

M.I.T. SPACE ENGINEERING RESEARCH CENTER

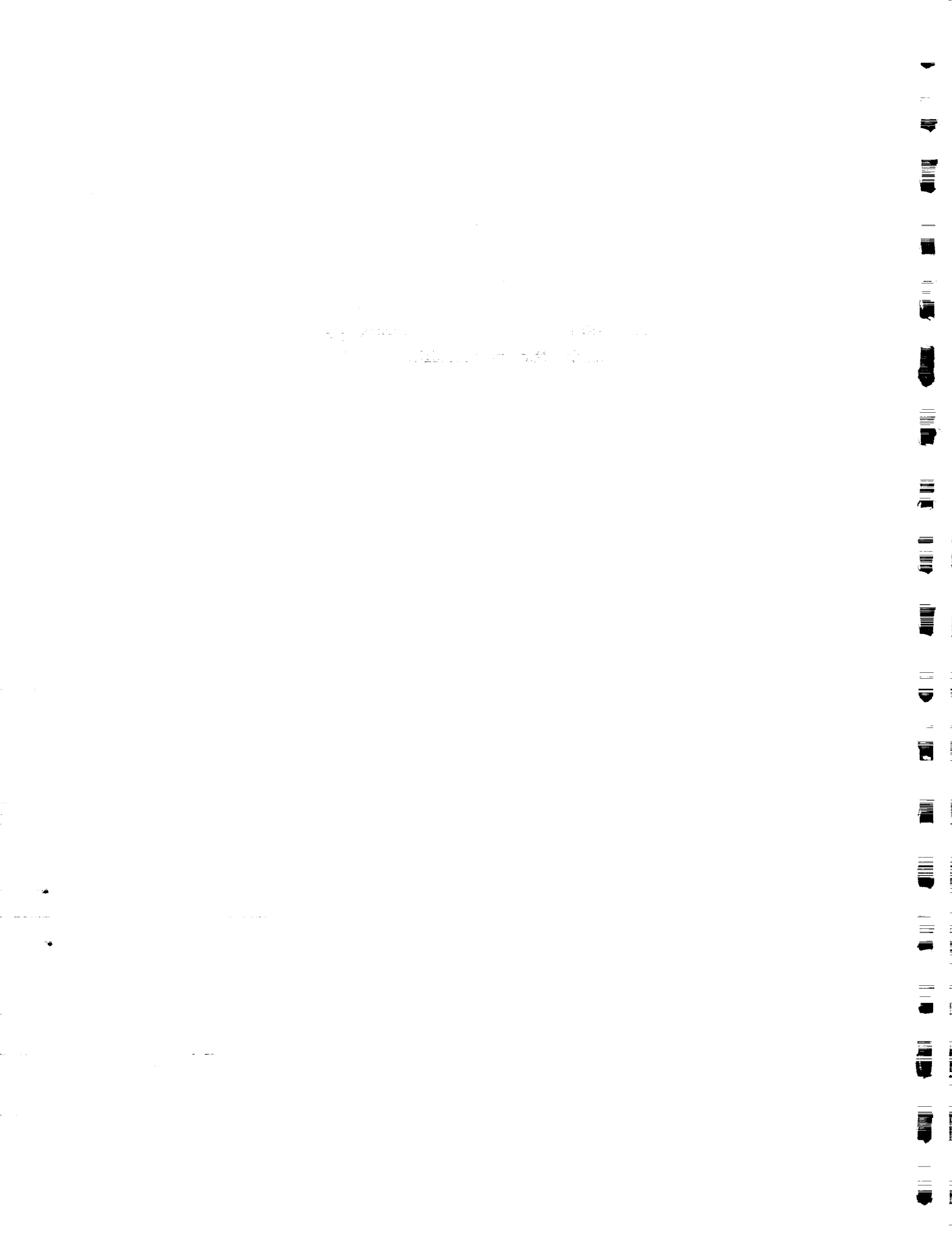
Semi-Annual Report: January 1992

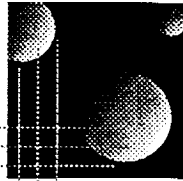
Professor Edward F. Crawley, Director

Dr. David W. Miller, Associate Director

April 1992 SERC # 4-92-R

(under the sponsorship of NASA)





*MIT
Space
Engineering
Research
Center*

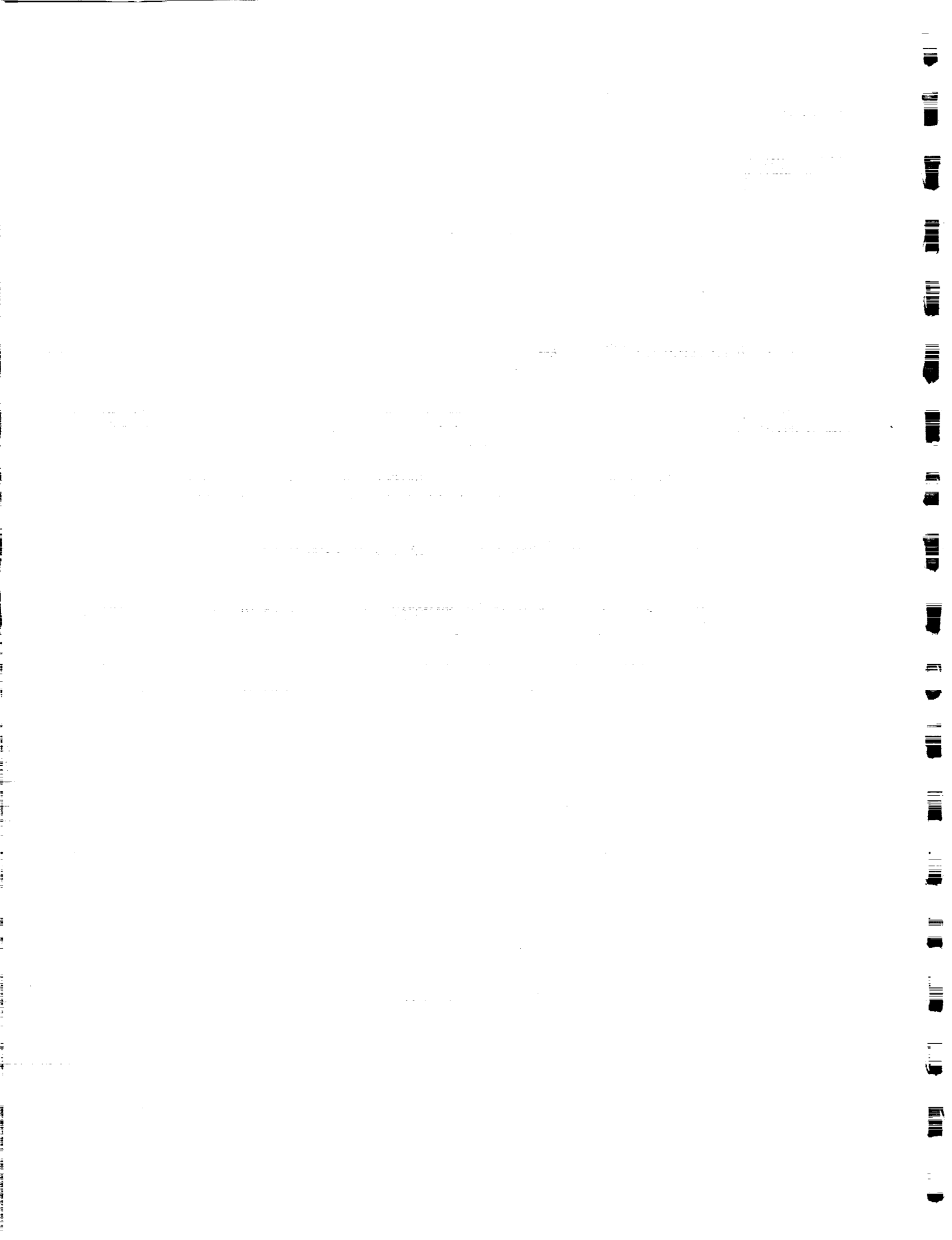
CONTENTS

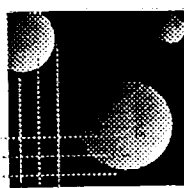
Overview, Objectives and Progress

- Executive Summary**

Presentations

- Interferometer Testbed: Overview and Hardware Summary**
- Passive Damping in the MIT SERC Controlled Structures Testbed**
- Finite Element Model and Identification Procedure**
- Physical Insight into the Simultaneous Optimization of Structure and Control**
- A Stochastic Approach to Robust Broadband Structural Control**
- MODE: Structural Test Article (STA)**
- The Middeck Active Control Experiment (MACE)**
- The Middeck Active Control Experiment: Gravity and Suspension Effects**
- The Middeck Active Control Experiment: Identification for Robust Control**
- Summary of Additional Research in Multivariable Identification and Control**
- Multivariable Identification for Control**
- Sensor and Actuator Technology Development**
- Implementation of Input Command Shaping to Reduce Vibration in Flexible Space Structures**
- Other Ongoing Research**
 - Pressure Actuator with Viscous Fluid Damping**
 - Passive Control/Damping**
 - End-Point Control of Flexible Manipulator Arms**
 - Embedded Electronics for Intelligent Structures**





MIT
Space
Engineering
Research
Center

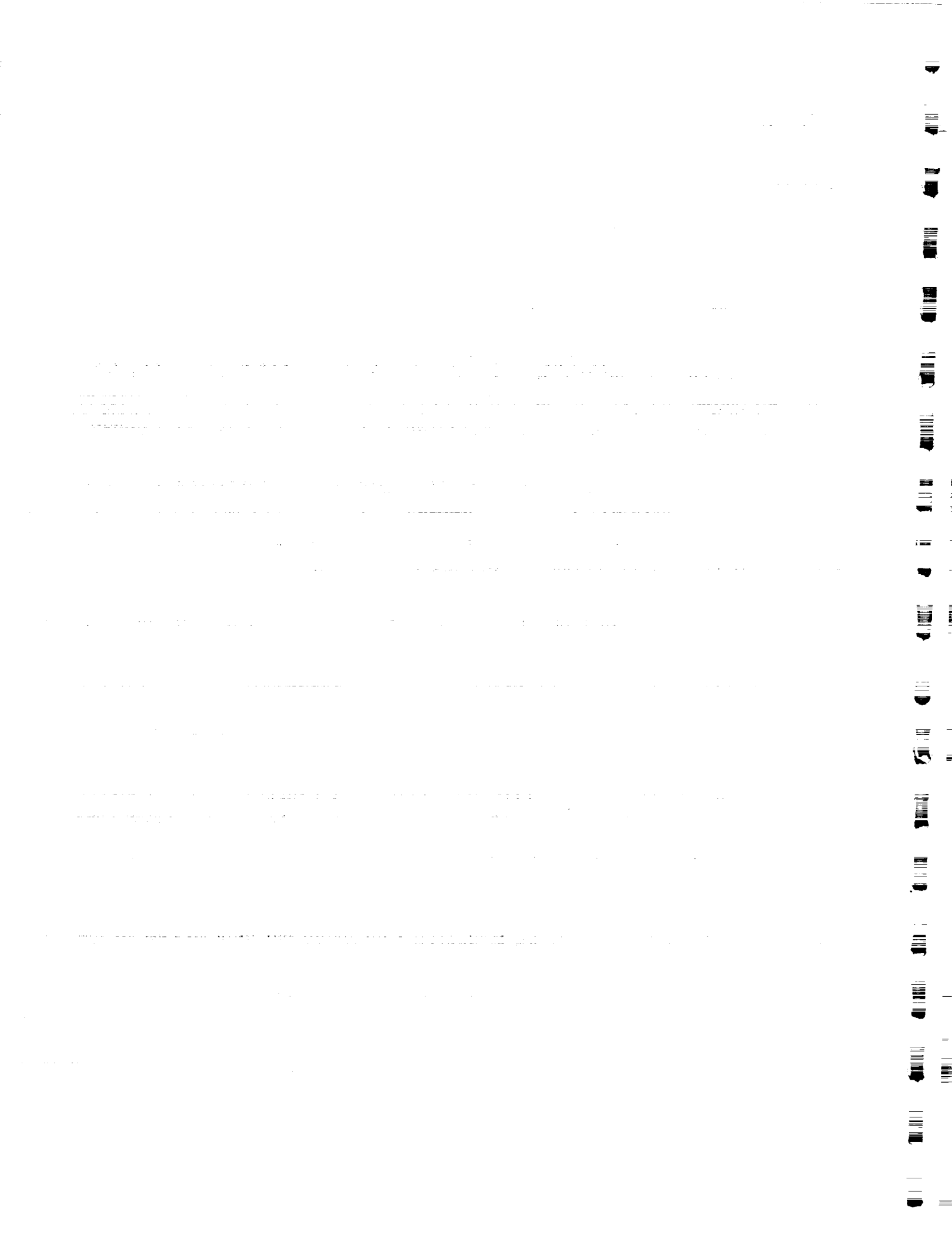
Overview, Objectives and Progress

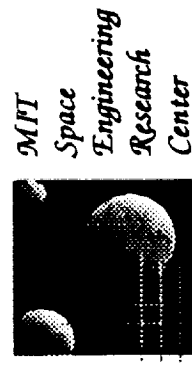
Executive Summary

The Space Engineering Research Center (SERC) at M.I.T., started in July 1988, has completed three and one-half years of research. This Semi-Annual Report presents annotated viewgraph material presented at the January 1992 Steering Committee and Technical Representative Review. Nine faculty and approximately 35 graduate students and like number of undergraduates through the Undergraduate Research Opportunity Program (UROP) participate in the activities of SERC, drawn from the Departments of Aeronautics and Astronautics, Electrical Engineering and Computer Science, and Mechanical Engineering.

The objective of the Space Engineering Research Center is to develop and disseminate a unified technology of controlled structures, to codify and disseminate this technology, and to train a generation of skilled engineers. The disciplinary research in CST continues and in this past year several notable milestones have been reached. The interferometer testbed became operational and is an active vehicle for CST researchers. The engineering model of the MACE multibody test article also was commissioned. It is a pathfinder for control of articulated flexible structures. The MODE experiment flew on STS-48. Its goals were to examine the dynamics of space structures in zero-gravity.

Moreover, there has been an ongoing effort toward developmental work in CST by the Space Engineering Research Center as we look ahead to the university/government/industry teaming of technologies for space applications with SERC as a model for university/government/industry cooperation.





INTERFEROMETER TESTBED: OVERVIEW AND HARDWARE SUMMARY

Andrew Nisbet

January 22, 1992

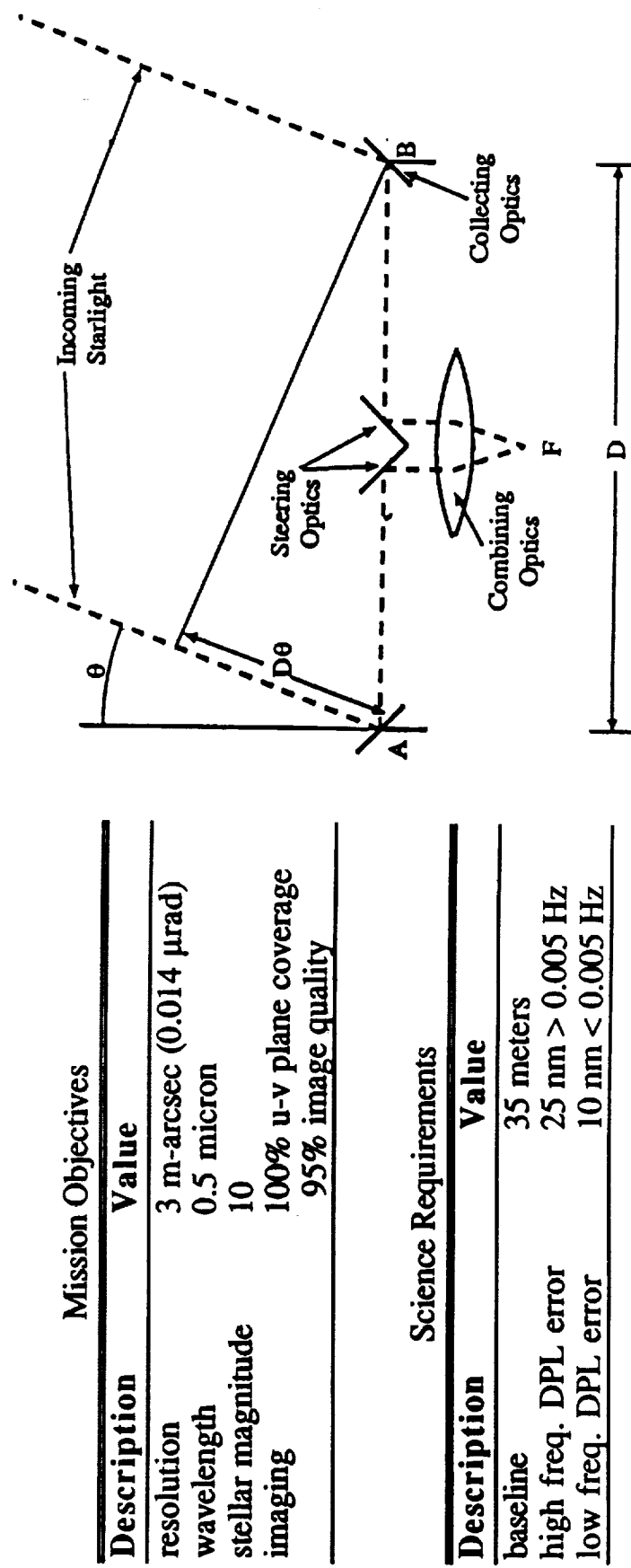
REFERENCE MISSION & SCIENCE REQUIREMENTS

MIT SERC WAS FOUNDED IN ORDER TO PURSUE RESEARCH IN CONTROLLED STRUCTURES TECHNOLOGY (CST). ONE OF THE FIRST STEPS TAKEN WAS TO SEARCH FOR A REPRESENTATIVE SCIENTIFIC MISSION THAT WOULD DEFINE STRINGENT CST REQUIREMENTS. AN OPTICAL INTERFEROMETER SPACECRAFT WAS CHOSEN BECAUSE IT CARRIES THE TOUGHEST REQUIREMENTS AND BECAUSE IT GIVES US SOME DEGREE OF COMMONALITY WITH OTHER TESTBEDS ACROSS THE COUNTRY.

CONSULTATION WITH ASTRONOMERS AT MIT, JPL, AND SAO LED US TO DEFINE THE SET OF MISSION OBJECTIVES SHOWN. FROM THE MISSION OBJECTIVES AND FROM THE PHYSICS OF INTERFEROMETRY, WE WERE ABLE TO DERIVE THE SCIENCE REQUIREMENTS FOR THE INSTRUMENT SIZE AND HIGH AND LOW FREQUENCY DIFFERENTIAL PATHLENGTH (DPL) ERRORS. THE FREQUENCY BOUND BETWEEN "HIGH" AND "LOW" IS DEFINED BY THE INVERSE OF THE INTEGRATION TIME.

Reference Mission & Science Requirements

- Needed scientific reference mission to define stringent CST goals: Optical Interferometer Spacecraft
- Consultation with astronomers produced the set of mission objectives shown below. The science requirements were then derived from the mission objectives.



Schematic of a two dimensional interferometer

SCIENCE REQUIREMENTS DERIVATION

THE INSTRUMENT MAXIMUM BASELINE DERIVED AS THE WAVELENGTH OVER THE DESIRED RESOLUTION.

THE HIGH FREQUENCY DPL LIMIT IS SET BY THE INTENSITY FUNCTION DERIVED FROM FOURIER ANALYSIS. HERE ϑ_l IS THE ALLOWABLE DPL. REQUIRING 95% IMAGE QUALITY MEANS THAT THE TERM MULTIPLYING $V(U)$ MUST BE EQUAL TO 0.95 OR GREATER.

THE LOW FREQUENCY DPL LIMIT IS SET BY THE MAXIMUM ALLOWABLE PHASE ERROR, FE , ALSO DERIVED FROM THE FOURIER ANALYSIS.

Science Requirements Derivation

- Baseline derived from resolution objective

$$\rho = \frac{\lambda}{D} = 0.003 \text{ arcsec}$$

- High frequency DPL limit derived from maximum intensity function

$$\begin{aligned} I_{\max} &= I_T + V(u) \cos\left(2\pi \frac{\partial\ell}{\lambda}\right) \\ &\approx I_T + V(u) \left(1 - \frac{1}{2} \left(2\pi \frac{\partial\ell}{\lambda}\right)^2\right) \end{aligned}$$

- Low frequency DPL limited derived from phase error

$$\phi_e = 2\pi \frac{\partial\ell}{\lambda}$$

REFERENCE SPACECRAFT DESIGN SUMMARY

IN A COMPLEMENTARY PROCESS TO THE TESTBED DEVELOPMENT, TWO THESIS PROJECTS HAVE BEEN CONDUCTED ON THE SYSTEMS LEVEL DESIGN OF AN INTERFEROMETER SPACECRAFT. THE VIEWGRAPH HIGHLIGHTS THE FEATURES OF THE DESIGN IN ITS CURRENT STATE.

- RWA: REACTION WHEEL ASSEMBLY
- LOS: LINE OF SIGHT

Reference Spacecraft Design Summary

Baseline	35 meters
Architecture	Deployable tetrahedral truss structure
Spacecraft Mass	3285 kg (truss) 12325 kg (total) incl. 25% margin
Payload Architecture	8 siderostats in non-redundant 2-D array
Telecommunications	TDRSS Ku-band compatible
Power Source	Body mounted solar arrays
Attitude Control	8 1200 Nms RWAs & mag. torque momentum dumping
Science Mode	217 sec integration time, continuous rotation about LOS

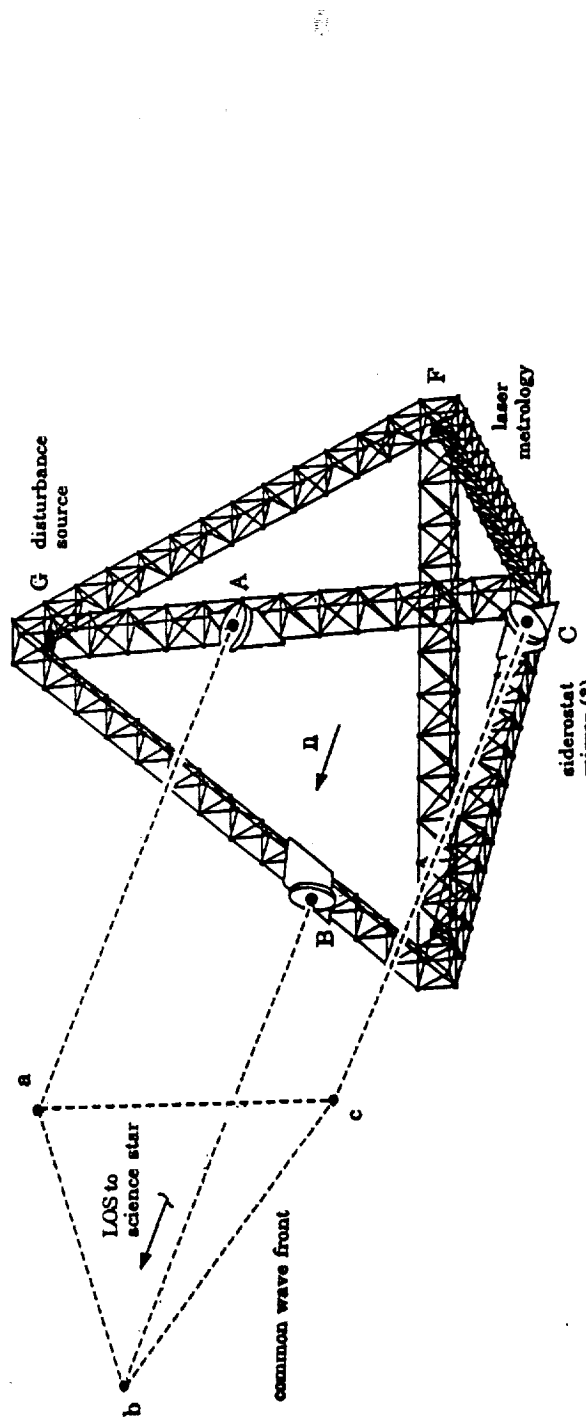
TESTBED REQUIREMENTS & PERFORMANCE METRIC

ONE OF THE SYSTEM DESIGN STUDIES DETERMINED AN EXPECTED DISTURBANCE LEVEL OF ABOUT 500 NM RMS DPL ERROR. THE PERFORMANCE GOAL FOR THE TESTBED IS TO ACHIEVE AN ORDER OF MAGNITUDE IMPROVEMENT OVER THE EXPECTED DISTURBANCE. THE 10 Hz LOWER FREQUENCY BOUND IS SET BETWEEN THE SUSPENSION MODES AND THE FIRST FLEXIBLE MODE.

IN THE TESTBED PROJECT, WE ARE CONSCIOUSLY ADDRESSING ONLY PART OF THE INTERFEROMETRY PROBLEM. FIRST, WE ARE ADDRESSING ONLY THE DPL ERROR IGNORING ERRORS FROM SUCH PROBLEMS AS WAVE-FRONT TILT. SECOND, WE ARE ADDRESSING ONLY THE CONTRIBUTION OF INTERNAL FLEXIBLE MOTION TO THE DPL ERROR (I.E., THAT FLEXIBLE MOTION WHICH CAUSES DISTANCES AF, BF, AND CF TO CHANGE). WE ARE NOT CONSIDERING THE DPL ERROR DUE TO RIGID BODY MOTION SINCE IT IS BEYOND THE SCOPE OF OUR RESEARCH EFFORTS. WE ARE ALSO NOT CONSIDERING THE DPL ERROR DUE TO EXTERNAL FLEXIBLE MOTION (I.E., THAT FLEXIBLE MOTION WHICH CAUSES DISTANCES AA, BB, AND CC TO CHANGE). THE SAME SOLUTIONS USED TO ADDRESS INTERNAL FLEXIBLE MOTION CAN BE APPLIED TO EXTERNAL FLEXIBLE MOTION. THE INTERNAL AND EXTERNAL FLEXIBLE CONTRIBUTIONS TO THE TOTAL DPL ERROR ARE APPROXIMATELY THE SAME MAGNITUDE.

Testbed Requirements & Performance Metric

- Structure is 1/10th scale truss-work tetrahedron with three siderostat locations. Performance requirement of 50 nm RMS differential pathlength error (DPL) above 10 Hz is an order of magnitude improvement over expected disturbance environment.



- Decision made to address only a subset of the DPL problem.
 - Errors due only to internal flexible motion will be considered, that due to external flexible and rigid body motion are not measured.

PERFORMANCE METRIC

THE PERFORMANCE METRIC WILL BE MEASURED BY LASER LEGS AF, BF, AND CF. THE PERFORMANCE METRIC AND GOAL IS AS SHOWN IN THE EQUATION. THE UPPER FREQUENCY BOUND OF 200 HZ IS SET FOR MEASUREMENT DEFINITION. EXPERIMENT HAS SHOWN THAT OVER 95% OF THE SYSTEM RESPONSE OCCURS BELOW 200 HZ.

- The performance metric as defined by internal flexible motion is measured by laser legs AF, BF, and CF. The performance goals for the testbed are:

$$\max \left(\begin{array}{l} (\text{AF} - \text{BF})_{\text{RMS}} \\ (\text{BF} - \text{CF})_{\text{RMS}} \\ (\text{CF} - \text{AF})_{\text{RMS}} \end{array} \right) \leq 50 \text{ nm over 10 - 200 Hz Bandwidth}$$

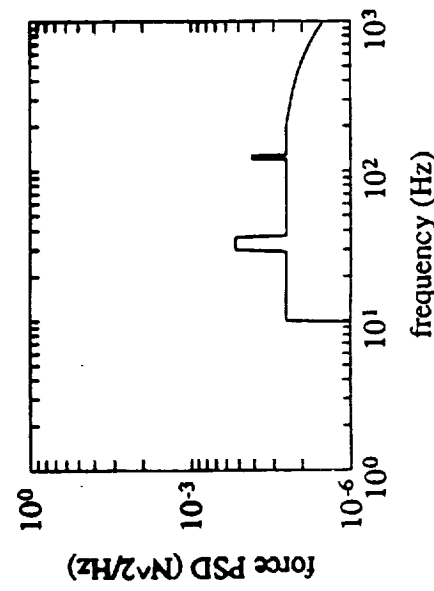
DISTURBANCE SOURCE & SIGNAL

DESIGN STUDIES IDENTIFIED AND CHARACTERIZED A VARIETY OF TYPICAL DISTURBANCE SOURCES WHICH PRODUCED A LEVEL OF ~500 NM RMS DPL ERROR. THE DISTURBANCE SOURCES WERE CATEGORIZED INTO NARROW-BAND SPIKES, LOW LEVEL BROADBAND NOISE, AND TRANSIENTS.

OUR EFFORTS HAVE BEEN TO APPLY REPRESENTATIVE DISTURBANCE SIGNALS TO A PIEZO-SHAKER IN ORDER TO GENERATE AT LEAST 500 NM RMS DISTURBANCE. THE FIGURE SHOWN IS A FORCE POWER SPECTRUM REPRESENTING LOW BROADBAND NOISE WITH SLOWLY VARYING REACTION WHEEL SPIKES. THIS SPECTRUM PRODUCED AN INSUFFICIENT LEVEL OF 80 TO 100 NM RMS.

Disturbance Source & Signal

- Reference mission design identified typical spacecraft disturbances and determined DPL response of ~500 nm RMS on structure with nominal level of damping (~1%).
 - Narrow band spikes (reaction wheel imbalances)
 - Broadband (fluid flow noise)
 - Transient (solar array or antenna drives)
- Disturbance Signals Applied To Piezo-Shaker:
 - A signal to represent low broadband noise with slowly varying spikes produced insufficient excitation in structure.

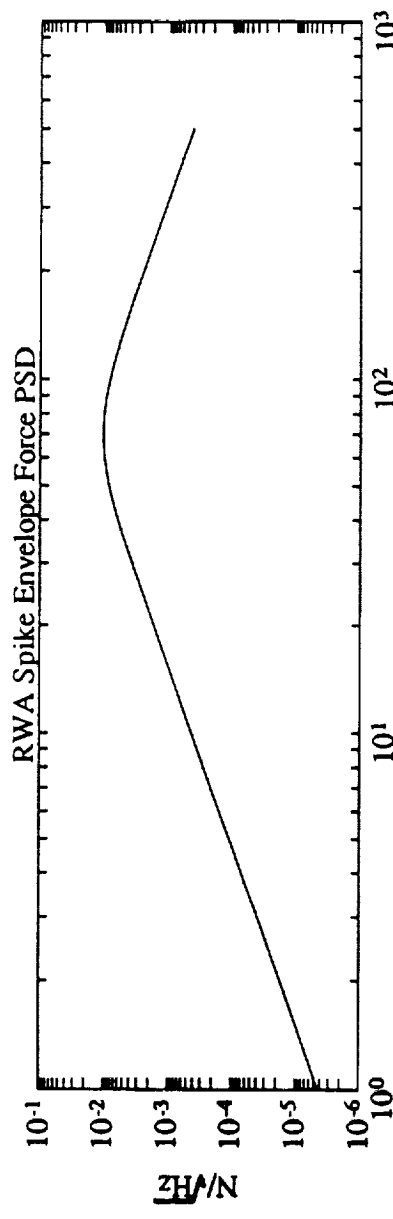


DISTURBANCE SIGNAL (CON'T)

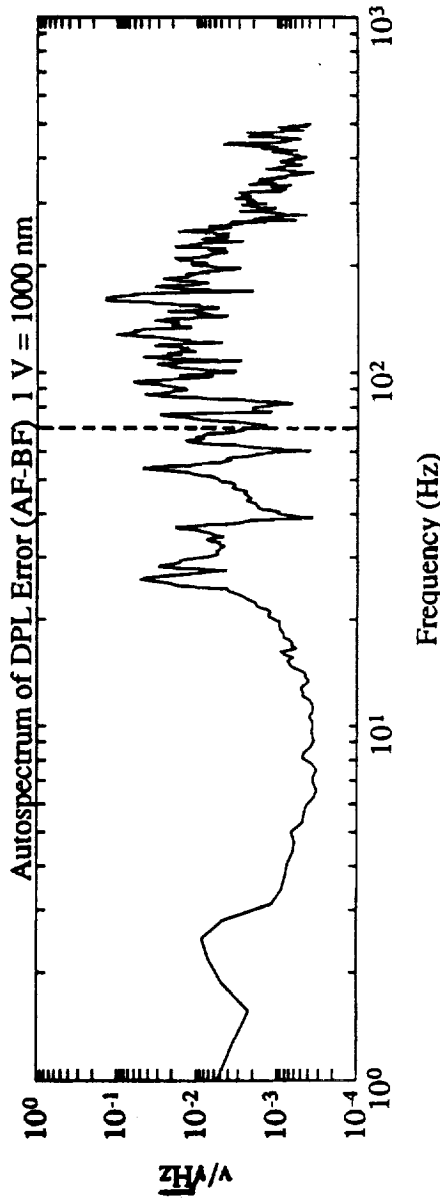
THE FIRST FIGURE SHOWS THE FORCE POWER SPECTRUM REPRESENTING THE FREQUENCY ENVELOPE OF REACTION WHEEL SPIKES AND THEIR HARMONICS. THIS WILL BE THE STANDARD DISTURBANCE SIGNAL THAT IS USED WITH THE TESTBED.

THE SECOND FIGURE SHOWS THE AUTOSPECTRUM OF THE RESPONSE BETWEEN LEGS AF AND BF. DISTURBANCE VARIED FROM 550 TO 770 NM RMS OVER THE THREE PATHLENGTH COMBINATIONS. THE VERTICAL LINE MARKS THE CORNER FREQUENCY OF DISTURBANCE. THERE ARE TWO IMPORTANT CONCLUSION FROM THIS DATA: 1) OVER 95% OF THE RESPONSE OCCURS BELOW 200 HZ, AND 2) THE RANGE FROM 100 TO 200 HZ IS AT LEAST AS IMPORTANT AS THAT FROM 10 TO 100 HZ.

- Disturbance Signal (con't):
 - Signal representing RWA spike envelope which increases with the square of the frequency up to wheels speed limit at 70 Hz. Some tail on the spectrum due to harmonics.



- This signal produces the following response with the desired level of disturbance (770 nm RMS). 96% of the total is below 200 Hz.



INTERFEROMETER TESTBED

"MOCK SIDEROSTATS" CAN BE SEEN AS THE THREE PLATES IN THE FOREGROUND. THESE ARE LOCATIONS A, B, AND C AND CONTAIN OPTICAL RETRO-REFLECTOR MOUNTS FOR THE LASER MEASUREMENT SYSTEM.

THE THREE-AXIS PIEZO-SHAKER (LOCATION G) CAN BE SEEN ON THE INSIDE OF THE TOP VERTEX.

THE "FOURTH VERTEX" (LOCATION F) CAN BE SEEN IN THE BACKGROUND. THIS LOCATION INCLUDES THE LASER HEAD, SPLITTING OPTICS, A RETRO-REFLECTOR, AND DETECTORS.

ACCELEROMETERS ARE DISTRIBUTED AT LOCATIONS AROUND THE TRUSS AND AT THE SIDEROSTAT LOCATIONS.

TWO ACTIVE STRUTS CAN ALSO BE SEEN AT LOCATIONS IN THE TRUSS WORK.

Interferometer Testbed

- "Mock siderostats" can be seen as the three plates in the foreground. These are locations A, B, and C and contain optical retro-reflector mounts for the laser measurement system.
- The three-axis piezo-shaker (location G) can be seen on the inside of the top vertex.
- The "fourth vertex" (location F) can be seen in the background. This location includes the laser head, splitting optics, a retro-reflector, and detectors.
- Accelerometers are distributed at locations around the truss and at the siderostat locations.
- Two active struts can also be seen at locations in the truss work.

TESTBED ARCHITECTURE

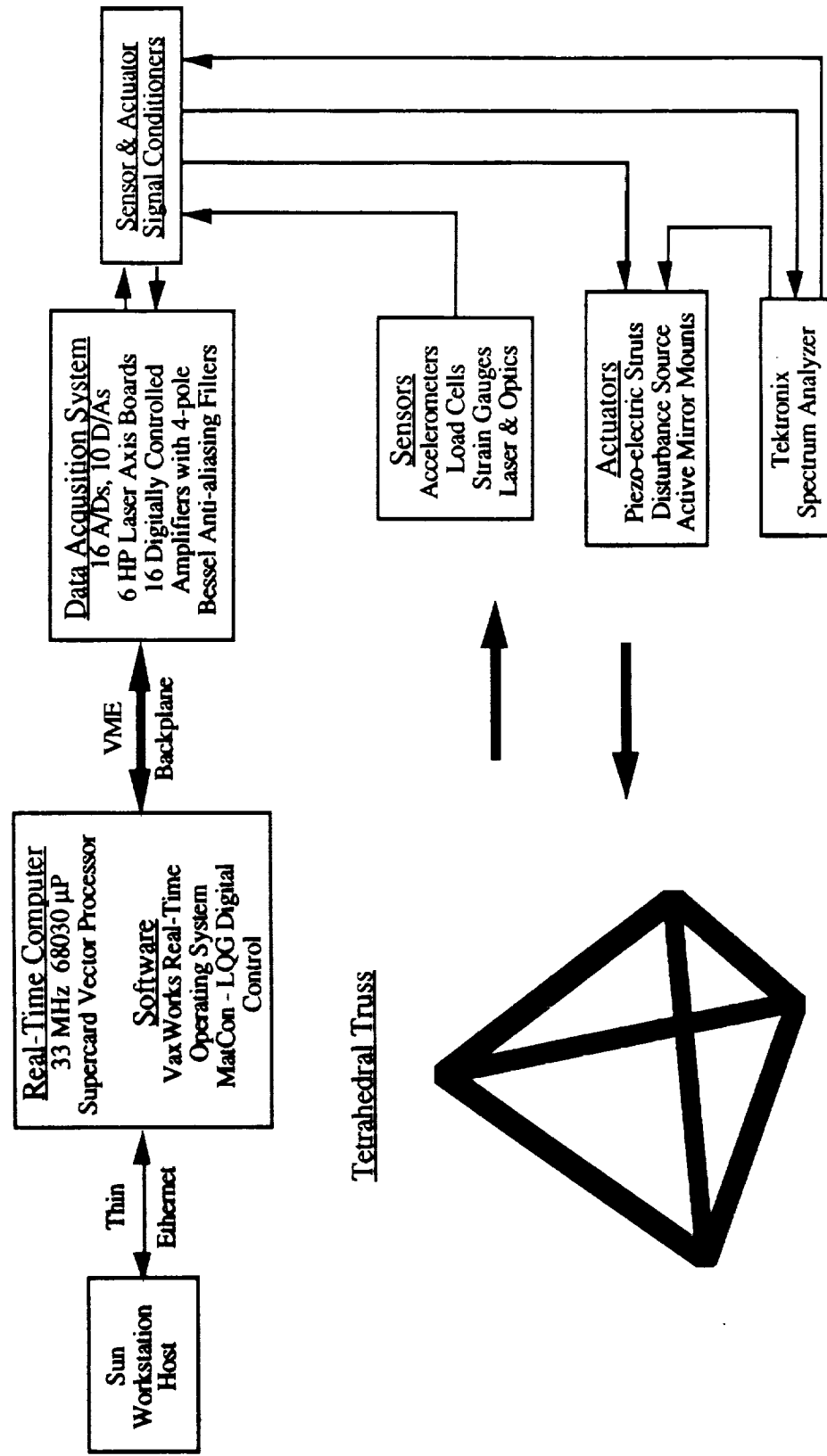
WE USE A SUN WORKSTATION AS A HOST FOR A REAL-TIME CONTROL COMPUTER WHICH IS USED FOR COMPUTING THE PERFORMANCE METRIC AND IMPLEMENTING CONTROLLERS. IT INTERFACES WITH THE SIX HP LASER CHANNELS, 16 A/D'S AND 10 D/A'S, AND 16 ANTI-ALIASING BESSEL FILTERS.

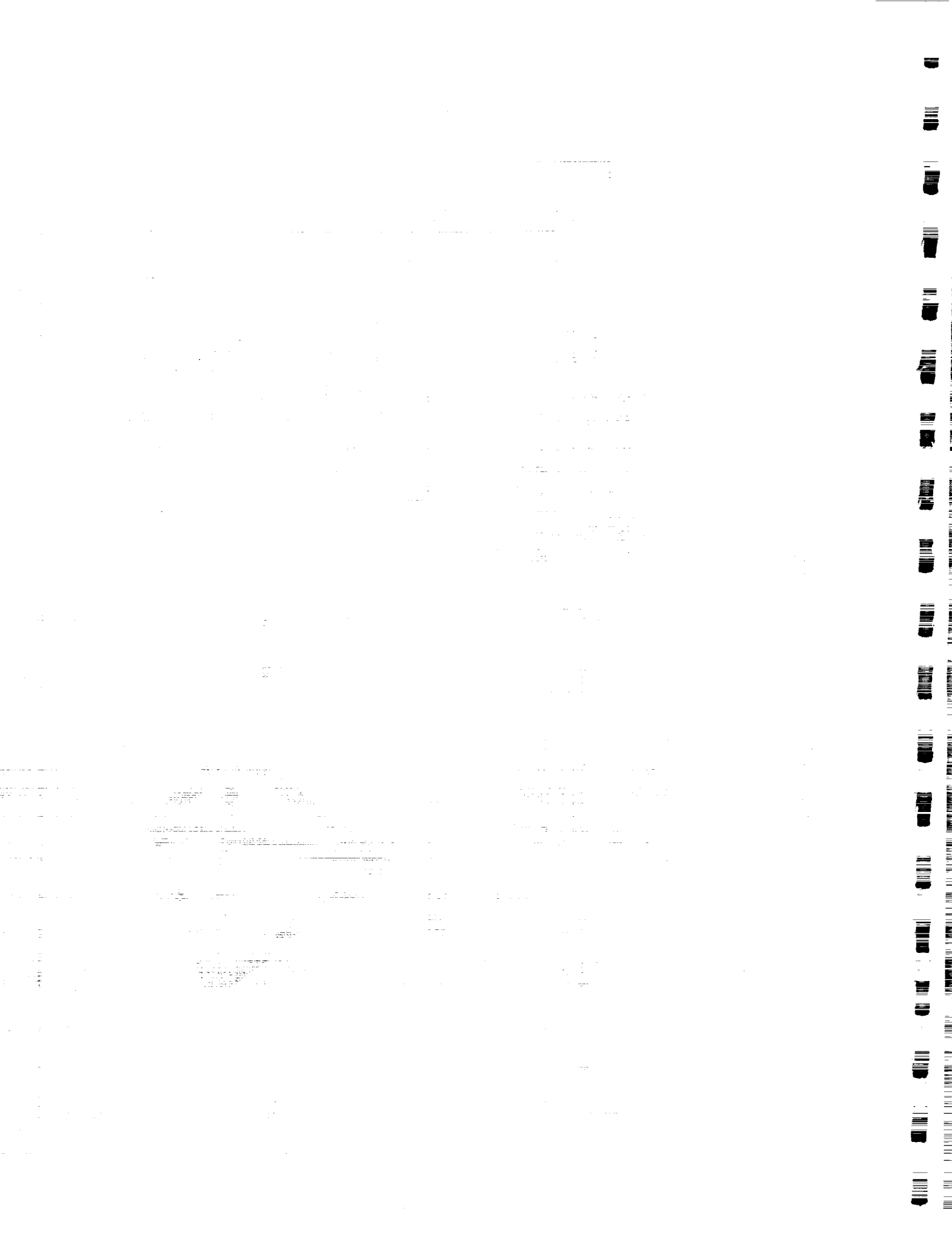
THE ARRAY OF SENSORS AVAILABLE FOR USE INCLUDE NUMEROUS KISTLER ACCELEROMETERS AT LOCATIONS ALONG THE TRUSS LEGS, THREE-AXIS SUNDSTRAND ACCELEROMETER MOUNTS AT THE SIDEROSTAT LOCATIONS, LOAD CELLS PLACED IN THE LOAD PATH OF THE ACTIVE STRUTS, STRAIN GAUGES ON THE ACTIVE STRUTS, AND THE THREE LASER LEGS.

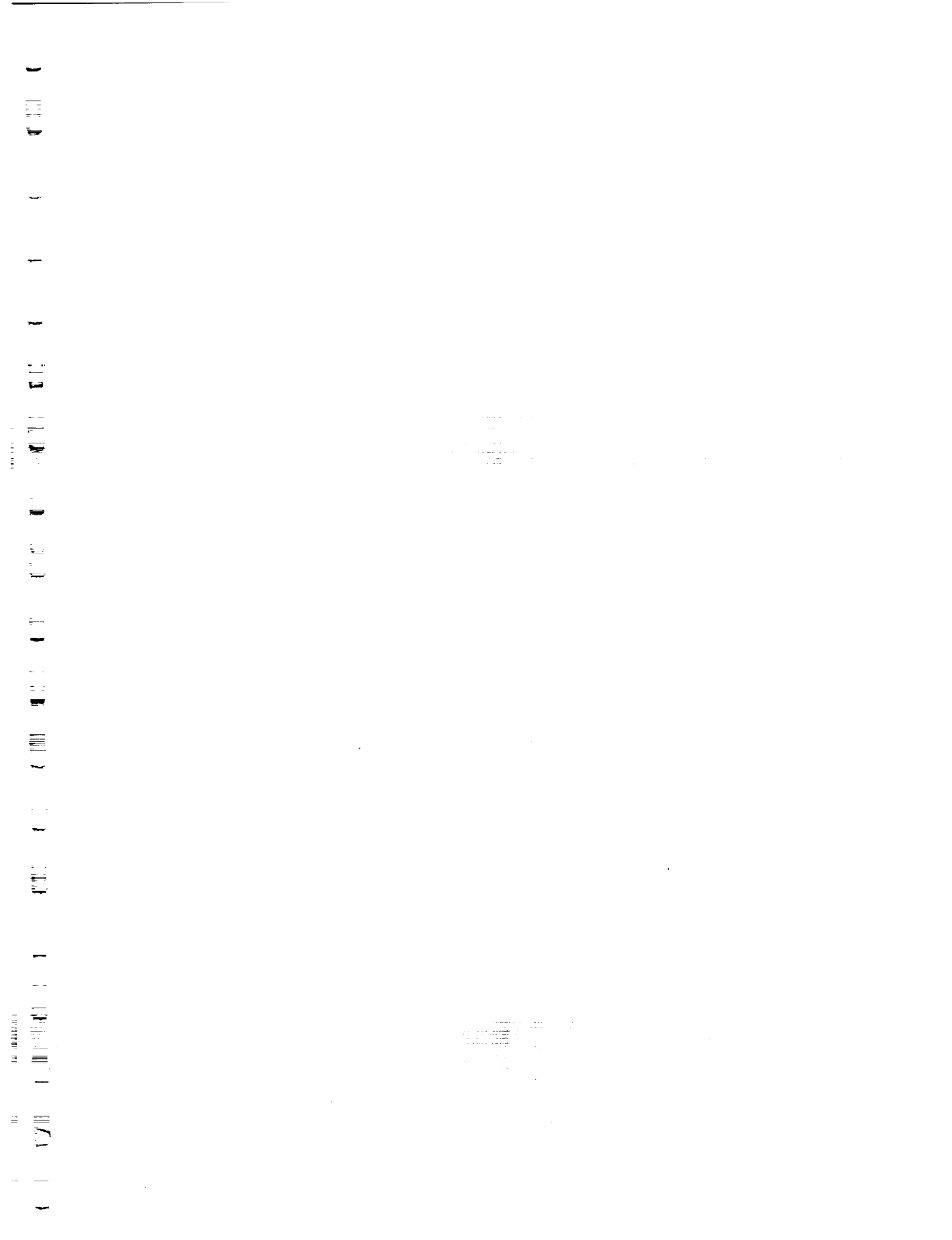
THE ACTUATORS FOR THE STRUCTURE ARE THREE PIEZO-ELECTRIC ACTIVE STRUTS THAT CAN BE PLACED ANYWHERE IN THE TRUSS, THREE PIEZO-ELECTRIC ACTIVE MIRROR MOUNTS AT THE THREE SIDEROSTAT LOCATIONS, AND THE DISTURBANCE SOURCE.

A TEKTRONIX SPECTRUM ANALYZER IS USED TO DRIVE THE DISTURBANCE SOURCE, TO MEASURE RELEVANT TRANSFER FUNCTIONS, AND TO HELP MONITOR THE PERFORMANCE METRIC.

Testbed Architecture







Passive Damping in the MIT SERC Controlled Structures Testbed

The talk outlines two damping mechanisms that have been developed and implemented on the MIT SERC Controlled Structures Testbed. Experimental results demonstrating viscoelastic (J-strut) and viscous (D-Strut) damping are presented. The two devices were designed to achieve different levels and frequency distributions of the damping added to the structure. The damping struts were constrained in size to be equal to or shorter than a regular strut on the truss which results in fewer restrictions on the placement passive struts. Some issues, such as the placement and sizing of the damping elements are still being developed, and will further progress will be achieved once a better finite element modal exists, as is discussed in the following talk.



Passive Damping in the MIT SERC Controlled Structures Testbed

Jonathan How, Gary Blackwood, and Eric Anderson

SERC Steering Committee Meeting
22 January, 1992

Viscoelastic Damping

The purpose of the viscoelastic J-struts is to add a relatively small amount of damping ($\eta_{max} \approx 10\%$) to many modes of the structure. While this will typically result in some improvement in the performance and disturbance attenuation, the primary purpose of this step is to raise the minimum level of damping in the first 36 modes. Since the D-struts are distributed relatively evenly throughout the structure and are similar to a regular strut, there is no significant change in global mass or stiffness distribution. The key benefits of these devices are that they are cheap and can be built at MIT.

The J-struts were designed and constructed at MIT SERC. They consist of a regular truss strut covered in two layers of ScotchDamp. A constraining layer of aluminum (roughly 50% the thickness of the strut wall) was then added. The entire device was cured to obtain the final product. It is expected that between 50 and 100 of these struts will be used on the structure, which has a total of over 700 struts.



ScotchDamp J-struts
installed on the bridge model

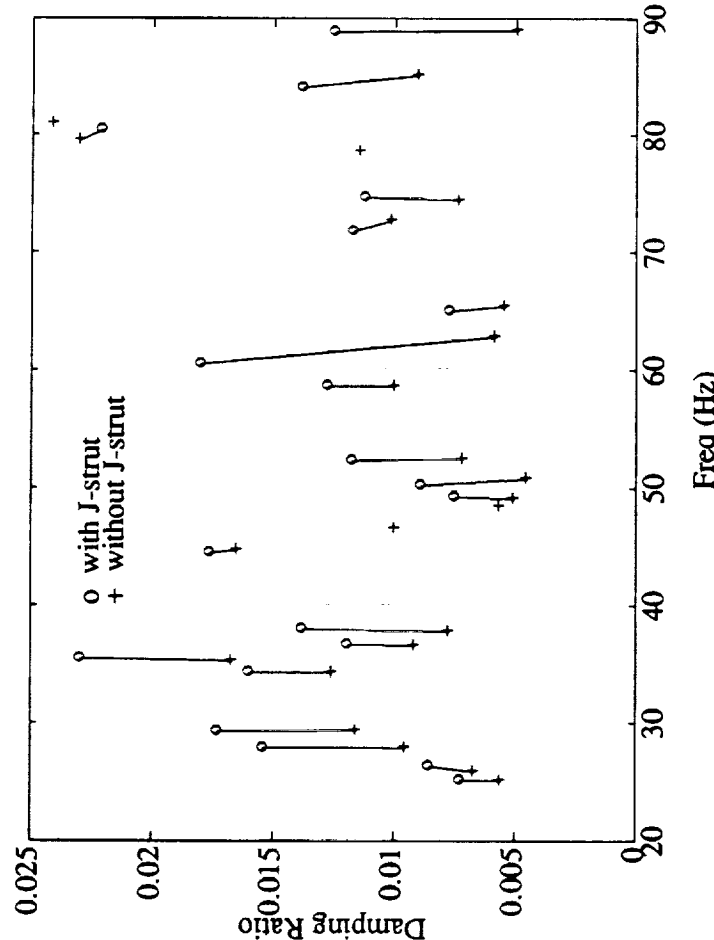
Viscoelastic Damping

- Purpose:
 - add damping to all modes so none too lightly damped
 - performance improvement and disturbance attenuation.
- No significant change in global mass or stiffness distribution.
- Low loss: $\eta_{max} \approx 10\%$ for struts built.
- Placed to maximize minimum added loss factor over first 36 modes.
- Inexpensive.

Results of Viscoelastic Damping

Fifty J-struts were added to the structure, placing them to maximize the minimum level of damping in the first 36 finite element modes. Transfer functions were collected between a suspended shaker and three accelerometers, of which one was collocated with the shaker. The same two shaker locations were used for tests with and without the J-struts. The transfer functions were identified in Matlab, and the figure is a comparison of the frequencies and damping ratios obtained for the two cases. The reversed pair at about 80 Hz is an indication of the level of error in the measurement and identification procedure. The predicted and measured damping increase in the first 20 modes (approximately 0.40 % for an average of 1.36 %) total of agree well.

Results of Viscoelastic Damping



- Average damping in 20 modes with J-struts: 1.34% (data from 3 accelerometers, 2 shakers)
- Average damping increase in 20 modes:
 - measured: 0.40% predicted: 0.44% – 0.52%

Viscous “Target” Damping

In contrast to the J-struts, the D-struts were designed to add a relatively large amount of damping in a narrow frequency range. Since the strut loss factors are much higher and the passive members are distributed less evenly, these devices can have a large effect on the global mass and stiffness values. Fewer D-struts will typically be used for a particular structure, as their role is to target specific modes to provide robustness/phase margin in active control rolloff and to lessen the effects of uncertainty. The placement and design of these struts will thus depend on the particular active control scheme that one intends to implement.

A complication of these dampers is that complex modes might have to be considered in the structure once they have been installed . The devices were modelled after the Honeywell D-Strut. Although the D-struts are more expensive than J-struts, similar hardware has been Space qualified. The D-strut is shorter than a regular strut, so a spacer (not shown) is typically included. This limits the effectiveness of the device, but this can be modified in later designs.

Viscous “Target” Damping

- Purpose:
 - provide robustness/phase margin in active control rolloff
 - lessen effect of uncertainty.
- Moderate effect on global mass and stiffness.
- High loss (5%-10% damping desired in a few modes).
- May have to consider complex modes after placement.
- Use the Honeywell D-Strut.
- Demonstrated on optical pathlength transfer function.
- Similar hardware has been Space qualified.

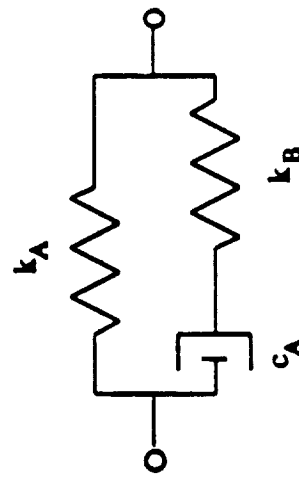
D-Strut Model and Component Tests

The D-strut can be effectively modelled as a lead-lag network. Typical predicted results of the loss factor and stiffness are presented in the graphs. Tests were performed to compare the 6 D-struts to the specifications, and the chart indicates how well they agree.



D-Strut Model and Component Tests

- Model:



$$Z(s) = k_A \frac{\omega_B s + \omega_A}{\omega_A s + \omega_B}$$

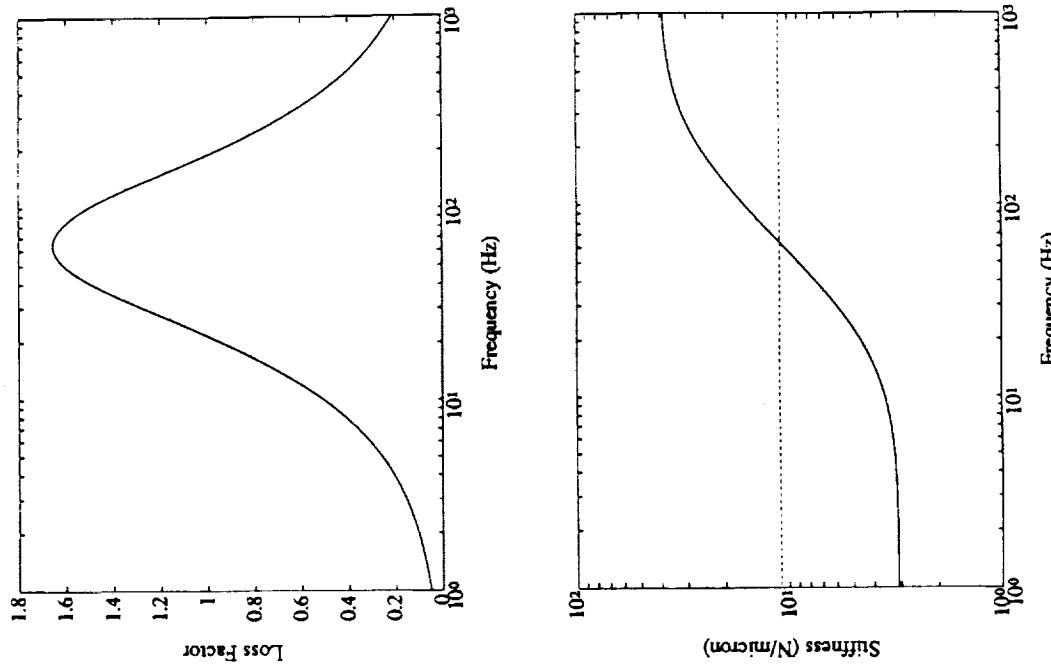
$$\omega_A = \frac{k_A k_B}{c_A (k_A + k_B)}$$

$$\omega_B = \frac{k_B}{c_A}$$

- Test results (100 nm rms):

	Component Tests			
param:	k_{DC}	f^*	η^*	ϕ^*
avg.	3.9 (N/ μ m)	78 Hz	1.41	55°
spec.	3.1 (N/ μ m)	64 Hz	1.66	59°

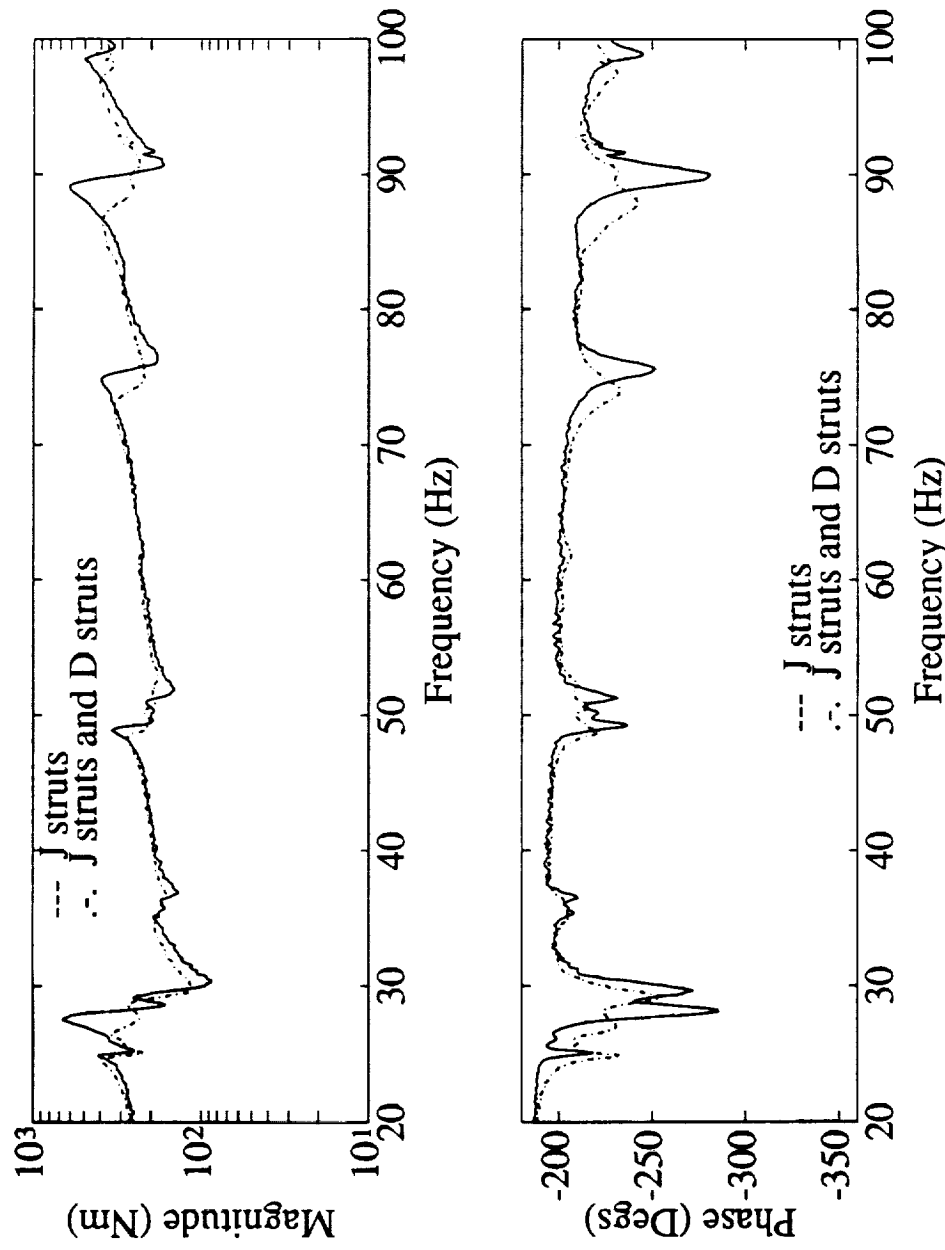
η^* Peak loss; ϕ^* Max. phase lead



Transfer Function Results of Target Damping

Consistent with the goal of placing the D-strut viscous dampers for a specific control task, the results are demonstrated on an optical pathlength transfer function. A discussion of the relevance of this transfer function is given in the following viewgraph. Note that the J-struts have already been placed in the structure. The goal of the next level of additional damping is to target the mode at 90 Hz which presents a difficulty for active controller due to the relatively large phase “blip” at that mode. Using the finite element model of the structure, this mode was isolated, and 5 D-struts were placed to maximize the damping in this mode. While the results indicate that some damping was achieved in other modes of the structure, and the frequency shifts indicate the influence on the global mass and stiffness values, what is most important is that a phase improvement of approximately 50° degrees was achieved in the target mode.

Transfer Function Results of Target Damping

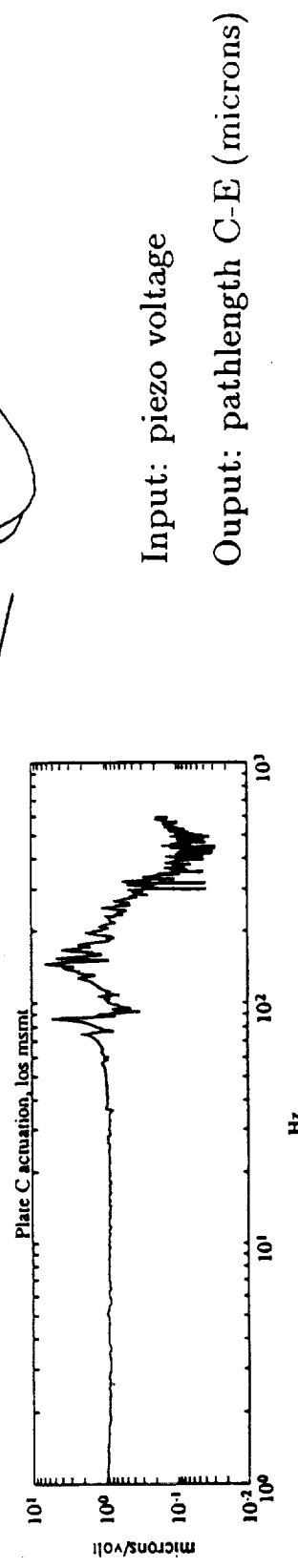
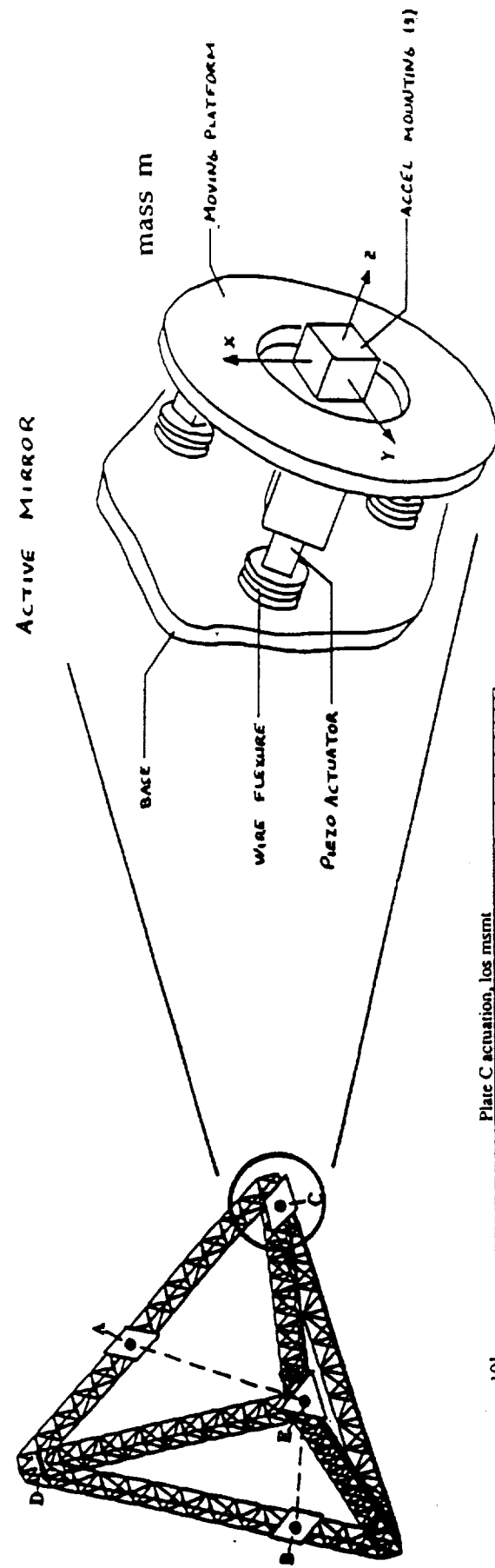


- 50° phase improvement on 90 Hz target mode

Pathlength Control Using Isolation Mounts

The viewgraph explains the relevance of the transfer function on the which the D-strut target damping was demonstrated. The mirror mount is located at one plate. The laser measurement between the fourth vertex (E) and the disturbance input that pistons the platform in the direction of E is given in the plot. A similar graph is presented to demonstrate the results of the D-struts.

Pathlength Control Using Isolation Mounts



Summary

The key results are that J-struts, while offering only a low peak loss factor, have a unit mass and stiffness comparable to the values of a regular strut. The D-struts are much heavier, but offer a much higher loss factor. The results indicate that the J-struts are effective in raising the overall level of damping in the structure, and that the D-struts are effective at targeting specific modes or frequency ranges of interest.

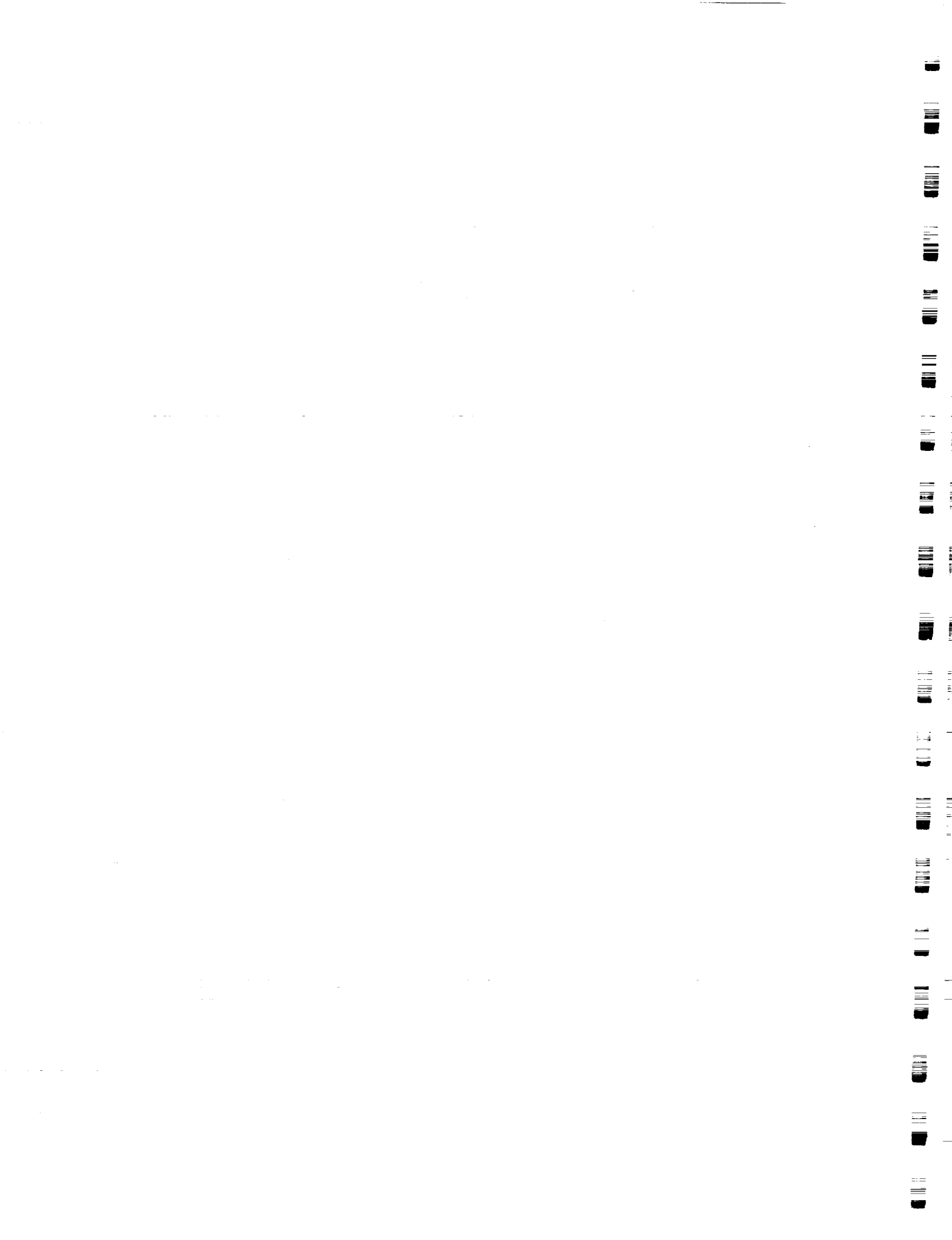
The research represented by this study is just part of the effort in an ongoing project that includes the development and implementation of piezoelectric shunting, the final placement of the viscoelastic J-strut dampers using modes from the updated finite element model, and the development of better targeting techniques for the placement of the D-struts.

Summary

- Features of the damper struts:

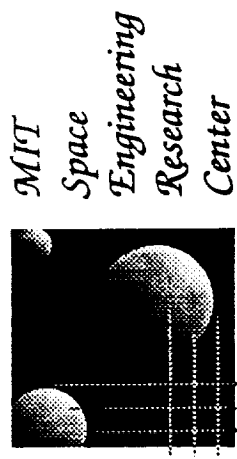
Strut	k_{∞}/k_{DC}	Peak Loss Factor (η^*)	Unit Mass (g) to Testbed	Mass Added
Nominal	1	< 0.005	39.5	—
J-Strut	1.12	0.07	57.3	1.41% (50)
D-Strut	9.8	1.41	232.9	1.53% (5)

- Ongoing work
 - place viscoelastic dampers using modes from the updated FEM
 - target damping for optical pathlength control
 - target damping for other global control approaches
 - piezoelectric shunting.



Finite Element Model and Identification Procedure

It was apparent from the work performed during the placement of the D-strut dampers discussed in the previous talk that, to be able to place the active or passive struts effectively, a finite element model that agrees better with the measured results must be developed. The purpose of this talk is to discuss the preliminary efforts at MIT SERC to bring the model and measurements of the SERC CST testbed into better agreement.



Finite Element Model and Identification Procedure

Jonathan P. How, Gary Blackwood, Eric Anderson, and
Etienne Balmes

SERC Steering Committee Meeting
22 January, 1992

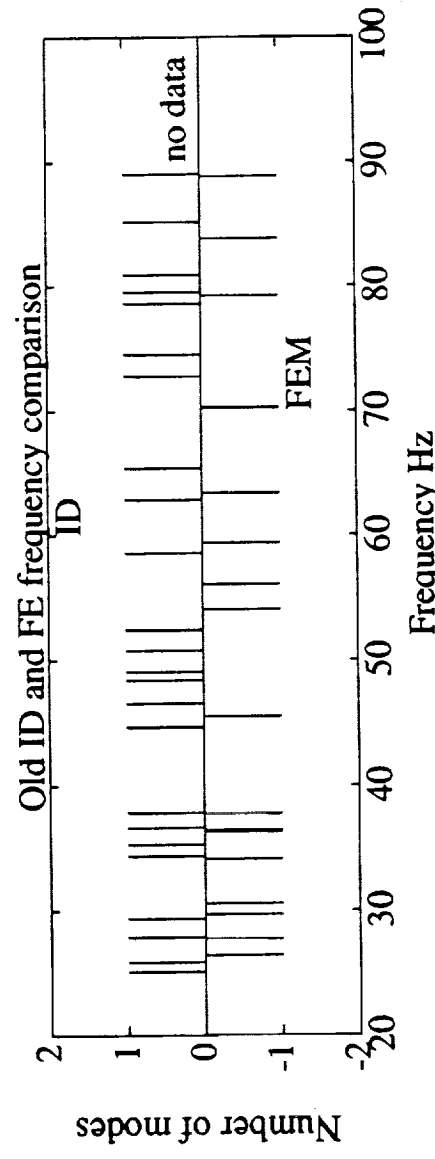
Finite Element Model Update

As mentioned, the large discrepancy between the frequencies of the finite element model and the identified data indicated that an update was necessary. The measured data is from the results collected during the damping augmentation tests. Although the agreement is reasonable for the first 8 modes, it is quite for modes above about 40 Hz. It was quite clear that a better model would be needed for sensor, actuator, damper placement, and initial control designs.

To determine which elements of the model should be modified, it is first necessary to develop a better understanding of the modal characteristics of the structure. This can be achieved by identifying the modal characteristics of the structure. This includes the frequencies, the damping ratios, and the residues. This process is related too, but an extension of identifying loop transfer function for the purpose of control designs. The identification procedure will be developed in the following slides.

Finite Element Model Update

- Large discrepancy between finite element model and identified frequencies indicate that update required.



- Agreement of modal frequency distribution:
 - poor at high frequencies
 - better for lower frequency modes dominated by first leg bending modes.
- Better model needed for sensor, actuator, damper placement, and initial control designs.

Identification Procedure

The hardware used during the test is listed. Some effort was made to ensure that every mode would be identified. This was achieved by a careful selection of the shaker locations to maximize the controllability of the least-controllable modes. These results were based on the old finite element model.

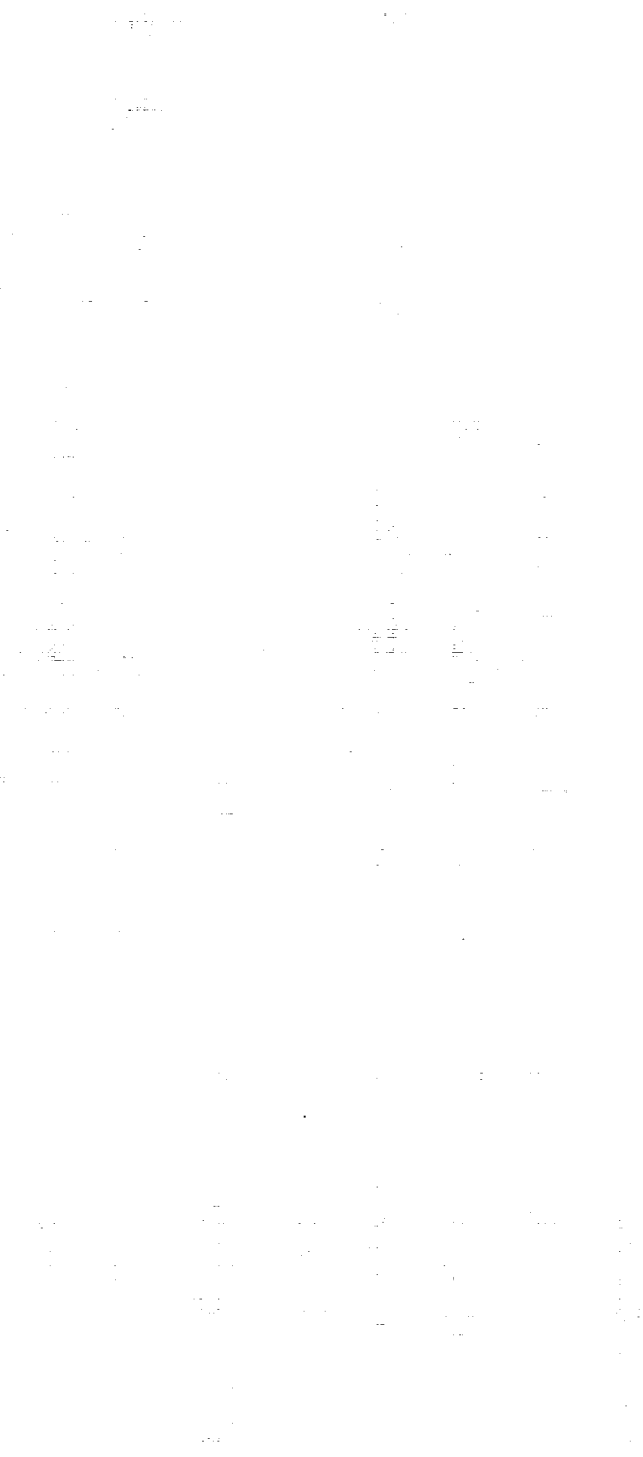
Identification Procedure

- Hardware:
 - 29 Kistler, 9 Sunstrand accelerometers
 - Brüel and Kjaer electromagnetic shaker
 - Tektronix scanner used to simultaneously measure all 38 channels.
- Selection of shaker locations:
 - 2142 possible locations reduced to 24 based on rankings using mean and maximum modal controllability.
 - goal: maximize controllability of least-controllable mode

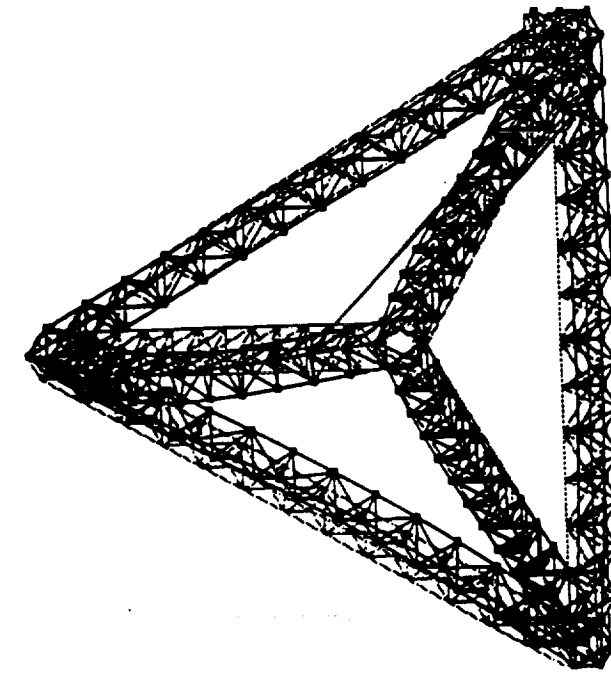
$$\max_i \left(\min_r |A_i^r| \right) \quad \begin{cases} A = \text{modal residue at input} \\ i = \text{input dof} (24) \\ r = \text{mode number (20)} \end{cases}$$

Testbed Mode Shapes

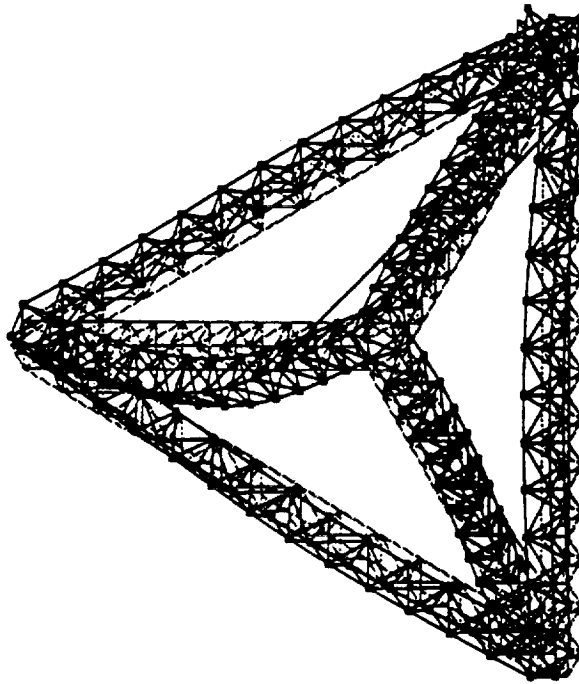
These finite element mode shapes for the two lowest frequency modes are presented for comparison with later results. The fourth vertex is at the lower righthand corner. The topmost corner in each figure is the location of the disturbance source. Leg 2 connects these two vertices. Mode 1 exhibits somewhat less Leg 2 motion than Mode 2.



Testbed Mode Shapes



Mode 1 (25.8 Hz)

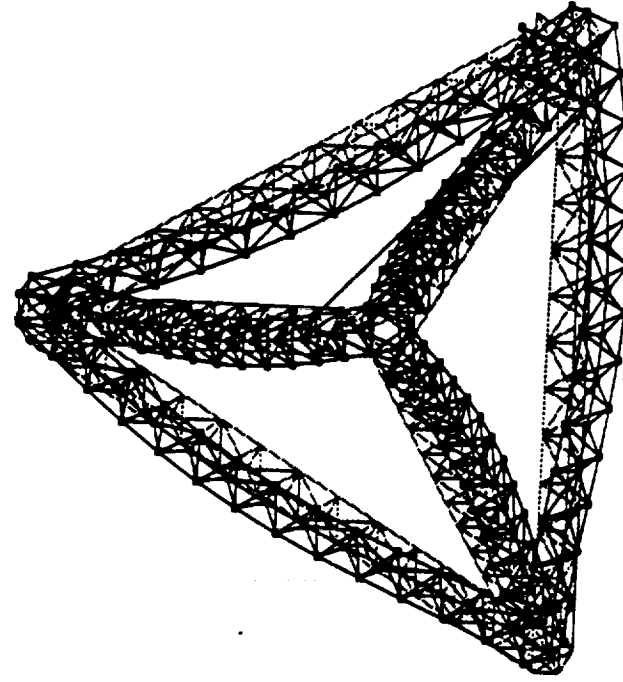


Mode 2 (27.2 Hz)

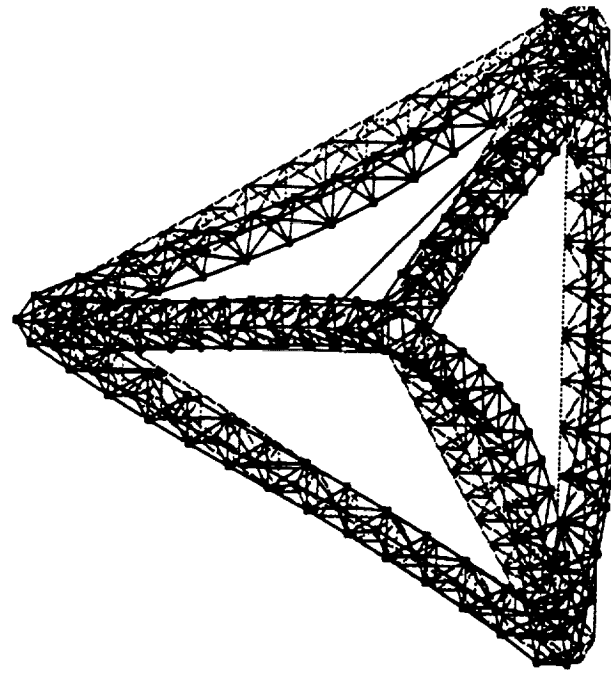
Testbed Mode Shapes

These finite element mode shapes for the modes 6 and 7 are presented for comparison with later results. Again, the fourth vertex is at the lower righthand corner. The topmost corner in each figure is the location of the disturbance source. Leg 2 connects these two vertices. As might be expected, these modes differ substantially from modes 1 and 2. In particular, it is clear that they exhibit somewhat more motion of Leg 2 than modes 1 and 2. This will be important for future comparisons since the shaker is located on this leg.

Testbed Mode Shapes



Mode 6 (36.1 Hz)



Mode 7 (36.3 Hz)

Interferometer Finite Element Model

The finite element model of the structure is quite large, with over 1500 degrees of freedom. Several characteristics of the model are listed. The most important points are that the model does exhibit closely spaced modes due to near symmetries in structure and that we have incorporated node flexibility through measured strut component test data. This data is at the component level only, but this could be modified by, for example, measuring the stiffness of an entire truss leg.

Interferometer Finite Element Model

- ADINA model, with 1500 degrees of freedom.
- Important attributes:
 - 1 beam element per strut
 - consistent mass matrix used
 - node flexibility incorporated through measured strut component test data
 - wires modelled as distributed masses
 - damping not modelled directly, included as modal damping in post processing
 - closely spaced modes due to near symmetries in structure
 - requires approximately 2 mins of Cray CPU time for the first 40 flexible modes.

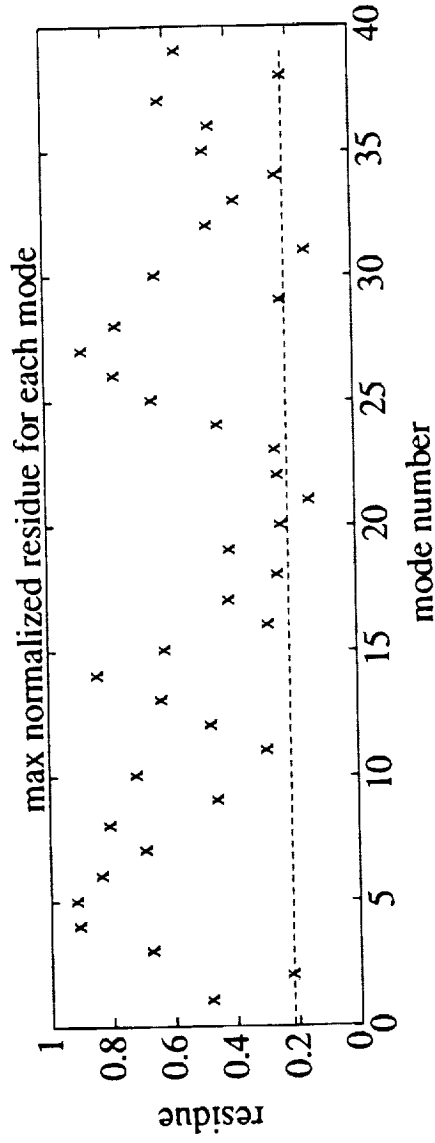
Shaker Locations

The top figure shows the level of controllability achieved in the first 20 modes, indicating that each should be measurable. In fact, the results indicate that the first 40 modes should all be reasonably disturbable from the 6 shaker locations. The resulting locations and directions of the shaker are show in the bottom left figure. As mentioned, 6 locations were required, with one location in each truss leg.

To accurately measure the collocated acceleration, a modification of the shaker tip was designed. The accelerometer is directly in the path of the applied force, parallel to the load cell, and housed in a steel load link. This design avoids any offset of the accelerometer which would make it sensitive to local rotations and introduce errors in the collocated measurements.

Shaker Locations

- Analysis resulted in one shaker location in each truss leg.



Shaker Tip:

- Shaker locations:

Data Analysis

Using 6 shaker locations and 38 accelerometers, over 220 transfer functions were measured. While interesting to look at, these are only useful if they can be modelled correctly and efficiently. To fit the large number of transfer functions taken, a modification of the least-squares approach coded by Roy Smith at UCSB was employed.

Data Analysis

- Transfer functions fit with modified least squares approach (R. Smith, UCSD).
- Leads to state space representation of measured data:
 - state space representation of each mode:

$$G_{fit}(s) := \begin{bmatrix} A & | & B \\ C & | & D \end{bmatrix}$$

- state space representation of each mode:

$$A_i = \begin{bmatrix} 0 & 1 \\ -\omega_i^2 & -2\zeta_i\omega_i \end{bmatrix} \quad B_i = \begin{bmatrix} 0 \\ 1 \end{bmatrix}$$

$$C_i = \begin{bmatrix} c_{1i} & c_{2i} \end{bmatrix} (38 \times 2)$$

- full model:

$$A = \text{BlockDiag}(A_i), B = \text{Col}(B_i), C = \text{Row}(C_i), D$$

Data Analysis

The A and B matrices are held fixed for each shaker location. As shown, B is of a very simple form. The use of a full C matrix adds extra flexibility to approach. The modal frequency and damping values were determined with `invfreqs` function in Matlab on several transfer functions. It was found that good fits require good estimates of the frequency and damping values of every mode in the frequency range of interest. This is but one of several curve fitting approaches currently employed at SERC. The advantages of this approach is that it is very simple to hold A and B fixed and then independently fit all 38 transfer functions simultaneously.

Data Analysis

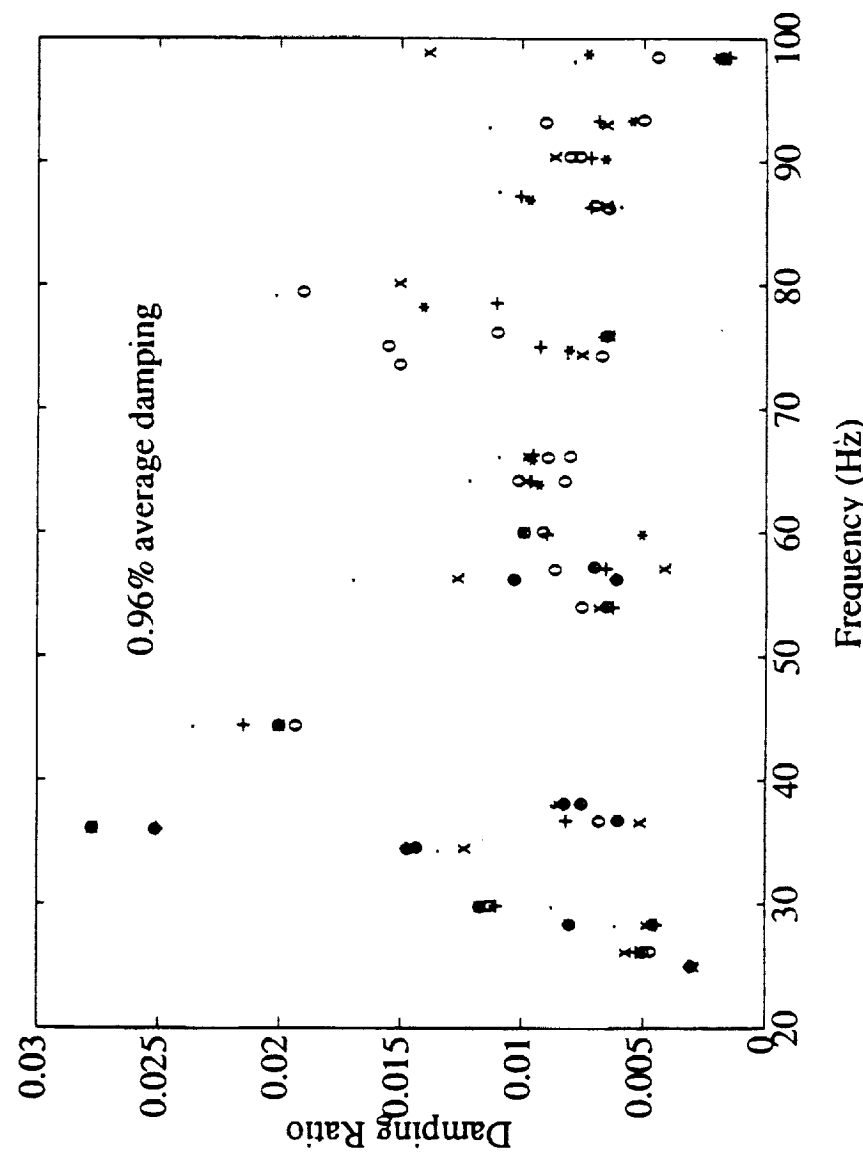
- The A and B matrices held fixed for each shaker location.
- Full C matrix adds extra flexibility to approach.
- Modal frequency and damping computed with `invfrequs` function in MATLAB on several transfer functions.
- Note: good fits require good estimates of the frequency and damping of every mode in the frequency range of interest.
- One of several curve fitting approaches employed at SERC.

Modal Frequency and Damping Comparison

The plot compares the frequency and damping values for the modes below 100 Hz for the six groups of transfer functions. The average damping in these modes is 0.96% (which agrees well with previous results). While the frequency values for each mode appear to agree well, there is some scatter in the damping ratios. This scatter results almost entirely from the identification procedure, but indicates the difficulties of developing an accurate multiple input/output model of a structure that is this complex.

Modal Frequency and Damping Comparison

- Six A matrices agree well in frequency, less so in damping.



Computational Procedure

Having developed the A and B matrices of the model, an iterative least-squares approach was employed to determine the best C and D choices. The equations presented here show how to select D from the previously known information. A similar process exists for C. It is also possible to perform an update of the A matrix given the new C and D matrices. However, due to difficulties that were experienced in the approach, this part of the process has not been performed.

Reference: Smith R. S., *Procedures for the Identification of the Precision Truss*, JPL D-7791.

Computational Procedure

- C and D matrix rows independently selected for each sensor.
- Example: Pick D

$$E_r = \left(\sum_{i=1}^m \|Y(j\omega_i) - G(j\omega_i)U(j\omega_i)\|^2 \right)^{\frac{1}{2}}$$

$$\begin{aligned} Z(j\omega_i) &= Y(j\omega_i) - C_b(j\omega_i - A_b)^{-1}B_b U(j\omega_i) \\ E_r(j\omega_i) &= Z(j\omega_i) - D(j\omega_i)U(j\omega_i) \end{aligned}$$

$$\text{Then } D_a = [\text{Re}(\bar{Z}) \text{ Im}(\bar{Z})] / [\text{Re}(\bar{U}) \text{ Im}(\bar{U})]$$

$$\text{where } \bar{Z} = [Z(1) \ Z(2) \ \dots \ Z(m)]$$

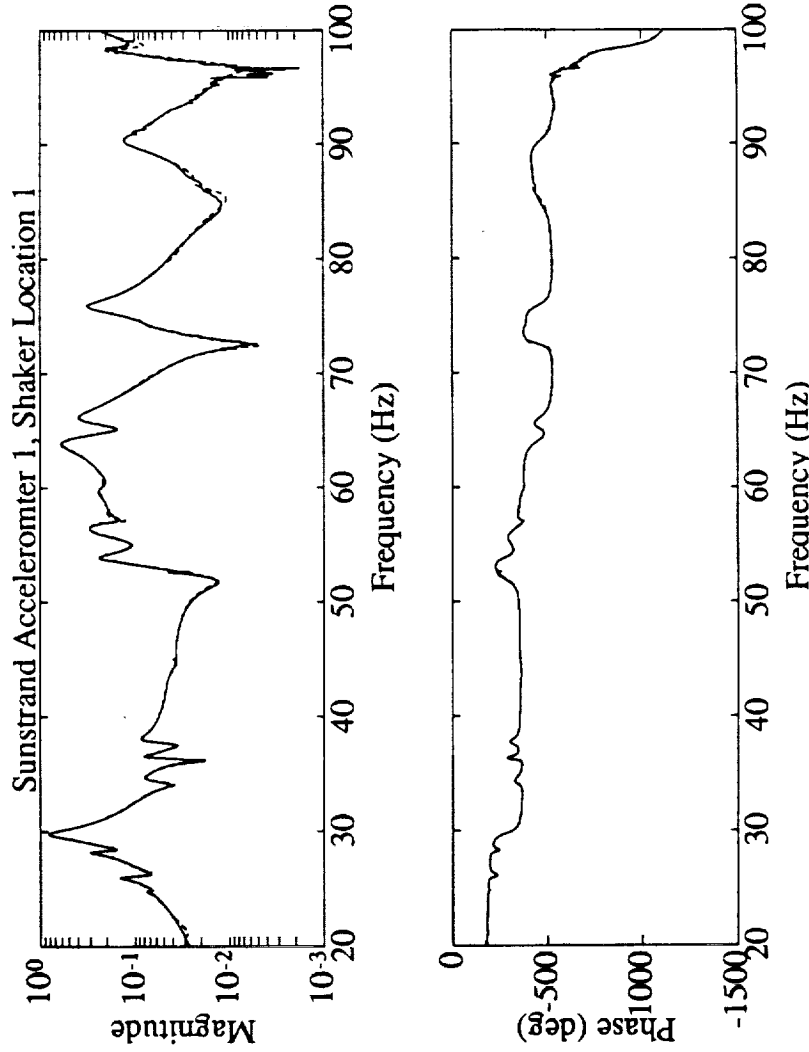
- Similar for the C matrix. Several iterations required.
- Software exists to perform an overall A matrix update.

Fit Comparison

The plot shows the agreement that is possible using this approach. As mentioned, it provides an effective tool for fitting hundreds of transfer functions, and it would appear that the results are good enough for initial control designs.

Fit Comparison

- Final fit comparison:



- Procedure effectively fits hundreds of transfer functions.
Results good enough for control designs.

Residue Analysis

Having developed the state-space model of the transfer functions, it is necessary to develop the residues for each mode so that the result can be compared with those of the finite element model. The equations shown here convert the residues of the acceleration transfer function to those of a displacement transfer function. Notice that the results are not constrained to be real, and are in fact complex.

Residue Analysis

- Need to compute displacement residues from approximate accelerometer transfer function.

$$\begin{aligned} G_{fit}(s) &= \sum_{i=1}^m \frac{c_{1i} + c_{2i}s}{s^2 + 2\zeta_i\omega_i s + \omega_i^2} + d \approx \frac{\ddot{y}}{f} \\ \overline{G}_{fit}(s) &= \sum_{i=1}^m \frac{b_{1i} + b_{2i}s}{s^2 + 2\zeta_i\omega_i s + \omega_i^2} + \frac{h(s)}{s^2} \approx \frac{y}{f} \end{aligned}$$

where $b_{1i} = -\frac{(1 - 4\zeta^2)}{\omega_i^2} c_{1i} - \frac{2\zeta}{w_i} c_{2i}$

$$b_{2i} = \frac{2\zeta}{\omega_i^3} c_{1i} - \frac{1}{w_i^2} c_{2i}$$

Residue : $\phi_i(x_{act})\phi_i(x_{sens})^H = (b_{1i} + b_{2i}s) \Big|_{s=j\omega_i}$

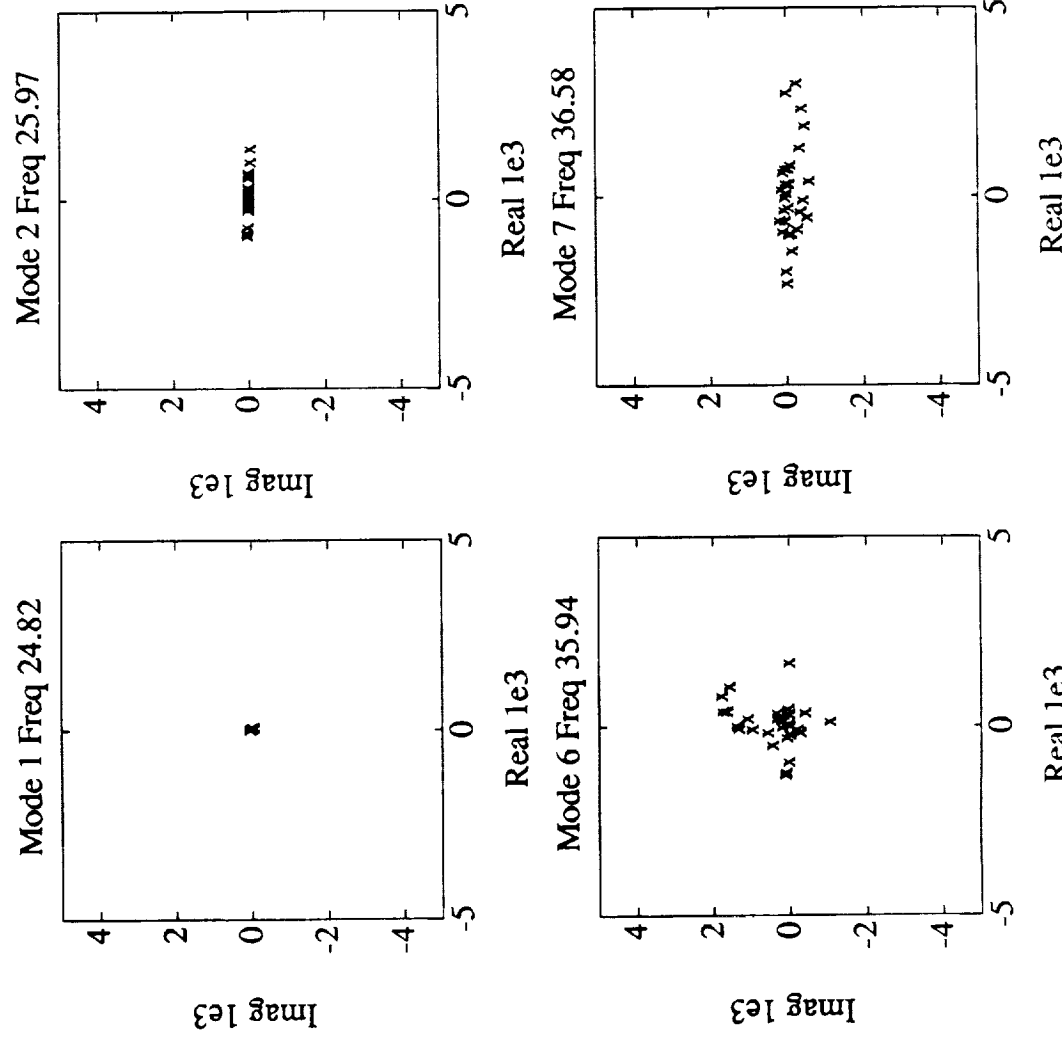
Typical Residues

These results present the residues of the four modes discussed previously from all 38 transfer functions with the shaker on Leg 2. For reference, a de-rotation of the residues using the collocated accelerometer phase measurement has been employed, which is why accurate measurements of this value were so important. Mode 1 showed little Leg 2 motion, and the residues are all relative small. Mode 2, a reasonably isolated mode in terms of frequency separation, showed some Leg 2 motion, and the residues are relatively large and almost entirely real.

In contrast, Modes 6 and 7, while both showing some Leg 2 motion, have closely spaced frequencies, and the resulting residues show large complex components. This indicates the difficulties of identifying a structure with closely spaced modes, as it is very difficult to decouple the effects of each mode in the residue analysis.

Typical Residues

- Residues rotated by phase at sensor collocated with shaker.

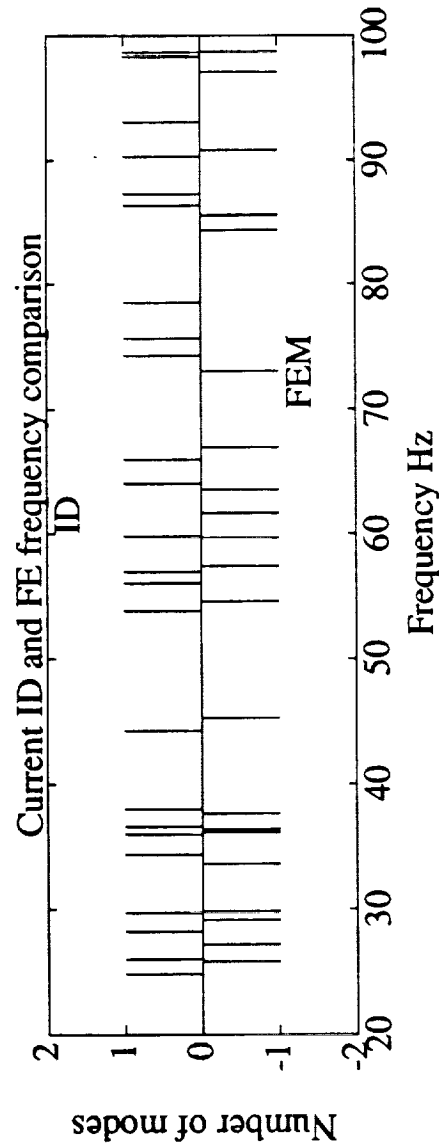


Current Status

Several changes have been included in both the structure and the model. Eigenvector studies illustrated the importance of plate flexibility, and the inclusion of these extra degrees of freedom in the FEM led to improved frequency agreement ($\leq 4\%$ error in first 9). The fourth vertex was also stiffened to improve the optical alignment, and the better agreement indicated in the figure illustrates that many local modes were present in the previous results.

Current Status

- Frequency comparison after structural and model updates:



- Modifications:

- eigenvector studies illustrated importance of plate flexibility, inclusion in the FEM lead to improved frequency agreement ($\leq 4\%$ error in first 9)
- fourth vertex stiffened to improve optical alignment, and better agreement indicates prior presence of local modes.

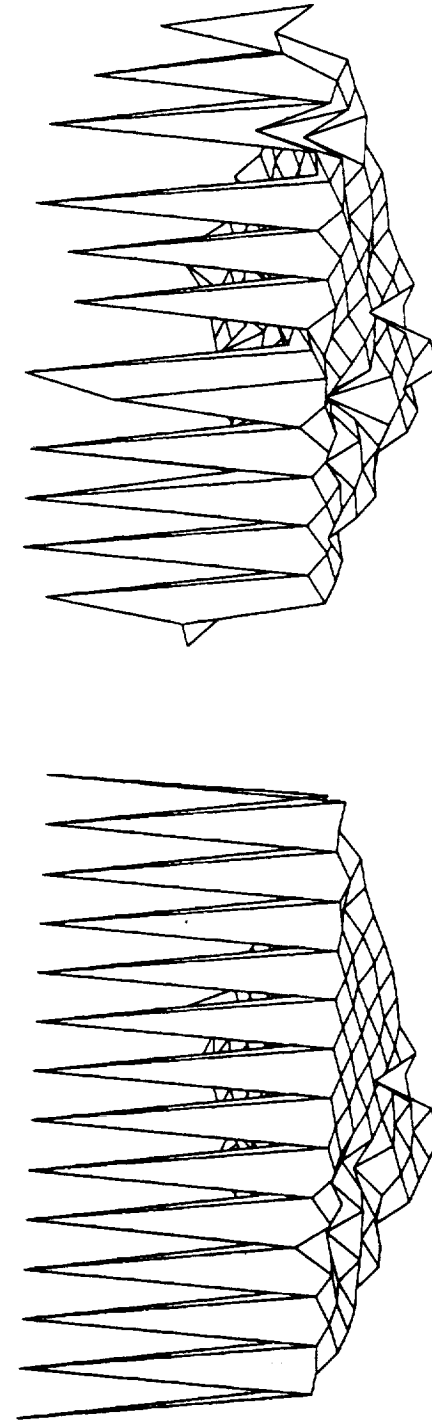
Identification/FEM Residual Comparison

To continue the comparison of the identified and modelled data, the Modal Assurance Criterion was computed. The figure on the left compares the model to model eigenvectors. The one on the right compares the model to measured. The correlation is good for the low frequency modes that are observable through Leg 2 (*i.e.*, not mode 1). Based on these results, it would appear that modes 6 and 7 have actually flipped. An issue in the comparison of these results is that the finite element model residues are real, but the measured residues can be complex.

Identification/FEM Residual Comparison

- Correlate identified and FEM residues for first 14 modes.
- Modal Assurance Criterion:

$$\text{mac}(x_1, x_2) = \frac{\|\sum_{i=1}^m \phi(x_1)_i \phi(x_2)_i^H\|^2}{(\sum_{j=1}^m \phi(x_1)_j \phi(x_1)_j^H) (\sum_{j=1}^m \phi(x_2)_j \phi(x_2)_j^H)}$$



Model/Measured

- Issue: FEM modes real, measured residues complex.

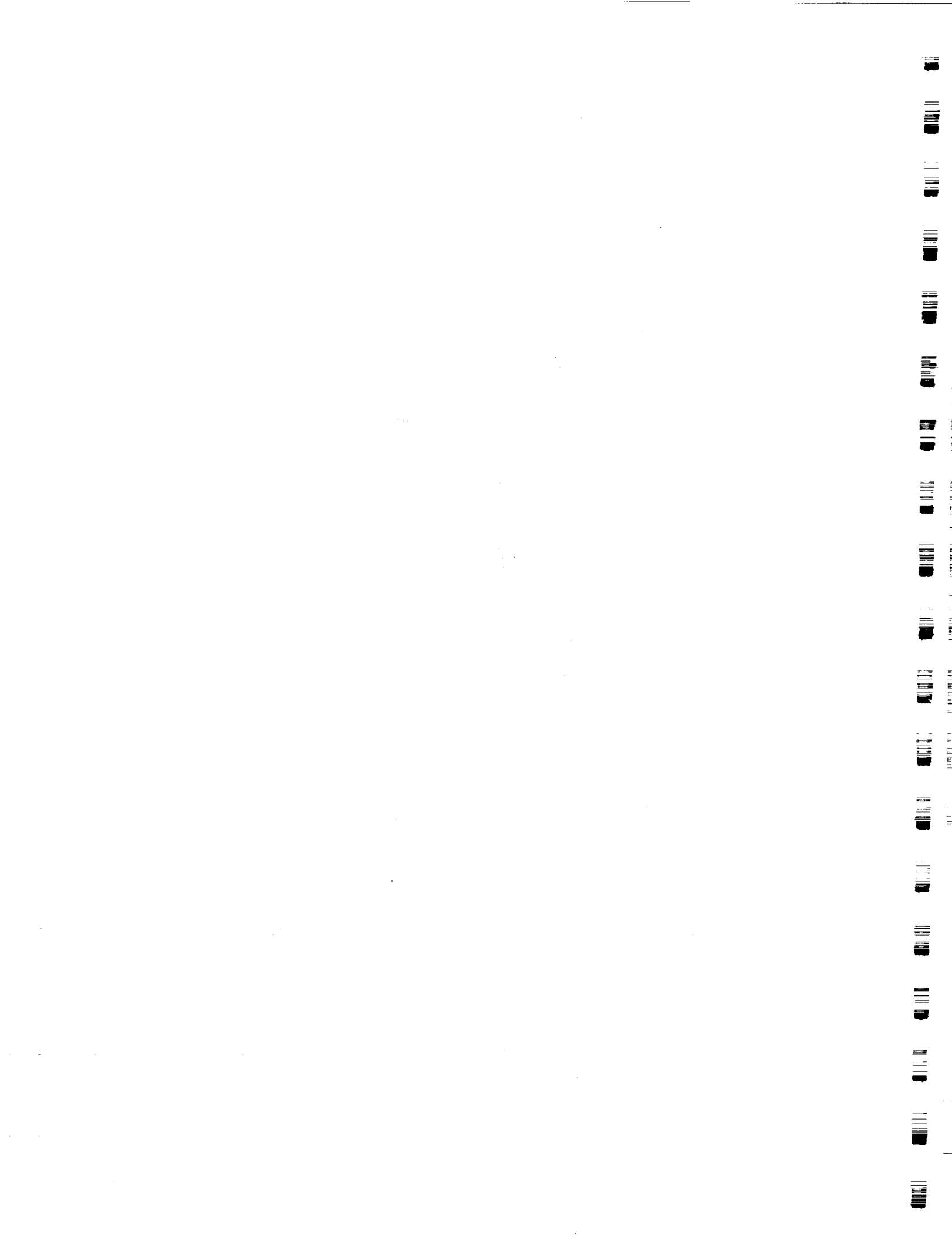
Model/Model

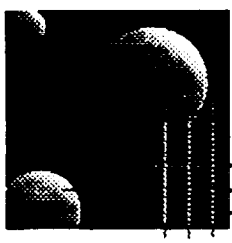
Future Work

To date, only coarse updates have been performed on the model. These will be continued as we try to account for other mismodelled dynamics. Eventually, as the agreement improves gradient type updates on the stiffness and mass matrices to match residues of higher frequency modes will be used. We are also in the process of improving the FEM suspension model with ID data. As mentioned, the goal is to develop the state space model so that it can be used for sensor, actuator, and damper placement, and then, hopefully, initial control designs.

Future Work

- Continue coarse FEM changes to correct plate flexibility and mass distribution assumptions.
- Apply gradient type updates on the stiffness and mass matrices to match residues of higher frequency modes.
- Improve FEM suspension model with 1D data.
- Develop state space model that can be used for sensor, actuator, damper placement, and initial control designs.

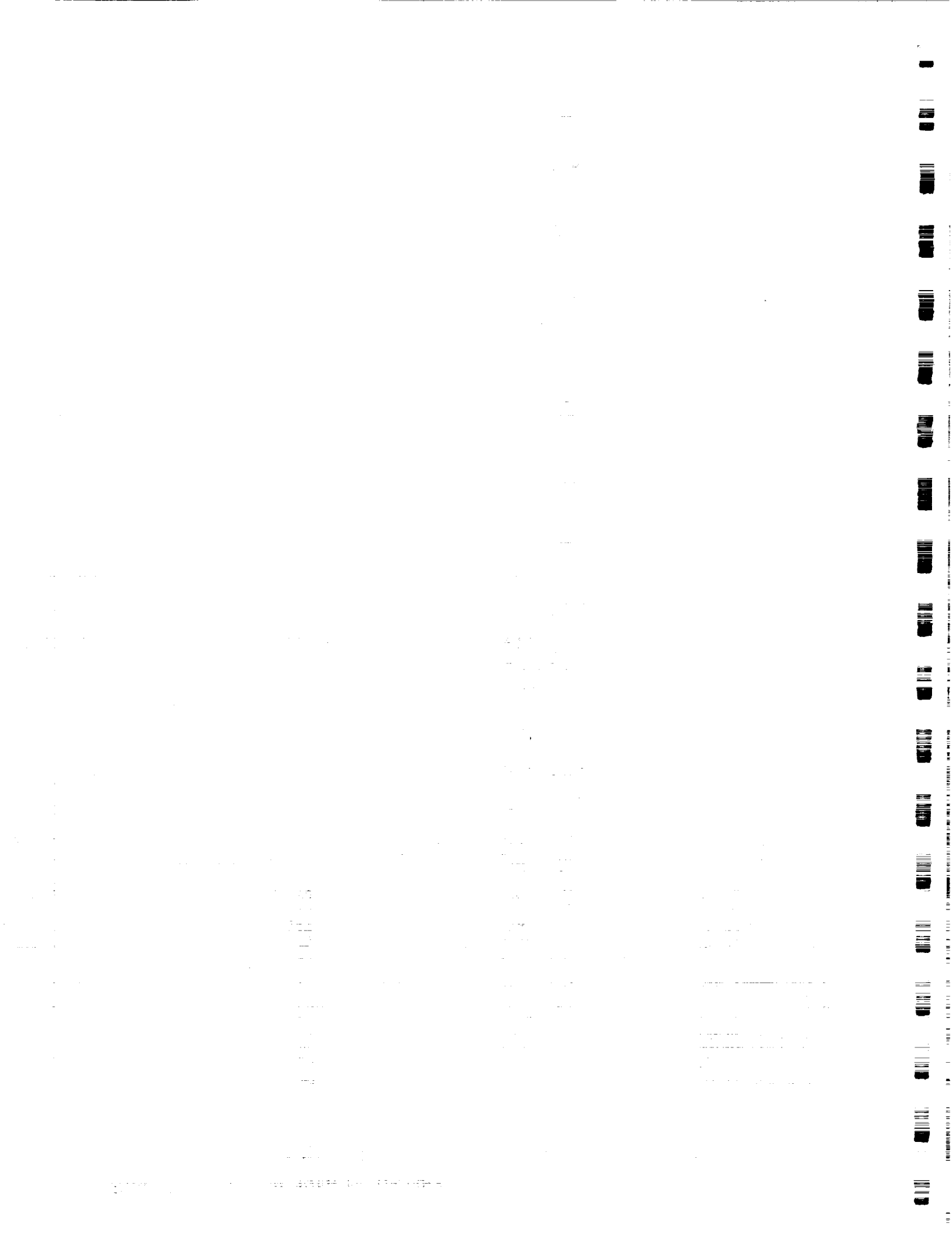




MIT
Space
Engineering
Research
Center

*Physical Insight into the Simultaneous Optimization
of Structure and Control*

Robert N. Jacques



Outline

- Description of simultaneous control/structure optimization and need for it.
- Need for physical insight
- Control/structure typical section and definition of modal properties
 - H_2 control design for typical section and behavior of performance with respect to modal properties
 - H_∞ control design for typical section and behavior of performance with respect to modal properties
 - Effects of more complex models

NEED FOR SIMULTANEOUS DESIGN

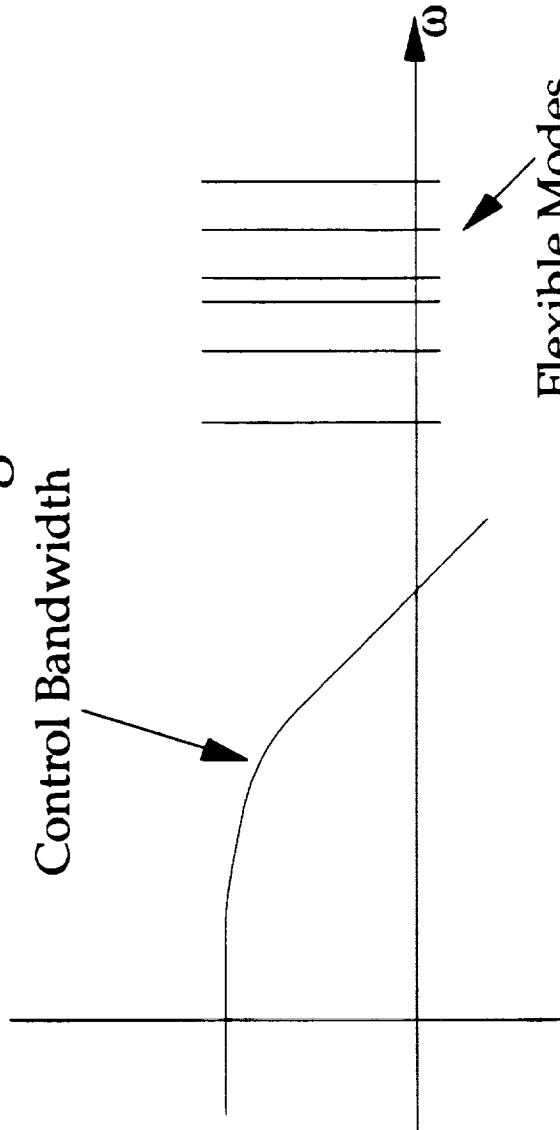
IN THE PAST, TYPICAL SPACECRAFT WERE FAIRLY RIGID AND HAD MODEST POINTING REQUIREMENTS. THIS USUALLY PLACED THE FREQUENCIES OF THE FLEXIBLE MODES OF THE SPACE WELL OUTSIDE OF THE BANDWIDTH OF THE ONBOARD RIGID BODY CONTROLLERS. THIS SEPARATION BETWEEN FLEXIBLE DYNAMICS AND CONTROL SIMPLIFIED THE DESIGN PROCESS. A GOOD DESIGN COULD BE ARRIVED AT BY DESIGNING THE CONTROL AND STRUCTURAL SUBSYSTEMS SEPARATELY.

CURRENT TRENDS HOWEVER ARE TOWARD SOFTER AND LARGER STRUCTURES WITH TIGHTER POINTING REQUIREMENTS. THIS FORCES THE CONTROL BANDWIDTH UP WHILE AT THE SAME TIME ALLOWING THE FREQUENCIES OF FLEXIBLE MODES TO COME DOWN. THE NET RESULT IS THAT SEVERAL TO MANY MODES OF THE SPACECRAFT CAN LIE WITHIN THE BANDWIDTH OF THE CONTROLLER. THE STRONG COUPLING BETWEEN THE STRUCTURE AND CONTROL THAT RESULTS IN DETERMINING DYNAMIC PERFORMANCE IMPLIES THESE SYSTEMS MUST BE DESIGNED TOGETHER TO OBTAIN GOOD PERFORMANCE.

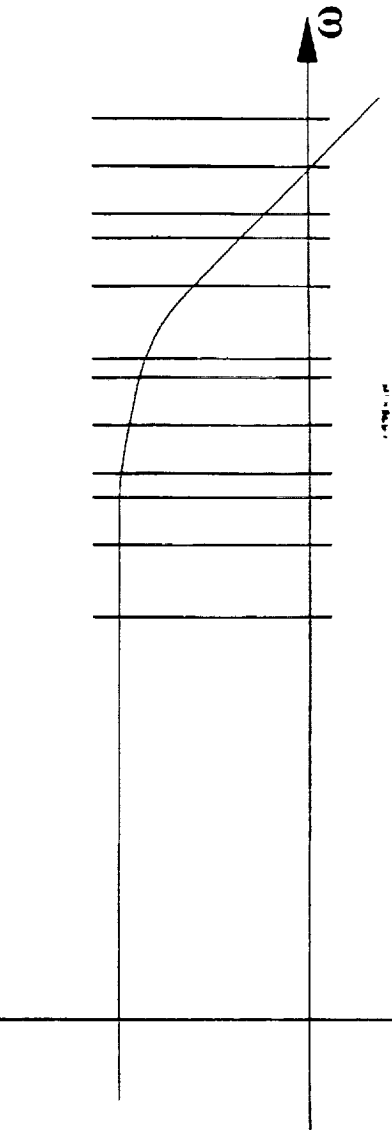
Need for Simultaneous Design

Past Designs

Control Bandwidth



Current Designs

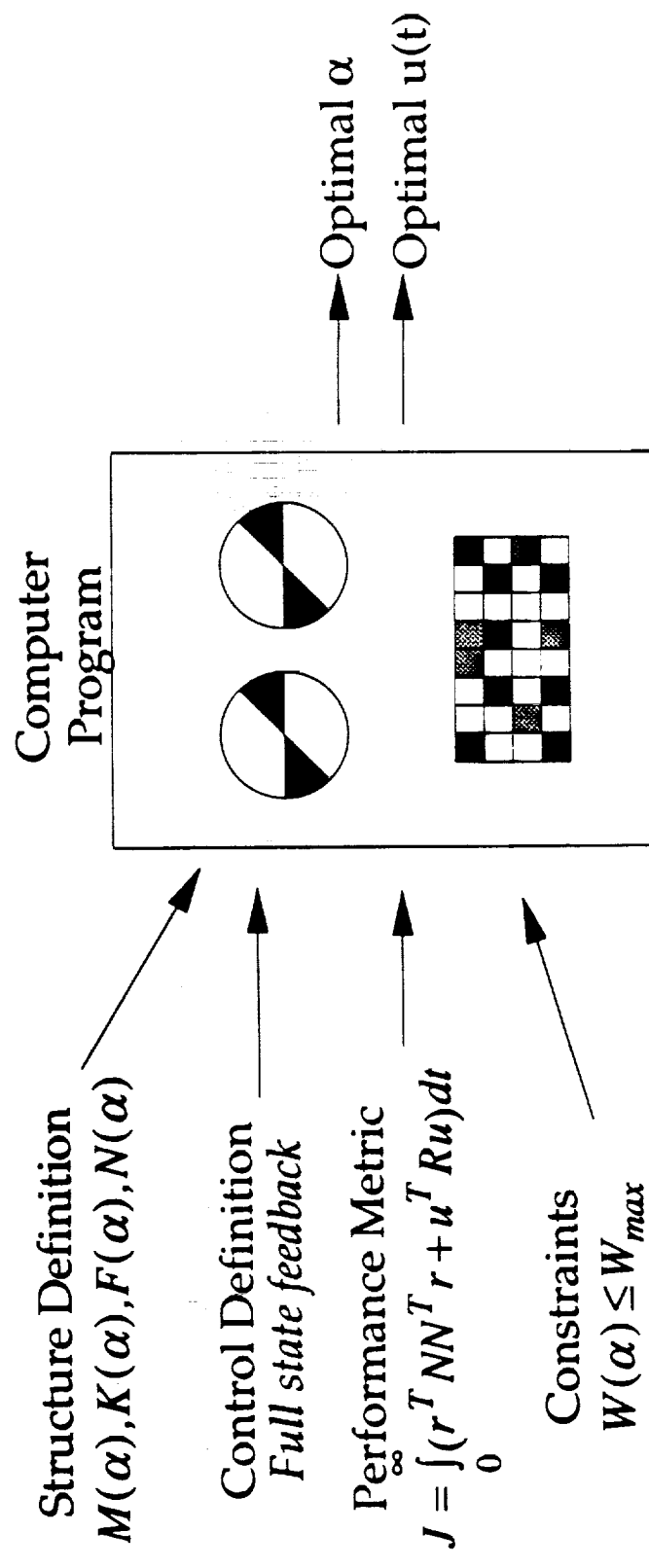


NUMERIC CONTROL/STRUCTURE OPTIMIZATION

ONE APPROACH TO THIS PROBLEM RELIES ON THE INTENSIVE USE OF NUMERIC OPTIMIZATION. THE ENGINEER FIRST THE STRUCTURAL DESIGN OF THE SPACECRAFT BY SPECIFYING CERTAIN QUANTITIES IN THE STRUCTURAL DESIGN (E.G. DIAMETERS OF MEMBERS IN A SPACE TRUSS). A CONTROL ARCHITECTURE IS SPECIFIED, BUT THE CONTROL GAINS ARE LEFT UNDETERMINED. FINALLY, THE ENGINEER SUPPLIES SOME MEASURE OF DYNAMIC PERFORMANCE AS WELL AS DESIGN CONSTRAINTS (E.G. A LIMIT ON THE TOTAL MASS). ALL OF THIS IS FED INTO A COMPUTER PROGRAM WHICH SEARCHES FOR A COMBINATION OF STRUCTURAL PARAMETERS AND CONTROL GAINS WHICH OPTIMIZES THE PERFORMANCE METRIC WHILE AT THE SAME TIME MEETING THE CONSTRAINTS.



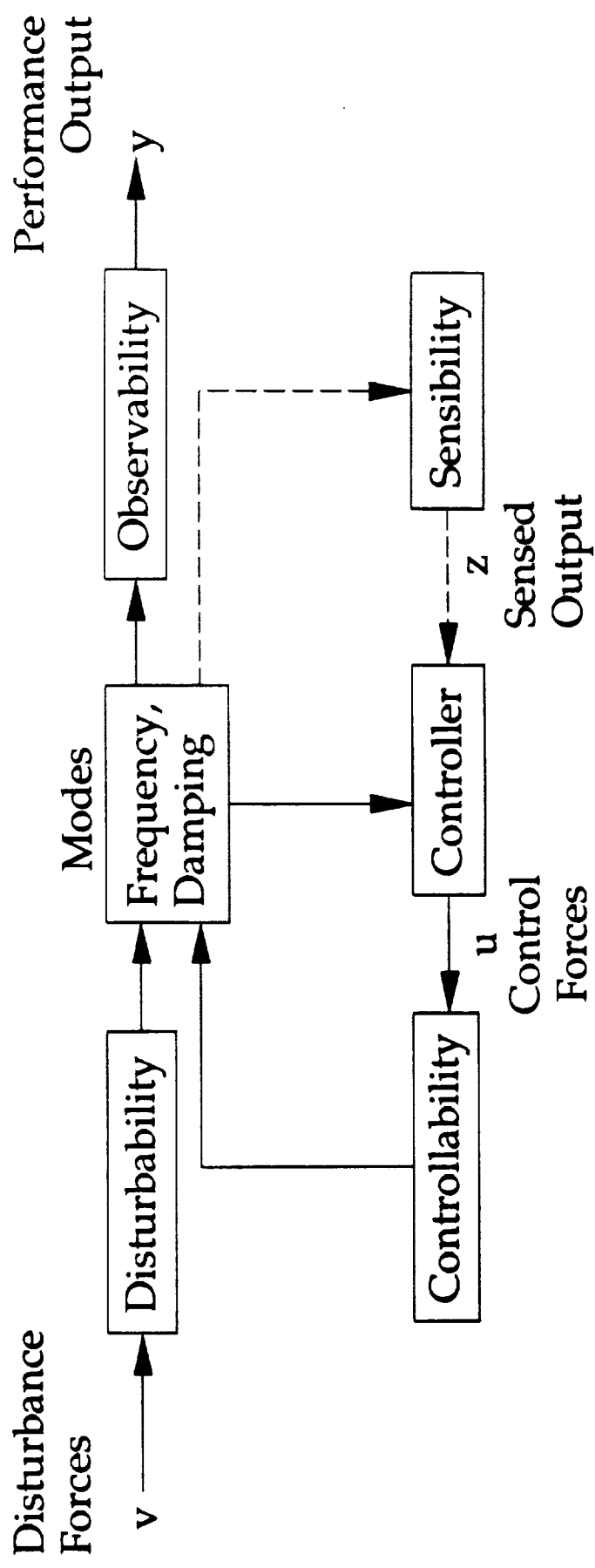
Numeric Control/Structure Optimization



APPROACHES TO CONTROLLED STRUCTURE DESIGN

WHILE NUMERIC OPTIMIZATION WILL YIELD THE BEST SOLUTION FOR THE DEFINED PROBLEM, IT DOES NOT GIVE MUCH INSIGHT INTO THE PROBLEM ITSELF. THIS INSIGHT IS CRUCIAL FOR CONTROLLED STRUCTURE DESIGN. EVEN IN SYSTEMS WHERE THE ULTIMATE DESIGN WILL BE DETERMINED THROUGH OPTIMIZATION, INSIGHT IS NECESSARY IN PROPERLY DEFINING THE OPTIMIZATION PROBLEM. ONE CAN THINK OF FIVE BASIC WAYS THAT AN ALTERATION TO A STRUCTURE CAN CHANGE ITS DYNAMIC PERFORMANCE. FIRST, IT CAN ALTER HOW THE DISTURBANCES INFLUENCE THE DYNAMICS (DISTURBABILITY). SECOND, IT CAN ALTER HOW THE DYNAMICS APPEAR IN THE DYNAMIC PERFORMANCE METRIC (OBSERVABILITY). THIRD IT CAN AFFECT HOW THE CONTROLLER ACTS ON THE STRUCTURE (CONTROLLABILITY). FOURTH, IT CAN CHANGE THE FREQUENCY AND DAMPING RATIOS OF THE MODES OF THE STRUCTURE. AND FINALLY, IT CAN CHANGE HOW WELL THE SENSORS CAN MEASURE THE DYNAMICS OF THE STRUCTURE (SENSIBILITY). HOWEVER, FOR THE REST OF THIS DISCUSSION, ONLY FULL STATE FEEDBACK CONTROLLERS WILL BE CONSIDERED AND SENSIBILITY WILL BE IGNORED. IT SHOULD BE MENTIONED AT THIS POINT THAT CHANGING A STRUCTURE ALSO AFFECTS THE ROBUSTNESS OF THE CONTROLLERS TO MODELLING ERRORS, HOWEVER THIS WILL ONLY BE TOUCHED UPON BRIEFLY.

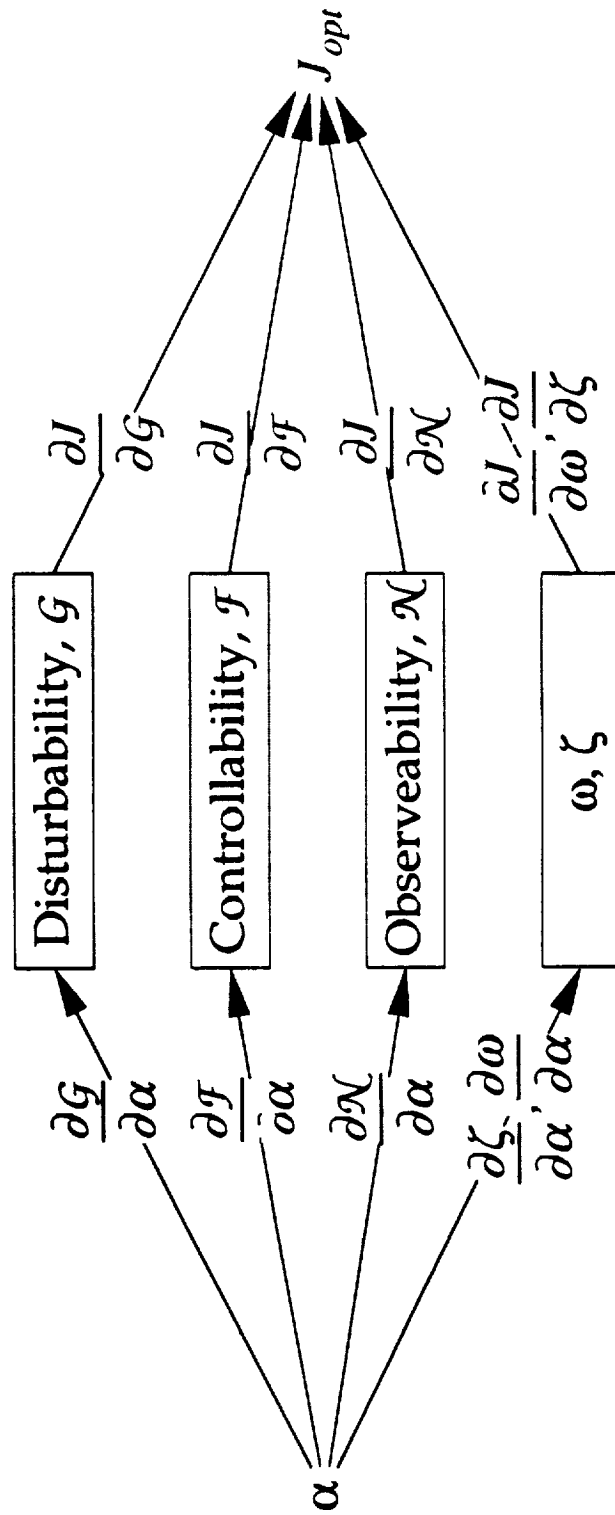
Approaches to Controlled Structure Design



RELATIONSHIP BETWEEN DESIGN PARAMETERS AND OPTIMAL CONTROL COST

IT IS USEFUL TO ENVISION AN ALTERATION IN THE STRUCTURE AS HAVING TWO STAGES OF EFFECTS ON THE OPTIMALLY CONTROLLED PERFORMANCE. FIRST, THE CHANGE IN THE STRUCTURE CHANGES ITS DISTURBABILITY, CONTROLLABILITY, OBSERVABILITY, FREQUENCIES AND DAMPING. FOR CLARITY, THESE QUANTITIES WILL BE CALLED MODAL PROPERTIES. SECONDLY, THE CHANGE IN THE MODAL PROPERTIES HAS AN EFFECT ON THE CLOSED LOOP PERFORMANCE. IT IS THIS LAST EFFECT WHICH WILL BE EXPLORED HERE. THIS ANALYSIS WILL SHOW WHICH MODAL PROPERTIES ARE THE MOST IMPORTANT UNDER WHICH CONDITIONS.

Relationship Between Design Parameters and Optimal Control Cost



PRELIMINARIES

ANY LINEAR STRUCTURE CAN BE DESCRIBED BY THE TOP EQUATION. A MORE USEFUL FORM IS THE MODAL STATE SPACE FORM SHOWN BELOW. THE STATE VECTOR BECOMES MODAL DISPLACEMENT AND FREQUENCY NORMALIZED MODAL VELOCITIES INSTEAD OF PHYSICAL DISPLACEMENTS AND VELOCITIES. A USEFUL FEATURE OF THE MODAL FORM IS THAT EACH OF THE MATRICES CORRESPONDS EXACTLY TO A DIFFERENT MODAL PROPERTY.

Preliminaries

Equation of Motion

$$M(\alpha)\ddot{r}(t) + D(\alpha)\dot{r}(t) + K(\alpha)r(t) = F(\alpha)u(t) + G(\alpha)v(t)$$

$$y(t) = N(\alpha)r(t)$$

Modal State Space Form

$$\frac{d}{dt} \begin{bmatrix} q \\ q' \end{bmatrix} = \begin{bmatrix} 0 & \omega \\ -\omega & -2\zeta\omega \end{bmatrix} \begin{bmatrix} q \\ q' \end{bmatrix} + \begin{bmatrix} 0 \\ \omega^{-1}\Phi^T F \end{bmatrix} u + \begin{bmatrix} 0 \\ \omega^{-1}\Phi^T G \end{bmatrix} v$$
$$y = [N\Phi \quad 0] \begin{bmatrix} q \\ q' \end{bmatrix}$$

where

$$r = \Phi q \quad q' = \omega^{-1}q \quad \Phi^T M \Phi = I \quad \Phi^T K \Phi = \omega^2 \quad \Phi^T D \Phi \approx 2\zeta\omega$$

DEFINITIONS

USING THESE MATRICES AS A GUIDE, ONE CAN ASSIGN MATHEMATICAL DEFINITIONS TO EACH OF THE MODAL PROPERTIES. NOTE THAT THERE ARE TWO DIFFERENT DEFINITIONS FOR DISTURBABILITY. ONE WHERE THE DISTURBANCE IS RECOVERY FROM A DISPLACEMENT DUE TO A STATIC FORCE (DISPLACEMENT DISTURBANCE) AND ONE WHERE THE DISTURBANCE IS RECOVERY FROM AN IMPULSIVE FORCE (VELOCITY DISTURBANCE). THE DIFFERING FREQUENCY DEPENDENCIES IN THESE TWO DEFINITIONS REFLECTS THE DIFFERENT IMPORTANCE OF STIFFNESS IN REJECTING THESE TWO TYPES OF DISTURBANCES.

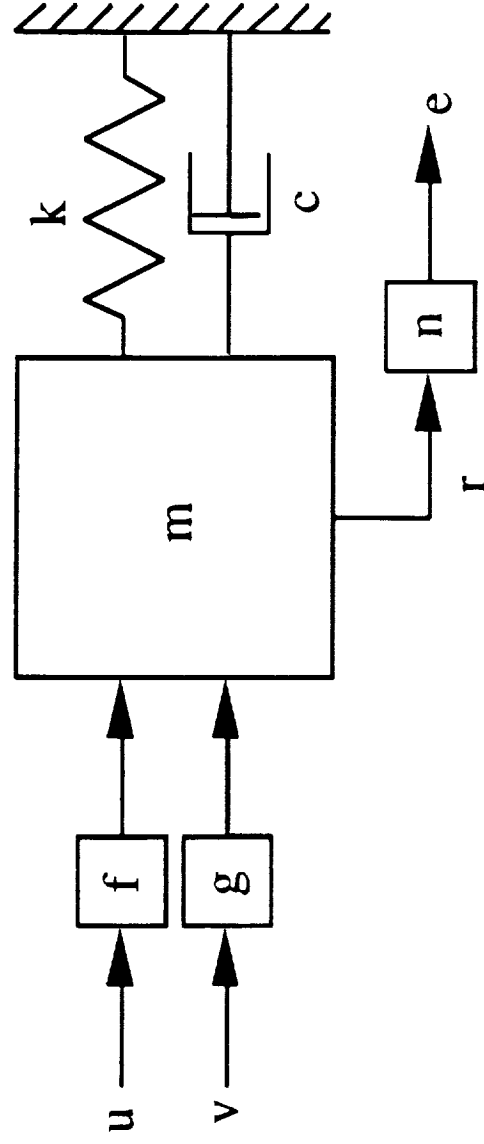
Definitions

Frequency	ω
Damping	ζ
Controllability	$\mathcal{T} = \omega^{-1} \Phi^T F$
Disturbability	$\mathcal{G}_d = \omega^{-2} \Phi^T G \quad \mathcal{G}_v = \omega^{-1} \Phi^T G$
Observability	$\mathcal{N} = N\Phi$

SINGLE MASS TYPICAL SECTION

IN ORDER TO BETTER UNDERSTAND THE INTERACTION OF THESE QUANTITIES IN DETERMINING DYNAMIC PERFORMANCE, IT IS USEFUL TO CONSIDER THIS SIMPLE SYSTEM. IN THIS CASE EACH OF THE MATRICES FOR MODAL PROPERTIES BECOMES A SINGLE SCALAR. A FURTHER ADVANTAGE IS THAT FOR THE PERFORMANCE METRICS CONSIDERED HERE, THE SOLUTIONS CAN BE PRESENTED IN CLOSED FORM, THUS MAKING THE FUNCTIONAL DEPENDENCE OF THE DYNAMIC PERFORMANCE ON THESE QUANTITIES MORE APPARENT.

Single Mass Typical Section



$$\omega = \sqrt{\frac{k}{m}} \quad \zeta = \frac{c}{2m\omega} \quad \mathcal{F} = \frac{f}{\omega} \quad \mathcal{G}_v = \frac{g}{\omega} \quad \mathcal{G}_d = \frac{g}{\omega^2} \quad \mathcal{N} = n$$

$$\dot{x} = Ax + Bu + Lv \quad y = Cx$$

$$x = \begin{bmatrix} q \\ q' \end{bmatrix} \quad A = \begin{bmatrix} 0 & \omega \\ -\omega & -2\zeta\omega \end{bmatrix} \quad B = \begin{bmatrix} 0 \\ \mathcal{F} \end{bmatrix} \quad L = \begin{bmatrix} 0 \\ \mathcal{G} \end{bmatrix} \quad C = [\mathcal{N} \quad 0]$$

OPTIMAL H₂ PERFORMANCE METRIC

A COMMONLY USED MEASURE OF DYNAMIC PERFORMANCE IS THE H₂ METRIC SHOWN. THE DISTURBANCE IS CHARACTERIZED AS THE EXPECTED VALUE OF THE OUTER PRODUCT OF THE INITIAL STATE. IT IS A WELL KNOWN RESULT OF MODERN CONTROL THEORY THAT THE PERFORMANCE OF THE OPTIMALLY CONTROLLED SYSTEM IS GIVEN BY THE EXPRESSIONS SHOWN.

Optimal H₂ Performance

Performance Metric

$$J = E \left[\int_0^{\infty} (y^2(t) + \rho u^2(t)) dt \right]$$

Disturbance Characterization

$$\begin{aligned} S = E[x(0)x^T(0)] &= \begin{bmatrix} G_d^2 V & 0 \\ 0 & 0 \end{bmatrix} \quad \text{Displacement} \\ &= \begin{bmatrix} 0 & 0 \\ 0 & G_v^2 V \end{bmatrix} \quad \text{Velocity} \end{aligned}$$
$$E[v^2] = V$$

Performance for Optimal Control

$$J = \text{tr}\{PS\}$$

where

$$PA + A^T P + C^T C - \frac{1}{\rho^2} PBB^T P = 0 \quad P = P^T > 0$$

CLOSED FORM SOLUTION

THIS EQUATION CAN BE SOLVED IN CLOSED FORM FOR THIS SIMPLE SYSTEM TO YIELD THE EXPRESSIONS SHOWN. NOTICE THE COST FOR BOTH TYPES OF DISTURBANCES HAS TWO COMPONENTS. THE FIRST IS A SCALING FACTOR THAT REFLECTS THE TRANSMISSION OF THE DISTURBANCE TO THE OUTPUT, WHILE THE SECOND REPRESENTS THE ATTENUATION OF THAT TRANSMISSION THROUGH THE APPLICATION OF DAMPING AND CONTROL.

Closed Form Solution

- Control influence parameter

$$\beta = \left| \frac{\mathcal{N}f}{\omega\rho} \right|$$

- Displacement Disturbance

$$J_{opt} = \frac{V G_d^2 \mathcal{N}^2}{\omega} \frac{1}{\beta^2} \left(\sqrt{\beta^2 + 1} \sqrt{4\zeta^2 + 2\sqrt{\beta^2 + 1} - 2} - 2\zeta \right)$$

- Velocity Disturbance

$$J_{opt} = \frac{V G_v^2 \mathcal{N}^2}{\omega} \frac{1}{\beta^2} \left(\sqrt{4\zeta^2 + 2\sqrt{\beta^2 + 1} - 2} - 2\zeta \right)$$

ASYMPTOTIC BEHAVIOR OF COST

MORE INSIGHT CAN BE GAINED BY CONSIDERING HOW THIS COST BEHAVES FOR LIMITING VALUES OF DAMPING AND CONTROL AUTHORITY. NOTICE THAT FOR LARGE VALUES OF DAMPING THE CONTROL INFLUENCE DROPS OUT WHILE FOR SMALL VALUES OF DAMPING, THE DAMPING RATIO DROPS OUT. THIS REFLECTS THE FACT THAT ONE IS ESSENTIALLY TRYING TO USE DAMPING AND CONTROL TO ACCOMPLISH THE SAME THING AND WHICHEVER ONE IS MORE AVAILABLE IS GOING TO THE MOST USEFUL. THIS IMPLIES THAT IF CONTROL IS GOING TO BE USED TO IMPROVE PERFORMANCE DIRECTLY, DAMPING SHOULD BE USED FOR SOMETHING ELSE, SUCH AS IMPROVING PERFORMANCE OF UNCONTROLLED MODES OR ADDING ROBUSTNESS TO THE CONTROL DESIGN. FOR LIGHTLY DAMPED SYSTEMS ONE OBTAINS TWO DIFFERENT BEHAVIORS OF THE COST DEPENDING ON THE LEVEL OF CONTROL. FOR LIGHT CONTROL LEVELS, THE COST IS INDEPENDENT OF THE CONTROL TYPE WHILE AT HIGHER CONTROL LEVELS, THE WEIGHTING ON CONTROL INCREASES FOR THE VELOCITY DISTURBANCE AND DECREASES FOR THE DISPLACEMENT DISTURBANCE.



Asymptotic Behavior of Cost

- Open loop or heavy damping
Velocity Disturbance
$$J_{opt} = \frac{V\mathcal{G}_d^2\mathcal{N}^2}{\omega} \frac{1}{4\zeta}$$
- Expensive Control, Light Damping
Velocity Disturbance
$$J_{opt} = \frac{V\mathcal{G}_d^2\mathcal{N}^2}{\omega} \frac{1}{\beta}$$

Displacement Disturbance

$$J_{opt} = \frac{V\mathcal{G}_v^2\mathcal{N}^2}{\omega} \left(\frac{1}{4\zeta} + \zeta \right)$$

- Cheap Control, Light Damping

Velocity Disturbance

$$J_{opt} = \frac{V\mathcal{G}_v^2\mathcal{N}^2}{\omega} \frac{1}{\beta}$$

Displacement Disturbance

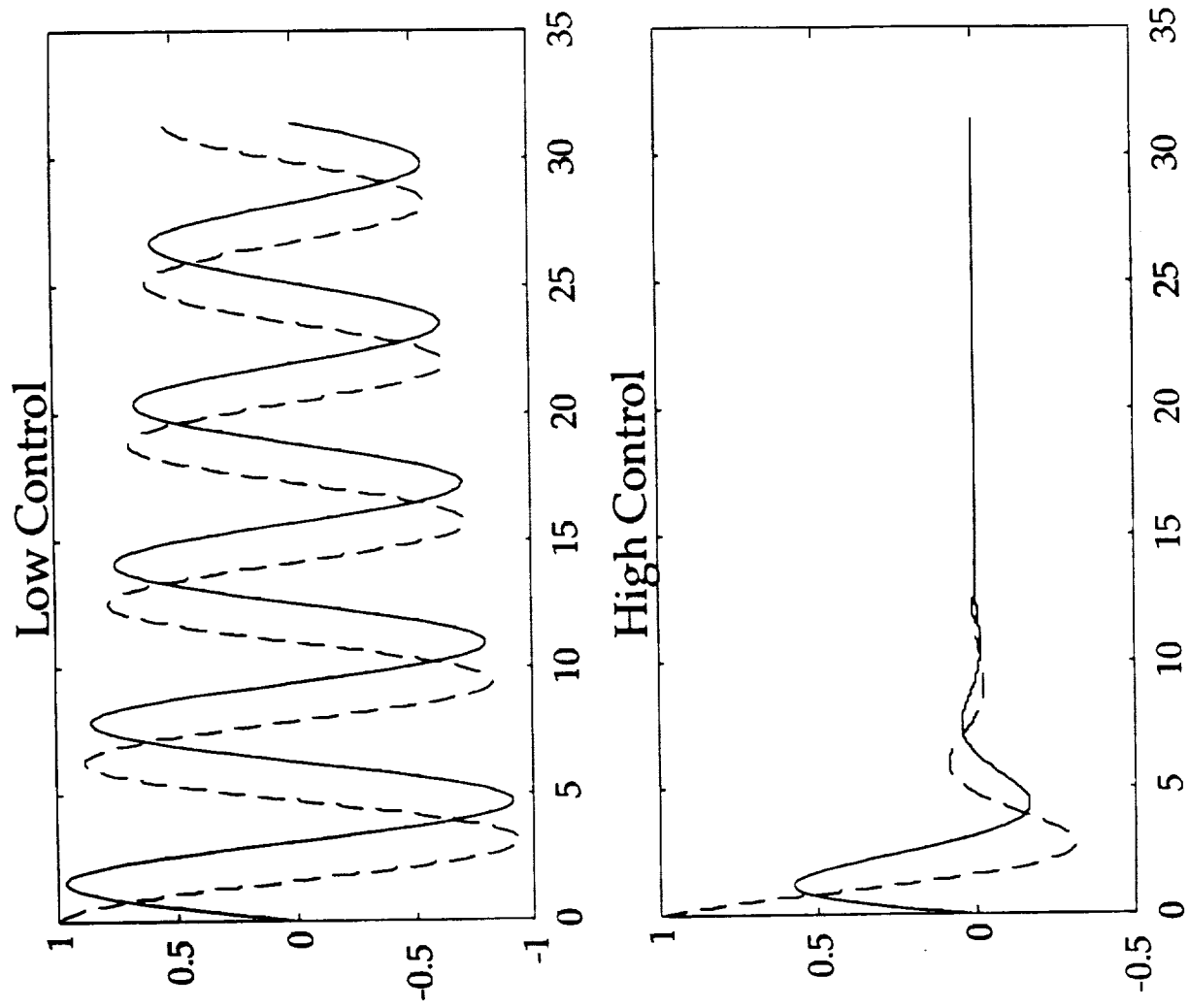
$$J_{opt} = \frac{V\mathcal{G}_v^2\mathcal{N}^2}{\omega} \frac{1}{\beta}$$

$$J_{opt} = \frac{V\mathcal{G}_v^2\mathcal{N}^2}{\omega} \sqrt{\frac{2}{\beta^3}} = \frac{V\mathcal{G}_v^2 \sqrt{2|\mathcal{N}|} \rho^3 \omega}{\sqrt{|\mathcal{F}|^3}}$$

DIFFERENCES BETWEEN CONTROL LEVELS

THESE DIFFERENCES CAN BE UNDERSTOOD BY LOOKING AT THE RESPONSES FOR A TYPICAL LIGHTLY CONTROLLED AND HEAVILY CONTROLLED SYSTEM. NOTICE THAT FOR THE LIGHTLY CONTROLLED SYSTEM, THE PHASE DIFFERENCE INDUCED BY THE TWO DIFFERENT DISTURBANCE TYPES HAS LITTLE EFFECT. THE PERFORMANCE IS DETERMINED BY THE TIME CONSTANT OF THE DECAY ENVELOPE. FOR THE HEAVILY CONTROLLED PLANT HOWEVER, IT CAN BE SEEN THAT THE COST IS DOMINATED BY THE AMPLITUDE OF THE FIRST OSCILLATION OF THE SYSTEM. NOTICE THAT THE ADDITION OF CONTROL MAKES IT POSSIBLE TO DECREASE THIS PEAK FOR THE VELOCITY DISTURBANCE BUT NOT FOR THE DISPLACEMENT DISTURBANCE. THIS PRODUCES THE DIFFERENT WEIGHTING ON CONTROL NOTED BEFORE.

Differences Between Control Levels



OPTIMAL H_{∞} PERFORMANCE

ANOTHER COMMONLY USED PERFORMANCE METRIC IS THE H_{∞} METRIC SHOWN. IN THIS FORMULATION THIS DISTURBANCE IS A WHITE NOISE FORCE ACTING ON THE DISTURBANCE INPUTS. THE OPTIMAL CONTROL SOLUTION FOR THIS PROBLEM CAN BE OBTAINED BY SOLVING THE RELATIONS SHOWN.

Optimal H_∞ Performance

Performance Metric

$$J = \sup_{\omega} (|y(j\omega)|^2 + \rho^2 |u(j\omega)|^2)$$

Disturbance Characterization

$$E[v(t)v(\tau)] = \delta(t - \tau)$$

Performance for Optimal Full State Feedback

$$PA + A^T P + C^T C - P \left(\frac{1}{\rho^2} BB^T - \frac{1}{\gamma^2} LL^T \right) P = 0$$

$$\gamma \geq \gamma_{min} \Leftrightarrow P = P^T > 0$$

$$J_{opt} = \gamma_{min}^2$$

CLOSED FORM SOLUTION

AGAIN, IT IS POSSIBLE TO SOLVE FOR THE OPTIMALLY CONTROLLED PERFORMANCE IN CLOSED FORM. NOTICE, THAT IF ONE IGNORES DISTURBABILITY IN THIS PROBLEM, THEN THE OPTIMAL OPEN AND CLOSED LOOP DESIGNS COINCIDE. THIS IMPLIES THAT A SEQUENTIAL DESIGN (WHERE THE STRUCTURAL DESIGN PRECEDES THE CONTROL DESIGN) WILL YIELD JUST AS GOOD A DESIGN AS SIMULTANEOUS OPTIMIZATION. IT IS NOT UNCOMMON FOR SITUATIONS TO OCCUR IN WHICH THE DISTURBABILITY CAN BE IGNORED. OFTEN, IN PROBLEMS WHERE THE DISTURBANCE IS HIGHLY DISTRIBUTED OR POORLY KNOWN, THE DISTURBABILITY IS VERY INSENSITIVE TO STRUCTURAL CHANGES AND HENCE CAN BE IGNORED. THEREFORE, THERE IS AT LEAST ONE CLASS OF PROBLEMS WHERE SIMULTANEOUS DESIGN MAY NOT BE NECESSARY.

Closed Form Solution

Closed Loop

$$J_{opl} = \begin{cases} G^2 \left(\frac{\mathcal{F}^2}{\rho^2} + \frac{\omega^2}{\mathcal{N}^2} 4\zeta^2 (1 - \zeta^2) \right)^{-1} & \zeta \leq \frac{1}{\sqrt{2}} \\ G^2 \left(\frac{\mathcal{F}^2}{\rho^2} + \frac{\omega^2}{\mathcal{N}^2} \right)^{-1} & \zeta \geq \frac{1}{\sqrt{2}} \end{cases}$$

Open Loop

$$J_{ol} = \begin{cases} G^2 \left(\frac{\omega^2}{\mathcal{N}^2} 4\zeta^2 (1 - \zeta^2) \right)^{-1} & \zeta \leq \frac{1}{\sqrt{2}} \\ G^2 \left(\frac{\omega^2}{\mathcal{N}^2} \right)^{-1} & \zeta \geq \frac{1}{\sqrt{2}} \end{cases}$$

EFFECTS OF SEVERAL MODES

THE TYPICAL SECTION PROBLEM DISCUSSED SO FAR HAD BUT A SINGLE MODE. IT IS USEFUL TO CONSIDER WHAT HAPPENS WHEN MORE MODES ARE PRESENT. UNFORTUNATELY, THE PRESENCE OF MORE MODES PREVENTS THE ATTAINMENT OF CLOSED FORM SOLUTIONS SO IT IS USEFUL TO CONSIDER A NUMERIC PROBLEM. FIRST, WHEN THE SYSTEM IS DESCRIBED IN THE MODAL STATE SPACE FORM DESCRIBED ABOVE, IT IS POSSIBLE TO BREAK THE GRADIENT UP INTO SEVERAL COMPONENTS. EACH OF THESE REPRESENTS THE EFFECT THAT CHANGING A STRUCTURAL PARAMETER WOULD HAVE IF ONLY ONE OF THE MODAL PROPERTIES WERE AFFECTED AT A TIME. THESE QUANTITIES ARE COMPUTED FOR THE BEAM PROBLEM SHOWN ON THE NEXT VIEWGRAPH. THE PERFORMANCE METRIC USED HERE IS THE H₂ METRIC ALREADY USED ON THE SINGLE MASS TYPICAL SECTION. THE NOMINAL DESIGN FOR THIS SYSTEM IS A UNIFORM THICKNESS, (1 CM) WITH THE LUMPED MASSES SET TO ZERO.

Effects of Several Modes

- Gradient of cost with respect to design variables

$$\frac{\partial J_{opt}}{\partial \alpha} = \text{tr} \left\{ P \frac{\partial S}{\partial \alpha} + H \left(P \frac{\partial A}{\partial \alpha} + \frac{\partial A^T}{\partial \alpha} P + \frac{\partial}{\partial \alpha} (C^T C) + P \frac{\partial}{\partial \alpha} (B R^{-1} B^T) P \right) \right\}$$

$$\text{where } H \left(A - B R^{-1} B^T P \right)^T + \left(A - B R^{-1} B^T P \right) H + S = 0$$

- Definition of subgradients

Frequency

$$\delta J_{fre} = \text{tr} \left\{ H \left(P \frac{\partial A}{\partial \alpha} + \frac{\partial A^T}{\partial \alpha} P \right) \right\}$$

Observability

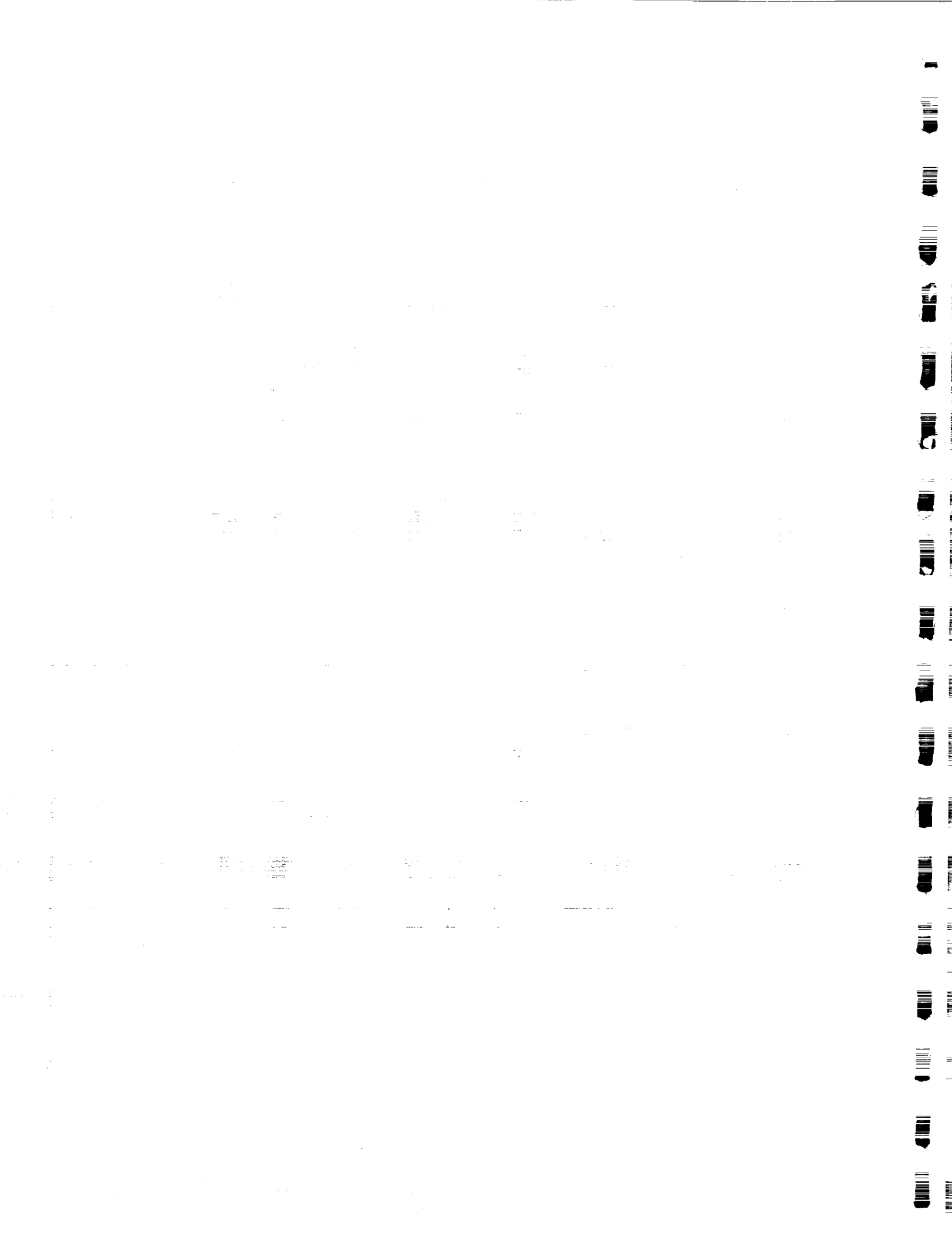
$$\delta J_{obs} = \text{tr} \left\{ H \frac{\partial}{\partial \alpha} (C^T C) \right\}$$

Disturbability

$$\delta J_{dis} = \text{tr} \left\{ P \frac{\partial S}{\partial \alpha} \right\}$$

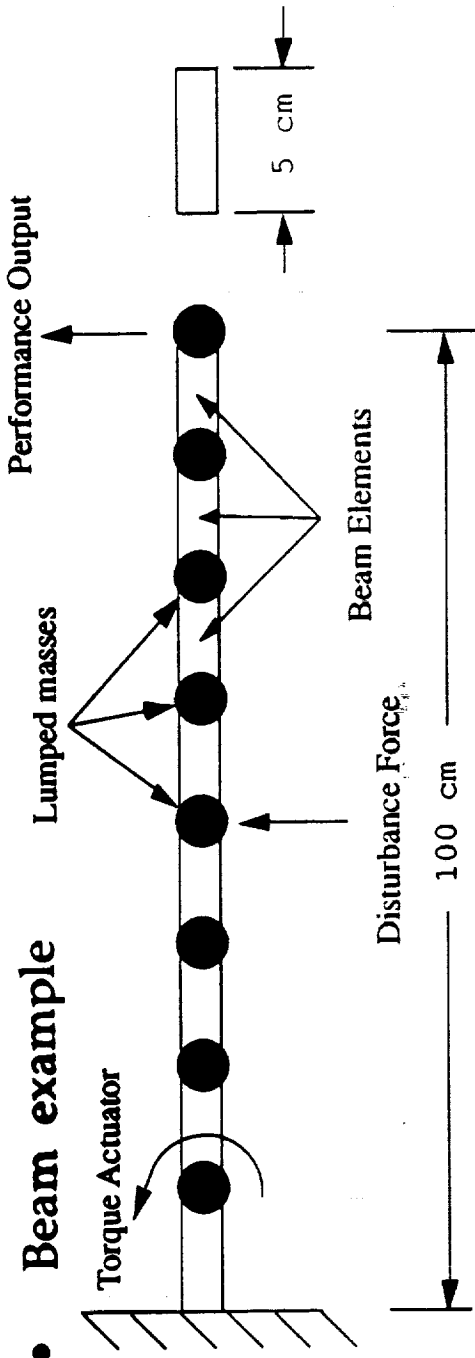
Controllability

$$\delta J_{con} = -\text{tr} \left\{ H P \frac{\partial}{\partial \alpha} (B R^{-1} B^T) P \right\}$$



Effects of Several Modes (cont)

- Beam example



- Properties

- Bernoulli-Euler aluminum beam (eight finite elements)
- Performance metric: Tip displacement
- Actuator: Torque applied near root
- Disturbance: Transverse force at midspan
- Design variables: Element thicknesses and lumped mass values
- Mass constraint: Mass must be less than or equal to that of a uniform beam of 1cm thickness with no lumped mass (nominal)

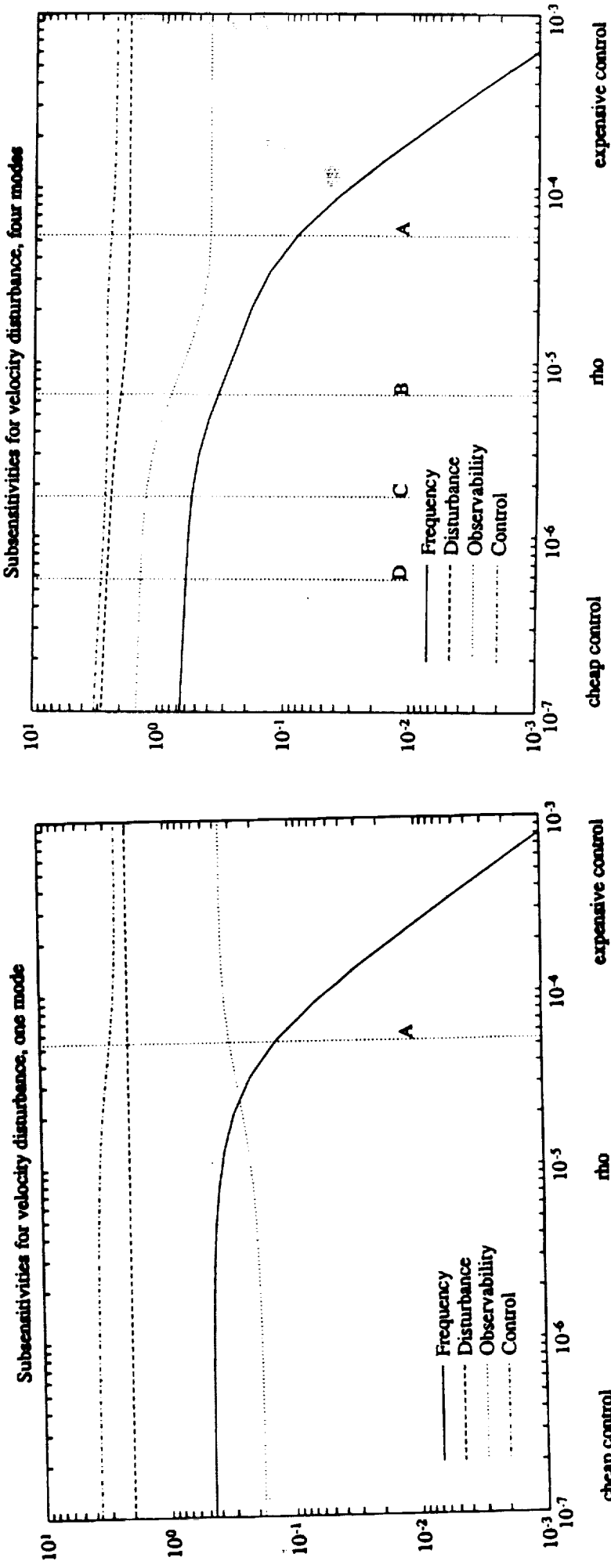
NORMALIZED SUBGRADIENTS VS. CONTROL PENALTY FOR NOMINAL DESIGN

THESE GRAPHS DEPICT THE SIZE OF THE SUBGRADIENTS (NORMALIZED BY FUNCTION VALUE) FOR DIFFERENT LEVELS OF CONTROL PENALTY. THE PLOT ON THE RIGHT REPRESENTS AN ANALYSIS WHERE THE BEAM IS CONSIDERED TO HAVE ONLY A SINGLE MODE AND IS THEREFORE IDENTICAL TO THE RESULT OBTAINED FOR THE SINGLE MASS TYPICAL SECTION. THE PLOT ON THE RIGHT SHOWS THE RESULT OF AN ANALYSIS WHERE THE BEAM IS CONSIDERED TO HAVE FOUR MODES. THE LEFT SIDES OF THE PLOTS REPRESENT HIGH CONTROL WHILE THE RIGHT SIDES REFLECT THE EFFECT OF LOW CONTROL. NOTICE THAT FOR LOW LEVELS OF CONTROL, THE PLOTS ARE VIRTUALLY IDENTICAL, BUT AT HIGHER LEVELS, THE FOUR MODE MODEL IS SHOWING A MARKED DECREASE IN THE SENSITIVITY TO CONTROLLABILITY AND AN INCREASE IN THE SENSITIVITY TO DISTURBABILITY AND CONTROLLABILITY. THIS IS DUE TO THE FACT THAT THERE ARE MORE MODES THAN ACTUATORS. AT LOW LEVELS OF CONTROL, THE CONTROLLER IS PROVIDING ACTIVE DAMPING TO ALL MODES. THIS VELOCITY FEEDBACK IS SIMILAR FOR ALL MODES AND IT IS POSSIBLE TO IMPLEMENT CLOSE TO OPTIMUM CONTROL FOR EACH MODE. AT HIGHER CONTROL LEVELS, HOWEVER, ACTIVE DAMPING GIVES WAY TO SHAPE CONTROL WHICH CAN BE MARKEDLY DIFFERENT FOR EACH MODE. THIS MEANS THAT OPTIMAL CONTROL CANNOT BE GIVEN TO EACH MODE SIMULTANEOUSLY AND THE CONTROL USED MUST NOT BE AS EFFECTIVE AS IT WAS IN THE SINGLE MODE CASE. THE NET EFFECT IS THAT THE IMPORTANCE OF CONTROL IS LOWER THAN EXPECTED WHILE DISTURBABILITY AND OBSERVABILITY BECOME MORE IMPORTANT.

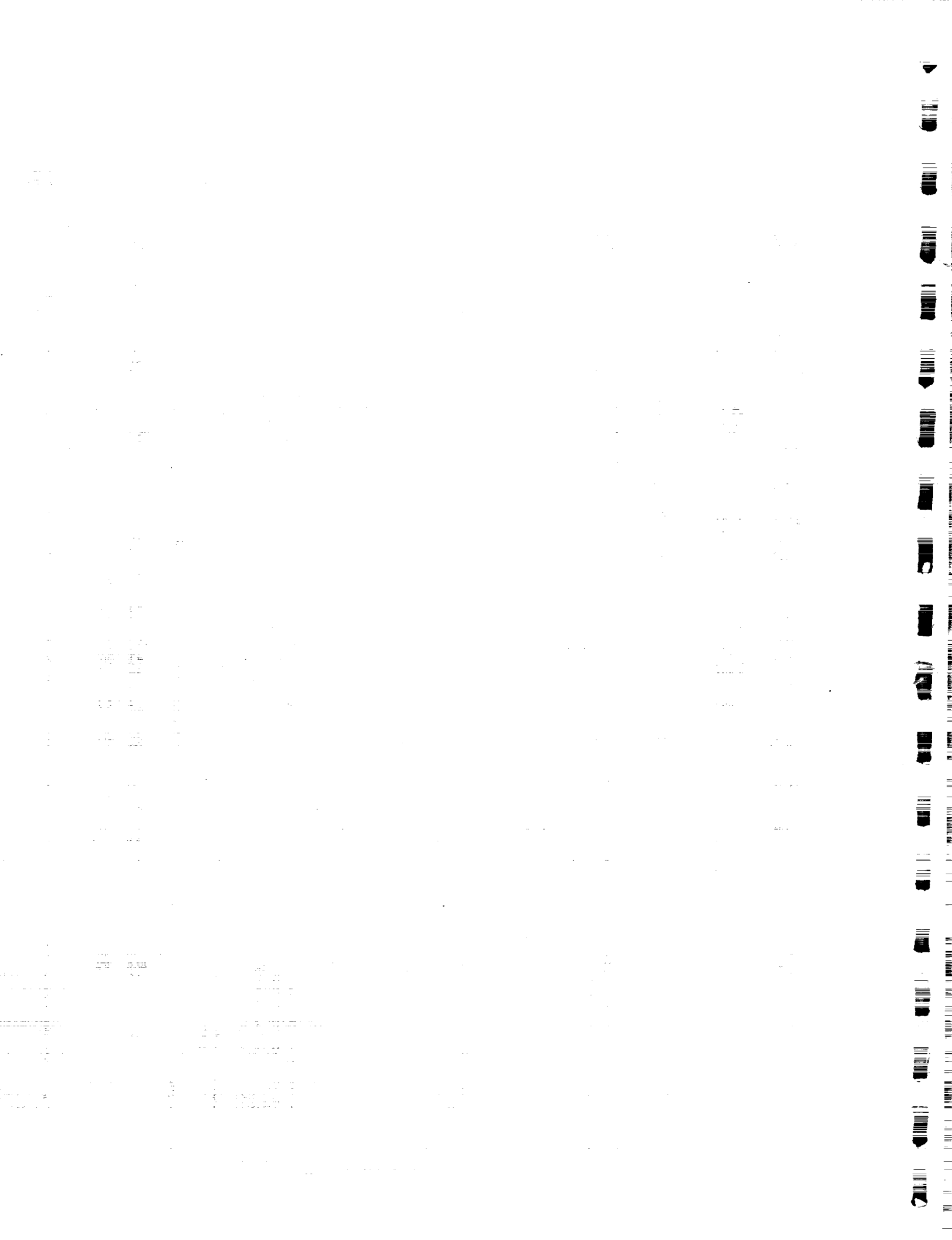
Normalized Subgradients VS. Control Penalty for Nominal Design

One mode Model

Four mode model

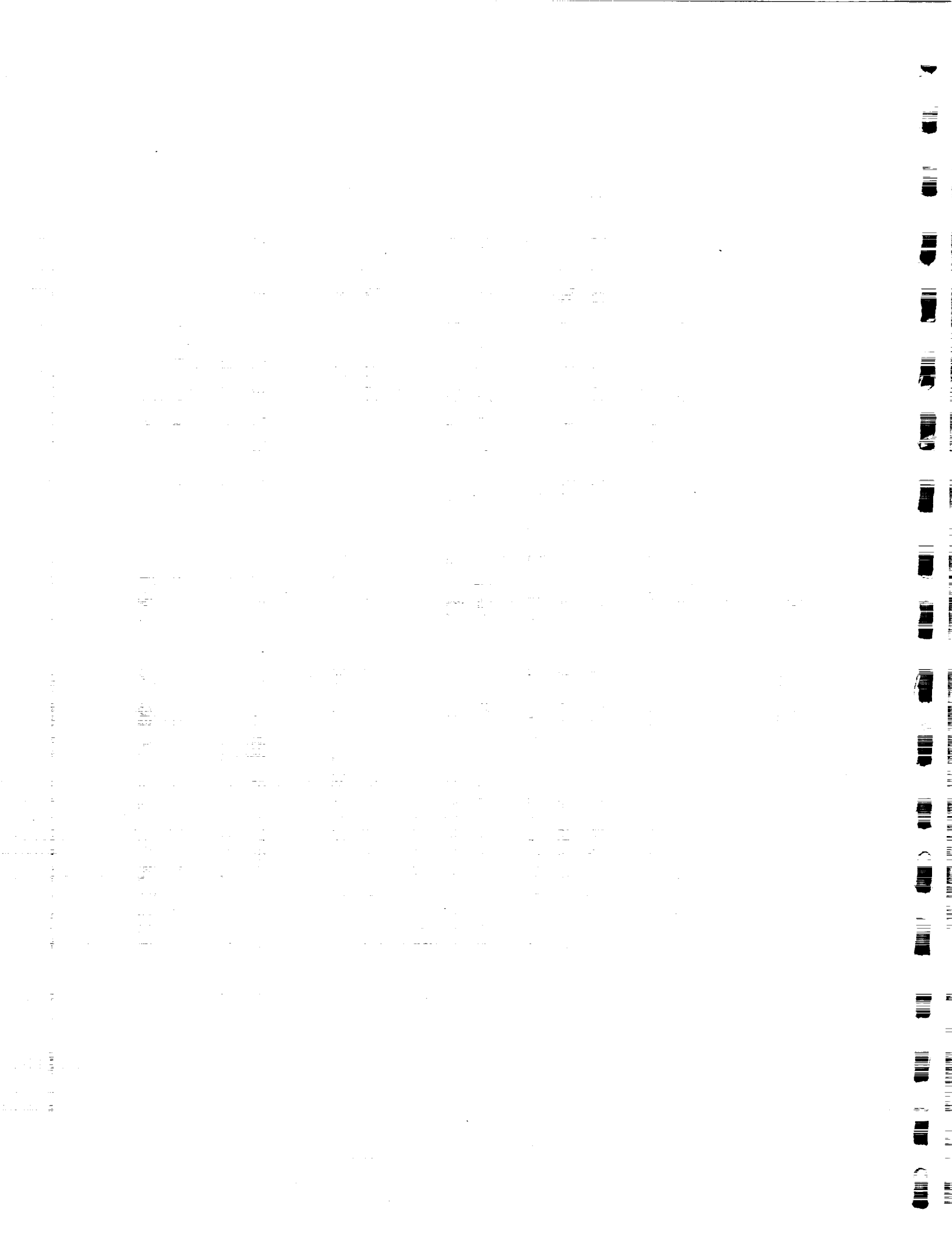


- More actuators than modes reduces importance of control influence parameter, β , at high levels of control



Conclusions

- It has been demonstrated that the typical section can yield useful insights into the simultaneous optimization of structures and control
- Damping should be used to improve performance of uncontrolled modes or to add robustness in controlled modes. It should not be used to improve performance in controlled modes directly
- At low control levels, actuators will provide active damping and the behavior of the performance for velocity and displacement disturbances will be identical.
- At higher control levels, the behavior of the performance will depend on the type of disturbance. In particular, velocity disturbance favor control more.
- For H_∞ problems, sequential design of structure and control might yield optimal design if performance is insensitive to disturbances
- In systems where there are more modes than actuators, the effectiveness of control at higher control levels will be diminished.





MIT
Space
Engineering
Research
Center

A Stochastic Approach to Robust Broadband Structural Control

Douglas G. MacMartin
Steven R. Hall

January 22, 1992

Goal

The goal of this research is to develop control methodologies for designing broadband active control systems for uncertain structures. In order to control many modes of such a structure, collocated feedback is required. For noncollocated sensors and actuators, there is almost no phase information about the transfer function in the modally dense regime, and therefore, nothing can be done to control the structure. However, using collocated and dual feedback, one can take advantage of the fact that the structure is positive real, and, hence, that any positive real compensator will not destabilize the structure. The resulting controllers are low-authority, and can be thought of as adding "active damping."

The approach taken here is to use a statistical model of the local dynamics near the sensor/actuator pair, rather than trying to develop a model that contains accurate information about every mode of the structure. Because the model only contains local information, it is robust to uncertainties elsewhere in the structure. Control design for this model is based on maximizing the power dissipated by the controller. This is equivalent to an impedance matching problem. In general, a noncausal compensator is required in order to match the impedance exactly at every frequency. Instead, the control design must find an optimal, causal approximation to this compensator.

Finally, experimental demonstration on the SERC interferometer testbed is desired. For this structure, a significant part of the open-loop performance degradation is above 100 Hz, where the global model is inaccurate. Local controllers, however, should be able to reduce the cost in this frequency region.

Goal

- Active broadband control of uncertain modally dense structures.
- Use collocated feedback.
 - Positive real controller guarantees stability.
 - Low authority or local control (“active damping.”)
- Use local acoustic or statistical model of structure.
- Maximize power dissipation.
 - Equivalent to impedance matching.
 - Cannot match impedance exactly at all frequencies due to causality constraint.
- Experimental demonstration on complex structures.

Local Models

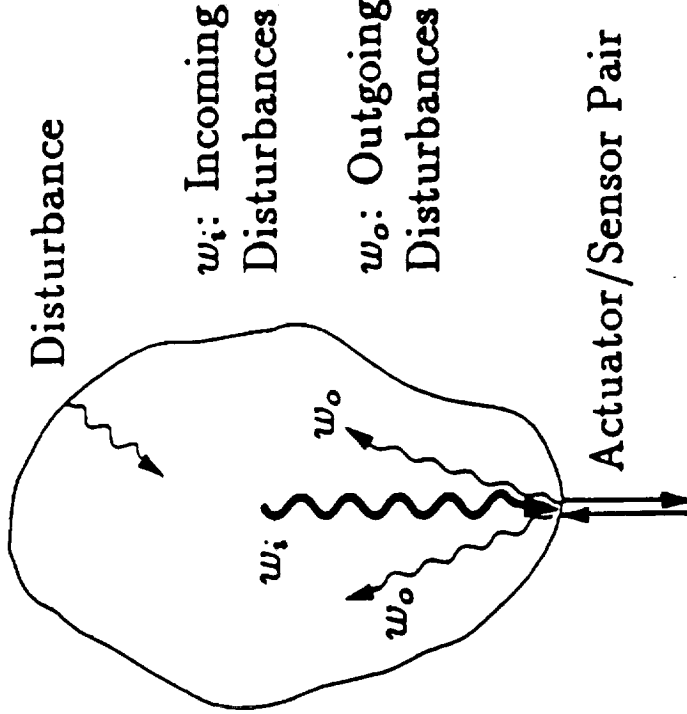
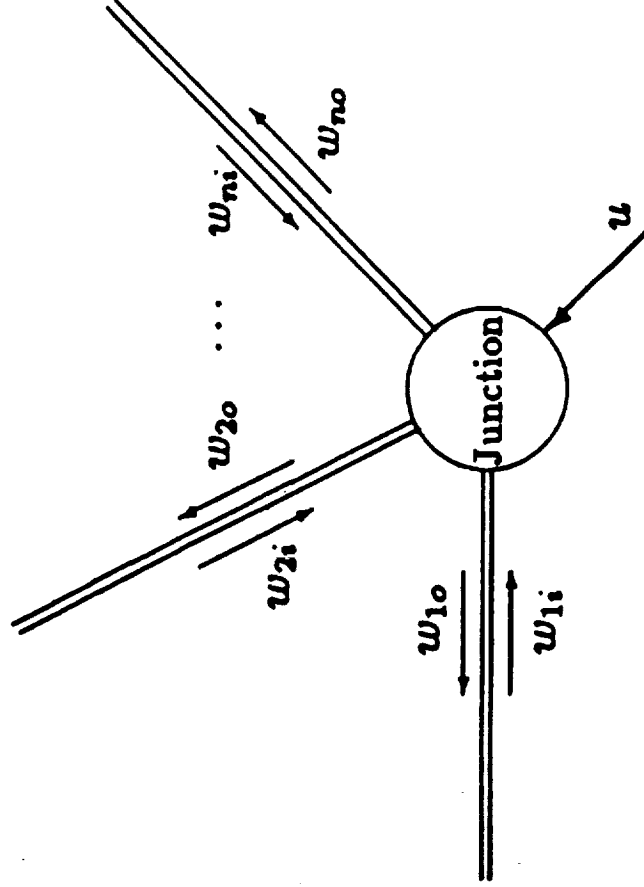
The current research builds on earlier research into optimal impedance matching in this lab. Miller *et al.* used a wave approach to model the structure. The structure in this case is modelled as a network of one dimensional wave-guides which meet at junctions. This approach results in a local model of the structure at the sensor and actuator location, and a model of the power dissipated by the control.

For complicated structures, the wave model can be difficult to identify. An alternative approach for obtaining a local model of the structure is to use the dereverberated driving point mobility. The structural response at a point can be considered to be the sum of two parts: a *direct field*, due to the local dynamics; and a *reverberant field*, which is caused by energy reflected back from other parts of the structure. The term “dereverberated” implies that the “reverberant” part of the response has been removed before computing the mobility.

Local Models

Travelling wave model

Dereverberated mobility model

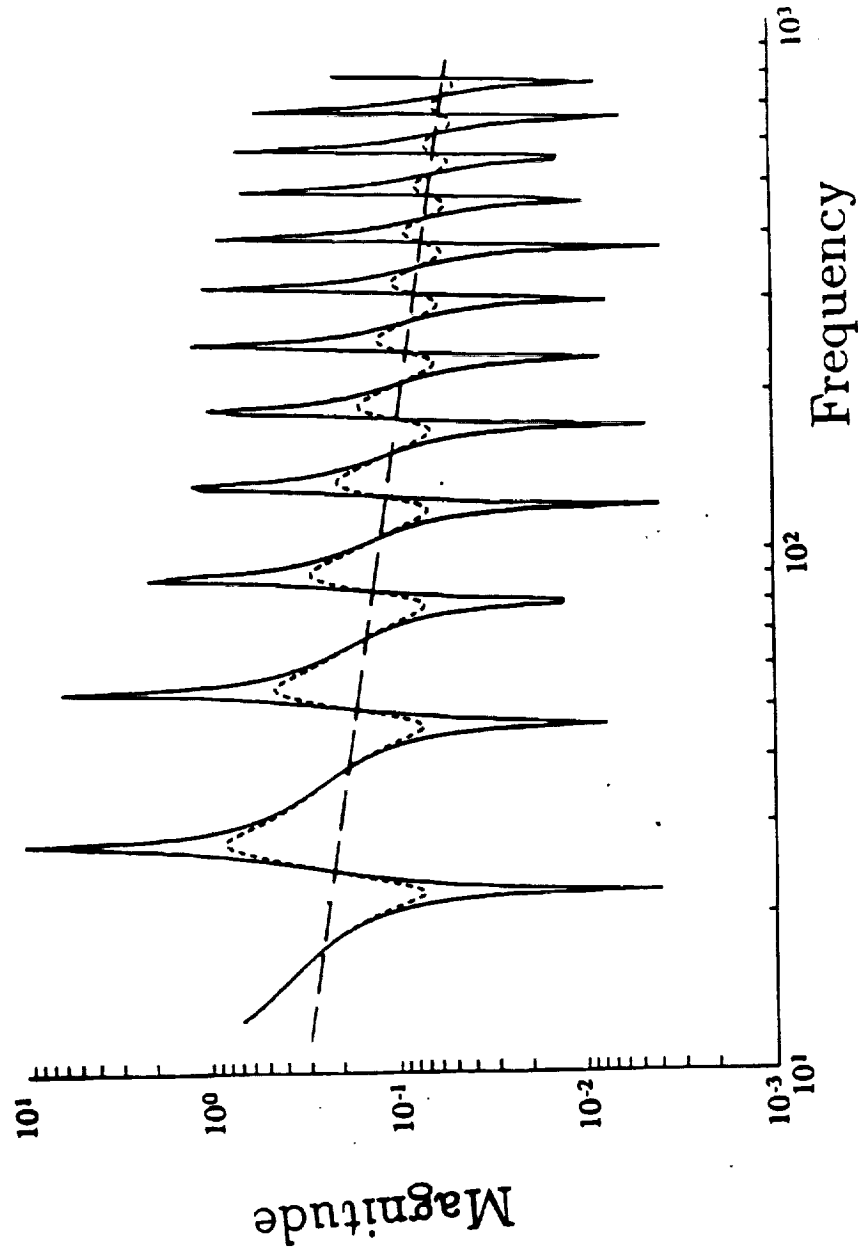


Computation of Dereverberated Mobility

The dereverberated mobility model can be obtained directly from an experimental transfer function by a logarithmic average, and thus can be applied to any arbitrary structure. The effect of considering only the direct, and not the reverberant field is the same as the effect of adding more and more damping to the structure until there is no returning wave at all. As more damping is added to the transfer function, the transfer function approaches the logarithmic average, as shown in the figure. The computation of the dereverberated mobility from an experimental transfer function is shown later.

Computation of Dereverberated Mobility

- From averaging transfer function:

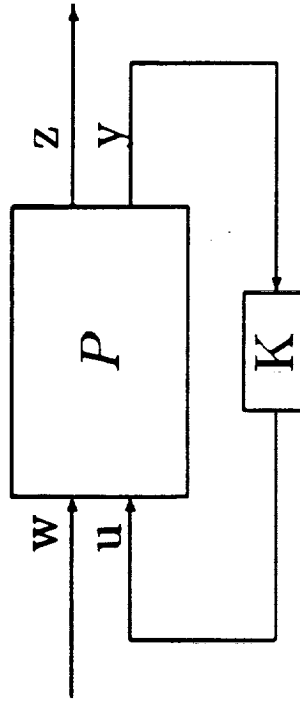


Power Flow

Previous results using a local model allow the power reflected back into the structure to be represented as a transfer function. The 2×2 transfer matrix P can be obtained in terms of state space representations for the dereverberated mobility $G(s)$. If $H(s)$ is the transfer function from the normalized disturbance input w to the output z , then H^*H is the reflected power flow at each frequency for unit input. The dissipated power per unit input is then $(I - H^*H)$. A compensator K is desired which minimizes, in an appropriate sense, the transfer function $H(s)$.

Power Flow

- Use local model only.
- Power dissipation related to input mobility G :



$$\begin{Bmatrix} z \\ y \end{Bmatrix} = \begin{bmatrix} G_1 I & G_1 G_0^\sim \\ G_0 & G \end{bmatrix} \begin{Bmatrix} w \\ u \end{Bmatrix}$$

- Define $H(s) = \frac{z(s)}{w(s)}$.
 - Analogous to reflection coefficient
 - Reflected power is $(H^* H)w^* w$
 - Dissipated power is $(I - H^* H)w^* w$

Impedance Matching

The maximum power dissipation is achieved with a non-causal impedance match. There are several ways to constrain the compensator to be causal. The problem with an \mathcal{H}_2 optimization of the power dissipation is that it does not guarantee closed-loop stability when the compensator is applied to the real structure. The compensator is derived based only on the local model, which does not include the information that energy which departs the junction will eventually return. As a result, the compensator may allow power to be generated at some frequencies, in order to achieve greater power dissipation at other frequencies.

If the worst case power flow is minimized, rather than the rms power, then the controller will not add power to the structure at any frequency, and hence the closed loop system is guaranteed to be stable. This also guarantees a positive real compensator. The drawback to this approach is that in general, the desired performance metric for the structure is the rms level of some quantity, rather than the worst case level. Thus while this approach guarantees stability, it is difficult to minimize the desired performance index. Both the \mathcal{H}_2 and \mathcal{H}_{∞} approaches were implemented experimentally on a 24 foot brass beam several years ago.

The goal now is to minimize the actual rms cost on the structure, and still guarantee stability, while using only local information about the structure.

Impedance Matching

- Maximum power dissipation is obtained if the compensator is the conjugate of the structural impedance.
 - This is noncausal \Rightarrow need best causal approximation.
- \mathcal{H}_2 optimization: No guarantee of stability on actual structure.
- \mathcal{H}_{∞} optimization: guarantees stability, but doesn't minimize desired performance metric.
- Goal: minimize actual rms cost and guarantee stability using only local information.

Control Problem

We want to minimize the best estimate of the global performance metric, given that we only have local knowledge and local control of the uncertain structure. There are several properties of the structure we can take advantage of to estimate the performance. First, a lightly damped structure approximately conserves energy. Second, a study of parametrically uncertain state space systems reveals additional properties; incoherence and equipartition. Incoherence states that, on average, the amplitudes of distinct modes are uncorrelated, while equipartition states that the average kinetic and potential energy of every mode at a similar frequency is the same. These assumptions are standard in Statistical Energy Analysis (SEA), and can be proven by averaging the state covariance over the probability distribution of the uncertain parameters. SEA is used primarily by mechanical engineers in vibration and acoustic analysis of complicated structures, often with hundreds or thousands of modes in the frequency range of interest.

Control Problem

- Minimize “global” mean-square performance metric $\langle y^T y \rangle$ using only local knowledge, local control.
- Use conservation of energy!
- Use characteristics of stochastic systems:
 - Incoherence: the amplitudes of distinct modes are uncorrelated,
 - Equipartition: the average kinetic and potential energy of every mode at a similar frequency is the same.

Control of Stochastic Systems

These assumptions, and the dereverberated mobility model can now be used to generate a cost functional expressed in terms of only the local information, that represents the best guess to the global performance metric. Using incoherence, the expected value of any quadratic performance metric can be related to a sum over the energies E_n of each individual mode, since the cross-terms are, on average, zero. This also uses equipartition, since the kinetic and potential energy contributions for each mode are lumped together into a single coefficient C_n . This sum can be approximated by an integral over frequency provided that the structure is modally dense.

The incoherence and equipartition assumptions can also be used to demonstrate that the incoming waves at a point have power proportional to the total structural energy, on a frequency by frequency basis. Using the power flow model obtained earlier (based on the dereverberated mobility model), the total power dissipated can now be expressed in terms of the energy. The key problem earlier in using the dereverberated mobility was that this local model did not include the fact that the actual structure is approximately conservative. Invoking conservation of energy, then, yields that the power dissipated by the control system, Π_{dis} , is equal to the power input from disturbance sources, Π_{in} , which can be easily characterized in terms of the power spectral density of the disturbances. Combining this with the previous result that the cost is related through an integral over frequency to the average modal energy yields a cost functional of the power flow $H^* H$ that is equivalent to minimizing the desired cost.

This cost combines features of both the \mathcal{H}_2 and \mathcal{H}_{∞} costs used in earlier research. It guarantees an \mathcal{H}_{∞} norm bound, and as a result, guarantees that the compensator dissipates power at all frequencies, and therefore stabilizes the actual structure. It also overbounds the \mathcal{H}_2 cost minimized originally with the Wiener-Hopf approach. The cost can be evaluated from state space data using the solution to a Riccati and a Lyapunov equation. The optimal compensator, however, must be found from numerical optimization.

Control of Stochastic Systems

- Incoherence \Rightarrow

$$\langle y^T y \rangle = \sum_{n=0}^{\infty} C_n E_n \simeq \int_{-\infty}^{\infty} C(\omega) E(\omega)$$

- Incoherence & Equipartition \Rightarrow incoming structural power is proportional to structural energy.

- Total power dissipated is therefore

$$\Pi_{diss} = \underbrace{(I - H(j\omega)^* H(j\omega))}_{\text{Relative Dissipation}} E(\omega)$$

- Conservation of energy \Rightarrow

$$\Pi_{diss} = \Pi_{in}$$

- The average (over uncertainty) cost is therefore:

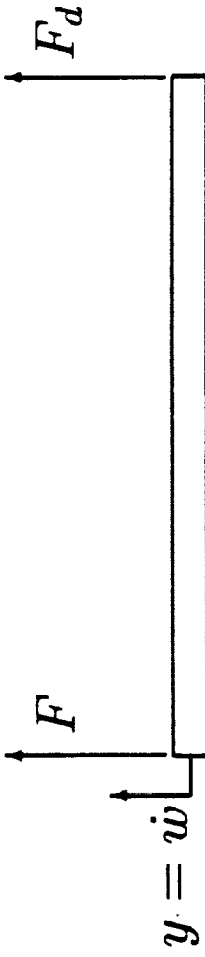
$$J = \frac{1}{2\pi} \int_{-\infty}^{\infty} C(\omega) \left[(I - H^* H)^{-1} H^* H \right] \Pi_{in}(\omega) d\omega$$

Example: Bernoulli-Euler Beam

To demonstrate the technique, consider a simple example of a Bernoulli-Euler beam, with a force actuator and velocity sensor at the left end, and a disturbance force at right end. The cost will be the rms difference between end point displacements. The dervative mobility is easily obtained from a wave model. (The local model is simply the transfer function of a semi-infinite beam.) As expected, the impedance match $K(s) = 1/G(-s)$ is non-causal, and cannot be implemented. A causal approximation must be obtained.

Example: Bernoulli-Euler Beam

- Free-free beam, force actuator and velocity sensor at left end, disturbance force at right end.
- Minimize difference between end-point displacements.



- Dereverberated mobility: (describes local dynamics)

$$G(s) = \frac{\sqrt{2}}{(\rho A)^{3/4} (EI)^{1/4}} \cdot \frac{1}{\sqrt{s}}$$

- Non-causal impedance match: (maximum dissipation)

$$K(s) = \frac{(\rho A)^{3/4} (EI)^{1/4}}{\sqrt{2}} \cdot \sqrt{-s}$$

Compensator Design

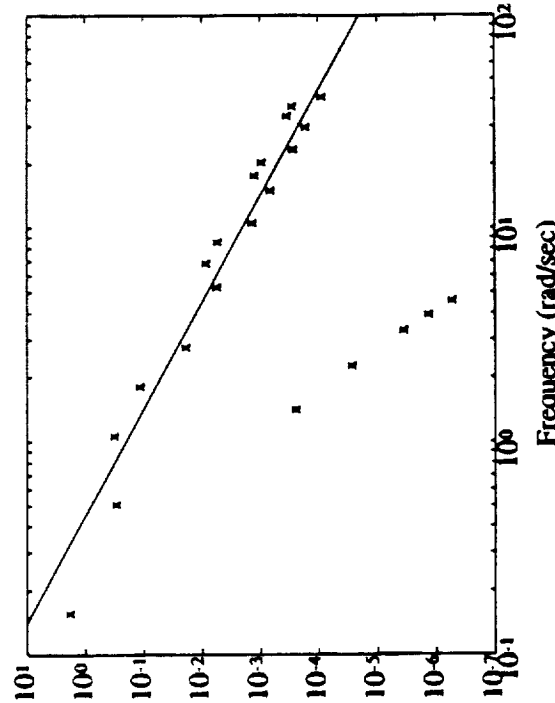
First, choose the input power $\Pi_{in}(\omega)$ based on the disturbance spectrum $V(\omega)$ and the dereverberated input mobility at the disturbance location $G_d(\omega)$. Then choose the weighting function $C(\omega)$ to approximate the modal cost, as shown in the figure. Finally, choose the desired compensator order and use numerical optimization to obtain the optimal compensator.

Compensator Design

- Choose $\Pi_{in}(\omega)$ based on disturbance spectrum $V(\omega)$ and derverberated input mobility at disturbance location $G_d(\omega)$.

$$\Pi_{in} = (G_d + G_d^*)V$$

- Choose $C(\omega)$ to approximate modal cost:



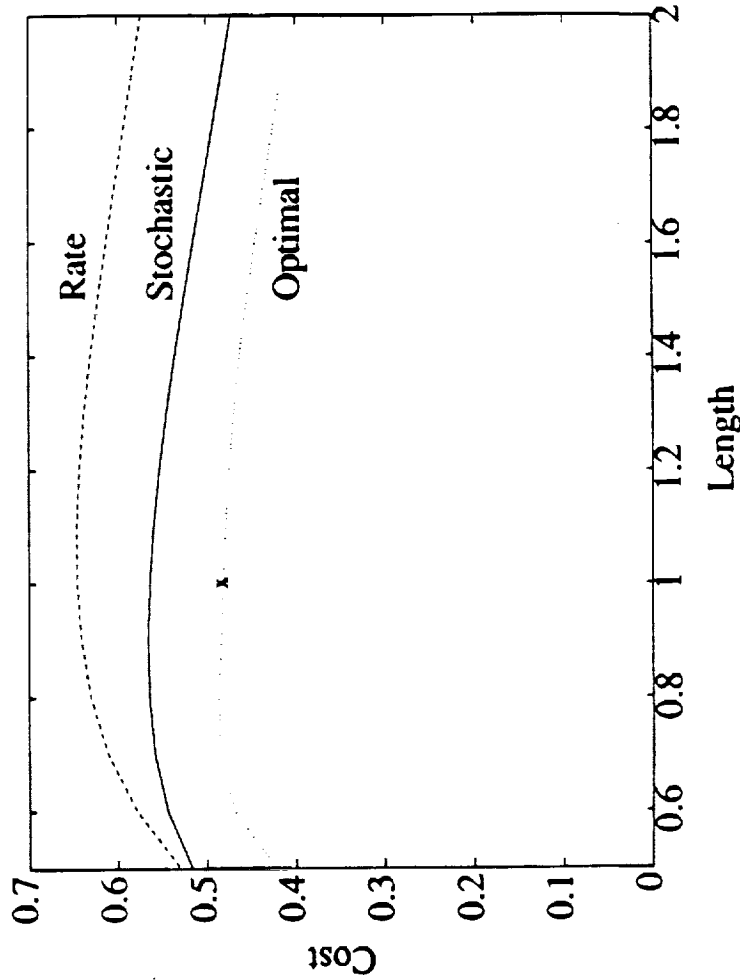
- Choose desired compensator order and use numerical optimization.

Performance

The cost is plotted as a function of the uncertain length of the beam for various compensators. The stochastic optimal compensator obtained here is better than rate feedback. The lowest curve on the graph is the locus of optimal compensators designed for each individual length; it is the lower bound on the achievable cost at each length. Any individual LQG compensator yielded an unstable closed loop system for small changes in length, due to the small control weighting used in the problem. Due to the weighting used to represent the input spectrum in this problem, the rate feedback solution is not particularly bad; in general it could be much worse than the stochastic optimal solution.

Performance

- Compare cost versus length of beam for various compensators.
 - LQG compensator unstable for small changes in length.



“Power” Dual Variables

In order to implement this approach using an active strut on the interferometer, the appropriate variables to be fed back must be identified. Each strut has a collocated strain gauge and load cell. The input and output variables in the dereverberated mobility model must be “power” dual; that is, their product should be the power flow into the structure. Since the piezo stack stiffness is high relative to the structure, it approximately commands displacement. Since force and velocity are dual, the integral of force is dual to the displacement. (That is, the compensator between these two variables fixes the transfer function between the force and velocity to be the same.)

“Power” Dual Variables

- Force into structure and relative velocity across active strut are dual.
- Piezo stack stiffness is high \Rightarrow commands displacement.
 - Can also command relative velocity.
- Want compensator $K(s)$ such that
 - Use integral of force feedback.

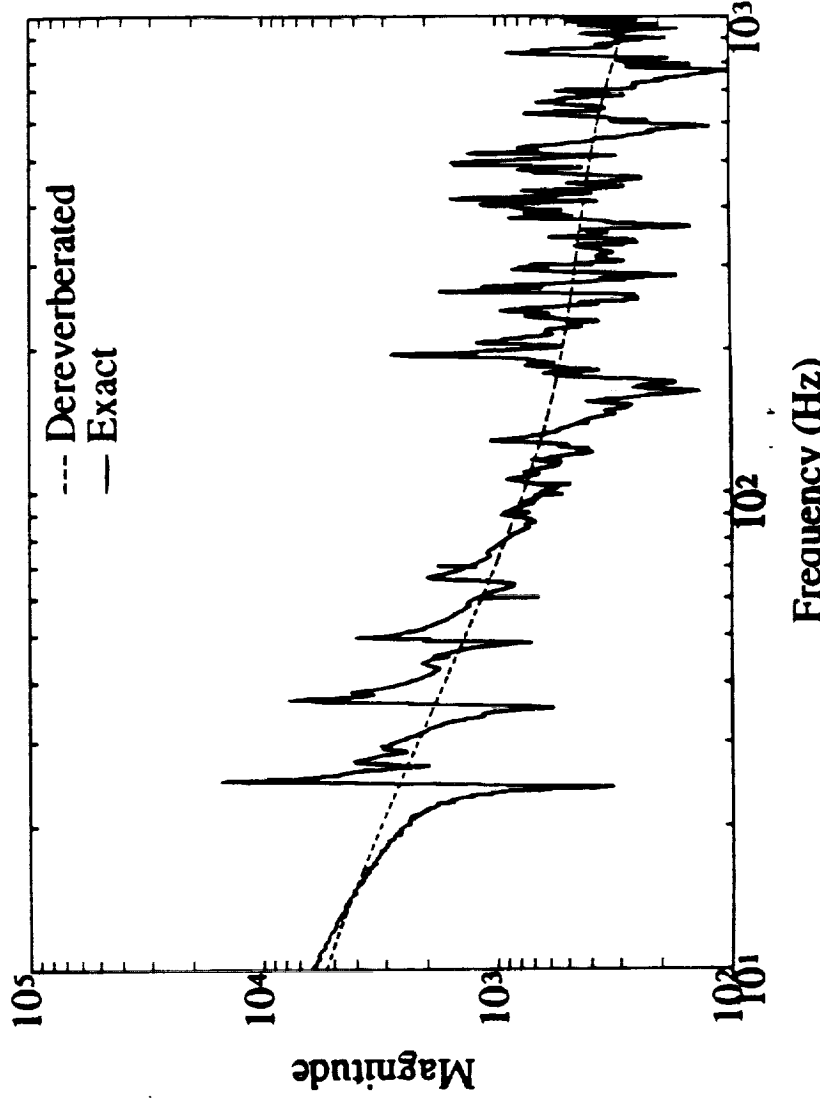
$$\begin{aligned}\dot{x} &= K(s)f \\ \Rightarrow x &= K(s) \left(\frac{f}{s} \right)\end{aligned}$$

Dereverberated Transfer Function

Experimentation on the interferometer is in progress, and preliminary results using constant gain impedance matching are given as part of the interferometer closed loop results presentation. The process by which the dereverberated mobility around an active strut can be identified is illustrated below. Since complex poles imply oscillation, and the dereverberated model assumes only the direct field, and hence no oscillation, the dereverberated mobility has only real poles and zeroes. Fitting the experimentally determined logarithmic magnitude with a transfer function containing only real poles and zeroes yields the dereverberated mobility. Only three poles were required to get a good fit of the transfer function.

Dereverberated Transfer Function

- Open loop transfer function from displacement to integrated force.
- Three (real) pole fit of log magnitude.



Conclusions

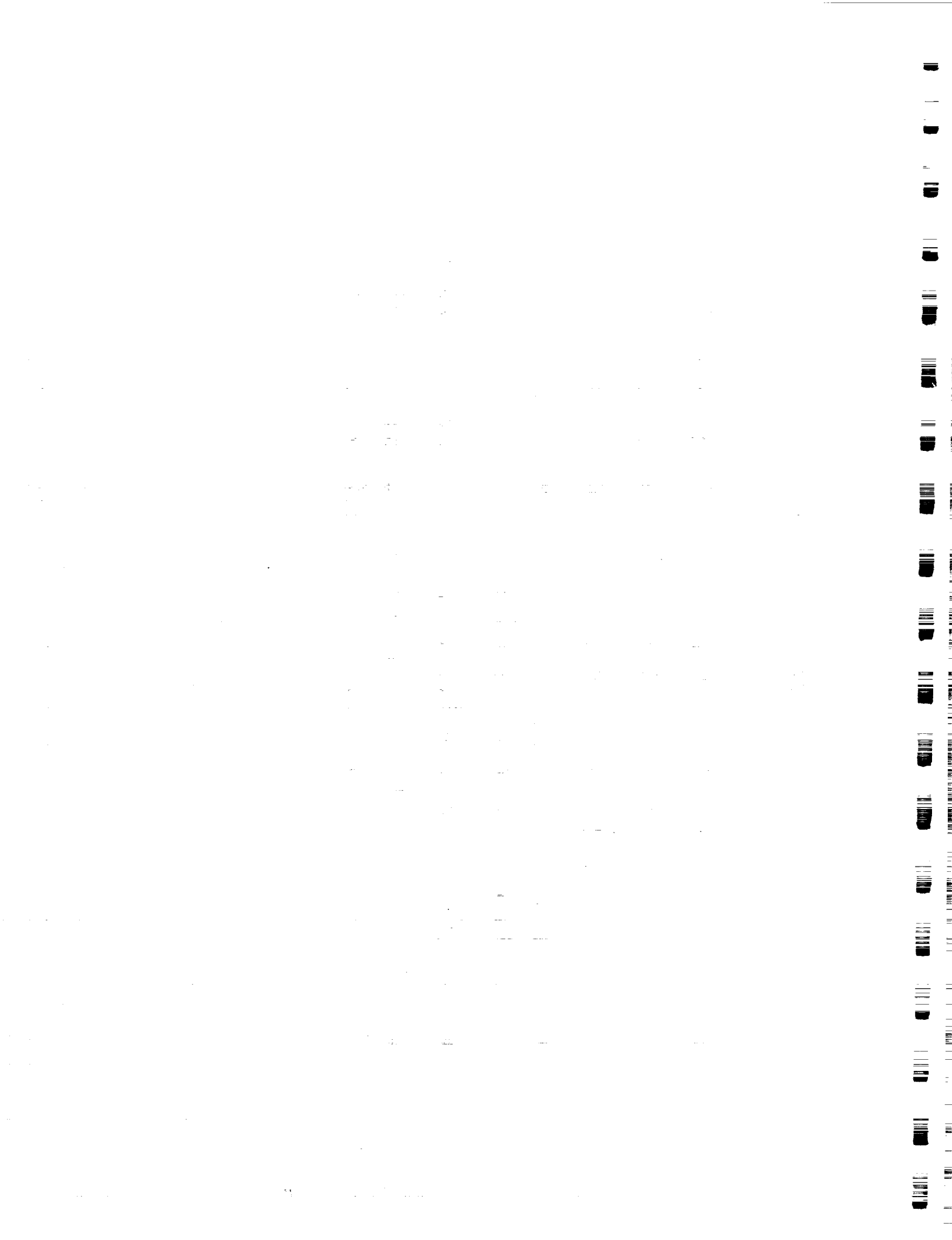
For the control of many modes of a structure, a global model that contains detailed information about each mode is likely to be highly inaccurate. A local model, however, will be robust to uncertainties elsewhere in the structure. Two approaches have been studied in SERC for developing local models for control design. A wave-based approach is easily applied to structures composed of one-dimensional waveguides. A more general approach is to use the dereverberated mobility, which can be obtained for any structure by averaging the experimental transfer function, or from a wave model of the structure.

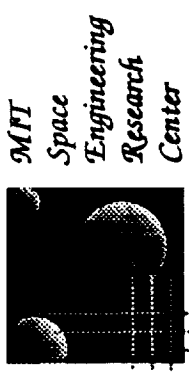
Control design using these local models is based on the minimization of the power flowing into the structure; the ideal compensator is a non-causal impedance match. An optimal controller can yield significantly better performance than rate feedback. Minimizing the \mathcal{H}_2 cost, or rms power flow does not guarantee closed-loop stability when the resulting compensators are applied to the actual structure. Minimizing the power in an \mathcal{H}_∞ sense guarantees stability, but it is more difficult to minimize the true performance index, which is generally an rms quantity.

One difficulty in applying many current robust control approaches to parameter uncertainty in structural control problems is that they do not take advantage of the fact that structures approximately conserve energy. In addition to taking advantage of conservation of energy, properties of parametrically uncertain structures can be used; equipartition and incoherence. These properties can be used in conjunction with a local model to develop a cost that will guarantee stability, as well as optimizing an rms performance index of the structure.

Conclusions

- Use local model of structure for broadband control.
 - Dereverberated mobility or travelling wave model.
 - Ideal compensator is a non-causal impedance match.
- Parameter-robust control for structures must take advantage of conservation of energy.
- Average covariance exhibits equipartition and incoherence.
- A cost functional can be obtained that uses these properties, and guarantees both stability and performance robustness.





*MIT
Space
Engineering
Research
Center*

MODE: STRUCTURAL TEST ARTICLE (STA)

Prof. E. Crawley
Prof. M van Schoor
Mr. Brett Masters
Mr. Mark Barlow

MIT
U. of Pretoria
MIT
MIT

PRECEDING PAGE BLANK NOT FILMED

Preview

- STA Objectives
- Hardware
- Data...
- Modeling
- Progress

MODE: Structural Test Objectives

- TO OBTAIN A DETAILED MODEL AND UNDERSTANDING OF ON-ORBIT STRUCTURAL DYNAMICS ON A COMPONENT ... SUB-COMPONENT SCALE.

Resonant and transient response influence on-board vibration / acoustic environment.

Incorrect modeling of dynamics can cause inadvertent CSI with attitude dynamics.

Detailed modeling is vital for robustness / performance of ~~precision-controlled~~ structures.

- UNDERSTANDING ON-ORBIT DYNAMICS WILL REDUCE UNCERTAINTIES BY:

comparison of earth test results with 0-gravity test results.

verifying and validating analytical models.

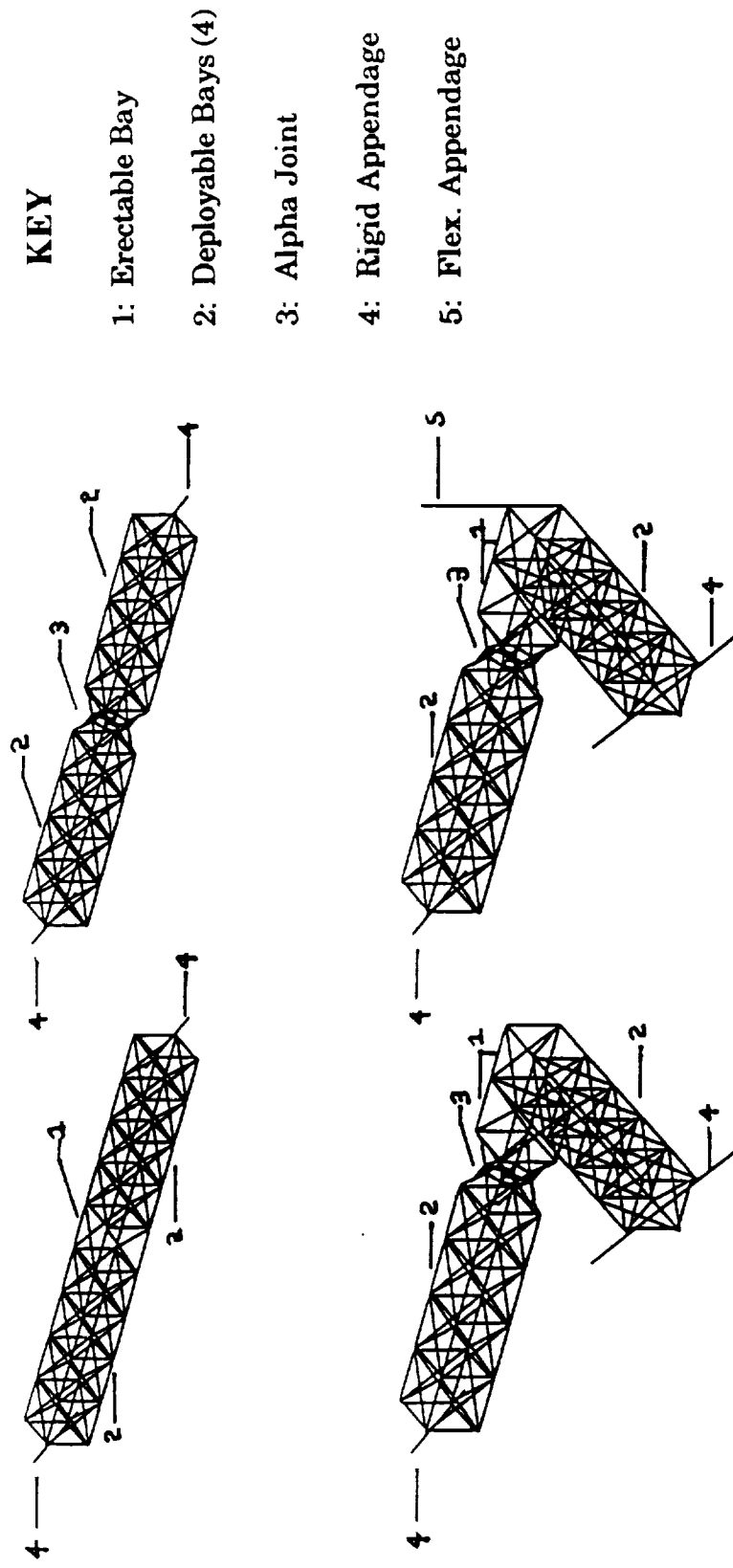
adding to the scant data base of quality data available on the dynamics of large flexible space structures in 0-gravity.

HARDWARE

FOUR TEST CONFIGURATIONS TESTED IN 0-GRAVITY WERE A BASELINE, CONSISTING OF TWO FOUR BAY DEPLOYABLE SECTIONS MATED WITH AN ERECTABLE MID-SECTION, BASELINE PLUS ALPHA, CONSISTING OF TWO FOUR BAY DEPLOYABLE SECTIONS MATED WITH A REPLICA SCALE ARTICULATING JOINT, AN "L" CONFIGURATION., TWO FOUR BAY DEPLOYABLE SECTIONS MATED AT A CORNER ARRANGEMENT OF TWO ERECTABLE BAYS PLUS THE ARTICULATING JOINT, AND FINALLY THE "L" WITH AN ADDED FLEXIBLE APPENDAGE AT THE L CORNER. THE TWO CONFIGURATIONS, THE BASELINE AND THE ARTICULATING JOINT, WERE PRIMARILY TWO DIMENSIONAL STRUCTURES WHERE AS THE "L" SHAPE IS TRULY THREE DIMENSIONAL.

ONE BAY OF ONE DEPLOYABLE SECTION HAD A THREE STAGE ADJUSTABLE PRE-TENSION. THE ARTICULATING "ALPHA" JOINT HAD A TWO STAGE ADJUSTABLE FRICTION CAM MECHANISM.

Hardware



Four Test Configurations of the STA

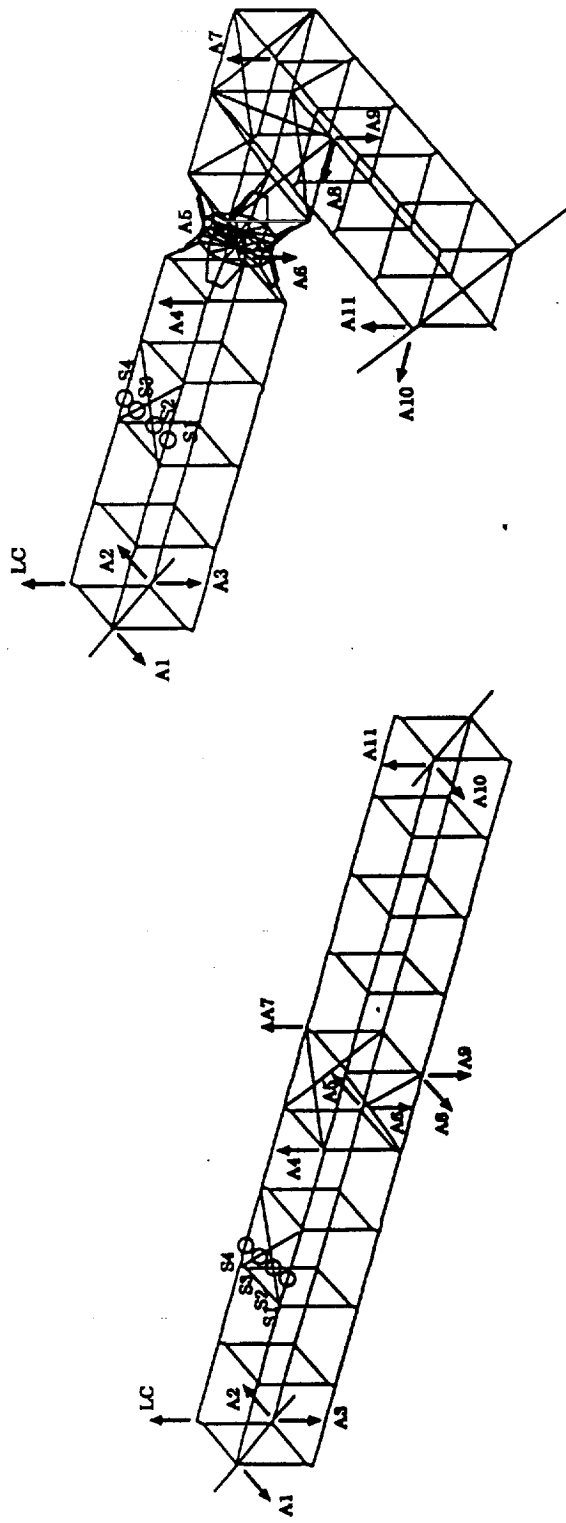
SENSORS AND ACTUATOR

ACCELEROMETER LOCATIONS WERE CHOSEN SO THAT WINDOWED MODES WOULD BE OBSERVABLE. THE STRAIN GAGES WERE IMPLEMENTED ON ONE FACE OF THE ADJUSTABLE PRELOAD BAY TO IDENTIFY LOADING CONDITIONS ON THE TENSIONING BRACES AND LONGERONS OF THE NON LINEAR COMPONENT. THE LOAD CELL WAS HOUSED IN THE PROOF-MASS-ACTUATOR ASSEMBLY SO THAT THE DRIVING FORCE COULD BE IDENTIFIED. SINE SWEEPS WERE PERFORMED IN THE DESIRED FREQUENCY WINDOWS. TIME DOMAIN DATA WAS STORED ON A WRITE ONCE READ MANY OPTICAL MEDIA AFTER CONDITIONING AND FILTERING IN THE EXPERIMENTAL SUPPORT MODULE. IN TOTAL NINE TEST PROTOCOLS WERE COMPLETED RECORDING OVER A BILLION DATA POINTS.

Sensors and Actuator

Sixteen sensor channels arranged and conditioned as full-bridge resistive gages

- four strain gage pairs located on one face of adjustable preload bay
- eleven accelerometers (piezoresistive) at predetermined locations
 - one load cell located in the proof-mass actuator housing



Sensor and actuator locations for Straight and L configurations.

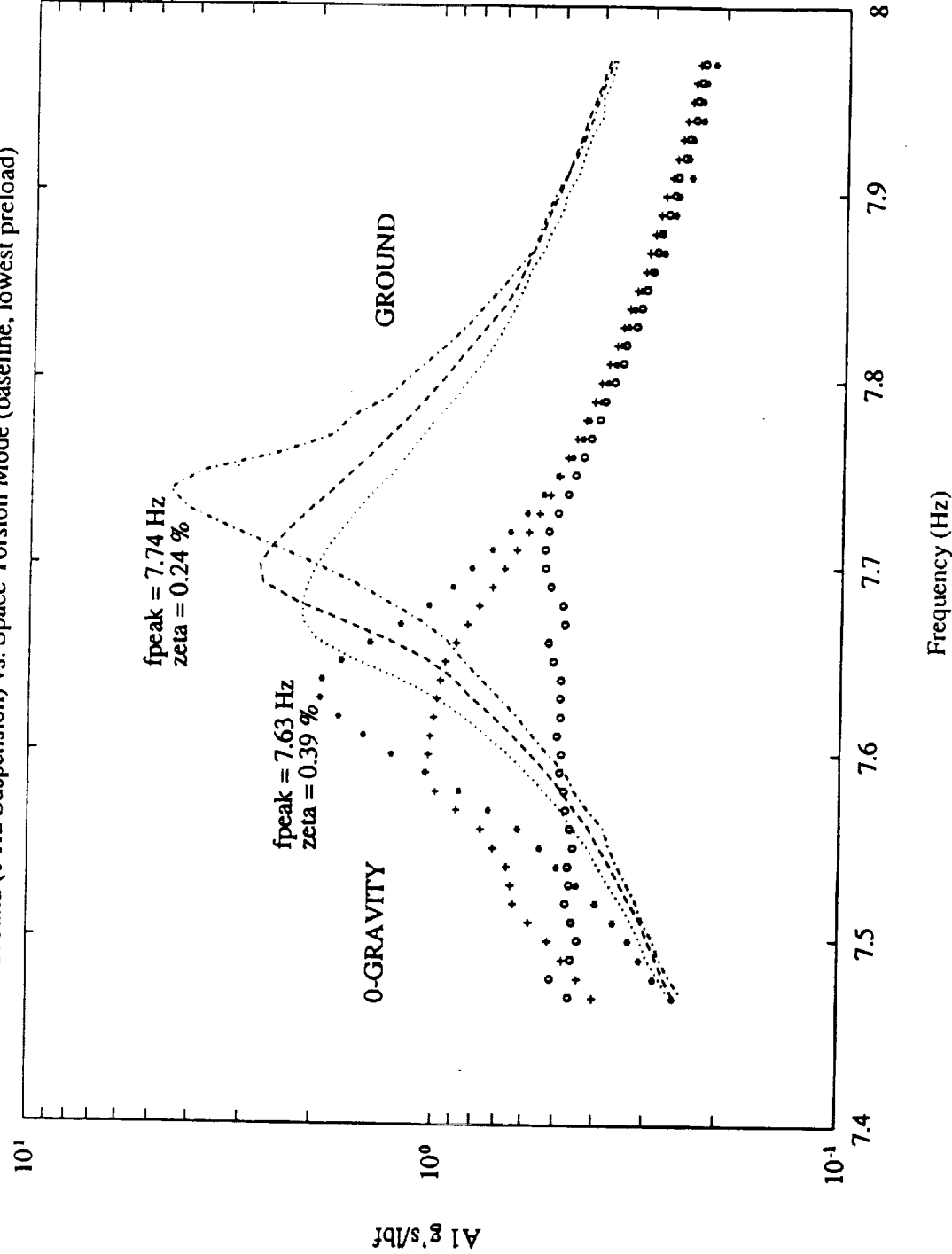
DATA

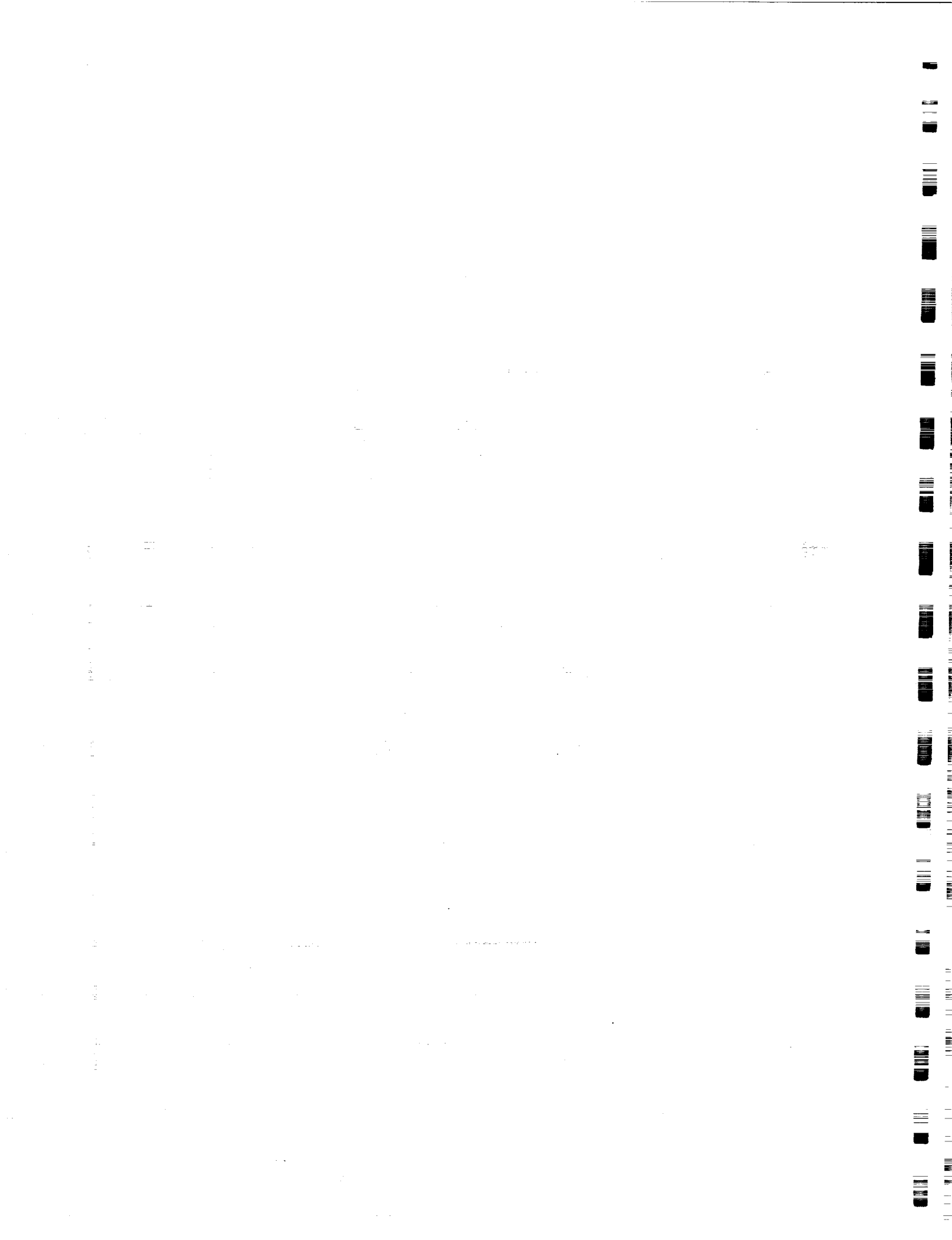
THE DATA SHOWN IN THE FIRST VIEW GRAPH IS AN OVER PLOT OF 0-GRAVITY VS ON ORBIT RESULTS FOR THE BASELINE CONFIGURATION TORSION MODE, WITH THE PRELOAD IN THE ADJUSTABLE BAY SET AT THE LOWEST LEVEL (APPROX 0.5 LB). THE DASHED, DOTTED AND DASH-DOTTED DATA REPRESENTS THREE DIFFERENT FORCING LEVELS (LOGARITHMICALLY SPACED, APPROX. 0.4, 2.5, 4.5 LBS RESPECTIVELY) OF 1-GRAVITY TESTING WITH NOMINAL, ONE HZ PLUNGE, SUSPENSION. THE STAR, CROSS AND CIRCLE DATA WAS THAT RECORDED ON ORBIT. IN BOTH SETS OF DATA THERE EXISTS A NOTICEABLE SHIFT IN RESONANT FREQUENCY WITH FORCING LEVEL AND A NOTICEABLE DIFFERENCE BETWEEN THE 1-G AND 0-G RESULTS.

THE DATA SHOWN IN THE NEXT VIEW GRAPH IS AN OVER-PLOT FOR THE ARTICULATING (ALPHA) JOINT CONFIGURATION, AGAIN FOR THE TORSION MODE. HERE, THE ALPHA JOINT CAM MECHANISM IS SET AT THE HIGH PRELOAD. THE DATA EXHIBITS SIMILAR DESTIFFENING WITH FORCE LEVEL AS NOTICED IN A MAJORITY OF THE GROUND DATA. AGAIN THE 0-GRAVITY DATA (NO SUSPENSION) IS SOFTENED, WHERE THE FREQUENCY SHIFT FOR THE LOWEST LEVEL OF FORCING, BELIEVED TO BE THE MOST LINEAR RESONANCE, WAS ON THE ORDER OF FOUR PERCENT.

Data

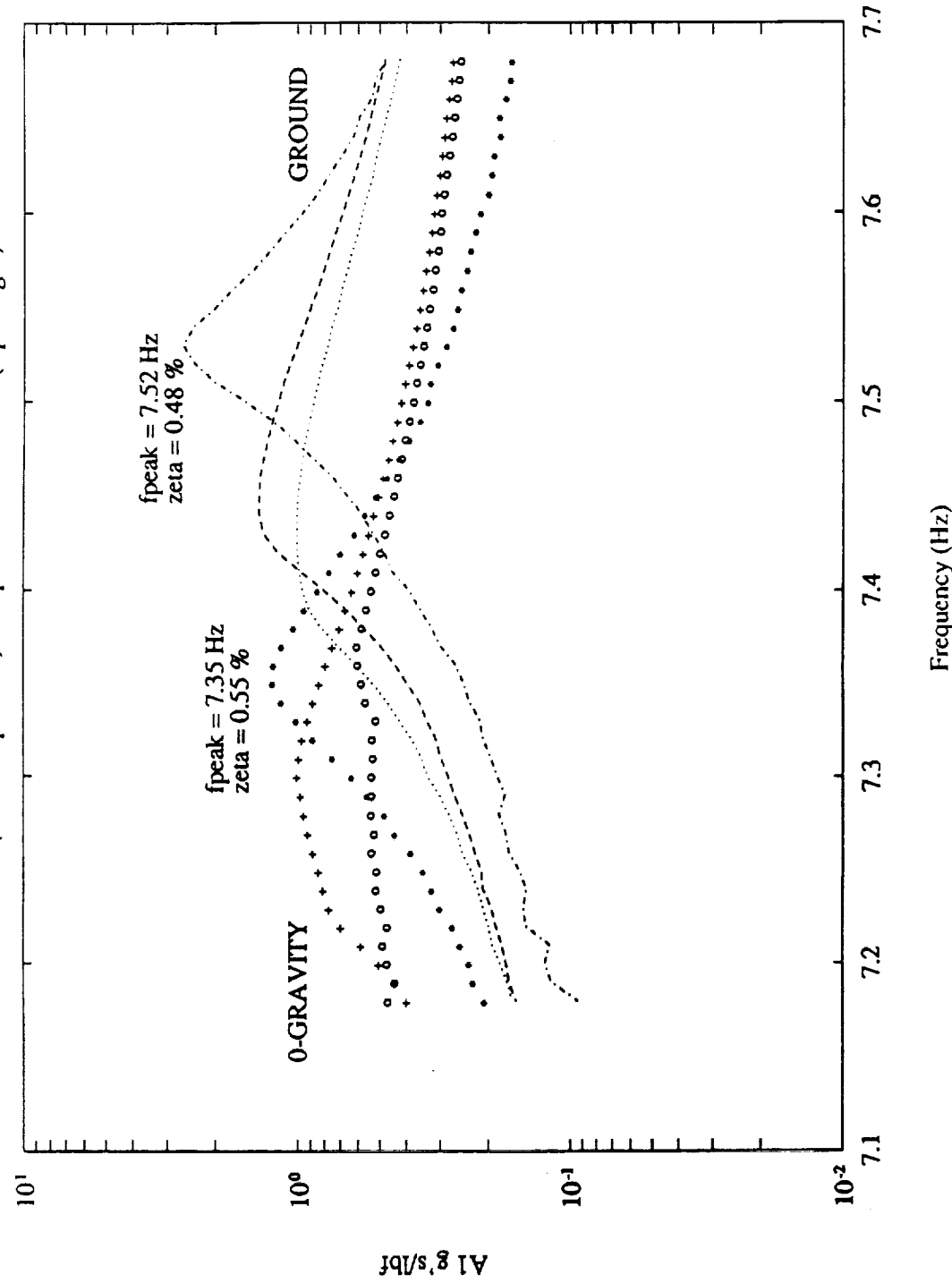
Ground (1 Hz Suspension) vs. Space Torsion Mode (baseline, lowest preload)





Data (cont.)

Ground (1 Hz Suspension) vs. Space Torsion Mode (alpha tight)

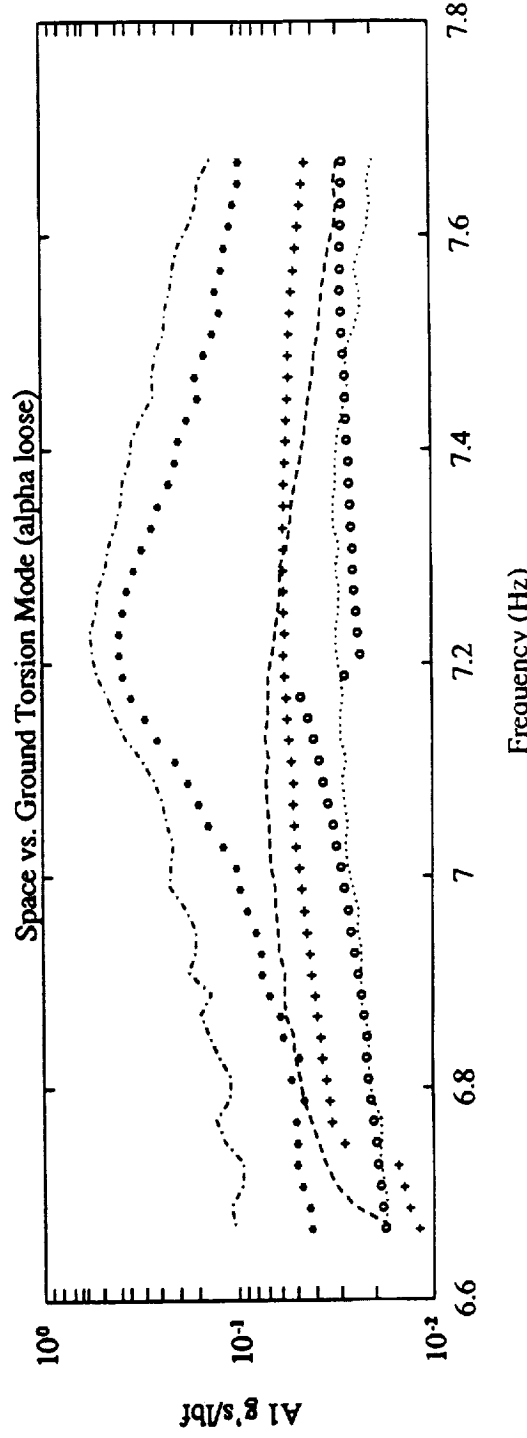
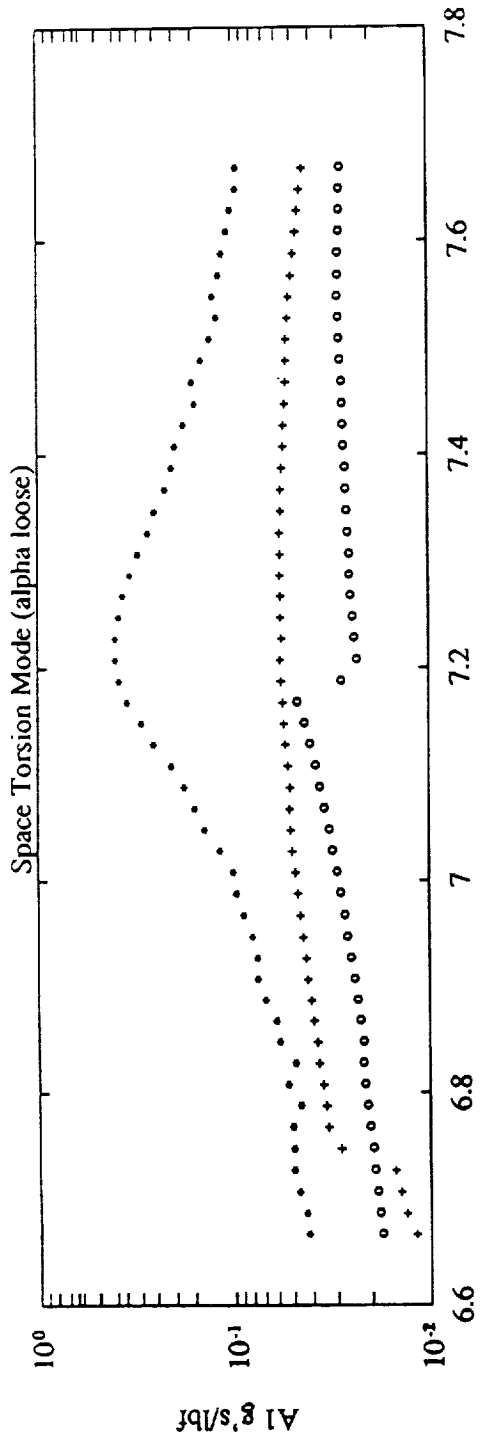


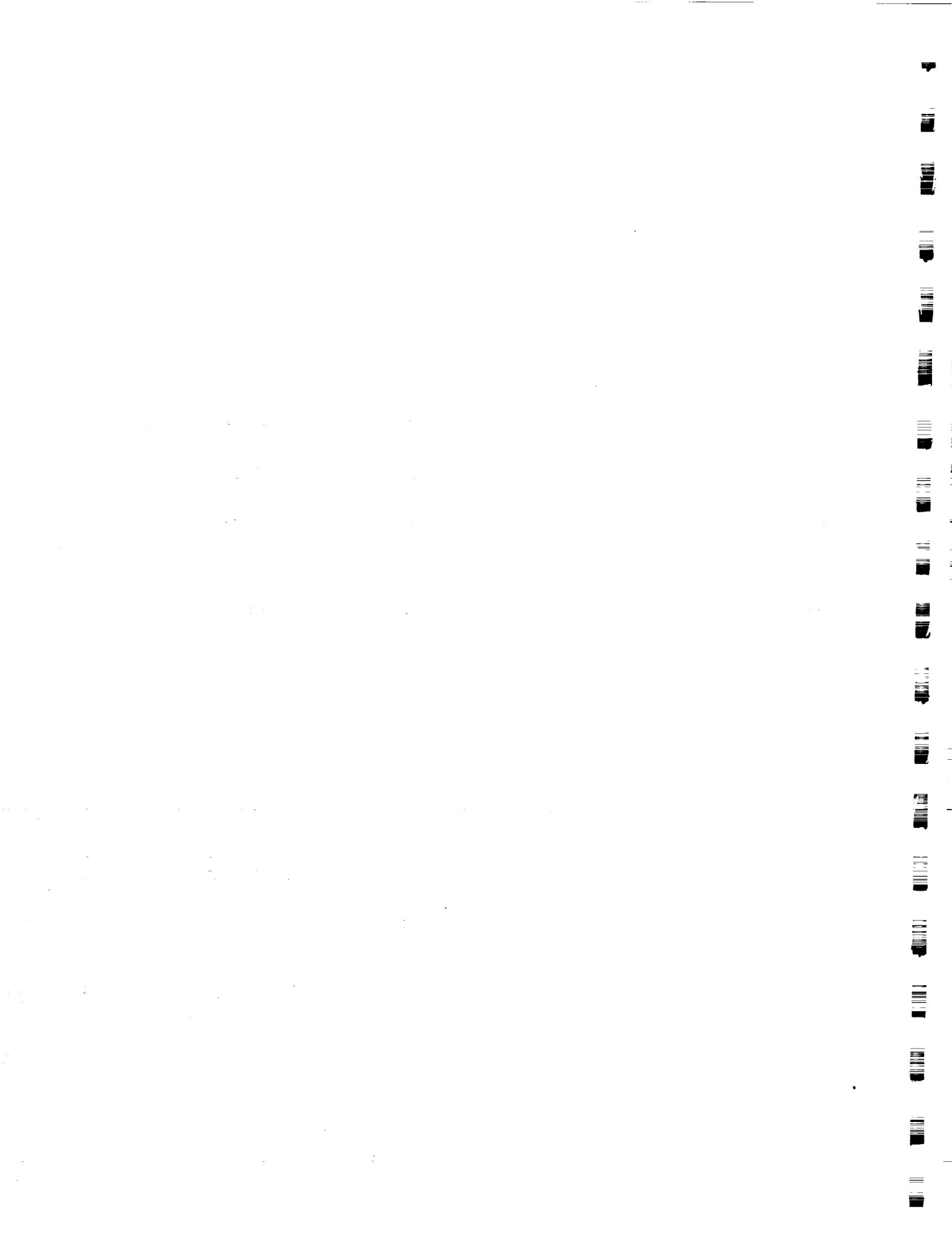
PRECEDING PAGE BLANK NOT FILMED

DATA (CONT.)

THE LAST VIEW GRAPH OF DATA WAS SEPARATED INTO 0-GRAVITY DATA AND AN OVER-PLOT OF 0-GRAVITY AND 1-GRAVITY DATA. THE DATA SHOWN IS FOR THE ALPHA JOINT CONFIGURATION WITH THE CAM MECHANISM LOOSE. THE STARS ARE THE LOWEST FORCING LEVEL, THE CROSSES ARE THE NEXT HIGHEST AND THE CIRCLES ARE THE HIGHEST. NOTE THAT FOR THE LOWEST FORCING LEVEL A RESONANCE IS STILL OBSERVABLE IN THE DATA. THE HIGHER FORCING LEVELS YIELD JUMP PHENOMENA IN 0-GRAVITY WHICH ARE NOT EVIDENT UNDER A 1-GRAVITY PRELOAD.

Data (cont.)





Preliminary Results

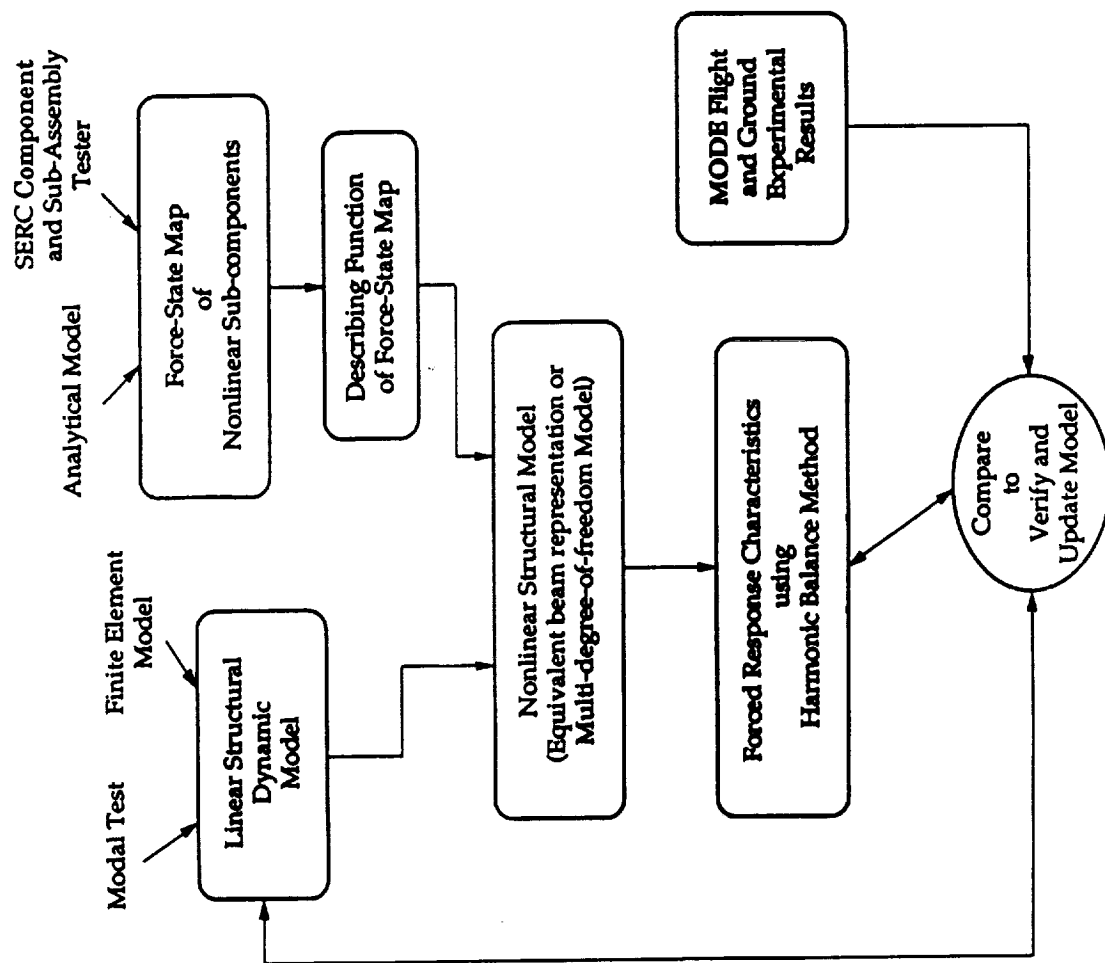
- MODES GENERALLY APPEAR SOFTER IN 0-GRAVITY
- RESONANCES EXHIBIT SIMILAR SHIFTS, ON THE GROUND AND IN 0-GRAVITY, RELATIVE TO INPUT FORCING LEVEL.
 - Some modes out of 0-gravity test windows!
- MODES ARE GENERALLY MORE DAMPED IN 0-GRAVITY.
- DATA EXHIBIT SOME ANOMALIES, TO BE EXPLAINED BY NON-LINEAR ANALYSIS?

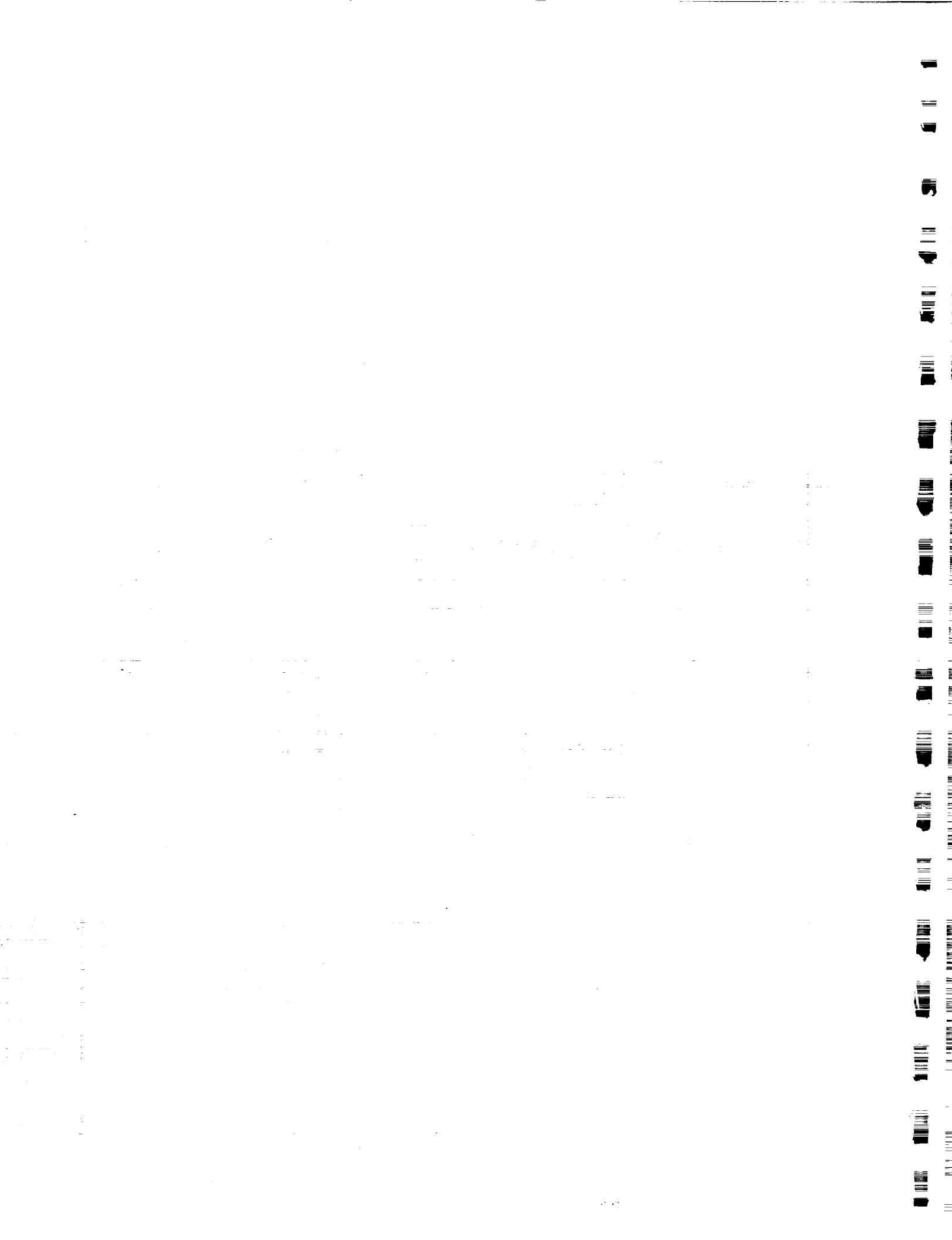
PROGRAM LOGIC

GROUND TESTING HAS BEEN PERFORMED AND IS DOCUMENTED BY BARLOW 1992 (*MIT M.S. THESIS*). THE GROUND TESTING ILLUMINATED SOME OF THE EFFECTS OF SUSPENSION TESTING ON A SPACE STRUCTURE. A LINEAR ANALYTICAL (FINITE ELEMENT) MODEL WAS ALSO DERIVED AND EMPLOYED AS A FIRST GENERATION MODEL OF SUSPENSION AND GRAVITY EFFECTS ON THE TESTING OF A TYPICAL SPACE STRUCTURE. RESULTS OF THE GROUND TEST PROGRAM TO DATE CAN BE FOUND IN "VARIATIONS IN THE MODAL PARAMETERS OF SPACE STRUCTURES", E.F CRAWLEY AND M.S. BARLOW AND M.C. VAN SCHOOR [PROCEEDINGS OF THE 33RD AIAA/ASME/AHS STRUCTURES, STRUCTURAL DYNAMICS, AND MATERIALS CONFERENCE , DALLAS, TX, 1992]. FURTHER WORK IS PROCEEDING ON THE IDENTIFICATION OF THE NONLINEAR COMPONENTS OF THE MODE STRUCTURE USING THE FORCE-STATE MAP TECHNIQUE. THE TECHNIQUE IS BEING DEVELOPED FROM SINGLE DEGREE OF FREEDOM QUASISTATIC PARAMETER IDENTIFICATION TO FULL SIX DEGREE OF FREEDOM IDENTIFICATION OF STIFFNESS AND DAMPING CHARACTERISTICS.

A SCHEMATIC OF THE COMPONENT TESTER IS INCLUDED. THROUGH SUBCOMPONENT IDENTIFICATION AND THE LINEAR FINITE ELEMENT MODEL A NONLINEAR STRUCTURAL MODEL IS BEING DERIVED. WITH THE NONLINEAR MODEL IN HAND PREDICTION OF THE FORCED RESPONSE CHARACTERISTICS IN 0-GRAVITY AND 1-GRAVITY WILL BE PERFORMED AND COMPARED WITH THE DATA BASE NOW AVAILABLE.

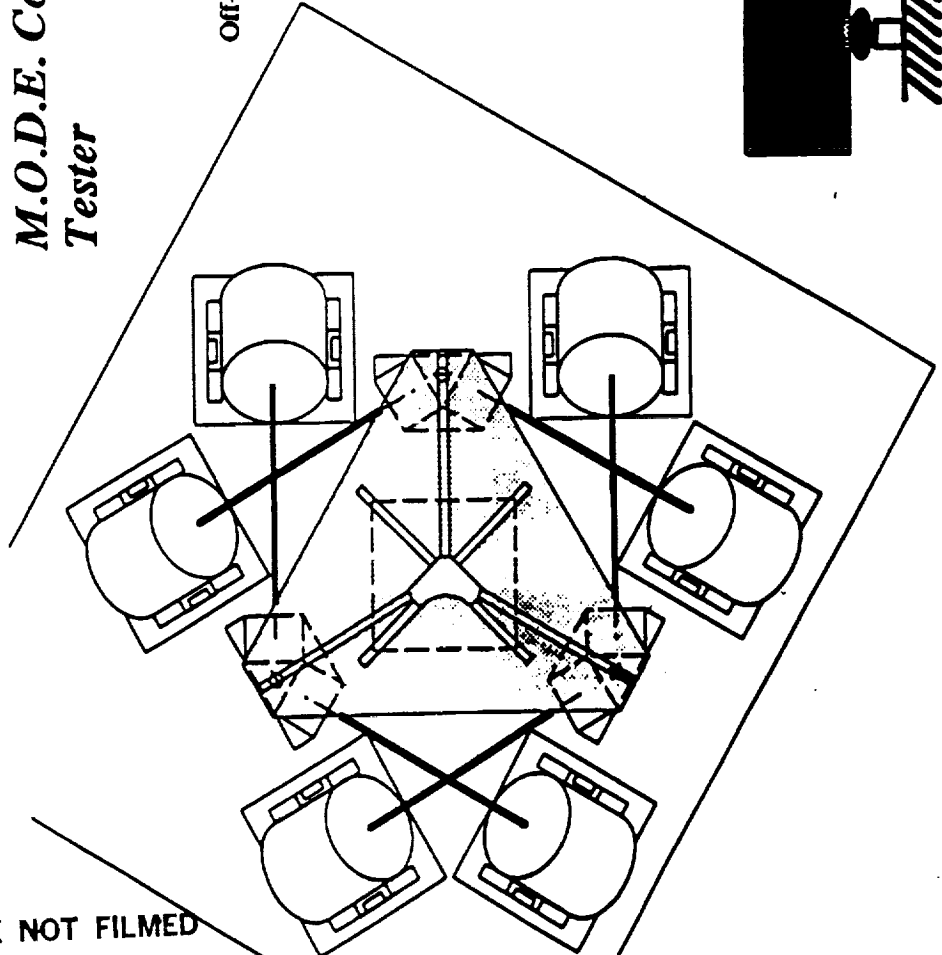
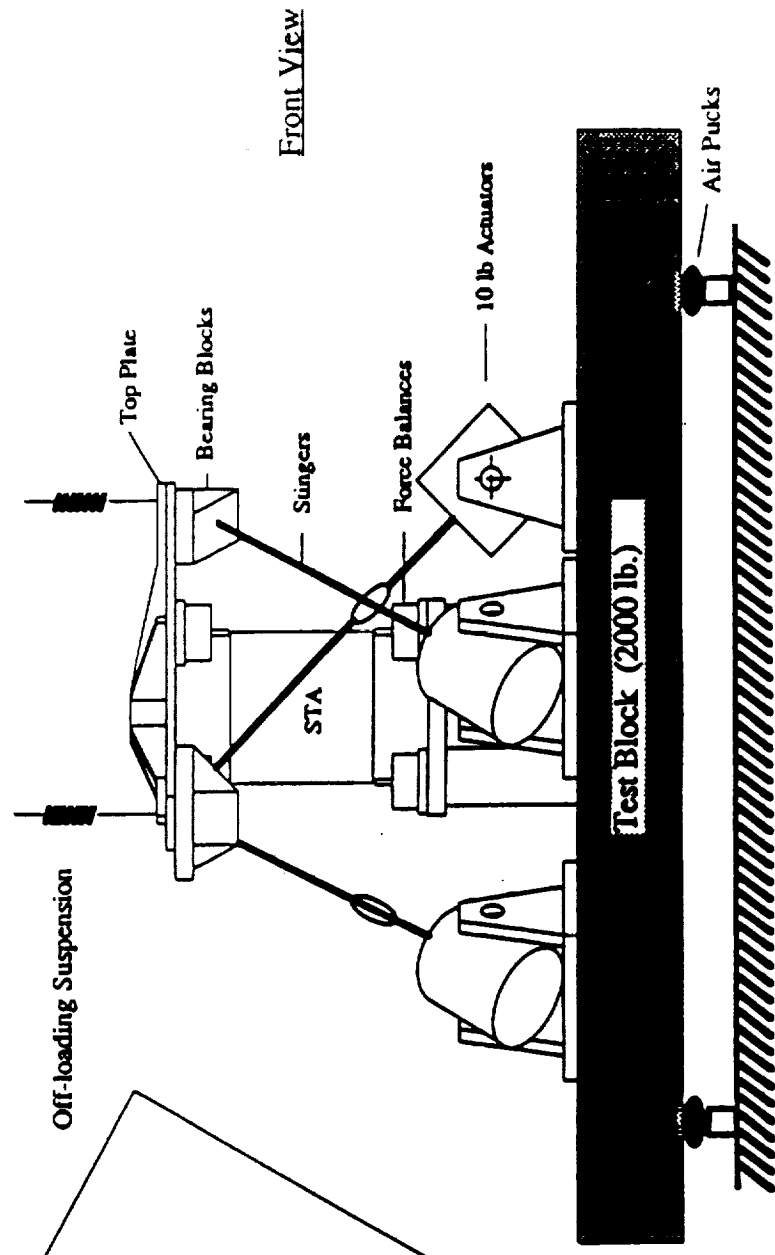
Program Logic



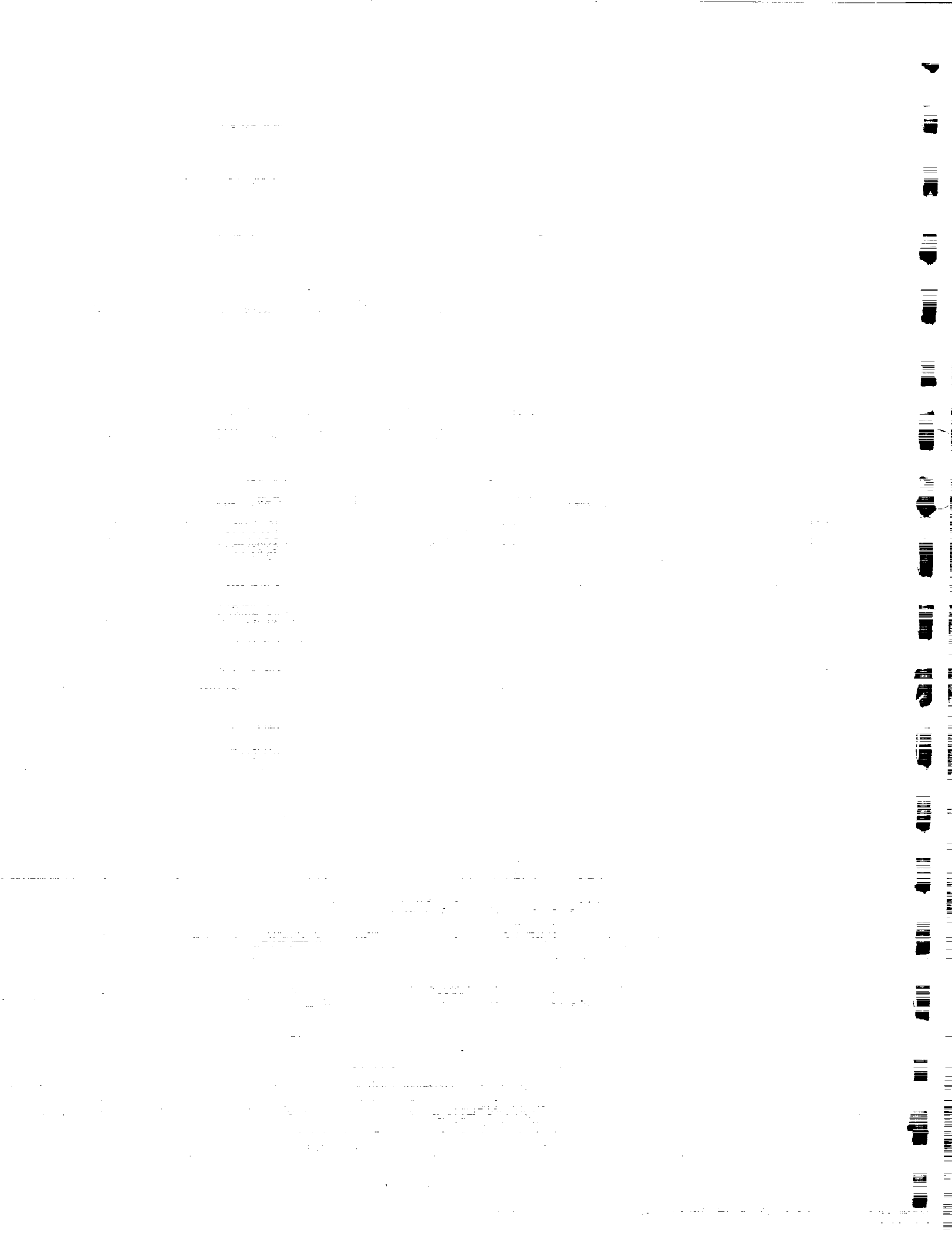


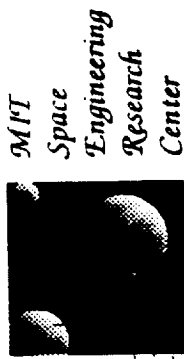
Progress

M.O.D.E. Component
Tester



PRECEDING PAGE BLANK NOT FILMED





MIT
Space
Engineering
Research
Center

**THE MIDDECK ACTIVE CONTROL
EXPERIMENT (MACE)**

Dr. David W. Miller

MIT

5th NASA/DOD CSI Technology Conference
March, 1992

THIS PRESENTATION DISCUSSES VARIOUS ASPECTS OF THE MIDDECK ACTIVE CONTROL EXPERIMENT (MACE) INCLUDING THE MOTIVATION FOR THE PROGRAM, THE ANALYTICAL MODELLING WORK, THE GROUND BASED EXPERIMENTAL CONTROL WORK AND A BRIEF DESCRIPTION OF THE FLIGHT OPERATIONS. MACE IS A NASA IN-STEP AND CSI OFFICE FUNDED SHUTTLE FLIGHT EXPERIMENT TENTATIVELY SCHEDULED FOR LAUNCH IN THE SUMMER OF 1994.

OUTLINE

The MODE Family of Experiments

Science Program

MACE Science Objective

Hardware Description

Science Approach

Suspension and Gravity Effects

MACE 1-g and 0-g Models

Gravity Influence on Control

Measurement Based LQG Control

Single-Input, Single-Output Topology

Single-Input, Two-Output Topology

Flight Experiment

Summary

MACE BUILDS UPON THE MIDDECK 0-GRAVITY DYNAMICS EXPERIMENT (MODE) CONCEPT. MACE IS DESIGNED TO TEST A TEST ARTICLE WHICH IS DEPLOYED ON THE SHUTTLE MIDDECK. EXPERIMENT CONTROL AND DATA ACQUISITION IS ACHIEVED BY CONNECTING A POWER AND DATA UMBILICAL BETWEEN THE TEST ARTICLE AND AN INSTRUMENTATION PACKAGE STORED IN ONE OF THE MIDDECK LOCKERS. WHILE MODE MEASURED THE GRAVITY DEPENDENT NONLINEAR BEHAVIOR OF TRUSS STRUCTURES AND CONTAINED FLUIDS DURING THE STS-48 MISSION IN SEPTEMBER, 1991, MACE IS DESIGNED TO INVESTIGATE THE GRAVITY DEPENDENT CLOSED-LOOP BEHAVIOR OF PRECISION SPACECRAFT.



THE MODE FAMILY OF EXPERIMENTS

Fluid Test Article (FTA)

Structural Test Article (STA)

Coupled Non-Linear
Dynamics of Fluids and
Structures in Zero
Gravity

Non-Linear Dynamics of
Jointed Truss Structures in
Zero Gravity

MACE Test Article

Influence of Gravity on the
Active Control of a
Multibody Platform

Flight #1:
September 1991

Flight #2:
June 1994

MACE is part of a logical sequence of cost-effective flight experiments designed to advance technology of interest to NASA in the area of controlled structures.

THE MACE PROGRAM FOLLOWS A FLEXIBLE, PRECISION SPACECRAFT THROUGH ANALYSIS AND GROUND TESTING TO ON-ORBIT OPERATION AND CONTROL REDESIGN. THE MOTIVATION IS TO EXPLORE A PLAUSIBLE PROCEDURE BY WHICH A REAL PRECISION SPACECRAFT MIGHT UNDERGO FLIGHT QUALIFICATION AND TO IDENTIFY ANY HURDLES WHICH MUST BE ADDRESSED IN MAKING THE SPACECRAFT OPERATE AS REQUIRED ONCE ON ORBIT. SUCH A PROGRAM OBJECTIVE IMPLIES THAT VARIOUS ISSUES MUST BE ADDRESSED DURING THE PROGRAM. THESE ISSUES RANGE FROM UNDERSTANDING HOW GRAVITY INFLUENCES ON STRUCTURAL DYNAMICS EFFECTS THE ABILITY TO PREDICT CLOSED-LOOP BEHAVIOR ON ORBIT TO TECHNIQUES FOR REDESIGNING THE CONTROL ONCE ON ORBIT.

MACE SCIENCE OBJECTIVE

Objective:

Develop a qualification procedure for flexible, precision spacecraft.

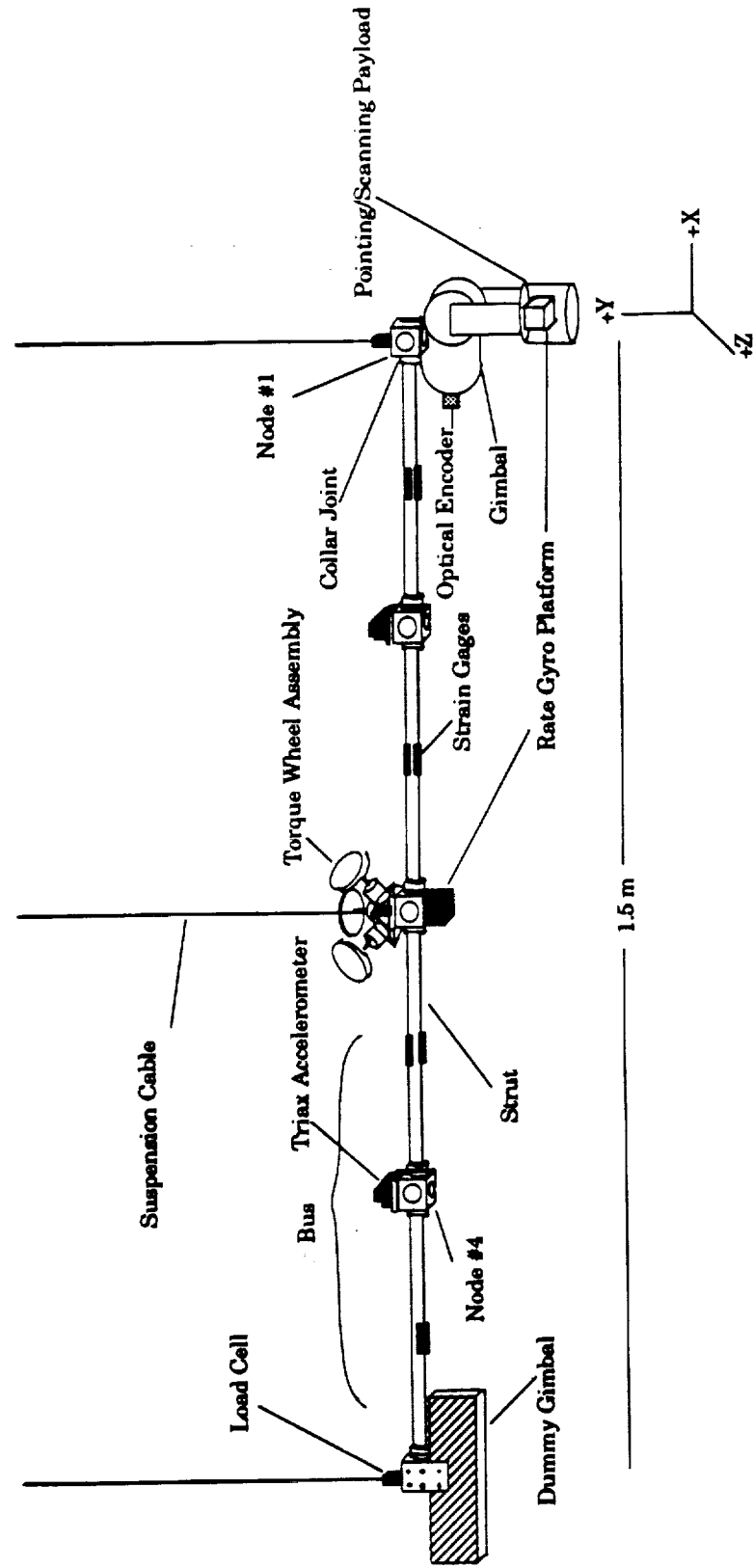
For future vehicles which cannot be dynamically tested on the ground in a sufficiently realistic zero-gravity simulation, this procedure will increase confidence in the eventual orbital performance of such spacecraft.

Implications:

- Understand direct gravity and suspension effects.**
- Develop analytical and ground test methods for predicting 0-g performance.**
- Develop techniques for system identification on orbit.**
- Develop controllers using on-orbit system identification data.**

A MULTIPLE PAYLOAD PLATFORM TEST ARTICLE WAS SELECTED IN ORDER TO BE REPRESENTATIVE OF A FUTURE MISSION ARCHITECTURE AND TO ENSURE SIGNIFICANT GRAVITY PERTURBATIONS TO THE STRUCTURAL DYNAMICS DURING GROUND TESTING. THE CURRENT CONFIGURATION OF THE HARDWARE CONTAINS ONE TWO-AXIS GIMBALLING PAYLOAD, AN ATTITUDE CONTROL TORQUE WHEEL ASSEMBLY AND VARIOUS INERTIAL AND STRUCTURAL SENSORS. WHEN THESE COMPONENTS ARE INTERCONNECTED BY A FLEXIBLE, LEXAM™ STRUCTURAL BUS, THE FUNDAMENTAL BENDING MODE HAS A FREQUENCY OF 1.7 HERTZ.

HARDWARE DESCRIPTION



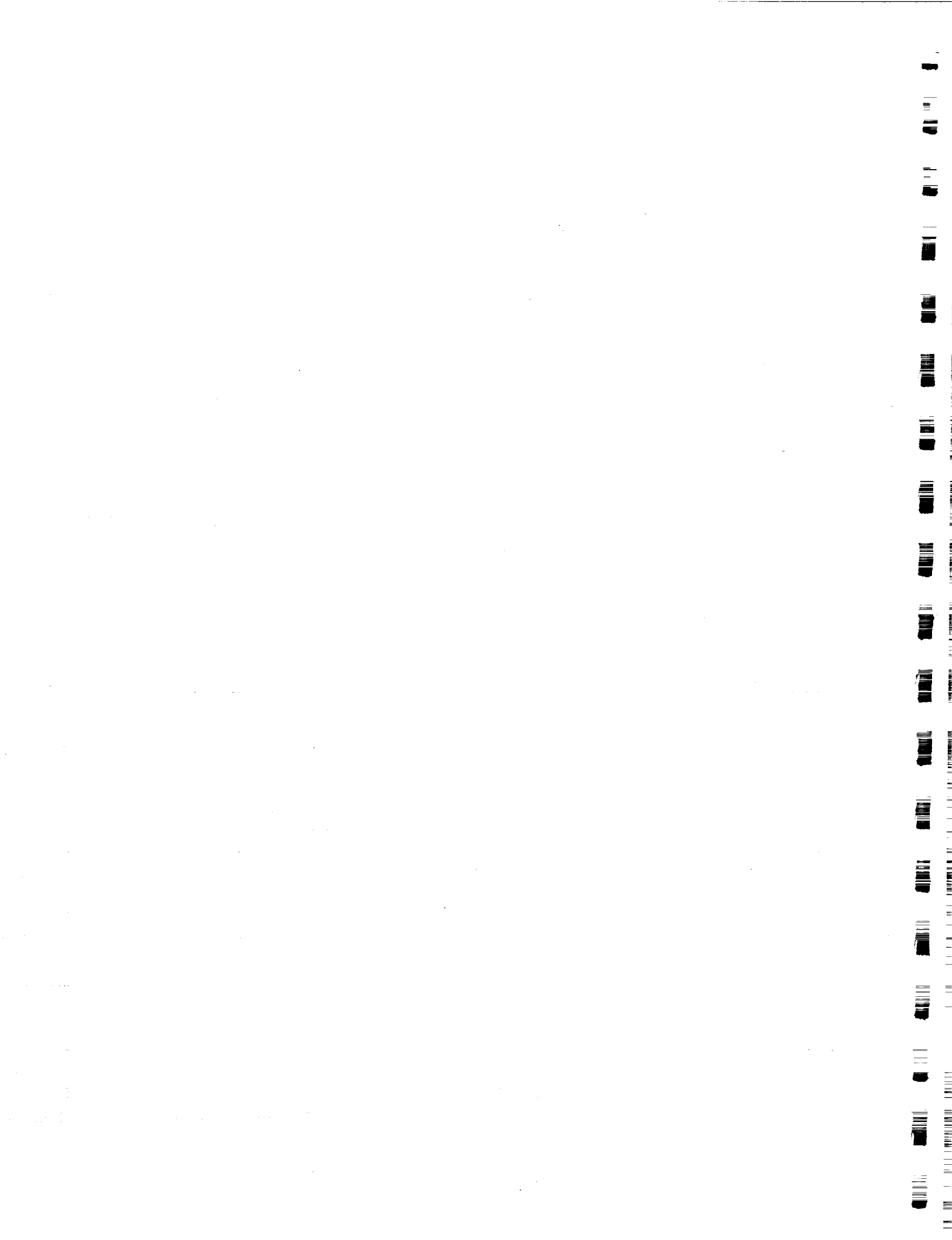
MAKING A PRECISION SPACECRAFT OPERATE AS REQUIRED ONCE ON ORBIT IMPLIES TWO APPROACHES. FIRST, THE CONTROL CAN BE BASED UPON ANALYTICAL PREDICTIONS OF 0-G BEHAVIOR. SECOND, THE BEHAVIOR OF THE SPACECRAFT CAN BE MEASURED ON ORBIT AND THE CONTROL CAN BE REDESIGNED. MACE FOLLOWS BOTH PATHS IN ORDER TO DETERMINE HOW MUCH PERFORMANCE CAN BE ACHIEVED THROUGH ANALYTICAL PREDICTIONS AND HOW MUCH ADDITIONAL PERFORMANCE CAN BE ACHIEVED THROUGH CONTROL REDESIGN BASED UPON ON-ORBIT MEASUREMENTS.

ANALYSIS AND GROUND TESTING ARE USED IN CONCERT IN ORDER TO DEVELOP PREDICTIONS OF ON-ORBIT BEHAVIOR. AN ANALYTICAL FINITE ELEMENT MODEL OF THE TEST ARTICLE IS DEVELOPED. VARIOUS GRAVITY AND SUSPENSION EFFECTS ARE INCORPORATED INTO THIS MODEL TO GENERATE PREDICTIONS OF 1-G BEHAVIOR. DATA FROM MODAL, OPEN-LOOP GROUND TESTING OF THE TEST ARTICLE IS USED TO REFINE THIS MODEL. ONCE REFINED, CONTROL IS DERIVED AND IMPLEMENTED ON THE SUSPENDED TEST ARTICLE. RESULTS OF THESE CLOSED-LOOP TESTS REVEAL DYNAMICS WHICH HAVE BEEN MISMODELED ENABLING FURTHER REFINEMENT OF THE FINITE ELEMENT MODEL.

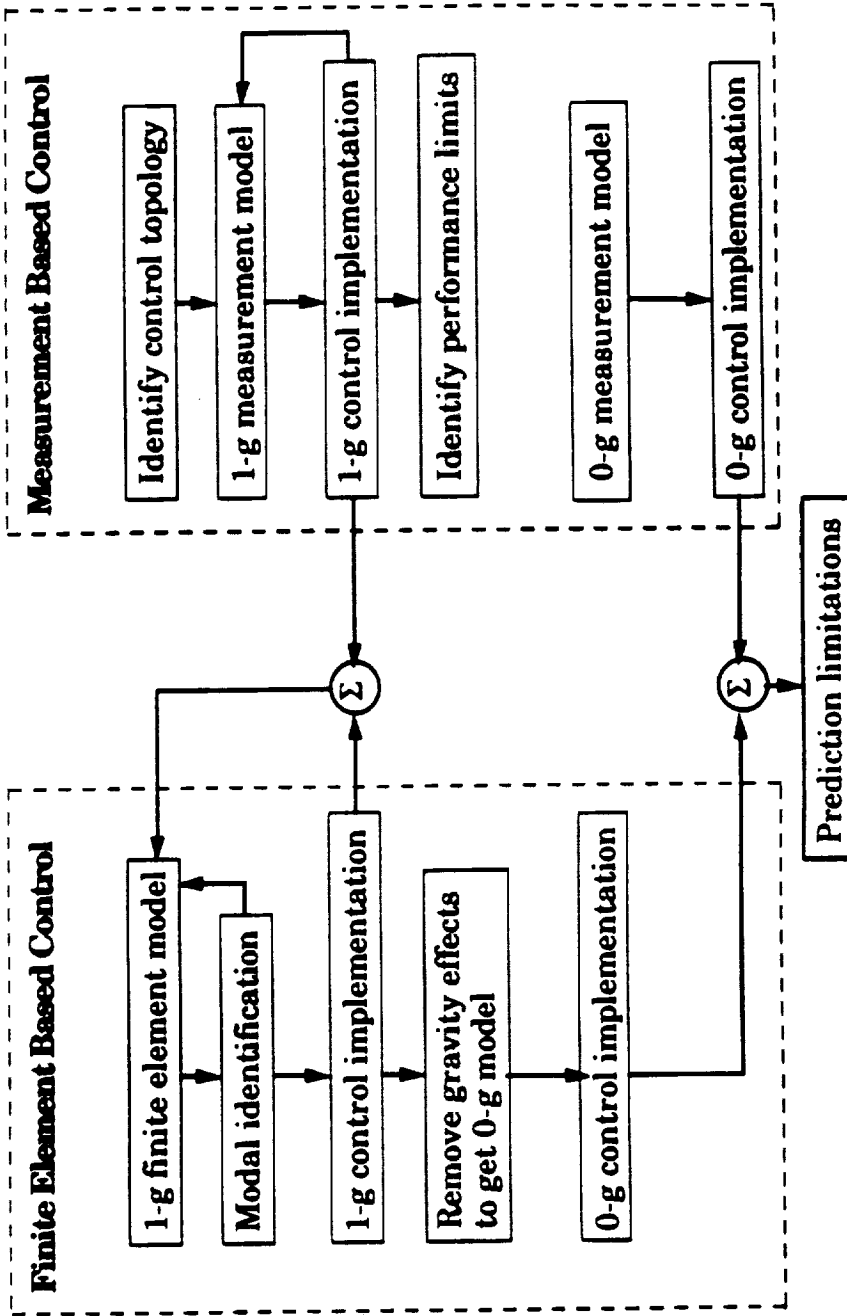
IN PARALLEL WITH THIS GROUND TEST EFFORT, CONTROLLERS ARE DERIVED BASED UPON MODELS GENERATED FROM GROUND TEST MEASUREMENTS. IT IS ARGUABLE THAT SUCH MODELS ARE MORE ACCURATE THAN FINITE ELEMENT MODELS. THEREFORE, THE PERFORMANCE ACHIEVED USING MEASUREMENT BASED CONTROL PROVIDES AN INDICATION OF THE MAXIMUM PERFORMANCE THAT IS PRACTICALLY FEASIBLE. THIS INFORMATION ALLOWS A DETERMINATION AS TO THE COST-BENEFIT OF FURTHER REFINEMENT OF THE FINITE ELEMENT MODEL. IN OTHER WORDS, IF BOTH FINITE ELEMENT AND MEASUREMENT BASED CONTROLLERS YIELD ABOUT THE SAME PERFORMANCE, FURTHER REFINEMENT OF THE FINITE ELEMENT MODEL MAY YIELD LITTLE IMPROVEMENT.

AT THIS POINT, THE GRAVITY EFFECTS ARE REMOVED FROM THE FINITE ELEMENT MODEL YIELDING A PREDICTION OF 0-G BEHAVIOR. THIS 0-G ANALYTICAL MODEL IS USED

TO DERIVE CONTROL FOR IMPLEMENTATION ON ORBIT. BY IMPLEMENTING THESE O-G
CONTROLLERS AT VARIOUS LEVELS OF CONTROL AUTHORITY, DEVIATIONS BETWEEN
MEASURED AND PREDICTED PERFORMANCE REVEAL LIMITATIONS IN PREDICTION
ACCURACY.



SCIENCE APPROACH



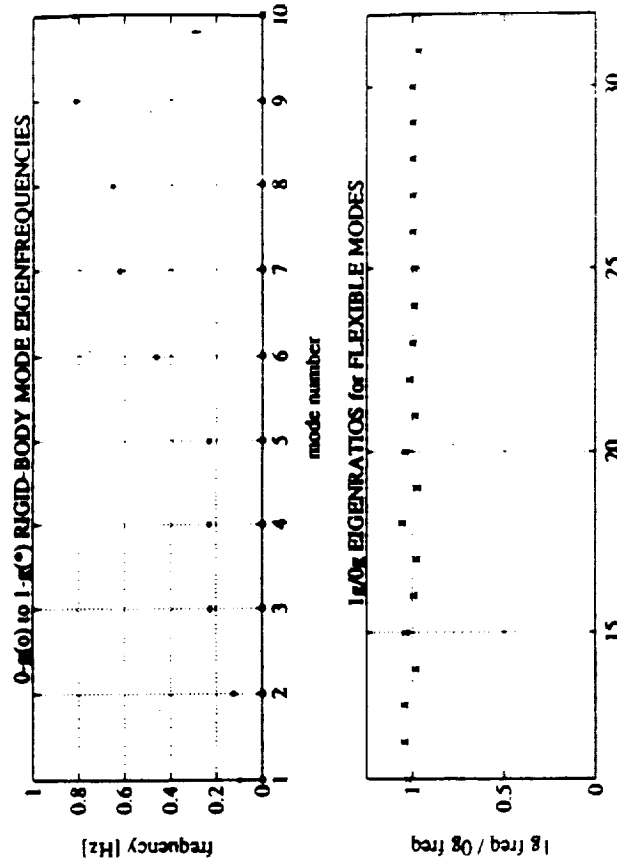
PRECEDING PAGE BLANK NOT FILMED

GRAVITY EFFECTS CAN PERTURB OPEN-LOOP BEHAVIOR BY SHIFTING FREQUENCIES AND DISTORTING MODE SHAPES. RIGID BODY MODES BECOME SUSPENSION MODES. THE FREQUENCIES OF FLEXIBLE MODES OF A STRUCTURE WITH 1% DAMPING CAN BE SHIFTED IN EXCESS OF THREE HALF POWER BANDWIDTHS. THIS HAS SERIOUS IMPLICATIONS FOR ROBUST CONTROL.

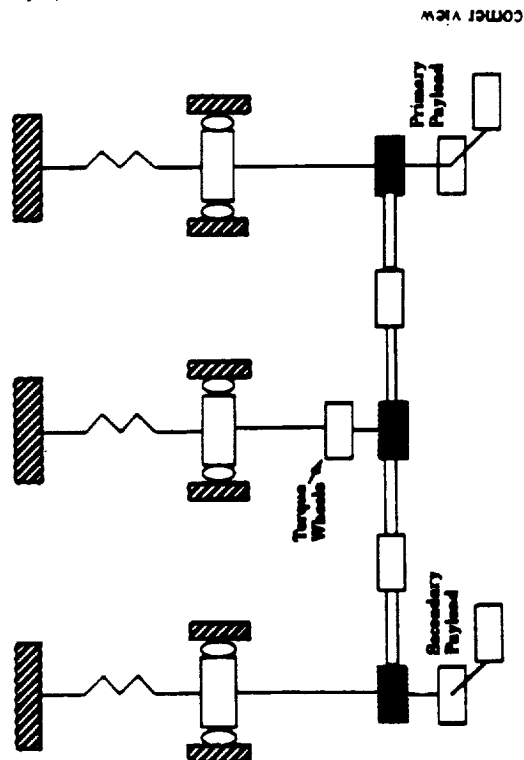
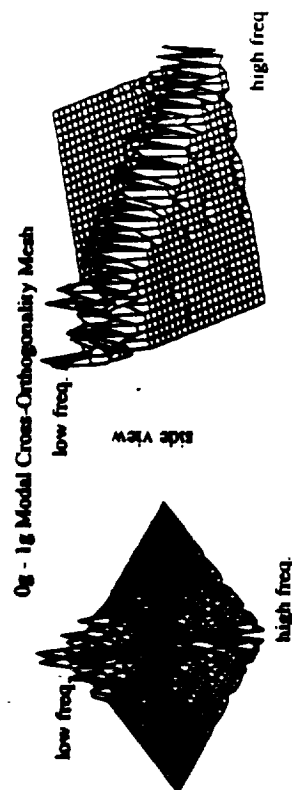
SUSPENSION AND GRAVITY EFFECTS

Classes of effect:

- Suspension
- Nonlinear
- Pre-load stiffness
- Static Pre-deformations
- Direct sensor & actuator



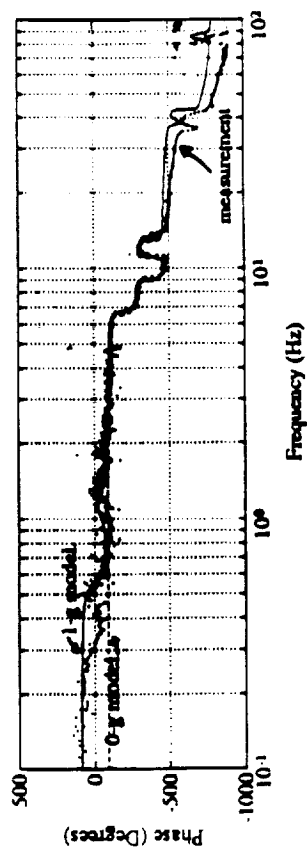
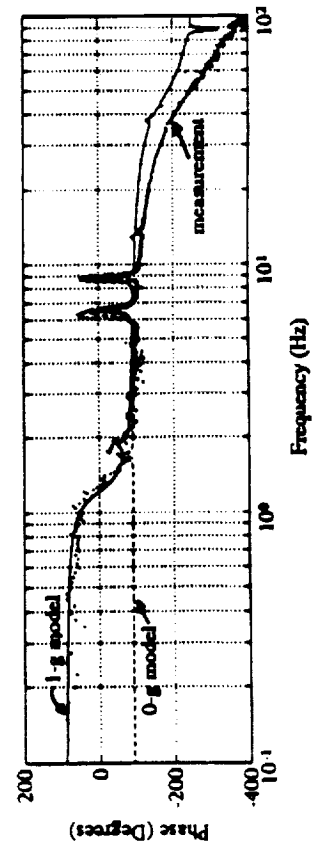
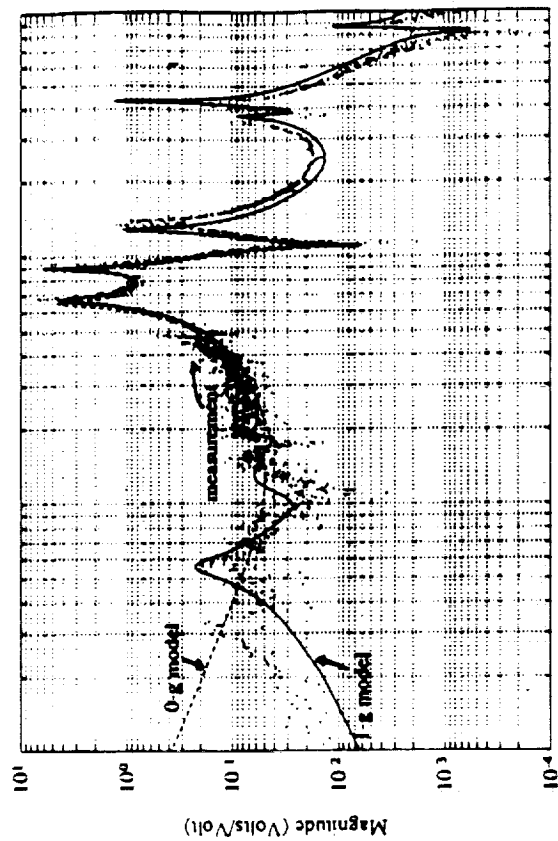
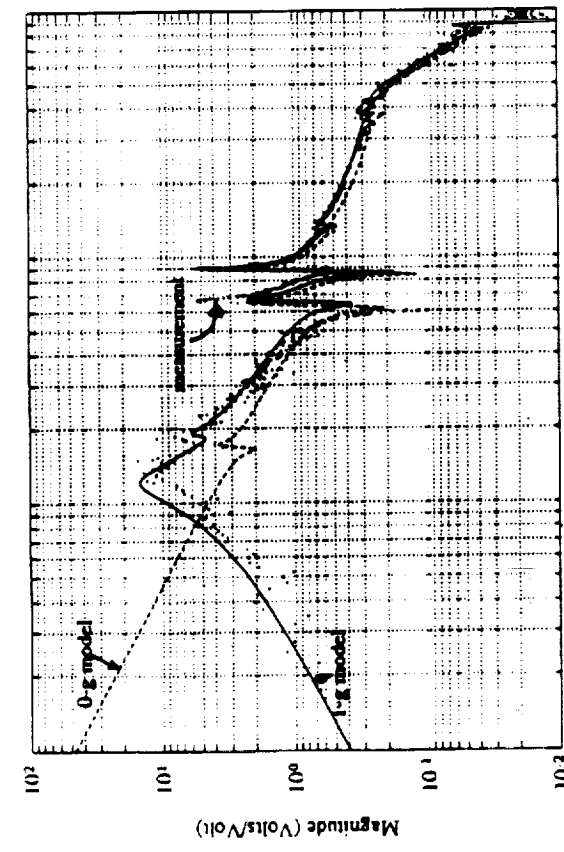
Gravity induced eigenvalue shifts.



Simplified model for study of gravity and suspension effects.

FINITE ELEMENT MODELS OF BOTH 0-G AND 1-G BEHAVIOR HAVE BEEN COMPARED WITH GROUND TEST MEASUREMENTS. THE 1-G FINITE ELEMENT MODEL PREDICTIONS OF TRANSFER FUNCTIONS WHILE INVOLVE MOTION OF THE TEST ARTICLE IN PRIMARILY THE VERTICAL PLANE COMPARE WELL WITH THE MEASURED TRANSFER FUNCTIONS.

MACE 1-G AND 0-G MODELS



Transfer function from z-axis
gimbal torque to z-axis payload
inertial angular rate.

Transfer function from z-axis
gimbal torque to z-axis bus inertial
angular rate.

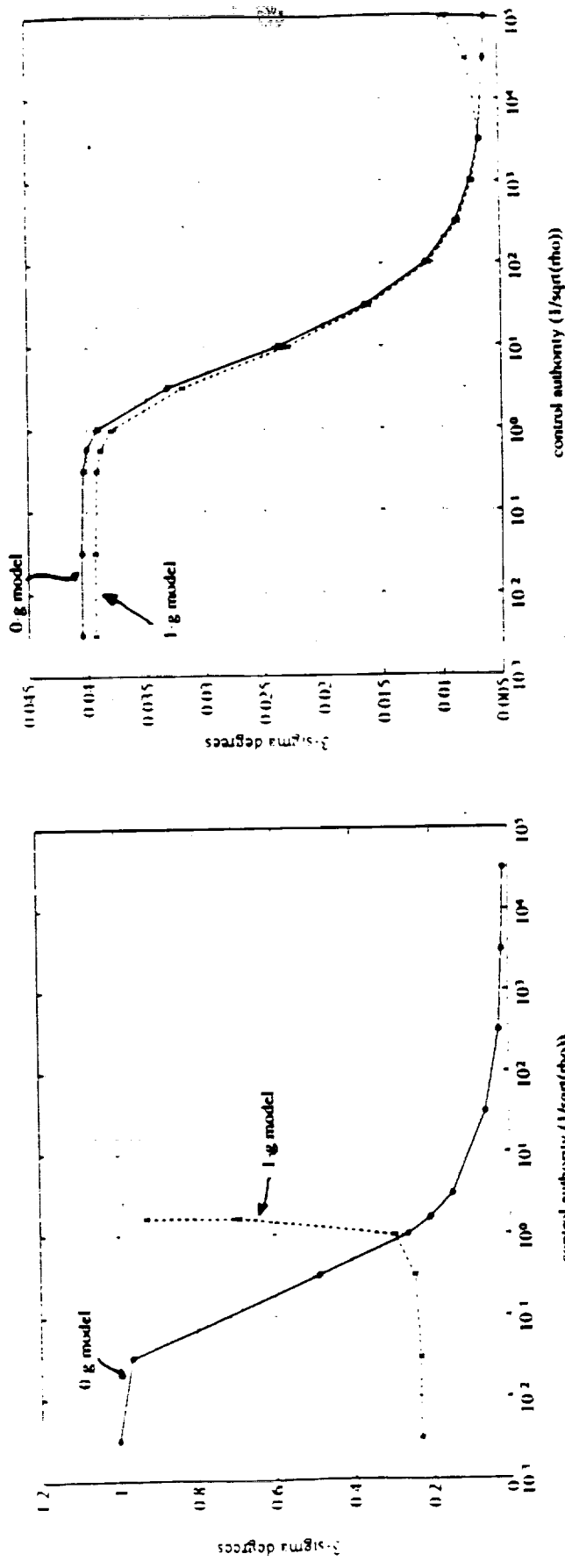
A CLOSED-LOOP ANALYSIS OR GRAVITY PERTURBATIONS WAS ALSO PERFORMED. A MODEL OF 0-G BEHAVIOR WAS USED TO DERIVE CONTROL. THE SPACECRAFT PERFORMANCE WAS THEN EVALUATED BY IMPINGING THIS 0-G CONTROL ON BOTH THE MODEL OF 0-G AND 1-G BEHAVIOR. AS MIGHT BE EXPECTED, WHEN THE 0-G CONTROL IS EVALUATED ON THE 0-G MODEL, PERFORMANCE IMPROVES WITH INCREASING CONTROL AUTHORITY. HOWEVER, A SUSPENSION MODE IN THE 1-G MODEL IS RAPIDLY DESTABILIZED WITH INCREASING CONTROL AUTHORITY.

IT WAS ALSO OF INTEREST TO INVESTIGATE THE GRAVITY PERTURBATIONS ON THE FLEXIBLE DYNAMICS. WITH THE SUSPENSION MODES REMOVED FROM THE 1-G MODEL, A PLOT WAS DERIVED SHOWING PERFORMANCE AS A FUNCTION OF CONTROL AUTHORITY. AGAIN, INSTABILITY OCCURS IN THE 1-G MODEL BUT AT A HIGHER LEVEL THAN THE SUSPENSION MODE. THEREFORE, BOTH SUSPENSION COUPLING AND FLEXIBLE MODE PERTURBATIONS ARE OF CONCERN WHEN EVALUATING A FLIGHT CONTROLLER IN A 1-G SIMULATION.

GRAVITY INFLUENCE ON CONTROL

Motivation:

Analyze implications of testing in a 1-g environment when control has been derived using a model of 0-g behavior.
Such a scenario would be typical of preflight qualification testing for a flexible spacecraft.



Performance vs. control authority
for entire model.

Performance vs. control authority
for flexible portion of model.

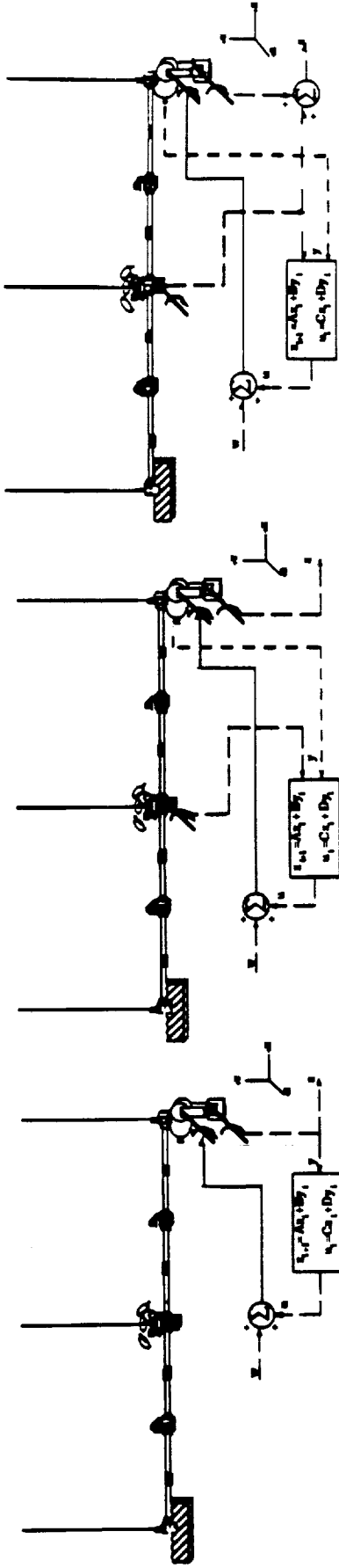
MEASUREMENT BASED CONTROL EXPERIMENTS HAVE ALSO BEEN CONDUCTED ON THE GROUND. THREE DIFFERENT CONTROL TOPOLOGIES WERE USED.

MEASUREMENT BASED LQG CONTROL

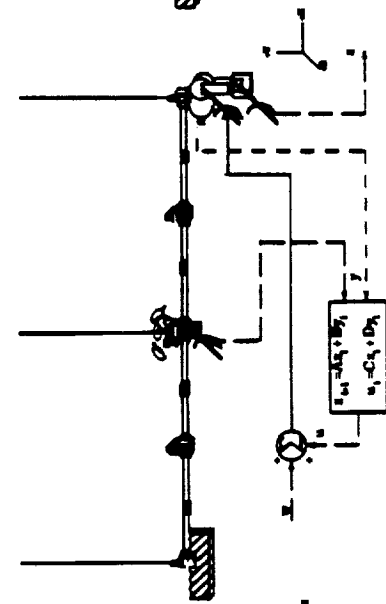
Three control topologies were implemented to minimize:

- 1 payload inertial angle by feeding it to gimbal torque.
- 2 payload inertial angle by feeding relative gimbal and bus inertial angles to gimbal torque.
- 3 payload and bus inertial angles by feeding gimbal relative and bus inertial angles to gimbal torque.

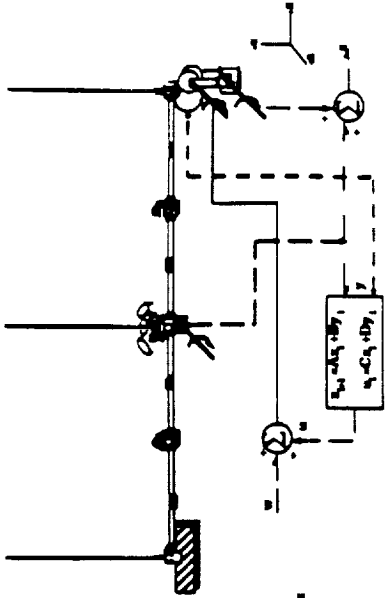
Additive white noise generated a gimbal torque disturbance.



**Topology #1: SISO
payload penalty**



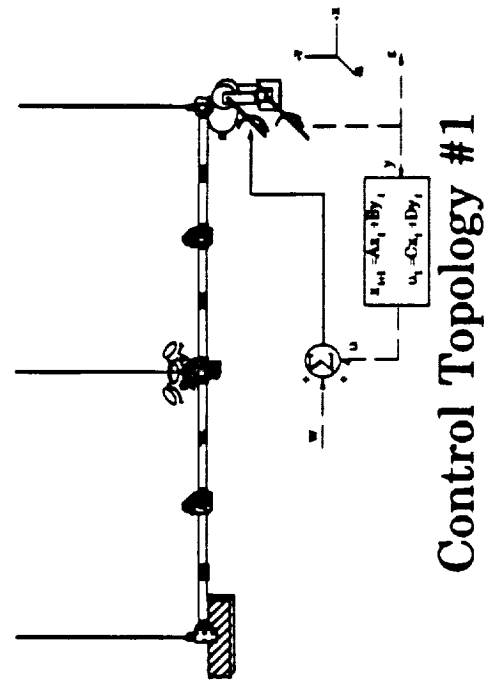
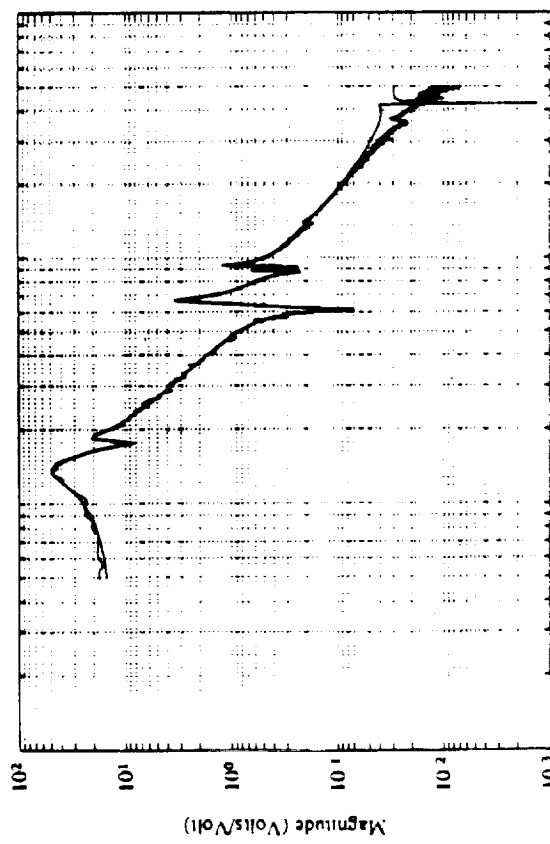
**Topology #2: SITO
payload penalty**



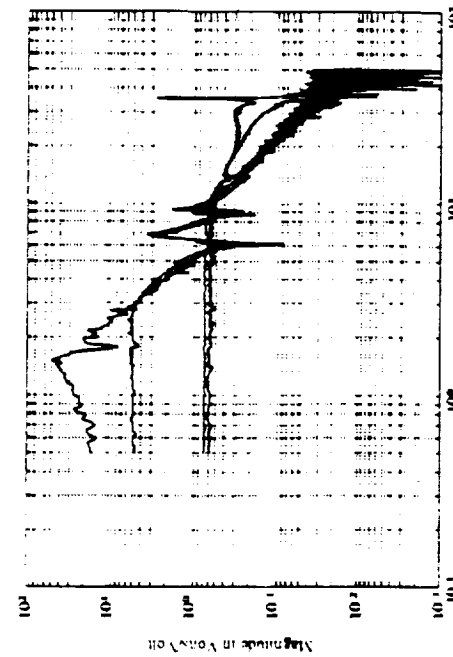
**Topology #3: SIT0
payload & bus penalty**

POLES, ZEROS, A GAIN AND A TIME DELAY ARE FITTED TO THE MEASURED TRANSFER FUNCTION. THESE PARAMETERS ARE USED TO GENERATE A STATE-SPACE MODEL. CONTROL BASED ON THIS MODEL EXHIBITED WELL OVER AN ORDER OF MAGNITUDE REDUCTION IN PAYLOAD POINTING ERROR. FOUR CURVES ARE SHOWN IN THE FIGURE IN THE LOWER RIGHT. THE HIGHEST CURVE IS THE OPEN-LOOP TRANSFER FUNCTION FROM THE WHITE NOISE GIMBAL TORQUE (DISTURBANCE) TO THE INERTIAL ANGLE OF THE PAYLOAD (PERFORMANCE METRIC). THE MIDDLE TWO CURVES SHOW THE CLOSED-LOOP TRANSFER FUNCTIONS FOR TWO DIFFERENT LEVELS OF LINEAR QUADRATIC GAUSSIAN (LQG) CONTROL AUTHORITY. THESE TRANSFER FUNCTIONS WERE MEASURED ONE DAY AFTER THE DATA FOR THE MODEL WAS MEASURED. WHEN THE CONTROL CORRESPONDING TO THE LOWER OF THESE TWO CURVES WAS IMPLEMENTED ONE MONTH LATER, THE CLOSED-LOOP BEHAVIOR WAS UNSTABLE DUE TO A SLIGHT SHIFT IN THE FREQUENCIES OF THE MODES NEAR 9 HERTZ. THE SECOND TO HIGHEST CURVE IN THE FIGURE SHOWS THE PERFORMANCE OF THE HIGHEST AUTHORITY, STABLE CONTROLLER DURING THESE TESTS PERFORMED ONE MONTH LATER. A MULTIPLE MODEL LQG DESIGN TECHNIQUE WAS USED TO DESIGN A CONTROLLER USING THE SAME, MONTH OLD DATA. THE PERFORMANCE OF THIS CONTROLLER IS SHOWN BY THE LOWEST CURVE IN THE FIGURE. HOWEVER, A MODE 34 HERTZ WAS NEARLY UNSTABLE DUE TO THE FACT THAT IT WAS NOT INCLUDED IN THE MODEL. THE MULTIPLE MODEL TECHNIQUE FORMULATES A CONTROLLER WHICH WILL BE STABLE FOR SEVERAL DIFFERENT MODELS. IN THIS EXPERIMENT, TWO MODELS WERE USED WITH THE FREQUENCIES OF THE MODES NEAR 9 HERTZ SLIGHTLY SHIFTED.

SINGLE-INPUT, SINGLE-OUTPUT CONTROL



Control Topology #1

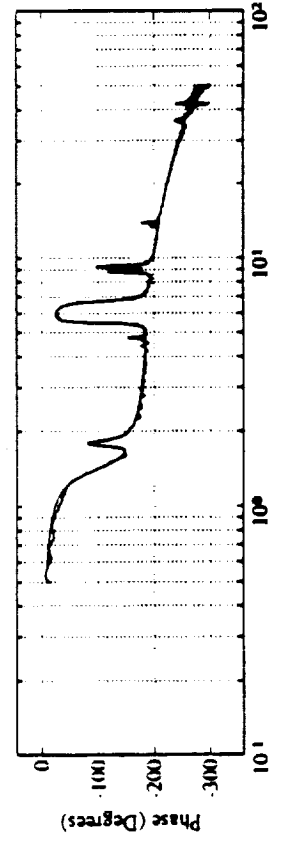
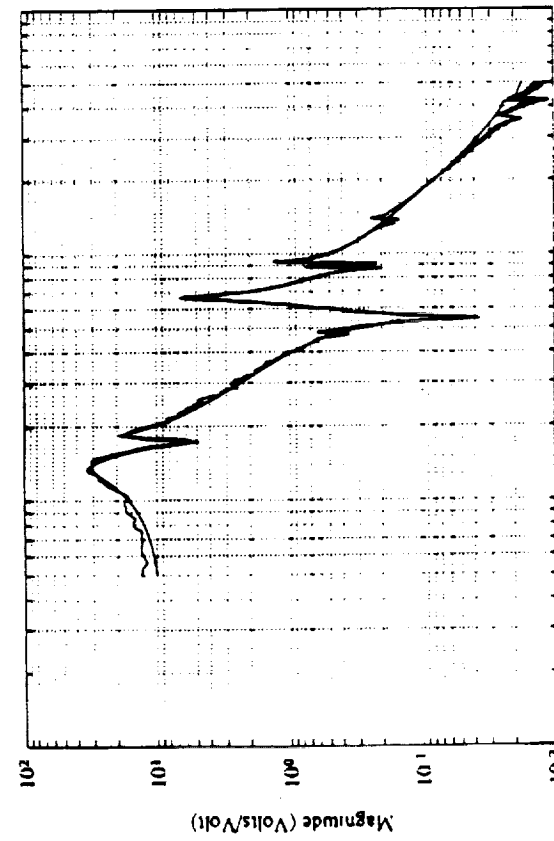


Measurement model and transfer function data from gimbal torque to payload inertial angle.

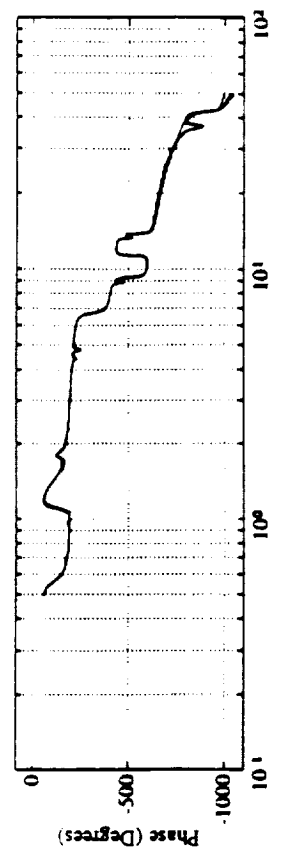
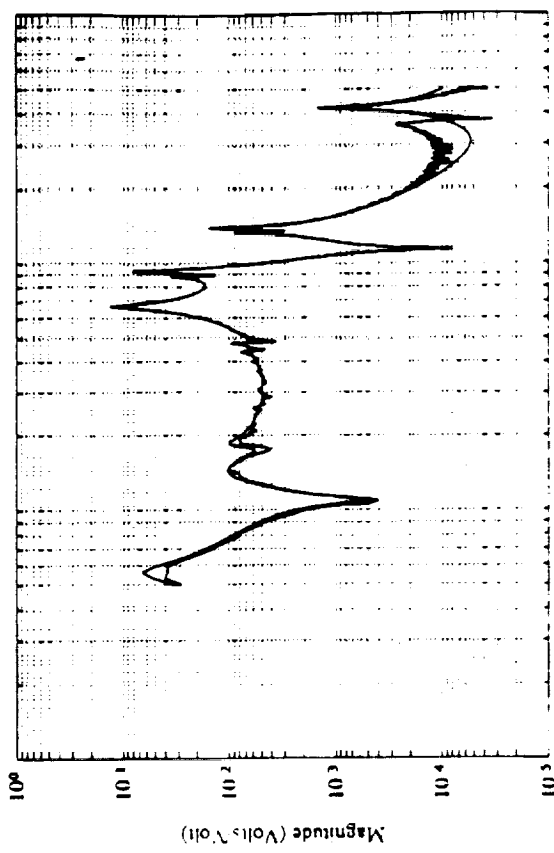
Transfer functions from gimbal to payload inertial angle

IN ORDER TO REALIZE THE SECOND AND THIRD CONTROL TOPOLOGIES, TWO ADDITIONAL TRANSFER FUNCTIONS NEEDED TO BE MEASURED. AGAIN, THESE TRANSFER FUNCTIONS WERE FITTED USING A NONLINEAR FREQUENCY DOMAIN FITTING ROUTINE WHICH MINIMIZES THE DIFFERENCE BETWEEN THE LOGARITHMIC VALUES OF THE COMPLEX TRANSFER FUNCTION DATA AND FIT. THIS ENABLES THE ROUTINE TO FIT THE POLES AND ZEROS EQUALLY WELL.

SINGLE-INPUT, TWO-OUTPUT MODEL



Measurement model and transfer function data from gimbal torque to gimbal relative angle.



Measurement model and transfer function data from gimbal torque to bus inertial angle.

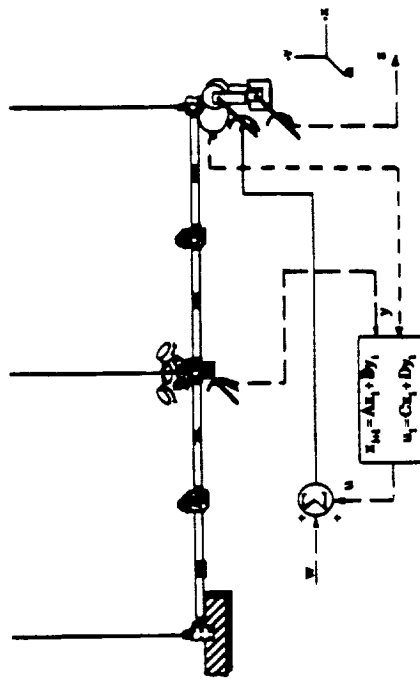
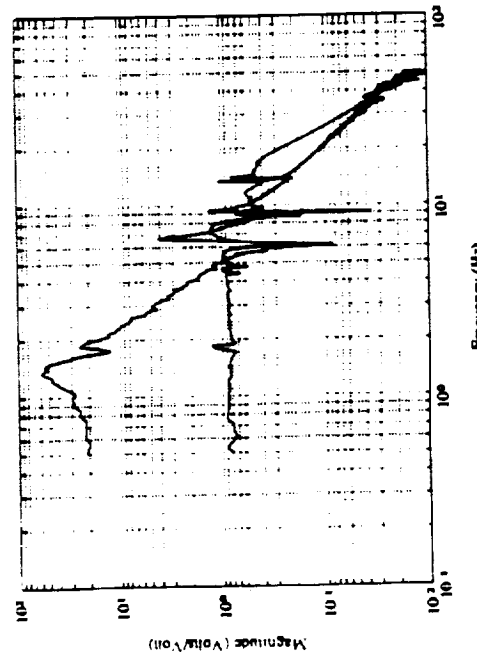
IN THE SECOND CONTROL TOPOLOGY, THE LACK OF PHASE MARGIN NEAR 9 HERTZ GENERATED A NEED FOR LEAD COMPENSATION. A PAIR OF ZEROS BELOW 9 HERTZ FOLLOWED BY A PAIR OF POLES JUST ABOVE 9 HERTZ RESTORED ADEQUATE MARGIN.

SINGLE-INPUT, TWO-OUTPUT WITH PAYLOAD PENALTY

The bus inertial angle, gimbal relative angle and measurement model make the payload inertial angle observable.

Plant inversion in the LQG compensator makes control highly sensitive to model uncertainty.

Lead compensation near 9 Hz. maintained adequate phase margin.

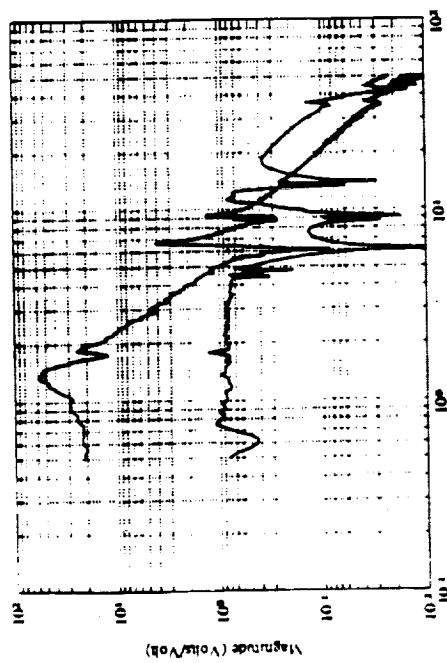


Transfer functions from gimbal to payload inertial angle

Control Topology #2

IN THE THIRD CONTROL TOPOLOGY, THE ADDITION OF THE BUS INERTIAL ANGLE TO THE PERFORMANCE METRIC FORCES THE CONTROL TO AUGMENT POINTING OF THE PAYLOAD WITH VIBRATION SUPPRESSION IN THE BUS.

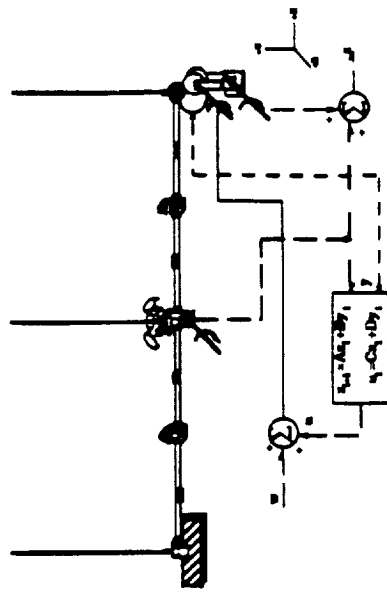
SINGLE-INPUT, TWO-OUTPUT WITH PAYLOAD AND BUS PENALTY



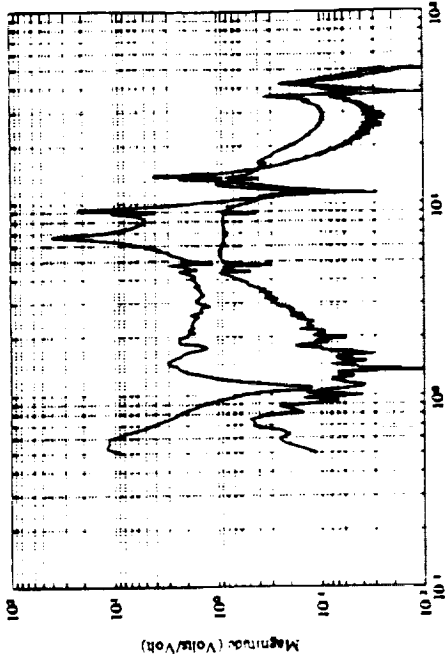
Transfer functions from gimbal to payload inertial angle

Transfer functions from gimbal to bus inertial angle

- Payload pendulum and first bending modes are suppressed
- In addition, higher frequency flexible modes are suppressed.
- An order of magnitude reduction in pointing error is achieved.

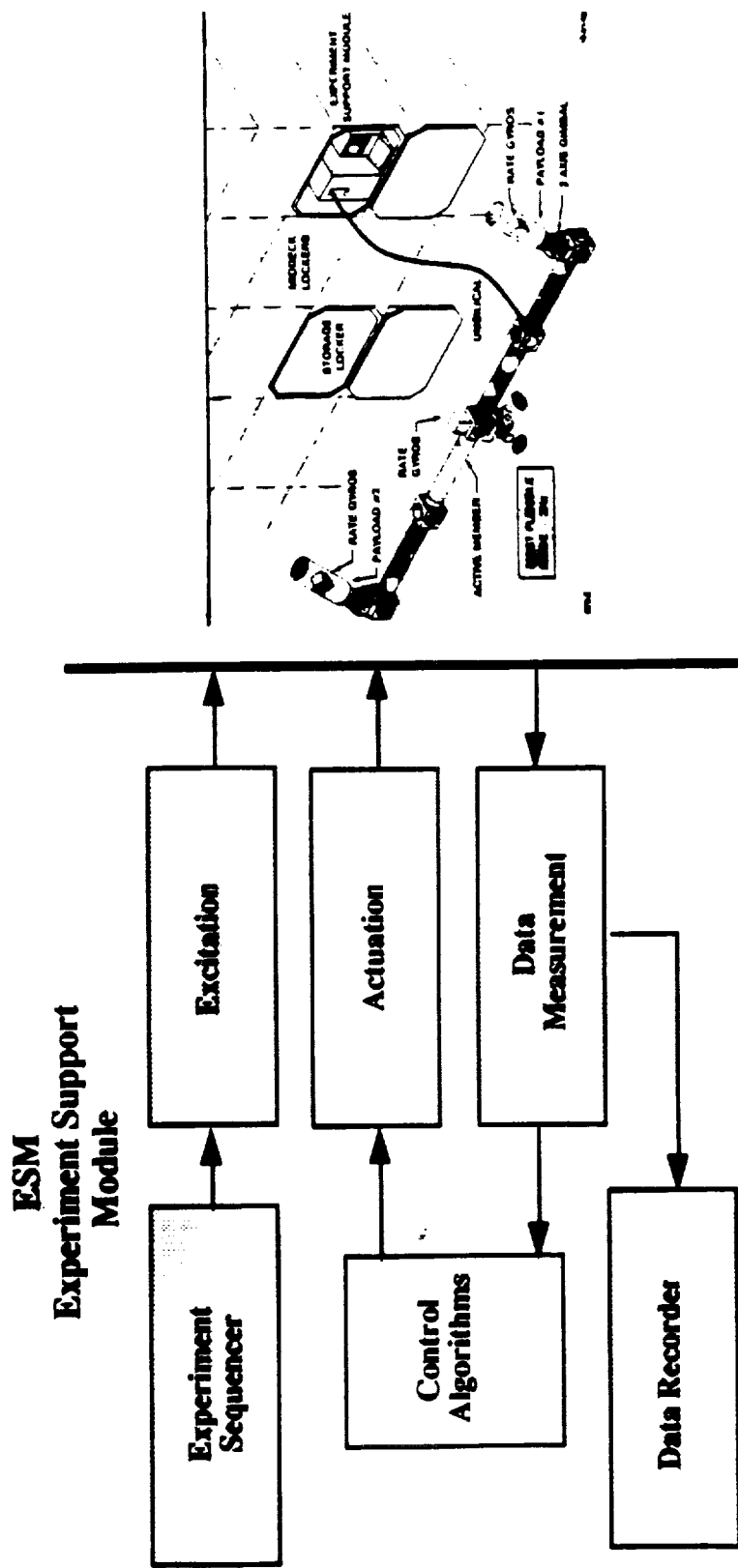


Control Topology #3



PRIOR TO DISCUSSION OF THE ON-ORBIT SCIENCE OPERATIONS, IT IS USEFUL TO BRIEFLY DESCRIBE SOME RELEVANT ASPECTS OF THE FLIGHT EXPERIMENT. THE TEST ARTICLE WILL BE STORED IN LOCKERS AND ASSEMBLED IN THE SHUTTLE MIDDECK. THE POWER AND SIGNAL WIRES ARE PRE-INTEGRATED INTO THE BUS ALLOWING SIMULTANEOUS MECHANICAL AND ELECTRICAL CONNECTIONS DURING ASSEMBLY. THE TEST ARTICLE IS LIGHTLY TETHERED IN THE MIDDECK TO PREVENT AIR CURRENTS AND CREW TIP OFF RATES FROM INDUCING DRIFT. THE TEST ARTICLE ELECTRONICS ARE CONNECTED THROUGH AN UMBILICAL TO AN ELECTRONICS PACKAGE STORED IN ONE OF THE MIDDECK LOCKERS. THIS ELECTRONICS PACKAGE CONTAINS THE FUNCTIONS OF EXPERIMENT SEQUENCING, REAL TIME FEEDBACK CONTROL AND DATA ACQUISITION AND STORAGE. OPERATIONS WILL OCCUR OVER THREE EIGHT HOUR DAYS OF ONE CREW MEMBER.

FLIGHT EXPERIMENT RESOURCES



- Three eight hour days of one crew member.
- Test article and support equipment stored in 3 middeck lockers.
- ESM stored in a fourth middeck locker.
- Wiring is pre-integrated in the test article for ease of assembly.

SELF-EXPLANATORY.

FLIGHT EXPERIMENT SCIENCE OPERATIONS

Conduct an open-loop identification at the beginning of each day.

Downlink first day's system identification data

- Assess functionality of test article and support electronics.
 - Restructure sequence of control protocols if necessary.
 - Develop 0-g measurement model for control derivation.
- Implement algorithms based on model of predicted 0-g behavior.

- The gravity and suspension effects in the 1-g model are removed and the control algorithms are derived.
- These tests determine the accuracy to which 0-g closed-loop performance can be predicted.

Implement algorithms based upon 0-g measurement model.

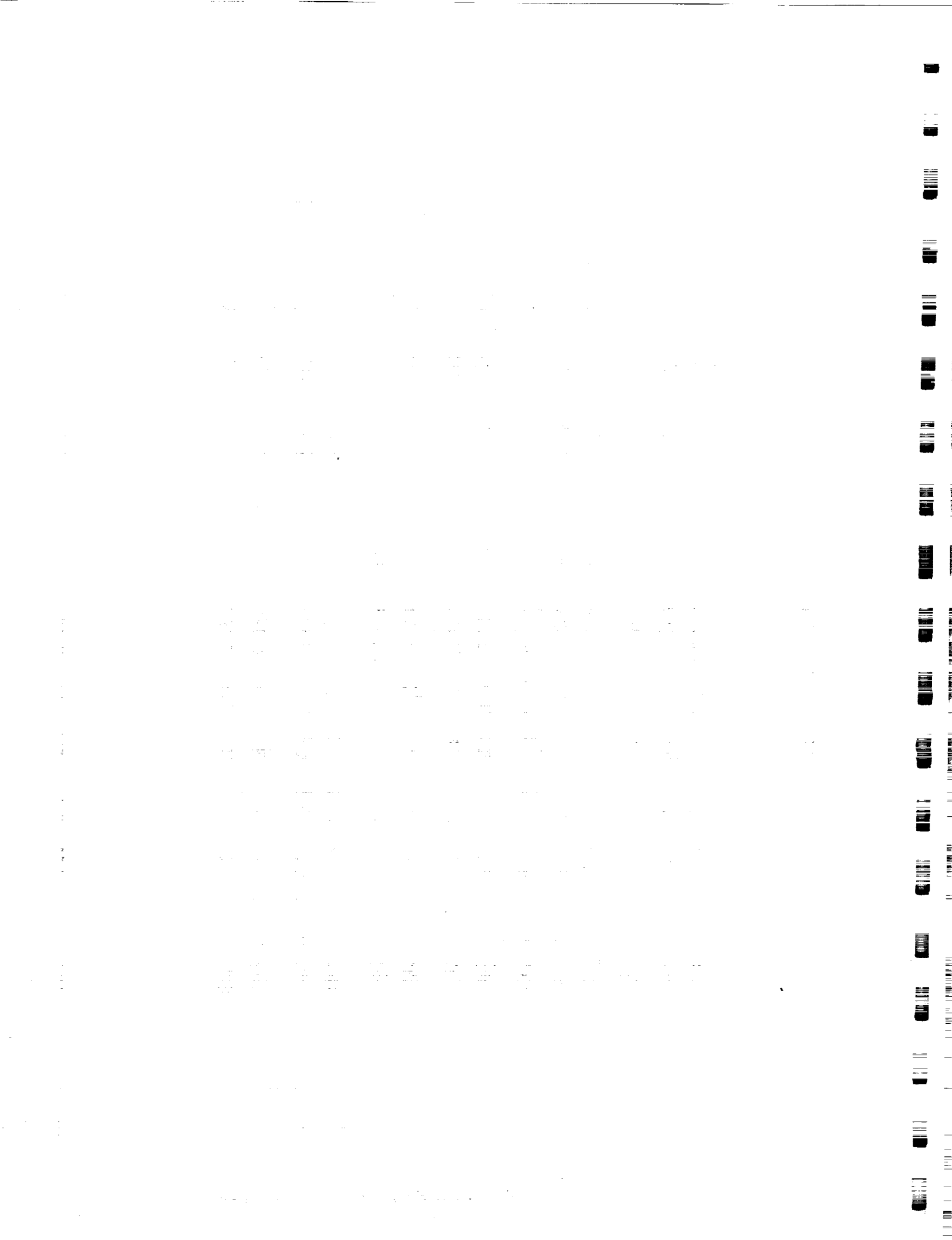
- Downlink of open-loop identification data and uplink of associated control algorithms.
- These tests identify the ability to which the test article's performance can be tuned on orbit.

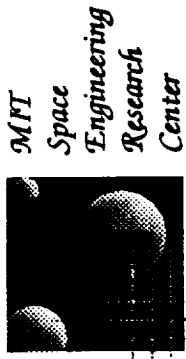
SELF-EXPLANATORY.

Space Engineering Research Center

SUMMARY

- The MODE family of flight experiments is designed to verify analytical tools developed to predict the gravity dependent behavior of proposed space structures.
- The MODE family of flight experiments uses reusable dynamic and control test facilities and exploits the shirt sleeve environment on the STS middeck.
- MACE investigates gravity dependent phenomena pertinent to the closed-loop dynamics of proposed space structures.
- Gravity and suspension effects perturb the MACE test article flexible modes when tested on the ground.
- Suspension mode stabilization can obscure important gravity influences on the flexible behavior during 1-g closed-loop testing.
- Measurement models have been used successfully to achieve over an order of magnitude improvement in pointing accuracy.





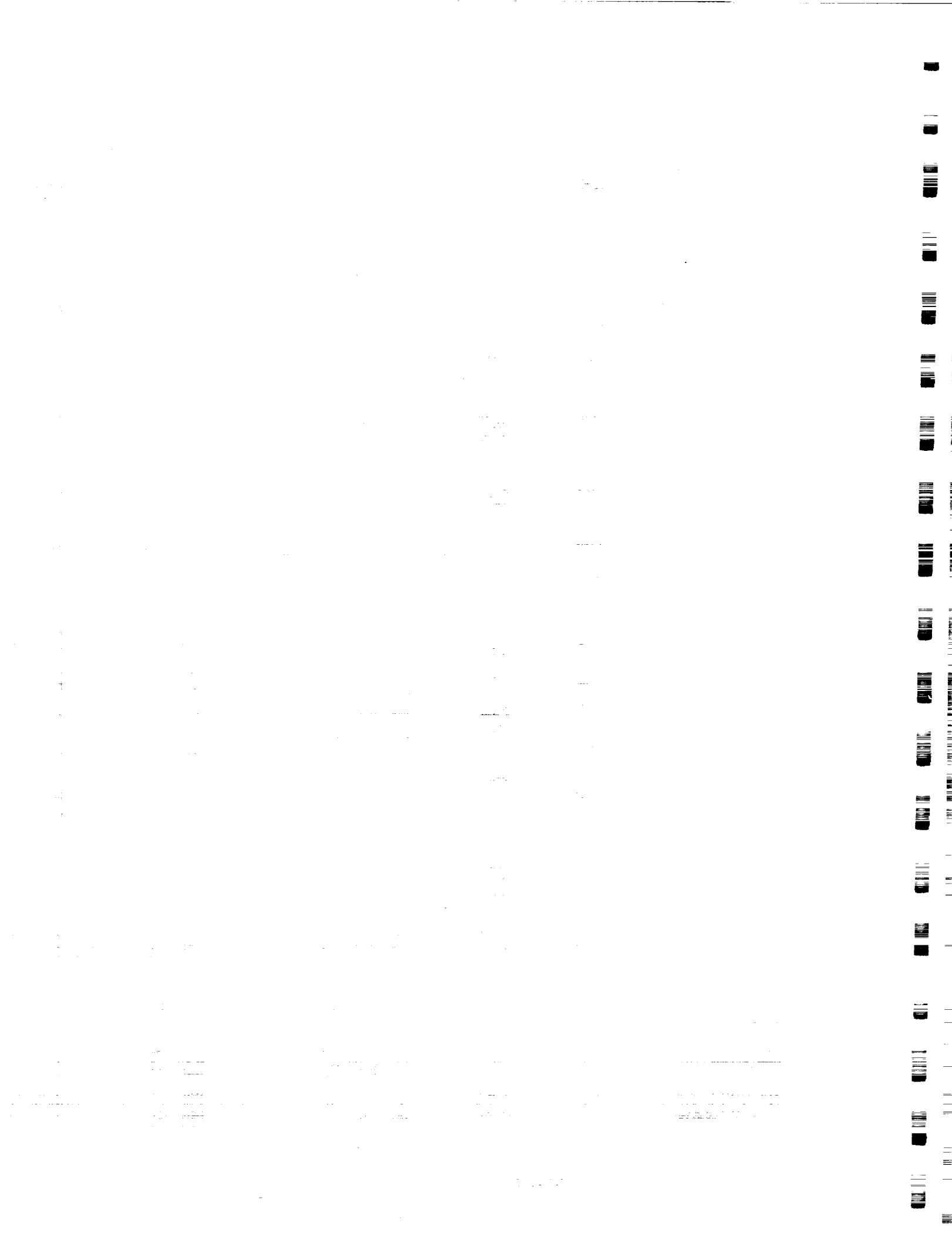
THE MIDDECK ACTIVE CONTROL EXPERIMENT:

GRAVITY AND SUSPENSION EFFECTS

Dr. E. F. Crawley
Dr. H. Alexander
Mr. Daniel Rey

MIT
MIT
MIT

SERC Steering Committee Workshop
January 22 and 23, 1992



OUTLINE

- Motivation and Objectives
- Approach
- Overview of Gravity and Suspension Effects
- Modelling of Gravity and Suspension Effects
 - Effects on Structure
 - Effects on Sensors and Actuators
- Application to MACE
 - EM Configuration Study and DM Modelling
 - Objectives
 - Approach
 - Results
- Conclusions
- Future Work

GRAVITY AND SUSPENSION INFLUENCES

THE MACE SCIENCE OBJECTIVE IS TO DEVELOP A QUALIFICATION PROCEDURE FOR FLEXIBLE PRECISION SPACECRAFT. THIS PROCEDURE WILL INCREASE THE CONFIDENCE IN THE EVENTUAL ORBITAL PERFORMANCE OF FUTURE VEHICLES WHICH CANNOT BE DYNAMICALLY TESTED ON THE GROUND IN A SUFFICIENTLY REALISTIC ZERO-GRAVITY SIMULATION.

CONTROLLED STRUCTURES IN PARTICULAR STAND TO BENEFIT FROM THE DEVELOPMENT OF SUCH A QUALIFICATION PROCEDURE AS IT IS MOST OFTEN NECESSARY TO PERFORM CLOSED-LOOP TESTS ON ACTUAL HARDWARE TO VERIFY THEIR STABILITY AND PERFORMANCE. SINCE, FOR PRACTICAL REASONS, THESE VERIFICATION TESTS ARE PERFORMED ON THE GROUND IT IS IMPORTANT TO UNDERSTAND THE EFFECTS OF GRAVITY AND OF THE SUSPENSION SYSTEM. IF INCLUDED IN THE SYSTEM MODEL IT IS POSSIBLE TO REFINE THE MODEL USING GROUND-BASED TEST DATA AND THEN REMOVE THE SUSPENSION SYSTEM AND GRAVITY EFFECTS FROM THE MODEL FOR A MORE ACCURATE ZERO-G MODEL.

GRAVITY AND SUSPENSION INFLUENCES

Motivation:

For those future spacecraft which cannot be dynamically tested on the ground in a sufficiently realistic zero-gravity simulation and for future controlled space structures whose closed-loop performance must be verified via ground-based tests it is important to understand the effects of gravity and of the suspension system.

Objectives:

- To identify and understand the effects of gravity and of a suspension system on the dynamics of a controlled structure.
- To develop and codify modelling techniques for the prediction of potential changes in the plant dynamics due to the presence or absence of gravity and a suspension system.
- To develop rule-of-thumb predictions for the magnitude of the various gravity effects based on beam equivalent approximations of the suspended structure.

APPROACH

TO DEMONSTRATE A POSSIBLE DESTABILIZING EFFECT OF GRAVITY ON A CONTROLLED STRUCTURE A SIMPLE ANALYSIS WAS PERFORMED ON A VERTICALLY SUSPENDED PINNED-FREE FLEXIBLE BEAM WHERE THE TIP SLOPE WAS REGULATED USING A TORQUE ACTUATOR PLACED AT SOME POINT ALONG THE BEAM LENGTH. A RITZ ANALYSIS WAS USED TO SHOW THAT FOR CERTAIN ACTUATOR POSITIONS THE EFFECT OF GRAVITY STIFFENING ON THE STRUCTURE CAUSED A PHASE REVERSAL OF THE EFFECTIVE INPUT. THIS ANALYSIS IS NOT FURTHER DESCRIBED IN THIS PRESENTATION.

PRELIMINARY RESEARCH EFFORTS WERE DIRECTED TOWARDS IDENTIFYING AND UNDERSTANDING THE DIFFERENT CLASSES OF GRAVITY AND SUSPENSION EFFECTS. AFTER WHICH IT WAS POSSIBLE TO FOCUS ON THE CONTINUOUS AND DISCRETE MODELLING OF THESE EFFECTS. SAMPLE PROBLEMS WITH KNOWN SOLUTIONS WERE USED TO CONFIRM THE MODELLING PROCEDURES.

VARIOUS SIMPLIFIED MACE CONFIGURATIONS WERE THEN STUDIED IN A PARAMETRIC DESIGN ANALYSIS TO SUPPORT THE MACE FLIGHT EXPERIMENT DESIGN AND FURTHER UNDERSTAND THE EFFECTS OF SUSPENSION AND GRAVITY. A HIGH ORDER MODEL OF THE MACE DEVELOPMENT MODEL WAS THEN DEVELOPED TO EXPERIMENTALLY VALIDATE THE MODELLING PROCEDURES AND FOR USE IN MODEL-BASED CONTROLLER DESIGN

THE FINAL STEP WHICH HAS YET TO BE PERFORMED IS THE DERIVATION OF A COMPLETE SET OF RULES-OF-THUMB TO IDENTIFY AT WHICH POINT THE GRAVITY AND SUSPENSION EFFECTS BECOME IMPORTANT.

APPROACH

- Motivate research with a simple example of gravity field perturbation to closed-loop performance.
- Identify and categorize gravity and suspension system effects.
- Develop an understanding of how to incorporate gravity effects into the system variational principle and its finite order approximation.
- Verify modelling techniques by applying them to sample problems.
- Perform parametric variation studies and experimental validation.
- Develop rules-of-thumb for when gravity and suspension system effects become important for suspended structures.

OVERVIEW OF GRAVITY AND SUSPENSION EFFECTS ON STRUCTURE

RECOGNIZING FIRST THAT THE EFFECTS OF GRAVITY AND SUSPENSION CAN BE CLASSIFIED AS EITHER DIRECTLY AFFECTING THE STRUCTURE OR DIRECTLY AFFECTING THE SENSORS AND ACTUATORS, A TABLE OF FURTHER CLASSIFICATIONS FOR THE DIRECT EFFECTS ON STRUCTURES IS SHOWN.

THE THREE DIVISIONS IN THE TABLE CORRESPOND TO THE DIRECT EFFECTS ON THE STRUCTURE DUE TO THE DISTRIBUTED GRAVITY LOADING, THE SUSPENSION BOUNDARY CONDITIONS AND THEIR COMBINATION.

OVERVIEW: Gravity and Suspension Effects on Structure

The following are direct effects on the structure and its model
(i.e. the A matrix of the controlled structure model.)

GRAVITY FIELD EFFECTS	SUSPENSION SYSTEM EFFECTS
1) FINITE DEFLECTIONS <ul style="list-style-type: none">distributed gravity loads will cause initial deformations of the suspended structure.	3) STATIC B. C. PERTURBATIONS <ul style="list-style-type: none">static translational stiffnesses in the horizontal and vertical directions are prescribed by the suspension system at each attachment point.
2) GRAVITY STIFFENING/DESTIFFENING <ul style="list-style-type: none">distributed gravity loads stress the deformed structure which leads to eigenfrequency shifts and eigenmode coupling.	4) DYNAMIC B.C. PERTURBATIONS <ul style="list-style-type: none">modal coupling with the suspension dynamic modes results in dynamic impedances at the attachment points.
5) DYNAMIC LOADING DUE TO GRAVITY FIELD AND SUSPENSION CONSTRAINTS <ul style="list-style-type: none">dynamic torques which result from center of mass axis offsets with respect to the suspension support plane(s).	

OVERVIEW OF GRAVITY EFFECTS ON SENSORS AND ACTUATORS

GRAVITY DIRECTLY AFFECTS THE DYNAMIC PERFORMANCE OF THOSE STRUCTURAL CONTROL ACTUATORS AND SENSORS WHOSE OPERATION IS BASED ON A TRANSLATING MASS. HARMONIC OSCILLATIONS OF THE SUPPORTING STRUCTURE CAUSE VARIATIONS IN THE ORIENTATION OF THE SENSOR OR ACTUATOR WHICH IN TURN PRODUCE DISTORTIONS OF THE DEVICE INPUT (ON THE STRUCTURE) OR OUTPUT. THE FORM OF THIS PERTURBING EFFECT OF GRAVITY IS THAT OF AN ADDITIVE PERTURBATION WHICH CAN AMPLIFY OR ATTENUATE THE DEVICE RESPONSE.

THE PROOF-MASS ACTUATOR AND THE ACCELEROMETER ARE THE ONLY TWO STRUCTURAL CONTROL DEVICES WHOSE PERFORMANCE IS THUS AFFECTED BY GRAVITY. THESE EFFECTS OCCUR EVEN IN THE DEVICE PERFORMANCE IS IDEALIZED. IN THE NON-IDEAL CASE THERE ARE ALSO EFFECTS SUCH AS GRAVITY INDUCED FRICTION. THESE EFFECTS ARE NOT STANDARD FOR A GIVEN DEVICE TYPE AND ARE THEREFORE NOT CONSIDERED.

COMPLEMENTARY TO THE DIRECT GRAVITY EFFECTS ON THE SENSORS AND ACTUATORS ARE THE INDIRECT EFFECTS WHICH ARE DUE TO CHANGES IN THE STRUCTURE. THESE EFFECTS ARE CAPTURED IN THE ANALYSIS OF DIRECT GRAVITY EFFECTS ON THE STRUCTURE.

OVERVIEW: Gravity Effects on Sensors and Actuators

Sensors and actuators are also sensitive to gravity field effects.

Perturbations to their performance result in changes to the control, output and feed-forward matrices (i.e. B, C and D matrices) of the model. Two types of effects can be identified:

1) Direct Effects:

The harmonic rotation of a translating mass device in a gravity field results in an additive perturbation to its ideal performance. To date, the only devices identified as being susceptible to this effect are the accelerometer and the proof-mass actuator.

Gravity loading can also result in non-ideal sensor and actuator performance; e.g. gravity induced friction in device.

2) Indirect Effects:

Perturbations to the structure (i.e. the A matrix) can result in perturbations to the sensor and actuator performance depending on their location and the extent of the perturbation to the structure.

MODELLING OF GRAVITY AND SUSPENSION EFFECTS ON THE STRUCTURE

THE EFFECT OF GRAVITY ON THE SMALL DISPLACEMENT EIGENPROBLEM FOR A SUSPENDED STRUCTURE IS TO LOAD THE STRUCTURE WITH A CONSTANT INITIAL STRESS. IT CAN BE SHOWN THAT THE EFFECT OF THIS STRESS IS RESTRICTED TO AN ADDITIVE PERTURBATION TO THE STIFFNESS MATRIX. REFERENCE: "CONCEPTS AND APPLICATIONS OF FINITE ELEMENT ANALYSIS", COOK, MALKUS AND PLESHA, THIRD EDITION, "STIFFNESS MATRIX FOR GEOMETRIC NONLINEAR ANALYSIS", YANG AND MC GUIRE. THIS ADDITIVE CHANGE TO THE STIFFNESS MATRIX CAN BE REPRESENTED IN MATRIX FORM AS THE GEOMETRIC STIFFNESS MATRIX OR THE STRESS STIFFENING MATRIX.

ADDITIONALLY, GRAVITY HAS THE EFFECT OF CAUSING INITIAL STATIC DEFORMATIONS WHICH CHANGE THE REFERENCE STRUCTURE. THE MODAL SOLUTIONS TO THE SMALL DISPLACEMENT EIGENPROBLEM ARE DEFINED AS OSCILLATING ABOUT THIS NEW REFERENCE.

THE EFFECTS OF THE SUSPENSION SYSTEM ARE CAPTURED BY INCLUDING A DESCRIPTION OF THE SUSPENSION SYSTEM IN THE STRUCTURAL MODEL BEFORE COMPUTING THE GEOMETRIC STIFFNESS EFFECTS.

MODELLING OF GRAVITY AND SUSPENSION EFFECTS ON STRUCTURE

Gravity

The effect of a constant stress on a structure in equilibrium is to alter its stiffness.

In a FEM this change to the stiffness matrix can be called the differential stiffness matrix or the geometric stiffness matrix. The geometric stiffness matrix is a function of the applied loading and to comprehensively incorporate the effect of gravity loading on the homogeneous system one should include its effects in the initial deformation calculations.

Suspension System

The effects of the suspension system on the structural dynamics are captured by including the suspension system in the system model before incorporating the effects of gravity.

GEOMETRIC STIFFNESS THEORY AND INITIAL STATIC DEFORMATION CALCULATION

TO CAPTURE THE EFFECTS OF GRAVITY LOADING ON THE UNFORCED SMALL DISPLACEMENT EIGENPROBLEM OF THE SUSPENDED STRUCTURE IT IS NECESSARY TO TAKE INTO ACCOUNT THE QUADRATIC STRAIN TERMS WHICH ARE WEIGHTED BY CONSTANT INITIAL PRE-STRESS TERMS THESE TERMS LEAD TO THE GEOMETRIC STIFFNESS MATRIX.

THE PROBLEM OF SOLVING FOR THE INITIAL STATIC DEFORMATIONS IS A NON-LINEAR PROBLEM AS THE CONSISTENT APPLIED LOADS ARE A FUNCTION OF THE NODAL DISPLACEMENTS AND THE GEOMETRIC STIFFNESS MATRIX IS A FUNCTION OF BOTH THE NODAL DISPLACEMENTS AND THE APPLIED LOADS. SOLVING FOR THE NODAL DISPLACEMENTS IS THEREFORE PERFORMED BY ITERATION. THE DEPENDENCY ON NODAL DISPLACEMENT BEING QUITE WEAK AT TIMES IT IS POSSIBLE TO APPROXIMATE THE SOLUTION WITH ONLY ONE ITERATION. THE PROCEDURE USED TO-DATE IN THE MACE PROGRAM IS TO APPLY THE LOADS IN STEPS AND TO ITERATE FOR EVERY STEP.

Geometric stiffness theory and initial static deformation calculation

The geometric stiffness matrix is obtained from the non-linear strain terms in the potential energy expression for an elastic structure in equilibrium:

$$\begin{aligned} U_p = & \int_V \left\{ \frac{1}{2} (\epsilon_i^T E \epsilon_i + 2\epsilon_i^T E \epsilon_q + \epsilon_q^T E \epsilon_q) - (\epsilon_i^T E \epsilon_{i0}^{(0)} - \epsilon_i^T E \epsilon_{q0}^{(0)} - \epsilon_q^T E \epsilon_{q0}^{(0)}) \right\} dV \\ & + \int_V \left\{ \epsilon_i^T \sigma_0 + \epsilon_q^T \sigma_0 \right\} dV \underset{\text{_____}}{=} \int_V u^T F dV - \int_S u^T \phi dS \end{aligned}$$

For finite deflections the initial static deformation calculation is a non-linear problem as both the deflection and the stiffness are functions of the loads. Iterations are therefore required to solve for the final equilibrium state:

$$q_{i+1} = [K(q_i) + K g(q_i, Q(q_i))]^{-1} Q(q_i)$$

MODELLING GRAVITY'S EFFECT ON ACCELEROMETERS AND PMA'S

THIS WORK IS DOCUMENTED IN THE RECENT AIAA PAPER NO92-2094: "DIRECT EFFECTS OF GRAVITY ON THE CONTROL AND OUTPUT MATRICES OF CONTROLLED STRUCTURE MODELS", D.A.REY, H. ALEXANDER, E.F. CRAWLEY.

MODELLING GRAVITY'S EFFECT ON ACCELEROMETERS AND PMAs

Harmonic rotation of an accelerometer or proof-mass actuator about an axis other the vertical axis or the device's sensitivity/actuation axis results in an additive perturbation to the device's output/input.

The harmonic rotation can be as a result of harmonic bending or torsional vibration of the supporting structure.

The output/input is either attenuated or amplified depending on the relative phasing of the coupled translation and rotation of the supporting structure, (with a possible phase reversal in the attenuation case).

In the case of torsion the output/input perturbation is about zero such that gravity makes torsional modes observable and gravity causes the PMA force actuator to induce torques.

The effects of gravity on the B and C matrices have been identified and non-dimensional sensitivity measures show that these effects are especially important at low frequencies but are only significant with near-horizontal oriented devices and at those points where the rotations are large with respect to the displacements.

MODELLING GRAVITY'S EFFECT ON ACCELEROMETERS AND PMA'S

THIS WORK IS DOCUMENTED IN THE RECENT AIAA PAPER NO92-2094: "DIRECT EFFECTS OF GRAVITY ON THE CONTROL AND OUTPUT MATRICES OF CONTROLLED STRUCTURE MODELS", D.A.REY, H. ALEXANDER, E.F. CRAWLEY.

INCLUDED IN THE PAPER IS AN APPLICATION OF THE MODELLING OF GRAVITY'S EFFECT ON ACCELEROMETERS TO THE MACE PROGRAM. A NON-DIMENSIONAL SENSITIVITY ANALYSIS PREDICTED THAT THE MODELLING OF GRAVITY'S EFFECT WAS NECESSARY FOR THE HORIZONTAL ACCELEROMETER ON NODE 2. IN TURN, IT WAS FOUND THAT THE TRANSFER FUNCTION FROM THE INNER GIMBAL TO HORIZONTAL ACCELERATION AT NODE 2 DID SHOW CONSIDERABLE IMPROVEMENT AFTER THE EFFECT OF GRAVITY WAS INCLUDED IN THE OUTPUT MATRIX.

MODELLING GRAVITY'S EFFECT ON ACCELEROMETERS AND PMAS

The output of an accelerometer mounted to a beam in uncoupled bending and torsion vibration is given by:

$$a_i = \sum_{r=1}^{N_b} \left\{ \left(g \sin(\Phi'_r(x_i)) \kappa_i^r \right) \eta_r^t(t) \right\} + \sum_{r=1}^{N_b} \left\{ \left(g \sin(\Phi_r^b(x_i)) \kappa_i^b - \omega_j^2 \Phi_r^b(x_i) \right) \eta_r^b(t) \right\}$$

In modal modelling terms this yields the following C matrix type terms:

$$X = \begin{bmatrix} \eta^t & \left| \eta^t \right| \eta^b & \left| \eta^b \right| \dot{\eta}^b \end{bmatrix}^T$$
$$C_{ij}^T = g \kappa_i^t \Phi_j^t(x_i)$$
$$C_{ij}^B = g \Phi_j^b(x_i) \kappa_i^b - \omega_j^2 \Phi_j^b(x_i)$$
$$C = \begin{bmatrix} C^T & \left| 0 \right| C^B & \left| 0 \right| \end{bmatrix}$$

The non-dimensional gravity effect ratio is thus:

$$\Gamma = \frac{\frac{g}{l} \hat{\Phi}_j^b \left(\frac{x_i}{l} \right) \kappa_i^b}{\omega_j^2 \hat{\Phi}_j^b \left(\frac{x_i}{l} \right)}$$

Similar expressions hold for the effective input of a PMA mounted to a beam in bending and torsion vibration.

APPLICATION TO MACE

HAVING DETERMINED HOW TO MODEL THE EFFECTS OF GRAVITY AND OF THE SUSPENSION SYSTEM ON THE MACE STRUCTURE IT WAS FIRST SOUGHT TO EXAMINE, FOR A VARIETY OF SIMPLE CONFIGURATIONS (~ 40 D.O.F.), WHAT THE EXTENT OF THE PERTURBATION TO BOTH THE OPEN-LOOP AND CLOSED-LOOP SYSTEMS WAS. THE OBJECTIVE OF THIS EM (ENGINEERING MODEL) CONFIGURATION STUDY WAS THUS TO HELP DETERMINE WHICH CONFIGURATION SHOULD BE ADOPTED FOR THE EM.

THE SECOND APPLICATION WAS TO APPLY THE GRAVITY AND SUSPENSION MODELLING METHODS TO THE HIGH ORDER (~380 D.O.F.) MODEL OF THE MACE DM (DEVELOPMENT MODEL) CURRENTLY SUSPENDED IN THE BASEMENT AT THE M.I.T. SPACE ENGINEERING CENTER. THE TWO OBJECTIVES BEING EXPERIMENTAL VALIDATION OF THE MODELLING METHODOLOGY AND THE DEVELOPMENT OF A DM MODEL SUFFICIENTLY ACCURATE FOR THE PURPOSES OF DESIGNING MODEL BASED CONTROLLERS.

APPLICATION TO MACE

MACE EM Configuration Study

Objectives:

Select a MACE Engineering Model baseline configuration based on open-loop and closed-loop susceptibility to gravity and suspension effects.

MACE DM Modelling

Objectives:

Develop a high fidelity model of the MACE DM for use in control system design.
Experimentally verify the gravity and suspension modelling techniques.

MACE EM CONFIGURATION STUDY

TO COMPARE 0-G AND 1-G RESULTS TWO SETS OF MODELS ARE DEVELOPED FOR EACH TEST CASE STUDIED. CHANGES IN THE EIGENSTRUCTURE AND IN THE KEY TRANSFER FUNCTIONS ARE USED TO ASSESS THE PERTURBATION TO THE OPEN-LOOP SYSTEM WHILE PERFORMANCE VS GAIN CURVES ARE USED TO ASSESS THE IMPACT ON THE CLOSED-LOOP SYSTEM.

THE BASELINE TEST CASE IS BASED ON THE MACE SYSTEM DESCRIPTION IN THE EXPERIMENT REQUIREMENTS DOCUMENT, THIS BASELINE TEST CASE IS FURTHER DESCRIBED IN A MACE TECHNICAL NOTE. THE SIX VARIATIONS ON THIS BASELINE ATTEMPT TO CAPTURE THE FUNDAMENTAL CHANGES OF GLOBAL STIFFNESS REDUCTION, SECTIONAL GEOMETRY CHANGES WHICH FIX THE PRINCIPAL AXES OF THE BUS, ADDITIONAL HORIZONTAL AND VERTICAL COUPLING GIVEN A NON-PLANAR STRUCTURE, FLEXIBLE APPENDAGE EFFECTS AND A FUNDAMENTAL CHANGE FROM A STRAIGHT BUS TO AN L-SHAPED BUS.



MACE EM CONFIGURATION STUDY

Approach:

Develop set of 0-g and 1-g models of various fundamental MACE EM geometries.

Study open-loop impact of gravity and suspension system using eigensystem and transfer function references.

Study closed-loop impact of gravity and suspension system by applying LQG to system with PD stabilized bus attitude and gimbal pointing loops.

Test cases studied:

Baseline - circular section struts, 1.7 Hz fundamental, payloads at 45° from the vertical, system planar in suspension plane.

$f = 1 \text{ Hz}$ - stiffness change to obtain 1 Hz fundamental.

$EI_z/EI_y = 3$ - rectangular section struts, stiffened about z.

$EI_z/EI_y = 1/3$ - rectangular section struts, destiffened about z.

Out-of-plane - performance payload is swung 45° out-of-plane.

Flex. App. - flap-type flexible appendages added to node 1.

L-shaped - downward 90° bend is put in bus at node 2.

MACE EM CONFIGURATION STUDY

ON THE FAR LEFT IS A SAMPLE ORTHOGONAL PROJECTION OF AN EIGENMODE FOR THE FLEXIBLE APPENDAGE TEST CASE UNDER 1-G. THE 5.9 Hz MODE IS SEEN TO HAVE COUPLING BETWEEN HORIZONTAL BENDING OF THE BUS (2ND MODE), VERTICAL BENDING OF THE FLEXIBLE APPENDAGE PAIR (2ND MODE) AND SUSPENSION PENDULAR BEHAVIOR.

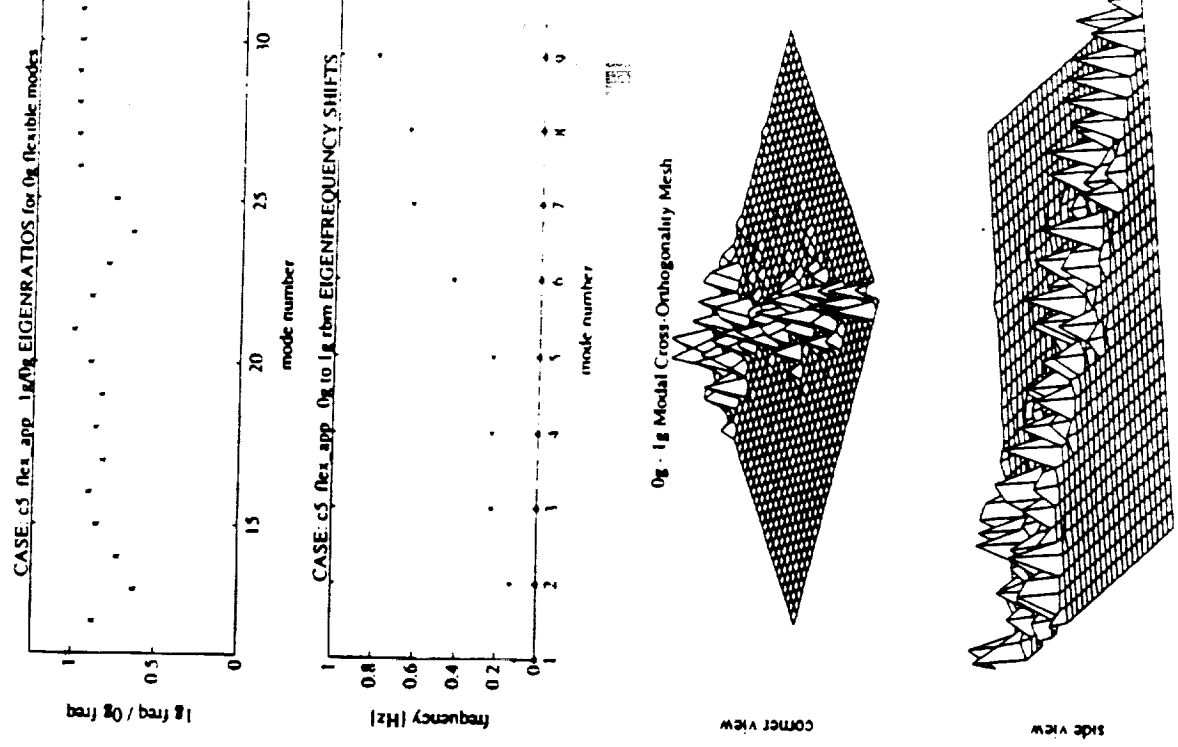
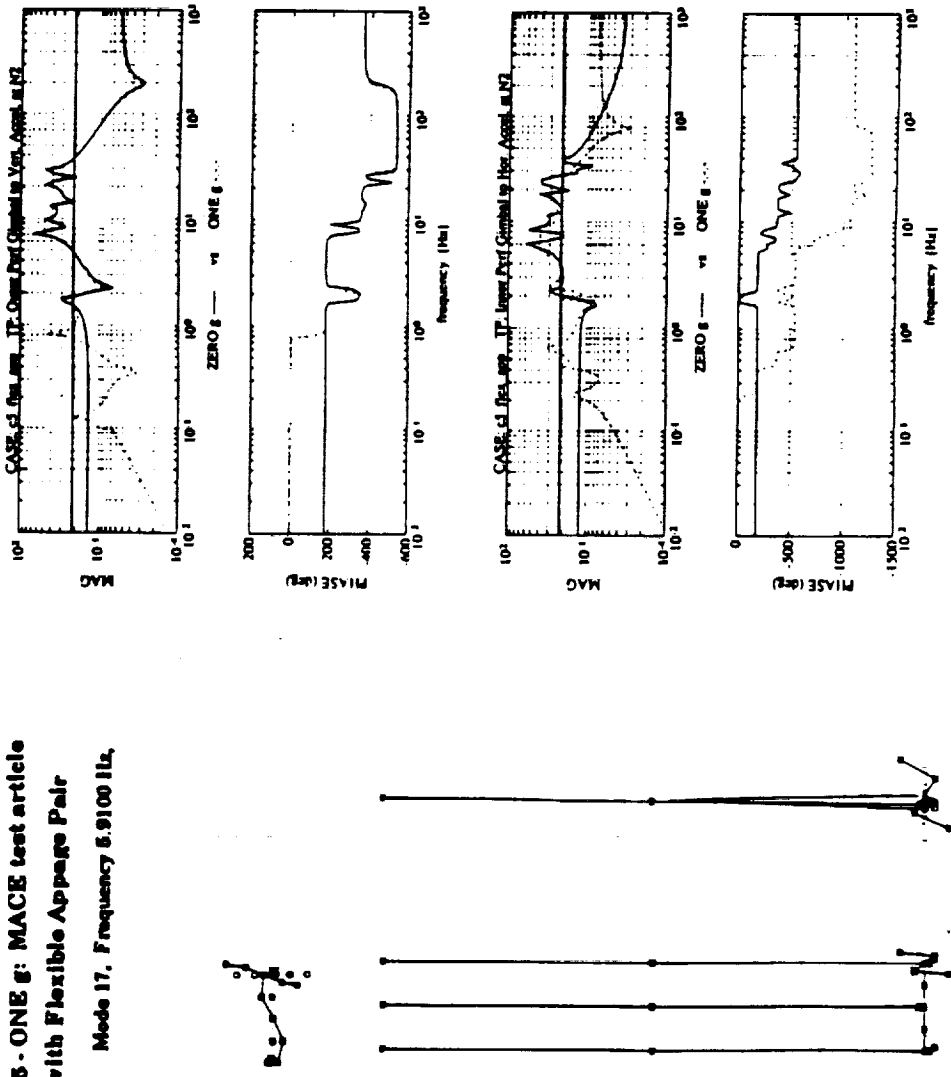
SAMPLE TRANSFER FUNCTIONS ARE SHOWN FOR THE SAME TEST CASE FROM OUTER PERFORMANCE GIMBAL TO VERTICAL ACCELERATION AT NODE 2, AND FROM INNER PERFORMANCE GIMBAL TO HORIZONTAL ACCELERATION AT NODE 2. THE SOLID LINE IS THE 0-G CASE AND THE DOTTED LINE IS THE 1-G CASE. AS EXPECTED, THE HORIZONTAL CASE IS MORE PERTURBED BY GRAVITY AND THE SUSPENSION SYSTEM THAN THE VERTICAL CASE. IN THE VERTICAL CASE WE CAN IDENTIFY THE LOW-FREQUENCY SUSPENSION RESONANCES ASSOCIATED WITH THE TILT AND BOUNCE MODES. IN THE HORIZONTAL CASE WE CAN IDENTIFY THE LOW-FREQUENCY SUSPENSION RESONANCES ASSOCIATED WITH THE PENDULAR AND COMPOUND PENDULAR MODES.

ON THE RIGHT WE HAVE A DESCRIPTION OF THE GRAVITY EFFECTS ON THE EIGENSYSTEM. THE EIGENVALUES FOR THE 1-G FLEXIBLE MODES ARE NORMALIZED W.R.T. TO 0-G EIGENVALUES, WHILE THE EIGENVALUES ASSOCIATED WITH THE RIGID-BODY MODES ARE NOT NORMALIZED AS THEY ARE SHIFTS FROM 0. THE MODAL CROSS-ORTHOGONALITY PLOT BETWEEN THE 1-G AND 0-G MODES SHOWS THAT THE RIGID-BODY MODES ARE PERTURBED THE MOST AND RESULT IN A HIGHLY COUPLED SUB-SPACE. THE FLEXIBLE MODES ARE ALSO AFFECTED BUT THE COUPLINGS ARE LIMITED TO THE CLOSER MODES.

MACE EM CONFIGURATION STUDY

Sample Open-Loop Results:

c6 - ONE 6: MACE test article
with Flexible Aperture Pair
Mode 17, Frequency 5.9100 Hz



MACE EM CONFIGURATION STUDY

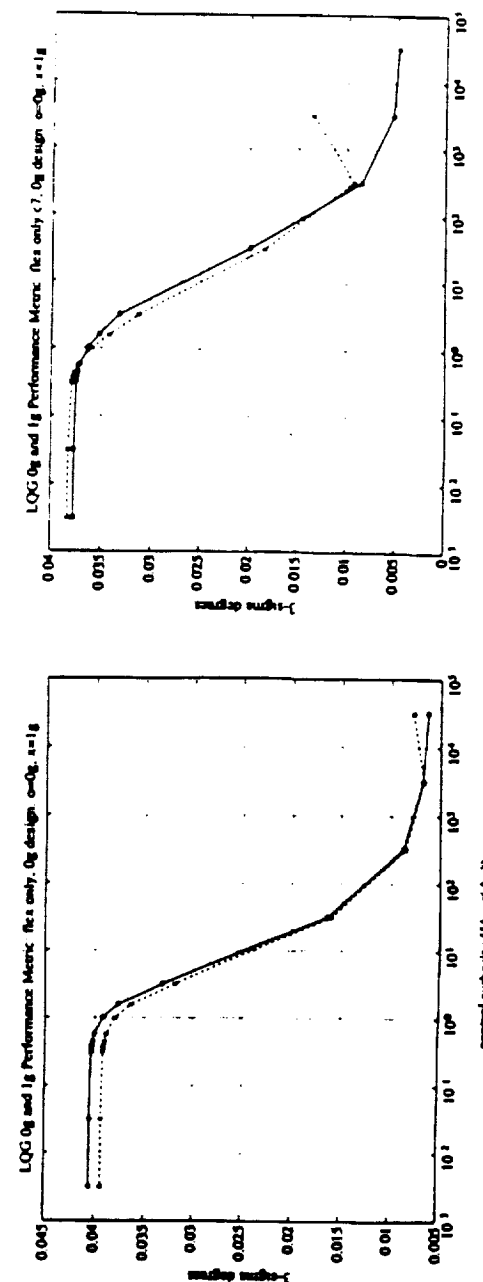
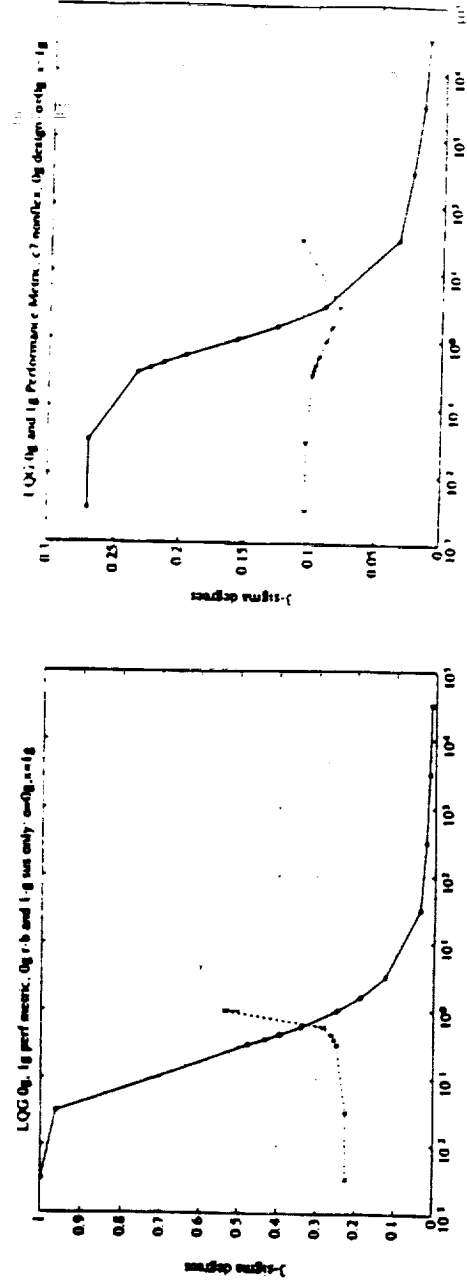
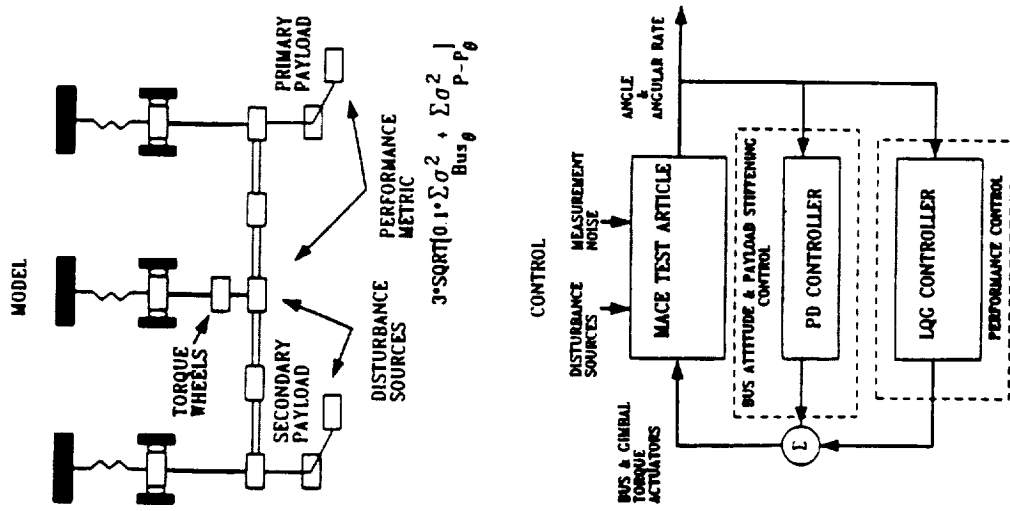
A PD CONTROLLER IS PLACED ON THE BUS ATTITUDE AND THE PAYLOAD TO PROVIDE A FUNDAMENTAL STIFFNESS TO THE 0-G RIGID-BODY AND MECHANISM MODES FOR COMPARISON WITH THE 1-G CASE. AN LQG CONTROLLER IS USED BASED ON WHITE-NOISE DISTURBANCES AT THE TORQUE WHEELS AND AT THE SECONDARY PAYLOAD. THE PERFORMANCE METRIC IS A WEIGHTED SUM OF THE 3 SIGMA VALUES OF BUS ATTITUDE STABILITY AND PAYLOAD POINTING STABILITY.

PERFORMANCE VS GAIN CURVES ARE SHOWN FOR TWO CASES. ON THE LEFT ARE THE CURVES ASSOCIATED WITH THE BASELINE TEST CASE AND ON THE RIGHT ARE THE CURVES ASSOCIATED WITH THE L-SHAPED TEST CASE. THE TOP CURVES ARE THE STANDARD CURVES FOR THE ENTIRE SYSTEM. THE BOTTOM CURVES ARE FOR THE SYSTEM WITH THE RIGID-BODY AND MECHANISM MODES TRUNCATED FROM BOTH THE LQG DESIGN AND EVALUATION. THE SOLID LINES ARE FOR THE PERF-COST CURVES FOR THE 0-G CLOSED-LOOP SYSTEM AND THE DOTTED LINES ARE FOR THE 1-G CLOSED LOOP SYSTEM. NOTE THAT THE CONTROL SYSTEM WAS DESIGNED FOR THE 0-G CASE SUCH THAT UNDER SUFFICIENTLY HIGH AUTHORITY THE SYSTEM TESTED ON THE GROUND GOES UNSTABLE. IT IS INTERESTING TO ALSO NOTE THAT THE FLEXIBLE MODES DO CONTRIBUTE TO THE EVENTUAL INSTABILITY BUT AT A HIGHER LEVEL OF GAIN. IN THE CASE OF THE L-SHAPED SYSTEM THE EFFECT OF THE FLEXIBLE MODE CONTRIBUTION IS LARGER THAN IN THE BASELINE CASE.

FURTHER DETAILS ARE GIVEN IN: "THE MIDDECK ACTIVE CONTROL EXPERIMENT", D. MILLER, R. SEPE, D. REY, E. SAARMAA AND E.F. CRAWLEY, 1992 CSI CONFERENCE PAPER.

MACE EM CONFIGURATION STUDY

Sample Closed-Loop Results:



MACE DM CONFIGURATION STUDY

THE SUSPENSION SYSTEM MODEL FOR A GIVEN SUSPENSION DEVICE PRESENTLY CONSISTS OF A SOFT LINEAR SPRING BETWEEN THE CEILING AND A SUSPENSION CARRIAGE WHICH IS CONSTRAINED TO A SINGLE PURE VERTICAL TRANSLATION DEGREE-OF-FREEDOM. THE STRUCTURE IS ATTACHED TO THE CARRIAGES WITH STIFF PINNED-PINNED RODS WHICH CAPTURE THE PENDULAR BEHAVIOR OF THE SUSPENSION.

THE SPRING STIFFNESSES ARE INDIVIDUALLY TUNED TO YIELD A LEVEL STRUCTURE (I.E. COLINEAR STRUCTURAL ATTACH POINTS) WHICH IS REPRESENTATIVE OF THE MASS-PROPORTIONAL STIFFENING OF THE INDIVIDUAL PNEUMATIC-ELECTRIC SUSPENSION DEVICES WHICH ARE INDIVIDUALLY TUNED USING A PRESSURE REGULATOR. SUCH A SUSPENSION TUNING RESULTS IN A BOUNCE MODE WHICH IS LARGELY DECOUPLED FROM THE STRUCTURAL FLEXIBILITY.

THE GEOMETRIC STIFFENING EFFECTS WERE CAPTURED BY PERFORMING A NONLINEAR LARGE DISPLACEMENT ANALYSIS WITH INCREMENTAL LOADING AND STIFFNESS REFORMATIONS AT EVERY STEP. THE INITIAL CONDITION IS THE STRUCTURE SUSPENDED WITH UNSTRETCHED SUSPENSION SPRINGS AND WITH CONCENTRATED DAMPING ELEMENTS TO DAMP THE SYSTEM RESPONSE. THE ITERATIONS ARE PERFORMED UNTIL THE STRUCTURE REACHES EQUILIBRIUM UNDER ACTUAL LOADING CONDITIONS. THE END RESULT OF THIS STEP IS A LINEAR MODEL OF THE STATICALLY DEFORMED STRUCTURE WITH GEOMETRIC STIFFENING EFFECTS INCLUDED. THE FINAL EIGENSOLUTION STEP IGNORES THE CONCENTRATED DAMPING ELEMENTS AND YIELDS EIGENMODES WHICH ARE SMALL DISPLACEMENTS ABOUT THE COMPUTED STATICALLY DEFORMED POSITION.

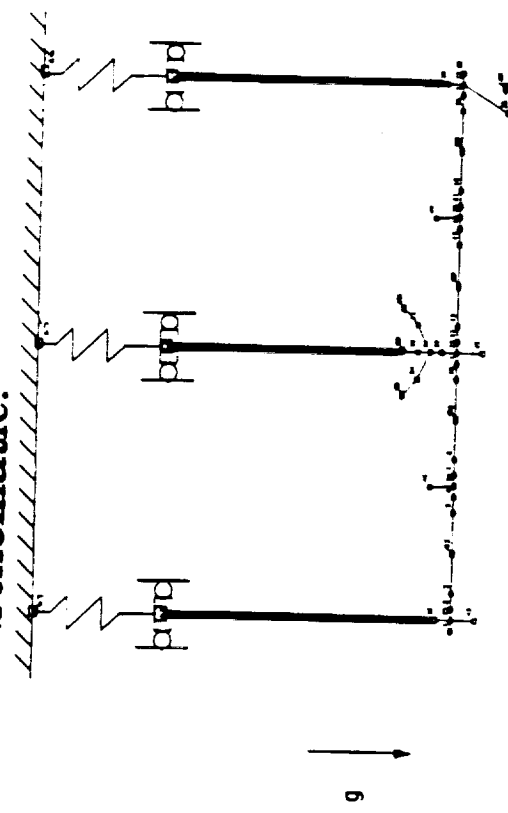
MACE DM CONFIGURATION STUDY

Approach:

Add a basic model of suspension system to 0g model and incorporate static pre-deformation and geometric stiffening effects.

Model pneumatic-electric suspension devices as soft tuned springs between ceiling and suspension carriages, constrain suspension carriages to vertical translation and attach structure to carriages via stiff pinned-pinned rods.
Compare low-frequency modal I.D. data with predicted transfer functions and tune if required.

MACE 1g DM Model Schematic:



MACE DM CONFIGURATION STUDY

PRELIMINARY RESULTS SHOW A GOOD QUALITATIVE AGREEMENT BETWEEN THE 1-G MODEL AND PRELIMINARY EXPERIMENTAL DATA. A SIGNIFICANT IMPROVEMENT IS ALSO OBSERVED IN THE LOW FREQUENCY PREDICTIONS FROM THE 0-G TO THE 1-G MODEL.

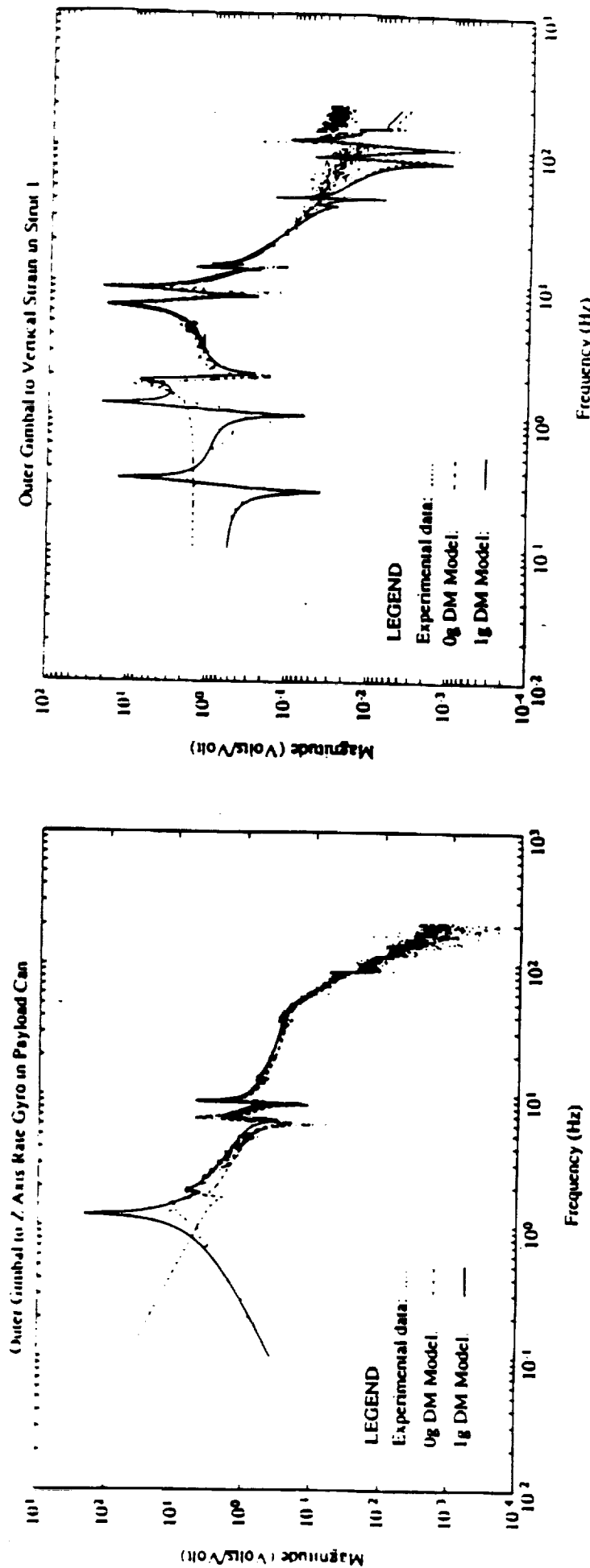
THE MODEL TUNING PROCESS IS NOW UNDERWAY.

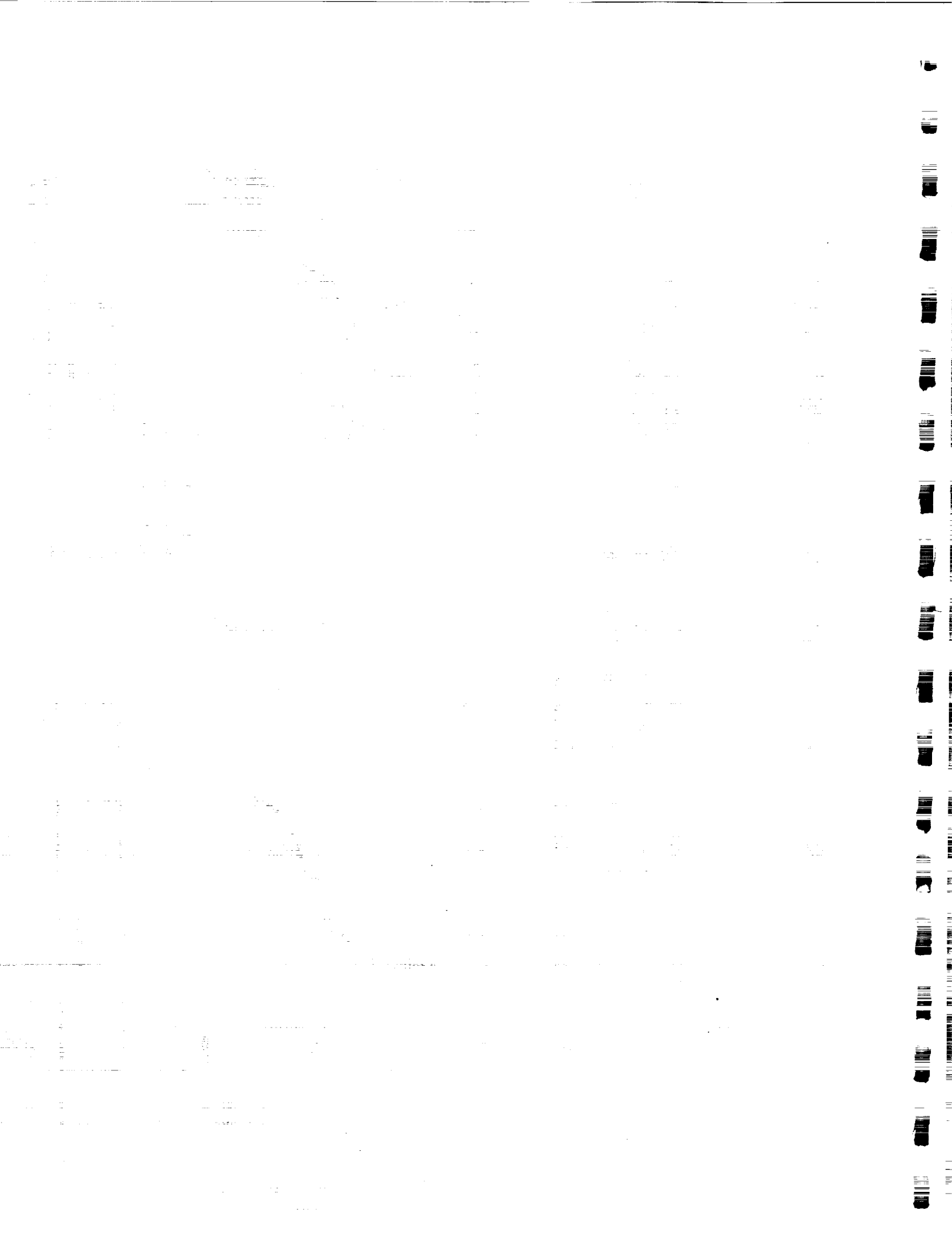
MACE DM CONFIGURATION STUDY

Status:

First iteration complete. Low frequency predictions have improved but some tuning is required including the addition of a higher order suspension model.

Sample Transfer Function Results:





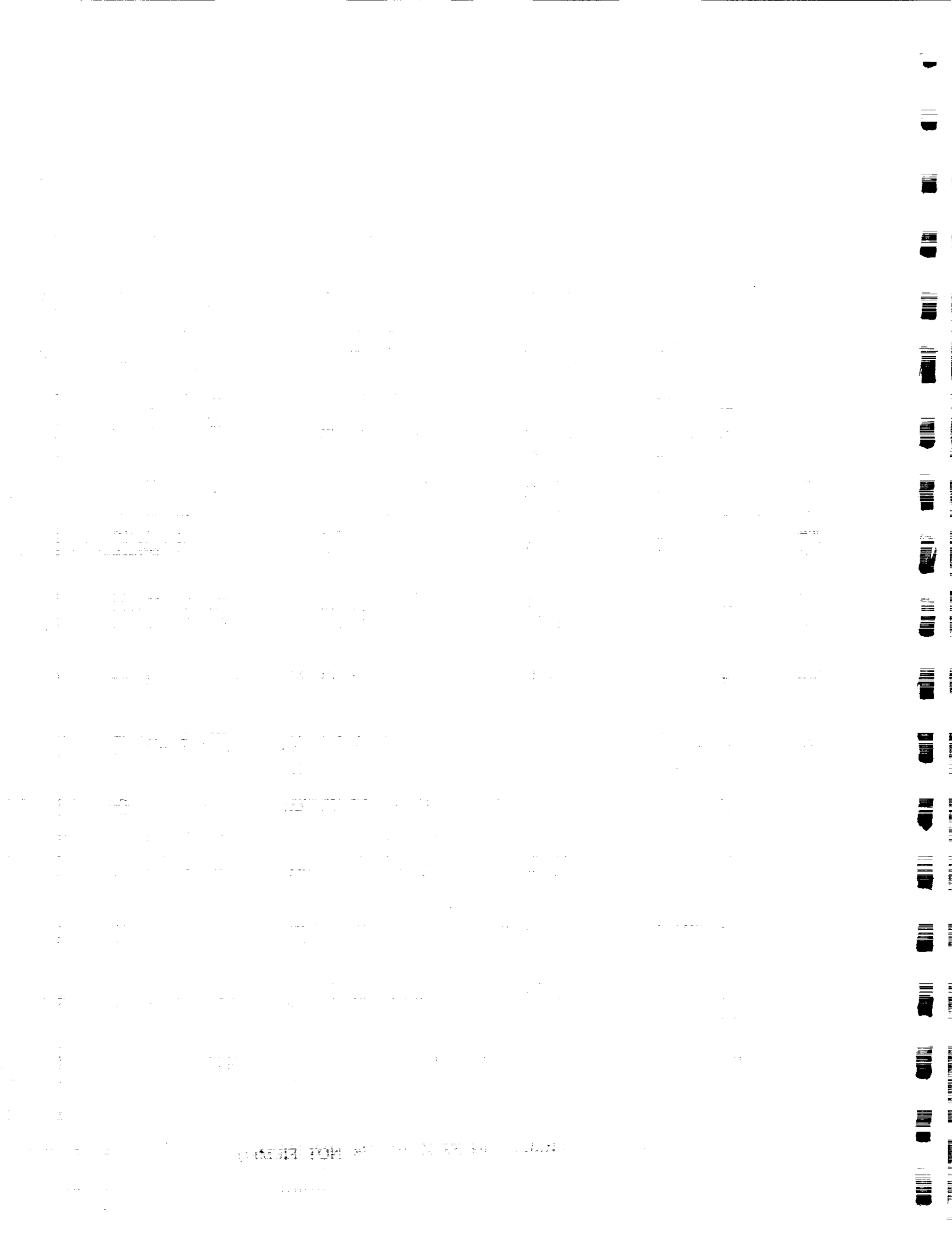
CONCLUSIONS

A gravity and suspension system modelling procedure has been developed which captures suspension effects, stiffness effects, static pre-deformation effects and direct sensor and actuator effects.

Preliminary experimental results are encouraging in that the agreement between model based transfer function predictions and measured transfer functions is good.

Clearly, the MACE test article is an effective test-bed for the research of gravity and suspension system effects and for the development of a space qualification procedure for flexible precision spacecraft as both the MACE DM and EM models have demonstrated a sensitivity to gravity and suspension effects.

LQG controllers designed for on-orbit operation but tested on the ground-based model were shown capable of first destabilizing suspension modes and then flexible modes at higher levels of control authority. This makes ground testing of candidate on-orbit controllers difficult.



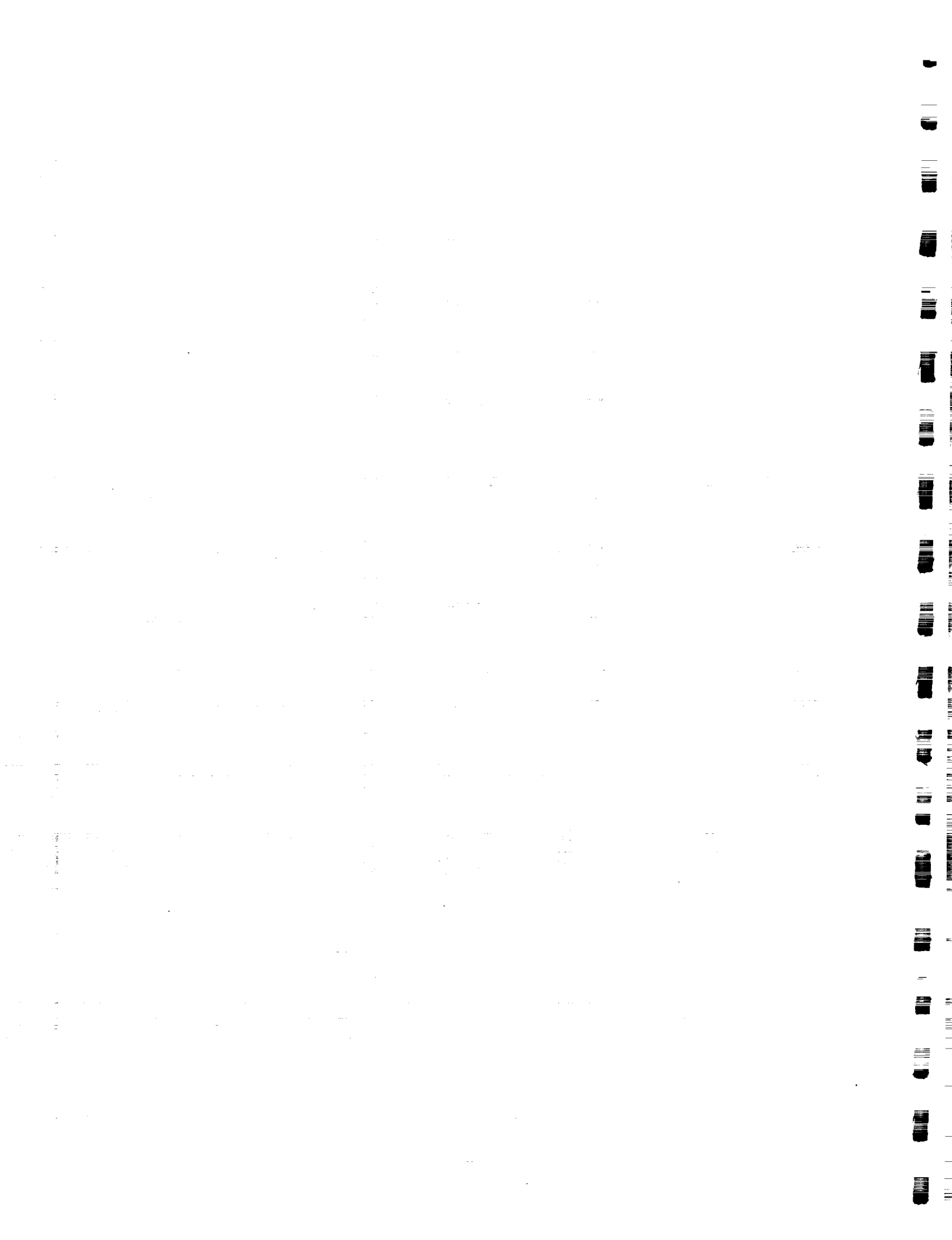
FUTURE WORK

Investigate impact of not reforming the mass matrix in the case of large deflections.

Tune the 1-g DM model and continue experimental validation using the MACE test article.

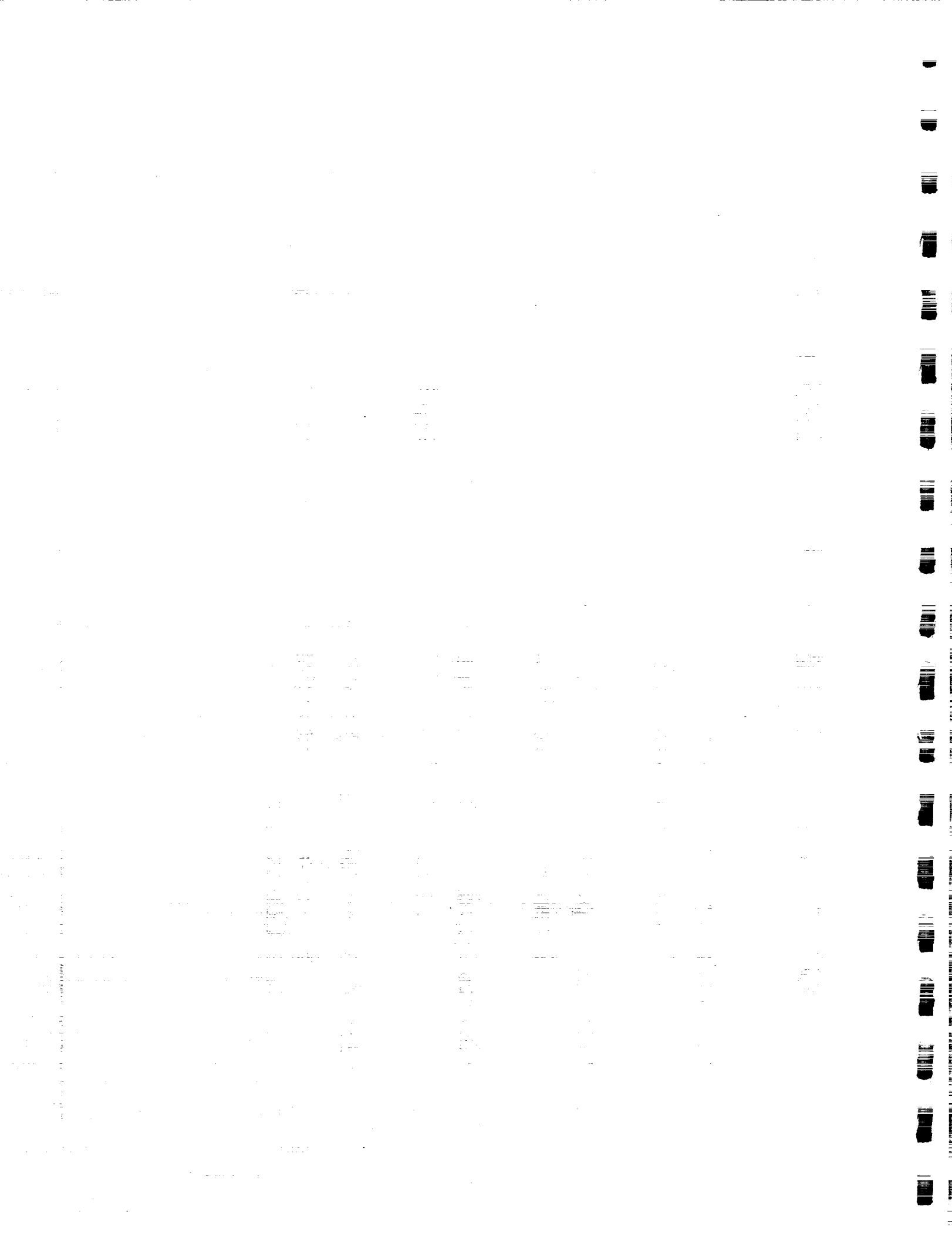
Derivation of gravity/suspension effect rules of thumb based on non-dimensional parameter descriptions of a suspended space structure.

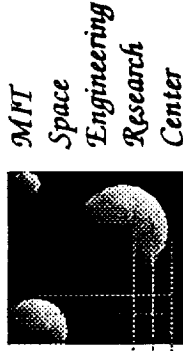
S.M. Thesis - “Gravity and Suspension Effects on Controlled Structure Models”



OTHER MACE RELATED RESEARCH

- Ken Chang, Prof. W. Seering:
Multiple Modes Input Shaping
- Marc Campbell, Prof. E. F. Crawley:
Interactive Control Systems
- Marco Quadrelli, Prof. A. von Flotow:
Non-Linear Multi-Body Modelling and Simulation.
- Dr. M. Mercadal, Dr. D. W. Miller:
Sensor and Actuator Selection under Control Topology Constraints





THE MIDDECK ACTIVE CONTROL EXPERIMENT (MACE):

IDENTIFICATION FOR ROBUST CONTROL

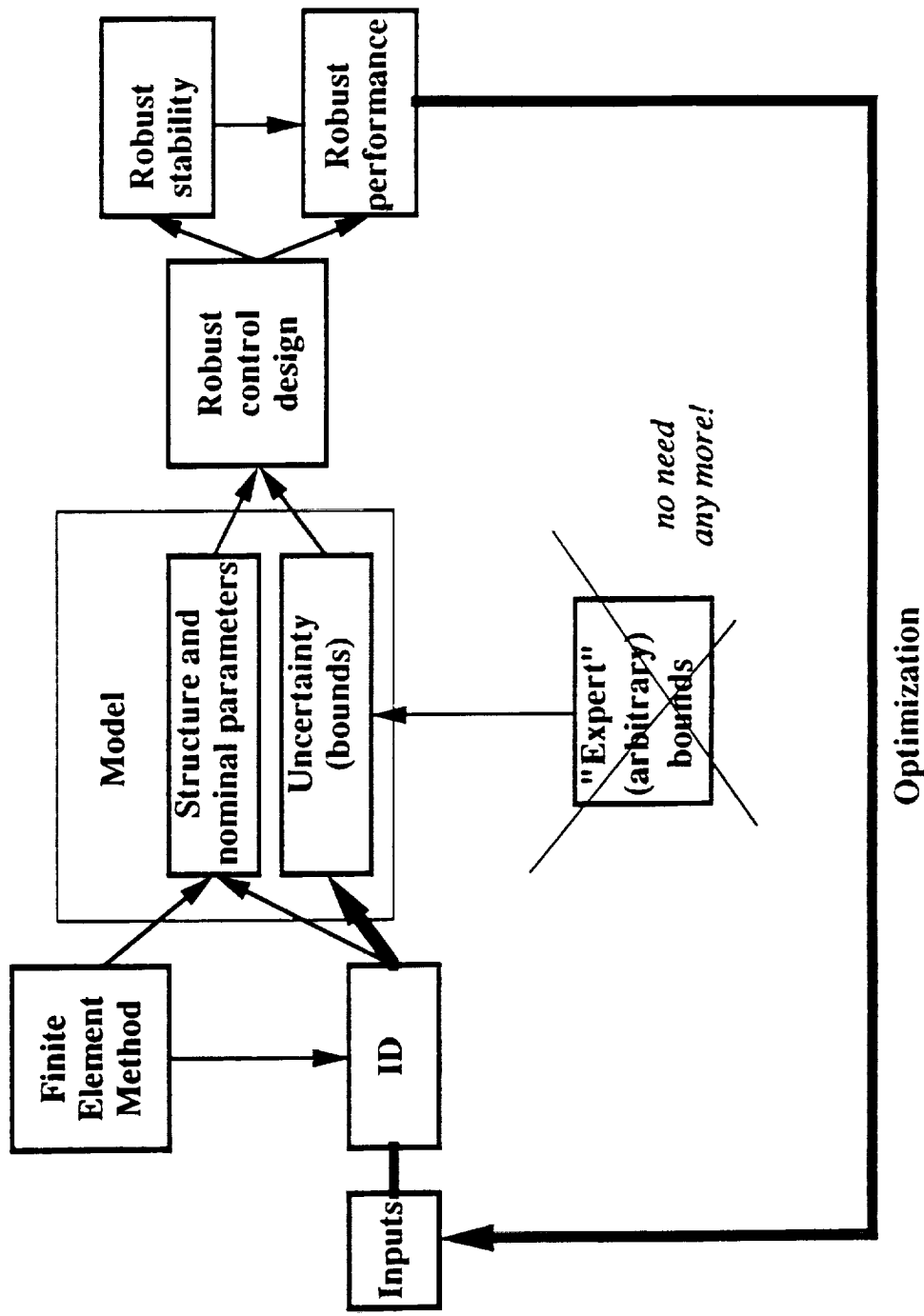
Dr. Valery I. Karlov

Moscow Aviation Institute (MAI)

INTEGRATION OF SYSTEM IDENTIFICATION AND ROBUST CONTROL IS CONSIDERED. THE IDENTIFICATION ALGORITHM IS AN EXTENDED KALMAN FILTER, THE ROBUST CONTROL ALGORITHM IS BASED ON COST AVERAGING TECHNIQUES OR ON PETERSEN-HOLLOT'S BOUNDS (MODIFIED FOR RANDOM CORRELATED PARAMETERS). THE IDENTIFICATION AND CONTROL PROBLEMS ARE COUPLED VIA OPTIMIZATION OF OPEN- AND CLOSED-LOOP INPUTS FOR THE IDENTIFICATION EXPERIMENT WITH THE OPTIMIZATION CRITERION BEING ROBUST CONTROL PERFORMANCE. THE APPROACH ALLOWS ELIMINATING "ARBITRARY" BOUNDS (OF UNCERTAIN MODEL PARAMETERS) IN ROBUST CONTROL DESIGN PROCEDURE AND PROVIDES REALISTIC OPTIMIZED BOUNDS.

Identification For Robust Control

Stages of Design



SYSTEM IDENTIFICATION CAN BE CONDITIONALLY SPLIT INTO THREE LEVELS SUBJECT TO ALGORITHM, MODEL AND WHAT IDENTIFICATION PROVIDES. THE THIRD LEVEL ALGORITHMS BASED ON USAGE OF EXTENDED KALMAN-TYPE FILTERS CAN IMPROVE THE RESULTS OF FIRST AND SECOND LEVEL ALGORITHMS. THE ADVANTAGES ARE IN PROVIDING HIGH-PRECISION ESTIMATES OF "DIRECT" PHYSICAL PARAMETERS (NATURAL FREQUENCIES, DAMPING RATIOS, MODE SHAPES) ALONG WITH REALISTIC BOUNDS (IN TERMS OF COVARIANCE MATRIX).

Three Levels of Identification

	①	②	③
A i g o r i h m	<ul style="list-style-type: none"> • Empirical Transfer Function Estimate • Eigen Value Analysis • 	<ul style="list-style-type: none"> • Least Square • Maximum Likelihood • Prediction Error • 	<ul style="list-style-type: none"> • Extended Kalman-type filters (state and parameter estimation)
M o d e l	<ul style="list-style-type: none"> • SISO • MIMO (deterministic) 	<ul style="list-style-type: none"> • TF • ARMAX $A(q)y(t) = B(q)u(t) + e(t)$ $t = 0, \dots, K$ 	<ul style="list-style-type: none"> • State-space $\dot{x} = A(\alpha)x + B(\beta)u + \xi$ $y = C(\beta)x + D(\beta)u + \eta, \quad t \in (0, T)$
P r o d u c t	<ul style="list-style-type: none"> • Model structure (number of modes, preliminary estimates) 	<ul style="list-style-type: none"> • Fitted estimates [but of "indirect" parameters $\gamma = \phi(\alpha, \beta)$] 	<ul style="list-style-type: none"> • High-precision estimates of "direct" parameters: <ul style="list-style-type: none"> - α (frequencies, damping ratios) - β (mode shapes, masses) • Realistic bounds

1. IN THE RICCATI EQUATION CONTROL PROBLEM THE OBJECT TO BE CONTROLLED IS A RICCATI EQUATION FOR THE AUGMENTED COVARIANCE MATRIX (INCLUDING BOTH STATES AND MODEL PARAMETERS). THE CONTROL IS INPUTS FOR IDENTIFICATION TAKING INTO ACCOUNT CONSTRAINT ON STRUCTURAL EXCITATION. THE CRITERION IS ROBUST CONTROL PERFORMANCE.
2. THE ESSENCE OF THE EQUIVALENT PROBLEM CONSISTS OF INTRODUCING A SUFFICIENT NUMBER OF HAMILTONIAN VARIABLES IN TERMS OF WHICH THE EQUIVALENT CRITERION CAN BE EXPRESSED.
3. THE NUMERICAL ALGORITHM IS BASED ON THE METHOD OF SUCCESSIVE APPROXIMATIONS FOR SOLVING A LINEAR-QUADRATIC BOUNDARY-VALUE PROBLEM.
4. THE EXTENDED KALMAN FILTER IS A SYSTEM OF FINITE-DIFFERENCE EQUATIONS DERIVED AS A RESULT OF THE ANALYTICAL SOLUTION TO A CONTINUOUS FILTER FOR EACH MODE.
5. PETERSEN-HOLLOT'S BOUNDS ARE MODIFIED FOR RANDOM CORRELATED PARAMETERS. THE CORRESPONDING MODIFIED RICCATI EQUATION IS DERIVED.

Basic Elements of The Approach

1. Non-linear problem of Riccati equation control for augmented covariance matrix:

$$\begin{bmatrix} P_x & P_{x\alpha} \\ P_{\alpha x} & P_\alpha \end{bmatrix}$$

2. Equivalent linear problem

(Received on the basis of non-traditional usage of RE analytical properties)

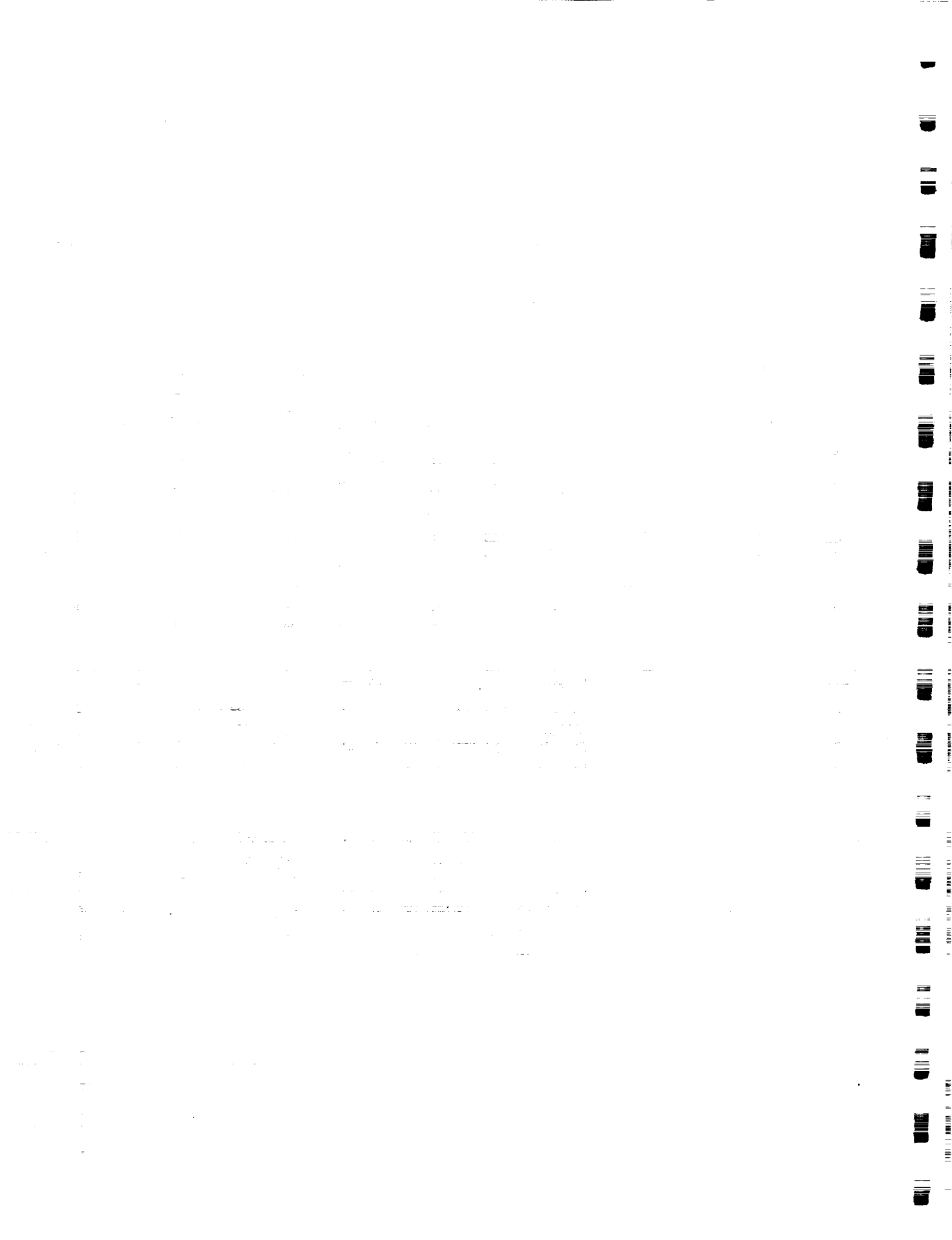
3. Converge numerical algorithm of optimization
4. Extended Kalman filter

(Solution on the basis of decomposition with respect to frequencies)

5. Robust control problem
 - Cost averaging techniques (use the "Post-ID" bounds directly)
 - Petersen - Hollot's bounds (need modification)

a). $SA_0^T A_0 S + (K + \beta \gamma NWN^T) - S(BR^{-1}B^T - \beta \gamma^T LVL^T)S = 0$
 $\beta < 1, VW = P_\alpha$

- b). Duality principle for design of dynamical feedback



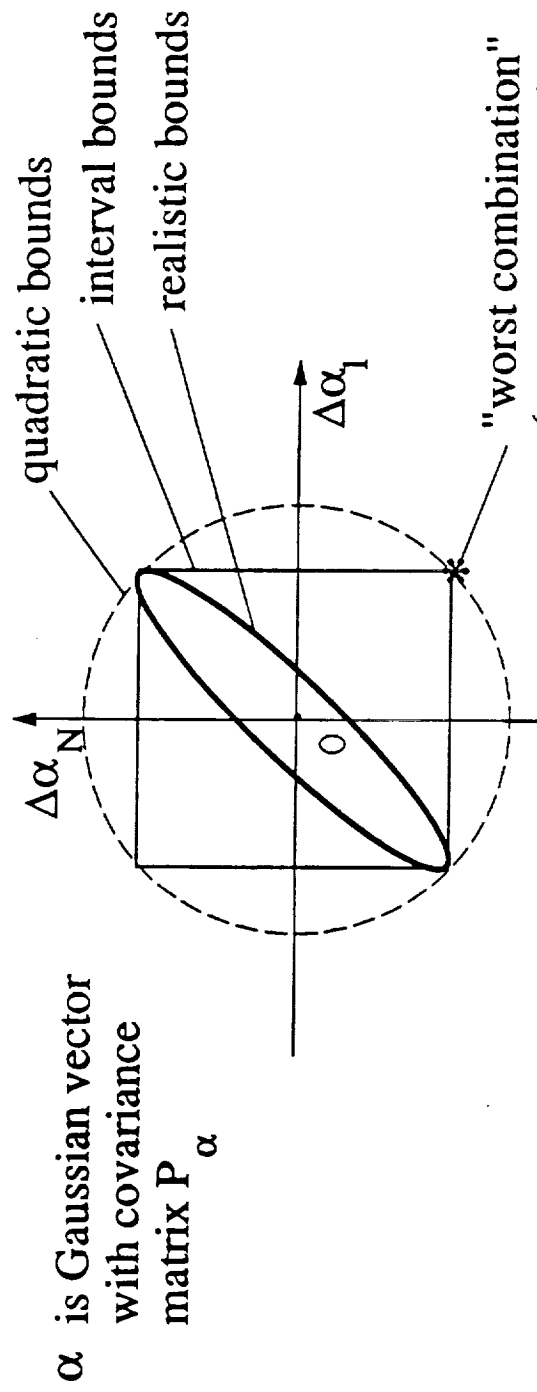
What The Approach Provides

- **Realistic statistical model of uncertainty**
(accuracy characteristics are received in the state-space model with "separated" noises in sensors and actuators)
- **Active ID:** Optimization of open- and close-loop inputs directly with respect to robust control performance
- **Taking into account constraints on excitation**
(desirable ID accuracy can be achieved with much less excitation, extremely important for experiments in the space)
- **Possibility to identify time-varying parameters**
(in case of moving rigid payloads)

PRECEDING PAGE BLANK NOT FILMED

THE QUADRATIC AND INTERVAL BOUNDS LEAD TO OVERCAUTIOUS RESULTS BECAUSE OF SPECIFYING "WORST COMBINATION" OF UNCERTAIN PARAMETERS WHICH, AS A RULE, DOES NOT OCCUR IN PRACTICE. THE REALISTIC BOUNDS TAKING INTO ACCOUNT COVARIANCES BETWEEN PARAMETERS PREVENT THIS "WORST COMBINATION". EVENTUALLY THIS DEGRADES CONSERVATISM OF THE BOUNDING ROBUST TECHNIQUES AND PROVIDES HIGH PERFORMANCE (COMPARABLE WITH THE PERFORMANCE PROVIDED BY THE THE AVERAGING ROBUST TECHNIQUES).

Advantages of "Post-ID" Model of Uncertainty



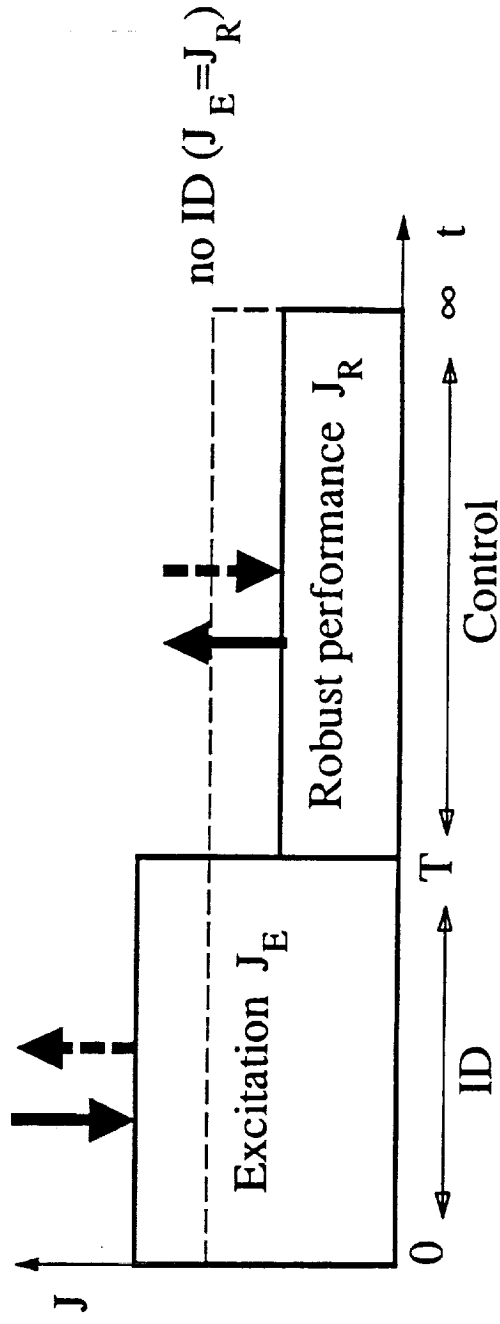
"worst combination"
(causes conservatism of robust control,
for large N dramatically)

- Reveals "cost" of different errors
- Reveals covariances between parameters
- Prevents non-realistic "worst combination" of parameters
(degrades conservatism of robust control)

PRELIMINARY RESULTS SHOW THAT OPTIMIZATION OF IDENTIFICATION EXPERIMENTS LEADS TO CONSIDERABLY INCREASING EXCITATION SUFFICIENT FOR ACHIEVING DESIRABLE ACCURACY OF IDENTIFICATION (IN TERMS OF ROBUST CONTROL PERFORMANCE). THUS THE DESIGNER CAN ESTABLISH ACCEPTABLE LEVEL OF DIMINISHED POINTING CONTROL ACCURACY DURING THE IDENTIFICATION EXPERIMENT TO ENHANCE THE ACCURACY OF ROBUST CONTROL ON THE NEXT TIME INTERVAL.

Advantages of Optimization

- Further degrading the conservatism
- Better coping with "difficulties" in the model, e.g. close modes (*excitation in optimal directions amplifies the difference between modes*)
- The best compromise between excitation and robust control performance



$$J = J_R + pJ_E \text{ where } p \text{ is a "price" of ID}$$

All J are quadratic forms

PRACTICAL REALIZATION OF THE ABOVE APPROACH FOR MACE CONSISTS OF THREE STAGES: 1) SIMULATION 2) GROUND EXPERIMENT AND 3) EXPERIMENT IN SPACE.

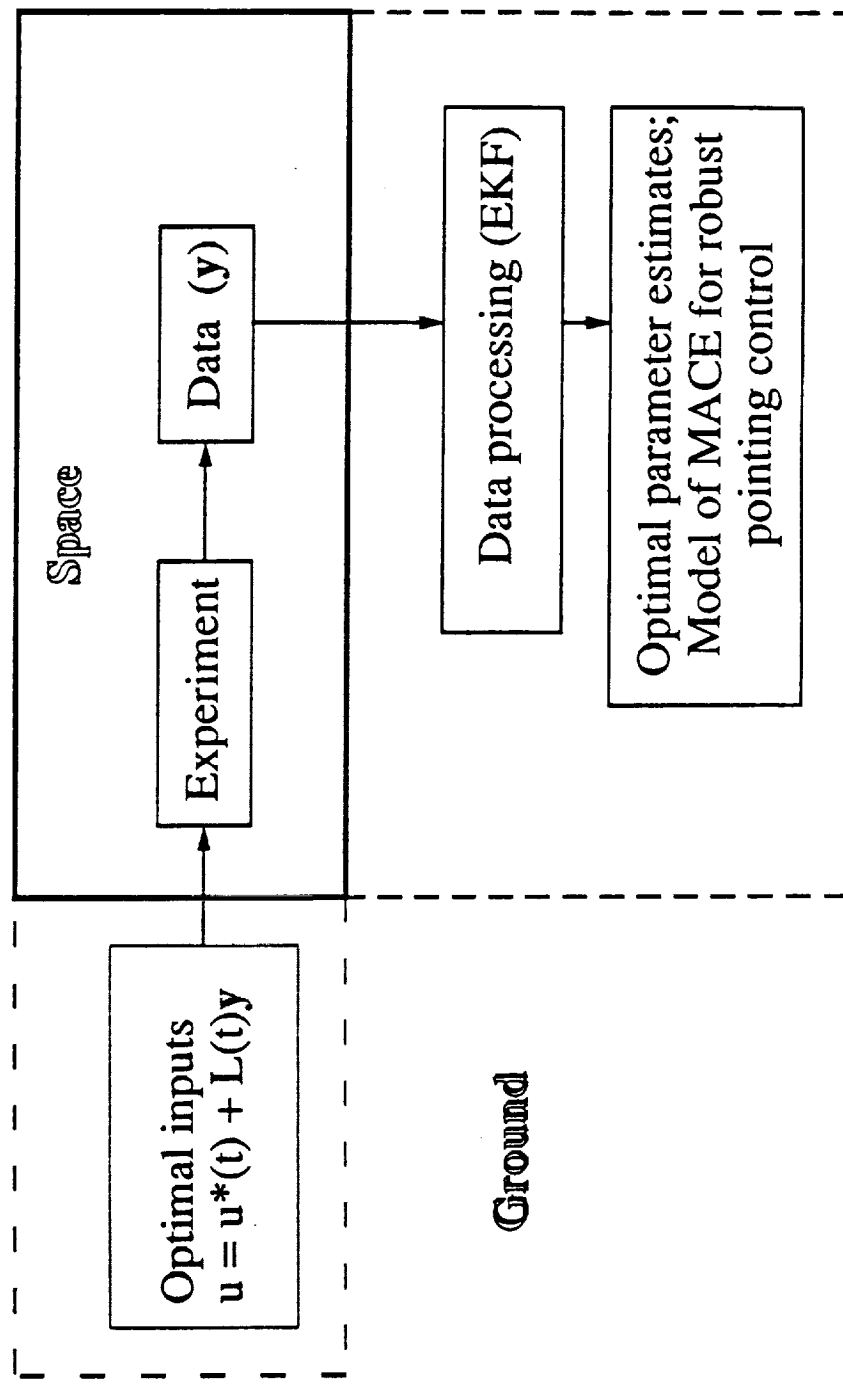
- 1) THE SIMULATION MODEL OF MACE WILL BE DERIVED TO CONFIRM CONVERGENCE OF IDENTIFICATION ALGORITHMS.
- 2) THE FEM STATE-SPACE MODEL WILL BE REFINED ON THE BASIS OF GROUND EXPERIMENTAL DATA.(AS A RESULT THE CONTRIBUTION OF GRAVITY AND SUSPENSION EFFECTS WILL BE REVEALED).
- 3) THE FEM STATE-SPACE MODEL WILL BE REFINED ON THE BASIS OF ON-ORBIT DATA. THE UNCERTAINTY OF PARAMETERS IN BOTH MODELS WILL BE REDUCED WITH RESPECT TO ROBUST CONTROL PERFORMANCE.

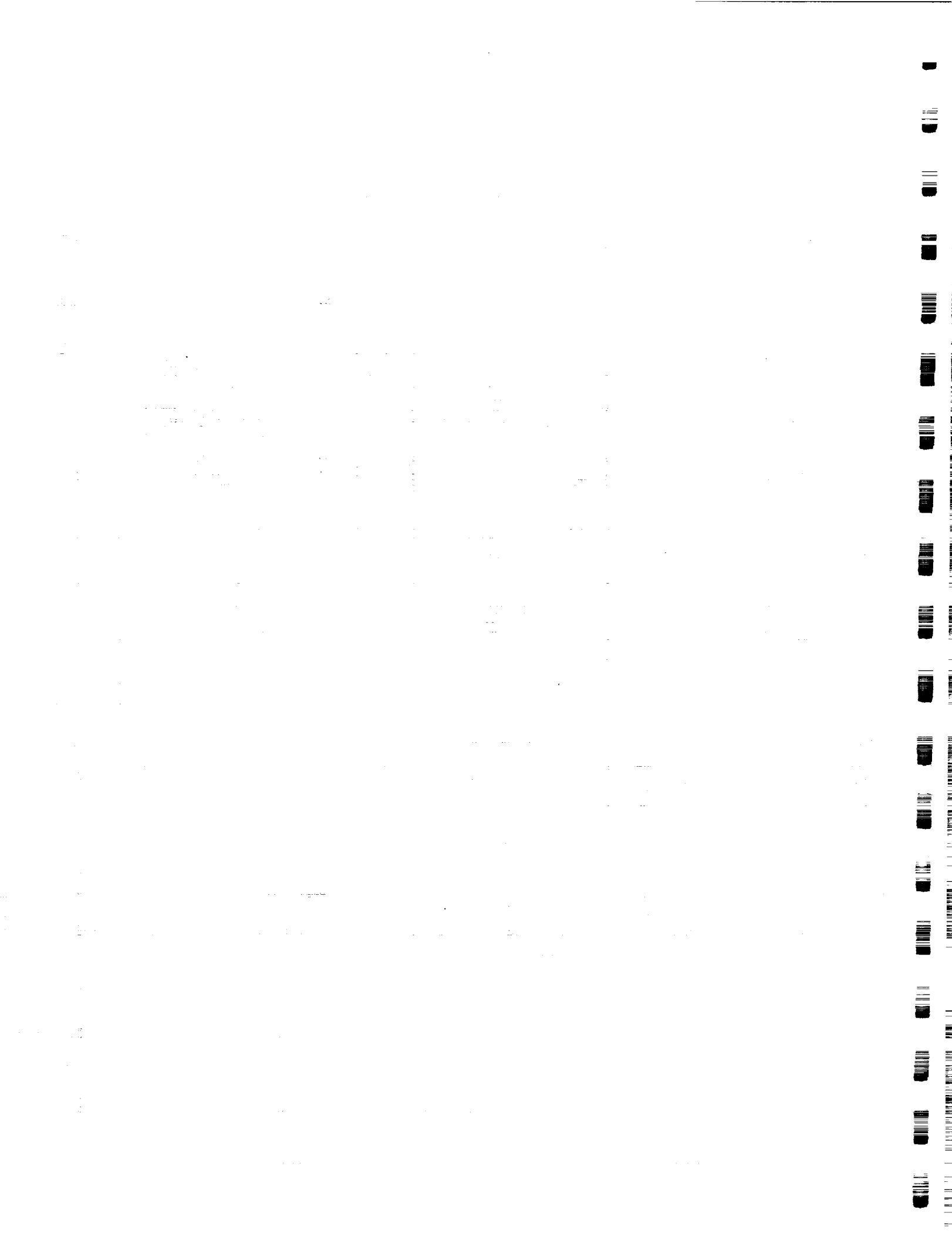
Practical Realization

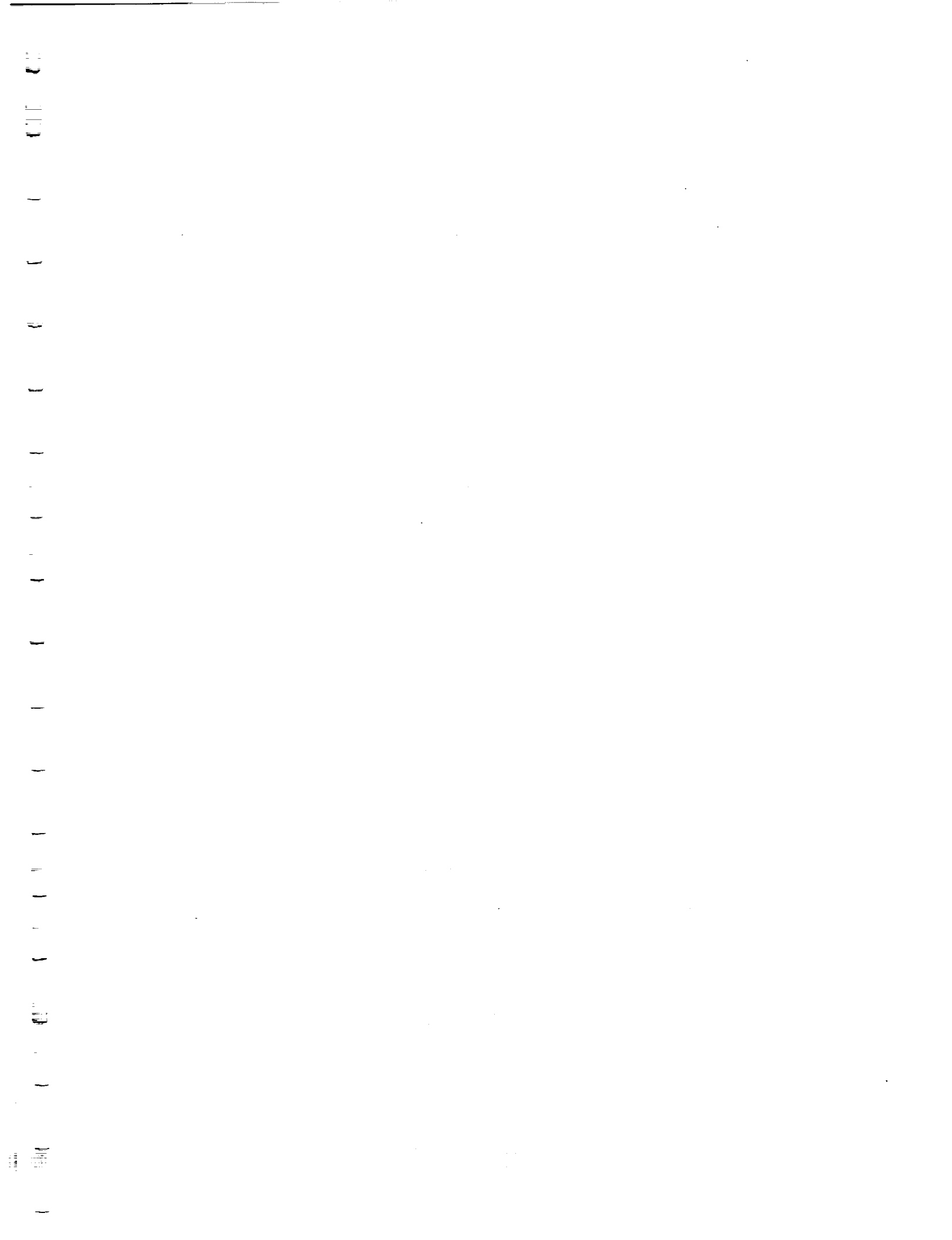
- Simulation of identification and robust control processes for MACE
(important for confirming convergence of parameter estimates to "true" ones)

- Ground experiment

- Experiment in space







IN THESE VIEWGRAPHS WE SUMMARIZE THE RESEARCH EFFORTS OF THE STUDENTS UNDER THE SUPERVISION OF PROFESSOR MICHAEL ATHANS. DUE TO TIME LIMITATIONS THEIR RESEARCH WILL ONLY BE HIGHLIGHTED, AND NO TECHNICAL DETAILS ARE PROVIDED.

WE WERE FORTUNATE TO HAVE DR. JOSEF BOKOR, OF THE HUNGARIAN ACADEMY OF SCIENCES VISITING MIT UNDER A FULLBRIGHT GRANT, PARTICIPATE IN OUR RESEARCH, ESPECIALLY IN THE AREA OF SYSTEM IDENTIFICATION. THE REST OF THE PARTICIPANTS ARE MIT GRADUATE STUDENTS.

FRANK AGUIRRE AND EDWARD BIELECKI STARTED THEIR RESEARCH IN THE FALL OF 1991. THEY ARE BOTH WORKING ON THEIR SM THESIS RESEARCH IN THE EE&CS DEPARTMENT. LEONARD LUBLIN IS PRESENTLY WRITING HIS SM THESIS IN THE A&A DEPARTMENT. KIRK GILPIN COMPLETED HIS SM THESIS IN THE EE&CS DEPARTMENT IN THE SUMMER OF 1991, AND IS NOW WORKING FOR HONEYWELL INC. JOEL DOUGLAS ALSO FINISHED HIS SM IN THE EE&CS DEPARTMENT IN MAY 1991, WORKED DURING THE SUMMER FOR LOCKHEED, AND RETURNED IN THE FALL TO CONTINUE HIS RESEARCH AND STUDY FOR HIS DOCTORAL THESIS. JOEL DOUGLAS WILL PRESENT IN THE FOLLOWING TALK HIS PROGRESS IN THE IDENTIFICATION OF THE MACE TEST ARTICLE.



SUMMARY OF ADDITIONAL RESEARCH IN MULTIVARIABLE IDENTIFICATION AND CONTROL

Michael Athans
Frank Aquirre
Edward Bielecki
Josef Bokor
Joel Douglas
Kirk Gilpin
Leonard Lublin

January 23, 1992

FROM A THEORETICAL POINT OF VIEW WE SEEK TO DEVELOP NEW COMPUTER-AIDED DESIGN METHODOLOGIES FOR THE ROBUST CONTROL OF MULTIVARIABLE SYSTEMS WITH BOTH PARAMETRIC AND OTHER DYNAMIC UNCERTAINTY.

OUR PROGRESS TO DATE IN THE ROBUST CONTROL OF SYSTEMS WITH PARAMETER UNCERTAINTY HAS BEEN DOCUMENTED IN THE FOLLOWING PUBLICATIONS:

J. DOUGLAS AND M. ATHANS, "ROBUST LQR CONTROL FOR THE BENCHMARK PROBLEM," PROC. AMERICAN CONTROL CONF., BOSTON, MA, JUNE 1991, PP. 1923-1924.

J. DOUGLAS AND M. ATHANS, "LINEAR QUADRATIC CONTROL FOR SYSTEMS WITH STRUCTURED UNCERTAINTY," SERC REPORT #12-91, MIT, SEPTEMBER 1991.

J. DOUGLAS AND M. ATHANS, "ROBUST LINEAR-QUADRATIC DESIGNS WITH RESPECT TO PARAMETER UNCERTAINTY," PROC. AMERICAN CONTROL CONF., CHICAGO, IL, JUNE 1992 (ALSO SUBMITTED FOR PUBLICATION TO THE IEEE TRANS. ON AUTOMATIC CONTROL).

THE IDEAS DEVELOPED ABOVE ARE BEING EXTENDED IN THE CURRENT RESEARCH OF J. DOUGLAS AND E. BIELECKI.

ROBUST MULTIVARIABLE CONTROL WITH PARAMETRIC UNCERTAINTY

- Novel Robust LQR control strategy derived by J. Douglas (SM thesis, two ACC papers) under assumption of full state feedback.
- Uncertain energy interpretation continuing by J. Douglas and E. Bielecki.
- Extension to Robust H_2/H_∞ version, with output feedback and dynamic compensation, topic of J. Douglas Ph.D. thesis with applications to MACE.

MOTIVATED BY THE NEED FOR RELIABLE MULTIVARIABLE IDENTIFICATION OF THE INTERFEROMETER TESTBED FOR VARIOUS ACTUATOR AND SENSOR LOCATIONS, WE DEVELOPED A SYSTEMATIC PROCEDURE FOR MIMO IDENTIFICATION, TOGETHER WITH THE REQUIRED SOFTWARE, AND TESTED IT ON THE INTERFEROMETER TESTBED.

OUR PROGRESS IS DOCUMENTED IN THE FOLLOWING PUBLICATIONS:

K. GILPIN, M. ATHANS, AND J. BOKOR, " IDENTIFICATION OF A LIGHTLY DAMPED STRUCTURE FOR CONTROL/STRUCTURE INTERACTIONS," SERC REPORT # 11-91, MIT, AUGUST 1991.

K. GILPIN, M. ATHANS, AND J. BOKOR, " MULTIVARIABLE IDENTIFICATION OF THE MIT INTERFEROMETER TESTBED," PROC. AMERICAN CONTROL CONF., CHICAGO, IL, JUNE 1992.

MORE RECENT VARIANTS OF THIS METHODOLOGY ARE CURRENTLY USED BY SEVERAL STUDENTS TO IDENTIFY SPECIFIC INTERFEROMETER-TESTBED CONFIGURATIONS AND THE MACE TRANSFER FUNCTION MATRICES.

MULTIVARIABLE IDENTIFICATION

- Systematic procedure for MIMO identification, together with required software, developed (K. Gilpin SM thesis; Gilpin, Athans, Bokor 1992 ACC paper). Blends:
 - Model reduction using Hankel matrix tools.
 - Initial SISO models using ordinary least squares and sinusoidal inputs.
 - Selective model refinement using nonlinear least squares.
 - Integration into MIMO model via residue matrix methods.
 - MIMO zero refinement using maximum likelihood identification based on white noise signals. Constrain MIMO poles, refine MIMO zeros.
 - Generation of singular values vs frequency.
- Methodology tested on interferometer testbed using accelerometer measurements. Extended to laser measurements (R. Jacques, F. Aquirre, and others). Will be used by Douglas for MACE.

OUR EXPOSURE TO THE COMPLEX INTERFEROMETER-TESTBED DYNAMICS, ITS DYNAMIC AND PARAMETRIC UNCERTAINTY, COUPLED WITH THE STRINGENT PERFORMANCE SPECIFICATIONS HAVE LED US TO A SIMULATION STUDY OF STUDYING SPECIFIC MIMO LQG-BASED DESIGN METHODOLOGIES WITH FREQUENCY WEIGHTS WHICH ARE ROBUST WITH RESPECT TO PARAMETER ERRORS AND HIGH-FREQUENCY UNMODELED DYNAMICS.

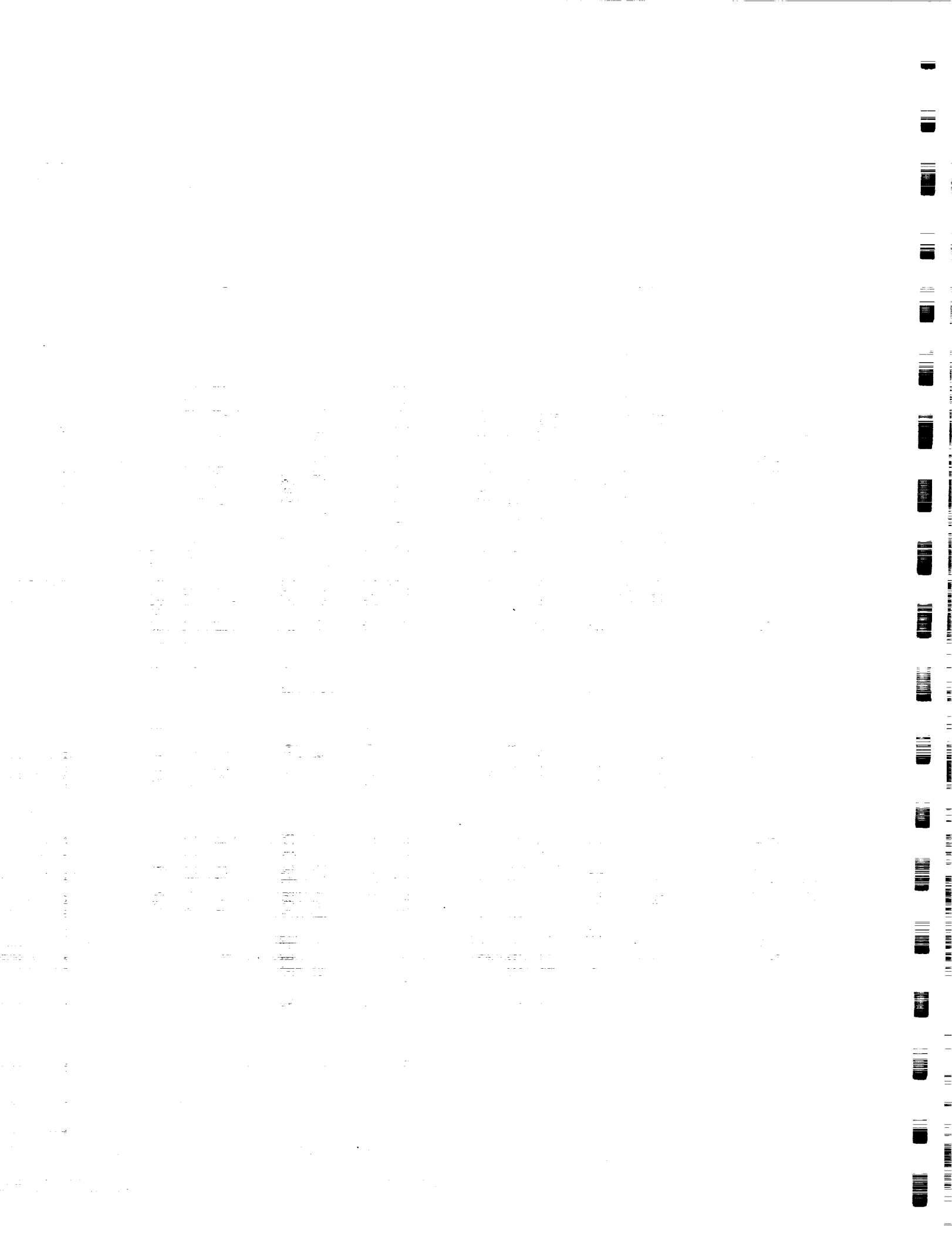
SUCH MODEL ERRORS INVARIABLY LIMIT THE PERFORMANCE (IN THE SENSE OF DISTURBANCE REJECTION) OF MIMO FEEDBACK CONTROL DESIGNS. TO UNDERSTAND THE COMPLEX TRADEOFFS INVOLVED WE STUDIED THE PROBLEM OF DESIGNING A MIMO CONTROLLER FOR A TWO-DIMENSIONAL TRUSS STRUCTURE USING A (TRUNCATED) FINITE-ELEMENT MODEL OF A BEAM. SUCH A MODEL APPROXIMATION INVARIAILY BRINGS INTO SHARP FOCUS THE IMPACT OF BOTH PARAMETRIC AND DYNAMIC UNCERTAINTY, SCALING, FREQUENCY WEIGHT SELECTION, STABILITY-ROBUSTNESS AND PERFORMANCE-ROBUSTNESS.

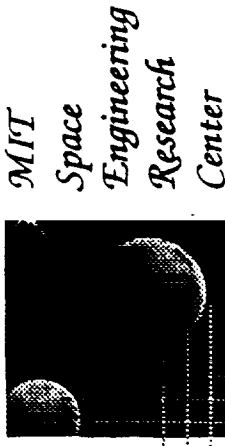
THE LESSONS THAT WE HAVE LEARNED FROM THIS DESIGN EXERCISE WILL BE VERY VALUABLE WHEN WE DESIGN HIGH-AUTHORITY DYNAMIC COMPENSATORS IN THE INTERFEROMETER TESTBED.

NO FORMAL DOCUMENTATION IS AVAILABLE AS YET ON THIS PROJECT. A SERC REPORT BASED ON L. LUBLIN'S SM THESIS IS UNDER PREPARATION.

MIMO DESIGN UNDER PARAMETRIC AND OTHER DYNAMIC UNCERTAINTY

- Goal is how to deal with complex dynamic plant errors in MIMO feedback control designs (e.g. interferometer) and to study impact of scaling and frequency weights.
- Developed H_2 (frequency-weighted LQG) MIMO controller for a 2-D truss using truncated beam model. Topic of L. Lublin SM thesis (being written right now). Simulation study, no hardware tests as yet.
- Parametric and high-frequency dynamics model errors limit superior disturbance-rejection performance.
- Phase information from Singular Value Decomposition provides partial information for stability robustness.
- We could not obtain significant reduction in conservatism associated with unstructured stability-robustness tests using this MIMO phase information.





Multivariable Identification for Control

Joel Douglas

January 23, 1992

AN IMPORTANT ONGOING RESEARCH ACTIVITY AT SERC IS THE DESIGN OF MULTI-INPUT MULTI-OUTPUT CONTROLLERS WHICH ARE ROBUST TO PARAMETRIC UNCERTAINTY. SINCE MOST OF THE CURRENT ROBUST DESIGNS REQUIRE A STATE-SPACE MODEL OF THE PHYSICAL SYSTEM, WE NEED TO DETERMINE HOW TO DERIVE SUCH A MODEL. ADDITIONALLY, WE DESIRE A MODEL WITH AS FEW STATES AS POSSIBLE, SO AS TO REDUCE THE ORDER OF THE CONTROLLER. THUS, WE WOULD LIKE A MINIMAL MULTIVARIABLE MODEL WHICH CAPTURES ALL THE NECESSARY DYNAMICS FOR CONTROL DESIGN.

MOTIVATION

- We want to study the design of robust multivariable controllers.
- Need a state-space model of system for design.
- How do we derive a minimal multivariable model?

THE FIRST STEP IN DERIVING A MIMO MODEL IS TO IDENTIFY EACH INPUT-OUTPUT LOOP. MANY TECHNIQUES EXIST TO DO SUCH A SISO IDENTIFICATION. ONE COMMON METHOD IS THE OUTPUT ERROR/NONLINEAR LEAST SQUARES TECHNIQUE. TYPICALLY, ONE WILL USE AN EQUATION ERROR/LINEAR LEAST SQUARES TO DETERMINE AN INITIAL GUESS FOR THE NONLINEAR METHOD.

FOR THE WORK ON MACE, WE USE A NEW NONLINEAR METHOD, IN WHICH WE PENALIZE THE DIFFERENCE IN THE LOG'S OF THE ESTIMATED AND MEASURED TRANSFER FUNCTIONS. THE REASON IS THAT MACE IS A LIGHTLY DAMPED SYSTEM, AND THIS METHOD PREVENTS A SMALL ERROR IN THE FREQUENCY OF A LIGHTLY DAMPED POLE TO APPEAR AS A LARGE ERROR IN THE COST FUNCTIONAL.

SISO Identification

- Well known techniques for Identifying SISO models.

- Output Error/Nonlinear Least Squares

$$Y(z) = G(z, \theta_f)U(z) + e_{oe}(z)$$

- Equation Error/Linear Least Squares

$$G(z) = G(z, \theta_f) + e(z)$$

- Results in a set of poles/zeros for each SISO loop.

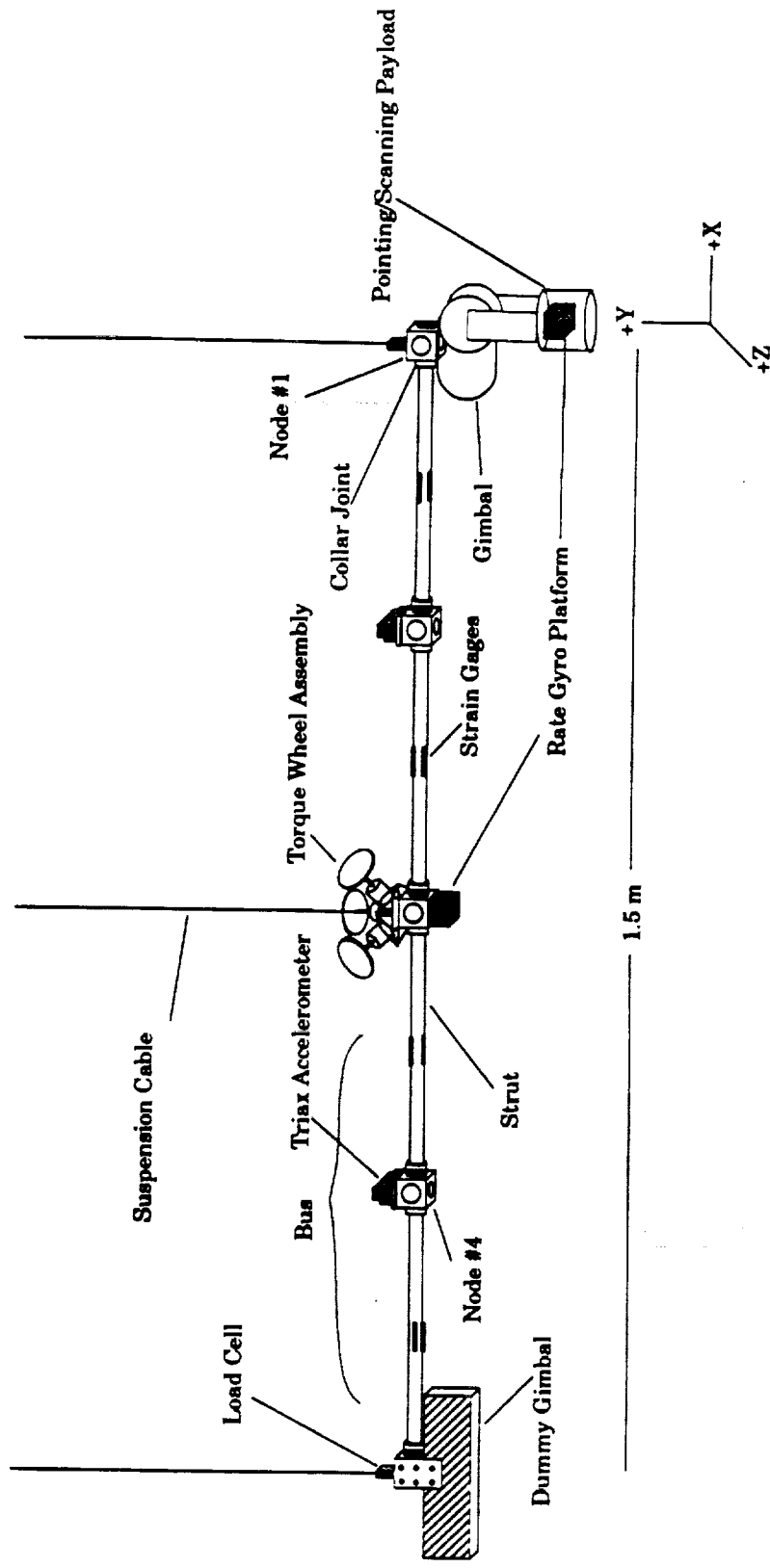
- Example on MACE

- Inputs: gimbal torque, torque wheel
 - Outputs: payload angle, encoder angle, bus angle
 - Nonlinear method with new cost function (Jacques):

$$J = \|\log G - \log G_m\|_2$$

A SCHEMATIC OF THE MACE DESIGN MODEL IS SHOWN. WE WOULD LIKE TO DO MIMO CONTROL ON MACE, AND SO A STATE-SPACE MODEL OF THE SYSTEM IS NEEDED. FOR THE FIRST MIMO MODEL, THE INPUTS ARE THE GIMBAL TORQUE AND THE TORQUE WHEEL, BOTH ACTING IN THE Z-DIRECTION. THE OUTPUTS ARE THE PAYLOAD ANGLE, THE RELATIVE ANGLE OF THE PAYLOAD TO THE BUS (DETERMINED BY AN ENCODER NOT SHOWN), AND THE BUS ANGLE MEASURED AT THE CENTER OF THE BUS. BOTH THE PAYLOAD ANGLE AND THE BUS ANGLE ARE DETERMINED BY MEASURING THE ANGULAR RATES, AND THEN INTEGRATING.

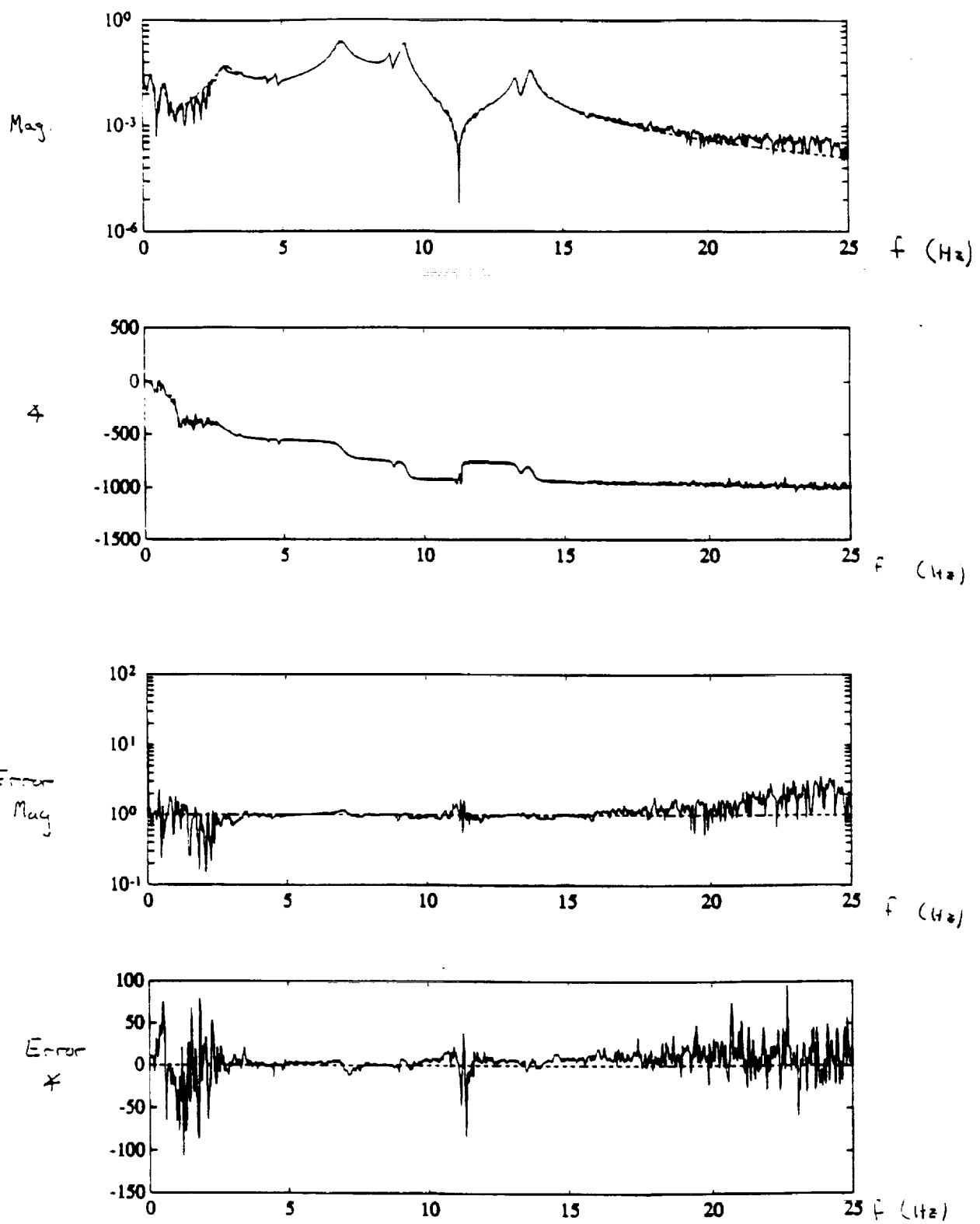
MACE SCHEMATIC



ONE OF THE SISO LOOPS IDENTIFIED USING THE NONLINEAR TECHNIQUE IS SHOWN. BOTH THE MEASURED AND MODELED TRANSFER FUNCTIONS ARE PLOTTED TOGETHER, AND ALSO THE DIFFERENCE BETWEEN THE TWO TRANSFER FUNCTIONS. THE TIME DELAY WAS MODELED USING A 4TH ORDER PADE APPROXIMATION.

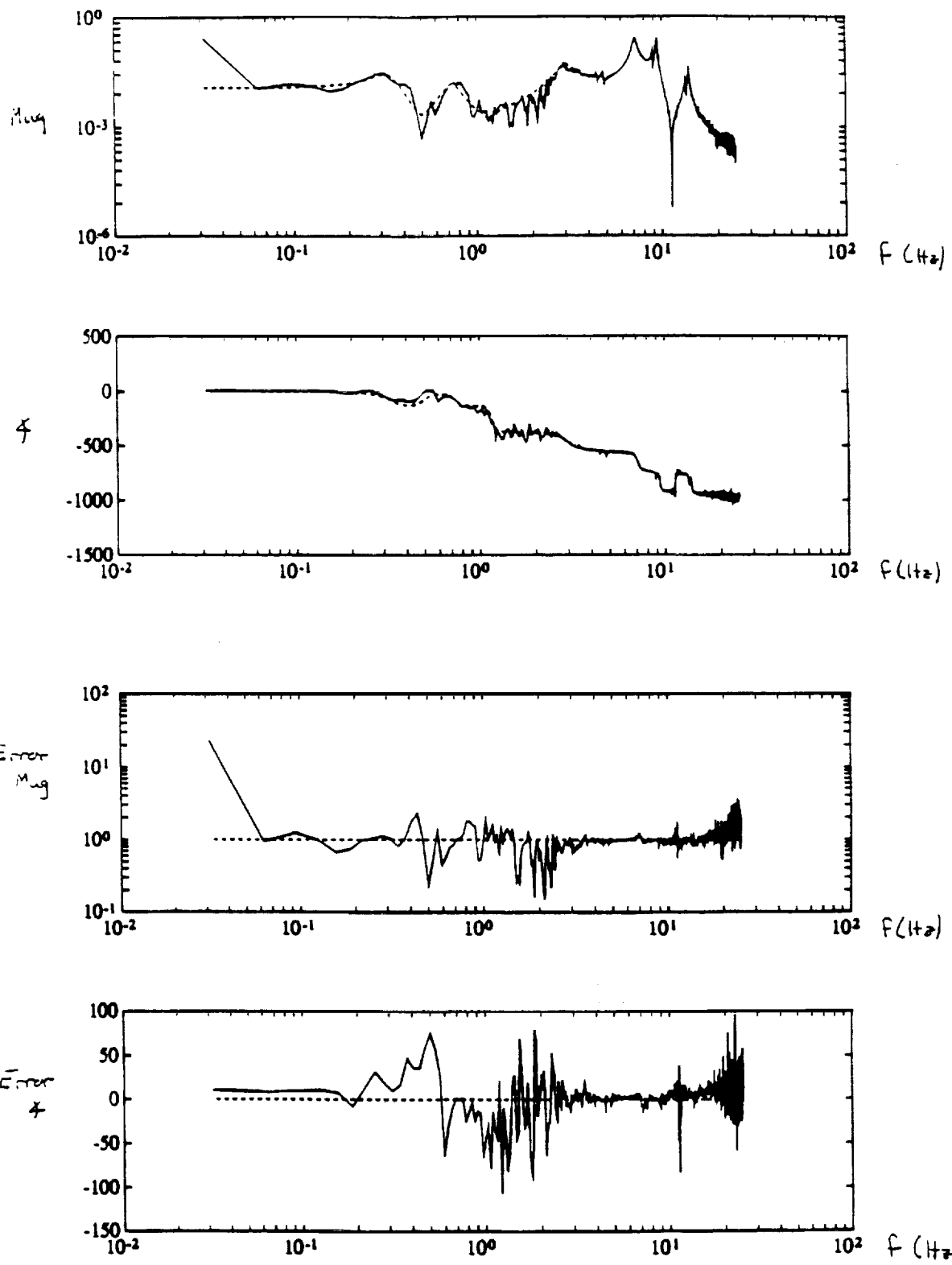
ON DOING THE IDENTIFICATION, WE FOUND THAT ONCE WE HAD FIT ALL THE LIGHTLY DAMPED POLES AND ZEROS, THE PHASE OF THE MODELED TRANSFER FUNCTION CLOSELY MATCHED THE PHASE OF THE MEASURED TRANSFER FUNCTION, BUT THE MAGNITUDE WAS INCORRECT. THIS WAS DUE TO A PAIR OF REAL ZEROS (ONE ZERO ON THE NEGATIVE REAL AXIS, THE OTHER ON THE POSITIVE REAL AXIS). THE APPROXIMATE LOCATION OF THESE ZEROS WAS FOUND USING THE FINITE ELEMENT MODEL, AND THEN THEN FIT INTO THE IDENTIFIED MODEL.

MACE EXAMPLE: TORQUE WHEEL TO ENCODER



THESE PLOTS ARE THE SAME AS THE PREVIOUS ONES, EXCEPT THAT THE FREQUENCY IS NOW IN A LOG SCALE. THIS EMPHASIZES THE LOW-FREQUENCY PORTION OF THE GRAPH. THE FIT AT LOW FREQUENCY IS NOT AS GOOD AS THE HIGHER FREQUENCIES BECAUSE THERE WERE LESS DATA POINTS TO MATCH.

MACE EXAMPLE: TORQUE WHEEL TO ENCODER



AS MENTIONED BEFORE, WE DESIRE TO COMBINE THE SISO TRANSFER FUNCTION ESTIMATES IN SUCH A WAY AS TO DETERMINE A MIMO STATE SPACE MODEL OF THE MACE SYSTEM. ADDITIONALLY, WE DESIRE A MINIMAL MODEL.

ONE METHOD TO DETERMINE A MIMO MODEL IS TO SIMPLY APPEND THE SISO TRANSFER FUNCTIONS TO CREATE A NON-MINIMAL MODEL. TO REDUCE THE MODEL, WE WOULD SIMPLY TRUNCATE UNOBSERVABLE OR UNCONTROLLABLE MODES. HOWEVER, THIS MAY CAUSE UNNECESSARY ERRORS. INSTEAD, WE WILL FOLLOW THE METHOD PROPOSED IN THE MASTERS THESIS OF KIRK GILPIN (SERC REPORT #11-91). THIS WILL PROVIDE A MINIMAL UNIQUELY DETERMINED MIMO STATE SPACE MODEL.

MIMO STATE SPACE MODEL

- State Space desired for ease of implementing control algorithms
- Goal is to determine minimal representation w/o truncation
- SM thesis by Gilpin

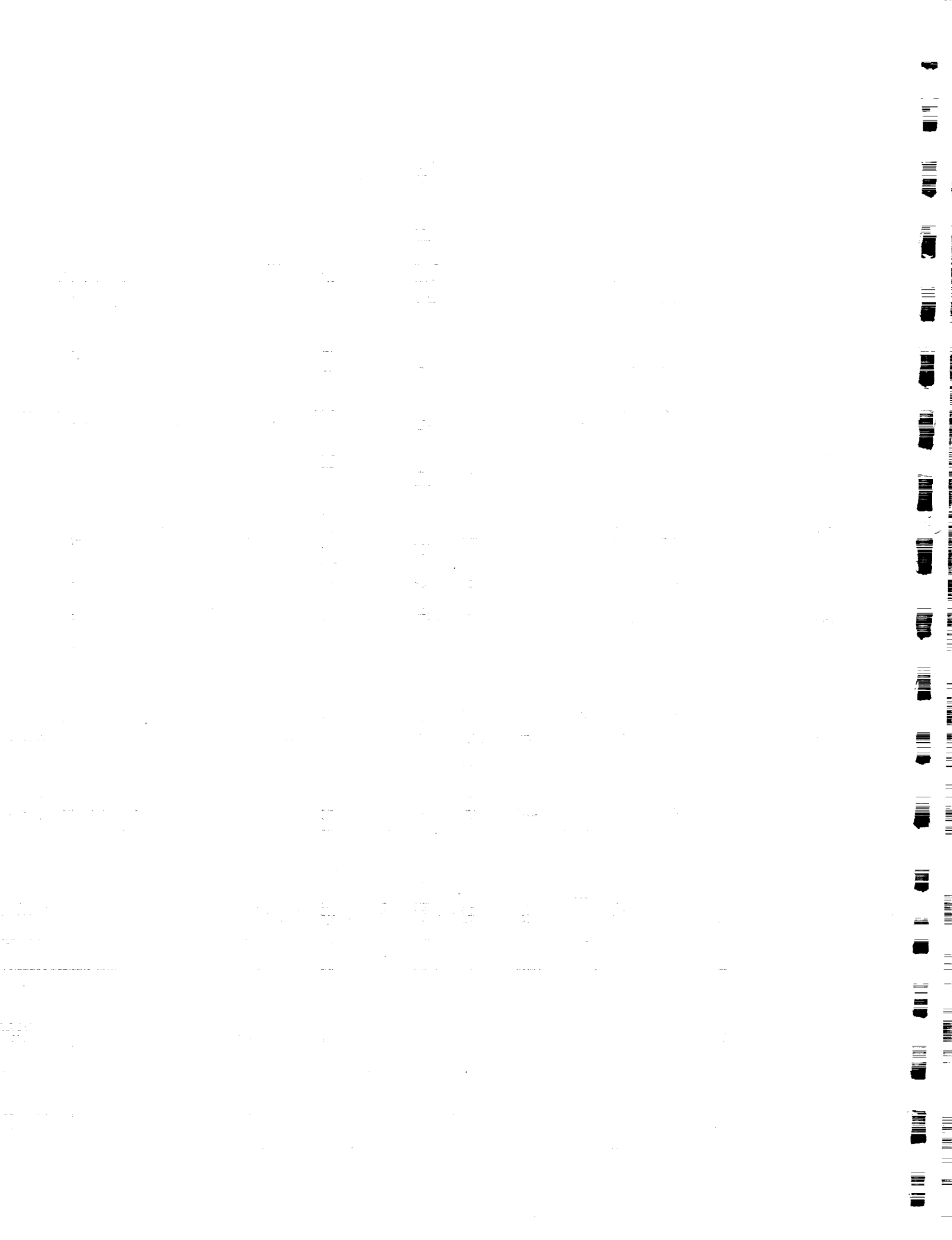
AS OF THIS TALK, WE HAVE IDENTIFIED THE SIX SISO TRANSFER FUNCTIONS OF THE MACE SYSTEM. WE ARE CURRENTLY WORKING ON COMBINING THESE TO DERIVE THE MIMO MODEL.

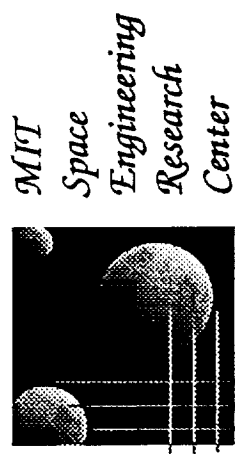
AS MENTIONED PREVIOUSLY, THE ULTIMATE GOAL IS TO DESIGN CONTROLLERS WHICH ARE ROBUST TO PARAMETER UNCERTAINTY. THIS MEANS WE MUST ADAPT OUR MIMO IDENTIFICATION TECHNIQUES SO THAT WE CAN IDENTIFY UNCERTAINTY BOUNDS ON PARAMETERS SUCH AS FREQUENCIES AND DAMPING RATIOS.

IN TERMS OF CONTROL, WE WISH TO FIRST CLOSE A MIMO LOOP ON MACE. ADDITIONALLY, WE WOULD LIKE TO EXTEND THE MASTERS THESIS OF JOEL DOUGLAS (SERC REPORT #12-91) FROM ROBUST FULL STATE FEEDBACK CONTROLLERS TO ROBUST OUTPUT FEEDBACK CONTROLLERS. COMBINING THIS NEW ROBUST METHOD OF CONTROL WITH IDENTIFICATION, WE WILL HAVE AN OVERALL PROCEDURE FOR THE IDENTIFICATION AND CONTROL OF UNCERTAIN SYSTEMS.

FUTURE WORK

- Identification
 - Combine SISO transfer functions using Gilpin's procedure.
 - Learn about identifying bounds on errors in frequencies, damping, mode shapes.
- Multivariable Control
 - Close a multivariable loop on MACE.
 - Extend robust full state feedback procedure of SM thesis to output feedback.
- Combine ID and robust control for overall procedure.





Sensor and Actuator Technology Development

Eric Anderson and Nesbitt W. Hagood

January 23, 1992

PRECEDING PAGE BLANK NOT FILMED

Sensor and actuator placement for robustness is the subject of a PhD thesis by Eric Anderson. This should be completed by Feb. 1993.

The self-sensing actuation is discussed in much greater detail in:

E. Anderson, N. Hagood, and J. Goodliffe, "Self-Sensing Piezoelectric Actuation: Analysis and Application to Controlled Structures," *33rd AIAA Structures, Structural Dynamics, and Materials Conf.*, Dallas, Apr. 1992, AIAA Paper 92-2645.

The nonlinear actuation modeling is work recently started that will consider nonlinearities in several different types of active materials.

Outline

- Sensor and Actuator Placement for Robustness
- Self-Sensing Actuators
- Nonlinear Actuation Models

The sensor/actuator selection problem has been recognized for a long time. Although there are many approaches available, most share a common attribute: the selection is based on a certain model. Notably, actuator and sensor noise have been considered (DeLorenzo, et al.), and costs based on the sensitivity of performance to uncertain parameters developed (Skelton).

The main point is that discussing the fine points of different schemes may be irrelevant if the models used are not very accurate.

Sensor/Actuator Selection

- Sensor and actuator selection/placement sets an *a priori* limit on closed loop performance.
- Correct placement can improve nominal performance for any specific control design technique.
- Placement problem has been investigated previously
 - open loop vs. closed loop algorithms
 - optimal vs. heuristic algorithms
- Degrees of freedom for sensor and actuator suite design:

Number	Type	Location
		subject to design constraints
- Placement is typically done using initial inaccurate model.

An explicit inclusion of the model uncertainty is included in robust control designs. It is believed that the uncertainty should also be represented in the sensor/actuator placement problem.



Sensor/Actuator Selection for Robustness

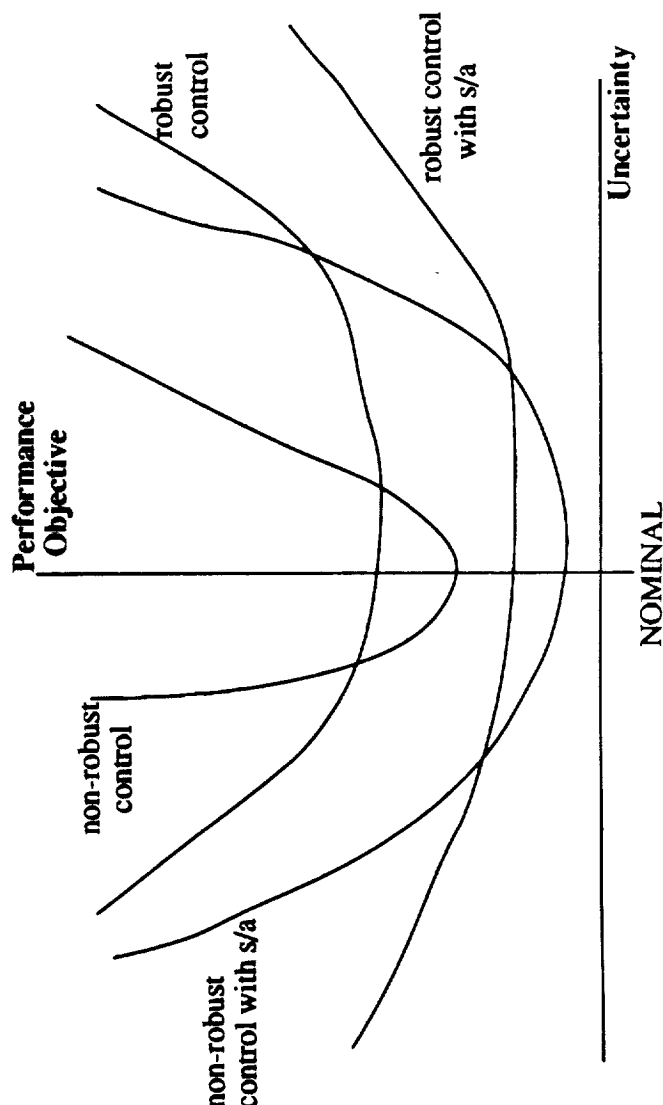
- **Concept:** Select sensors and actuators to minimize impact of model inaccuracies on achievable performance and stability.
- **Motivation:**
 - Placement and resulting closed-loop performance \stability are a strong function of model.
 - Only have uncertain model on which to base placement decisions.
 - Implies large uncertainties in *achievable* closed-loop performance or robustness.
- **Method:** Incorporate model uncertainty information into open or closed loop placement algorithms.

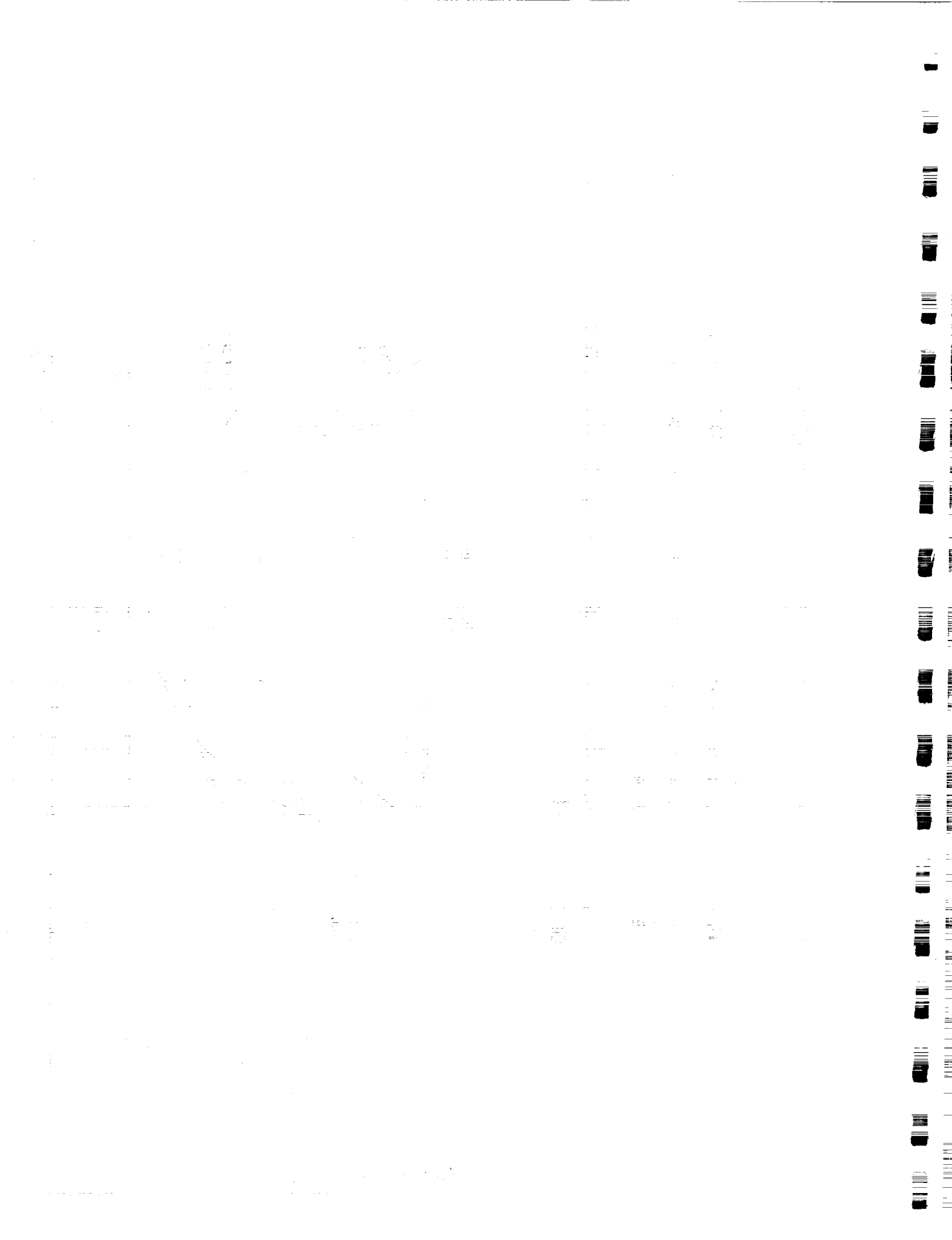
The plot is a qualitative speculation of the possible performance improvement. The performance objective (y-axis) is to be minimized in the presence of some number of uncertain parameters (x-axis).

Clearly, with appropriate s/a, the nominal performance can be improved. At this point, a debatable claim is that the s/a selection process incorporating uncertainty can achieve more robust closed loop results than robust control.

Achievable Performance Robustness

- Control design must use actuator and sensors it is given.
 - Example: Loss of controllability when actuator is unwittingly placed at a node.
- Can enable control task by introducing performance robustness through s/a set.





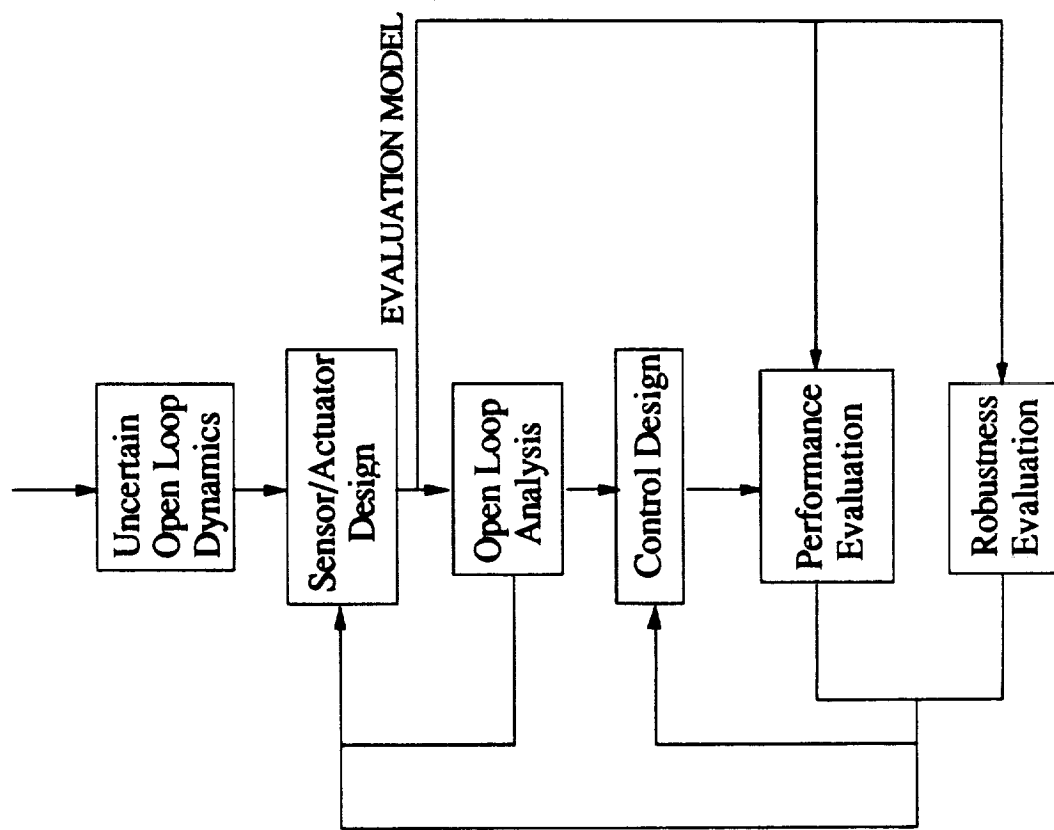
Methodology

- Model uncertainty strongly affects system matrices
 - Capture realistic error structure of finite element models
 - Introduce uncertainty early in analysis -> model set
- Open loop analysis:
 - 1) Heuristic reduction of s/a set
 - 2) Nominal Performance: Evaluate controllability/observability for each possible s/a set.
 - 3) Robust Performance: Evaluate expected value of controllability/observability over possible plants.
- Closed loop analysis
 - 1) Reduction of s/a set using open loop results
 - 2) Design controller for each s/a choice using standard techniques (e.g. LQG)
 - 3) Nominal Performance: Evaluate cost for each possible s/a set.
 - 4) Robust Performance: Evaluate expected value of cost over possible plants.

The important addition to the usual algorithm is the flow of robustness information back to the sensor/actuation selection.

System Design Methodology

Structural Constraints



The description of the uncertainty is critical. The errors typical of finite element modeling of complex built up structures must be represented. Regardless of the later ability to do in-line identification of control loops, an inaccurate model will be used to place the transducers. Further, any ground test of a large structure (if this is even feasible) may not accurately capture 0-g dynamics.

Representing the Uncertain System

- All system matrices affected by model uncertainty
- Focus on finite element errors, not ID errors
- Determine eigenvector uncertainty to expected errors:
 - Stiffness of components
 - Boundary conditions
 - Mass distribution
- Two approaches:
 - Range of possible plants/systems over all uncertain parameters
 - Sensitivity of nominal plant/system to uncertain parameters

Refer to Anderson PhD for much more complete description of the costs. To date, these results are very preliminary. It is important however to recognize the need for closed loop evaluation. A topic of current interest is whether one criterion can be used for the s/a selection and an entirely different one for the control design.

Figures of Merit

- Open loop analysis of sensor/actuator options used to reduce number of choices to manageable number
- Use controllability and observability gramians

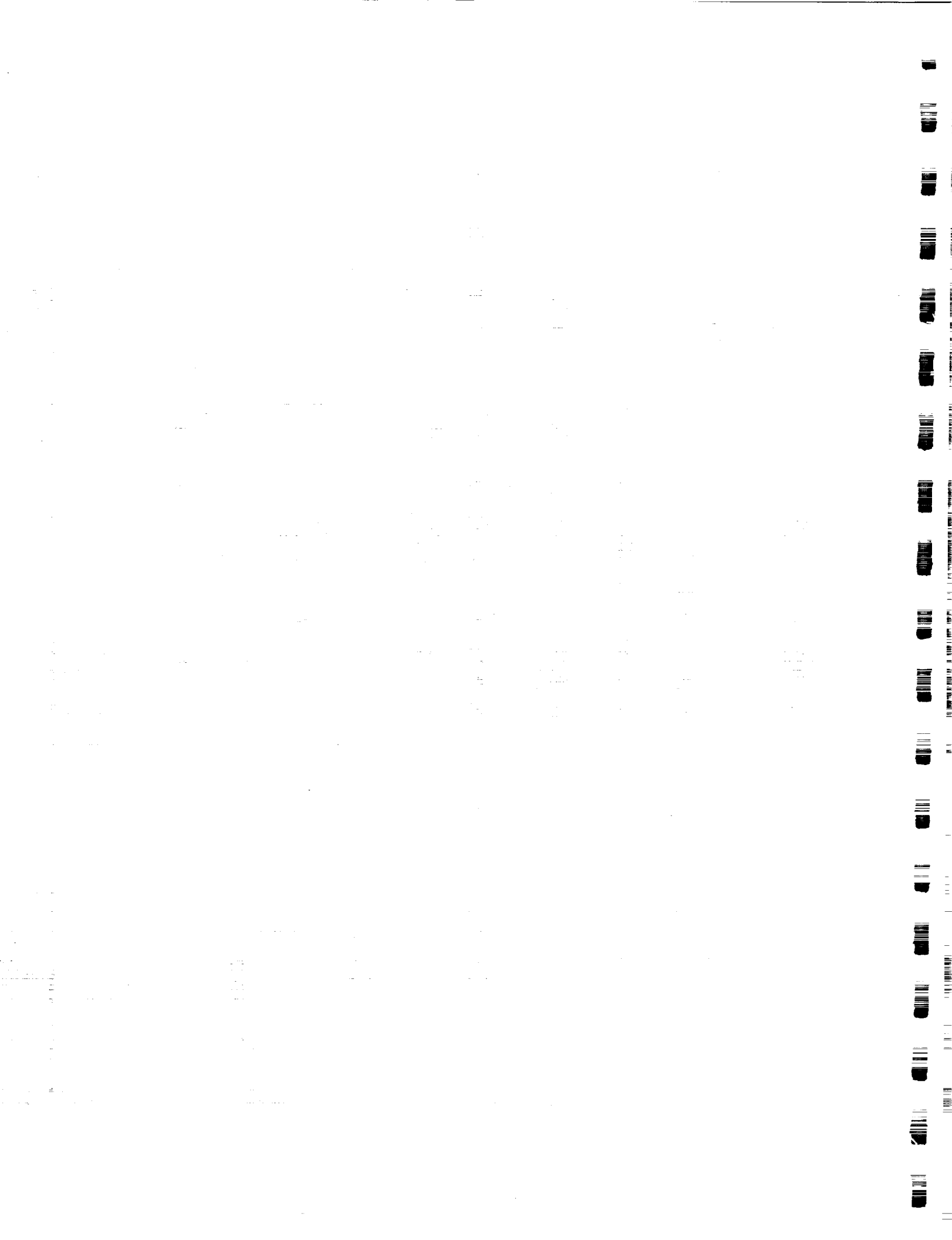
$$W_c(t_0, t_1) = \int_{t_0}^{t_1} \phi(t_1, \tau) B(\tau) \phi^T(t_1, \tau) d\tau$$

- Calculate with Lyapunov equation for each value of uncertainty
- $0 = A_i W_{c_i} + W_{c_i} A_i^T + B_i \Sigma_{ww} B_i^T,$
- Closed loop cost

$$J_{cl} = \text{tr}\{\langle Q C_i^T C_i \rangle\}$$

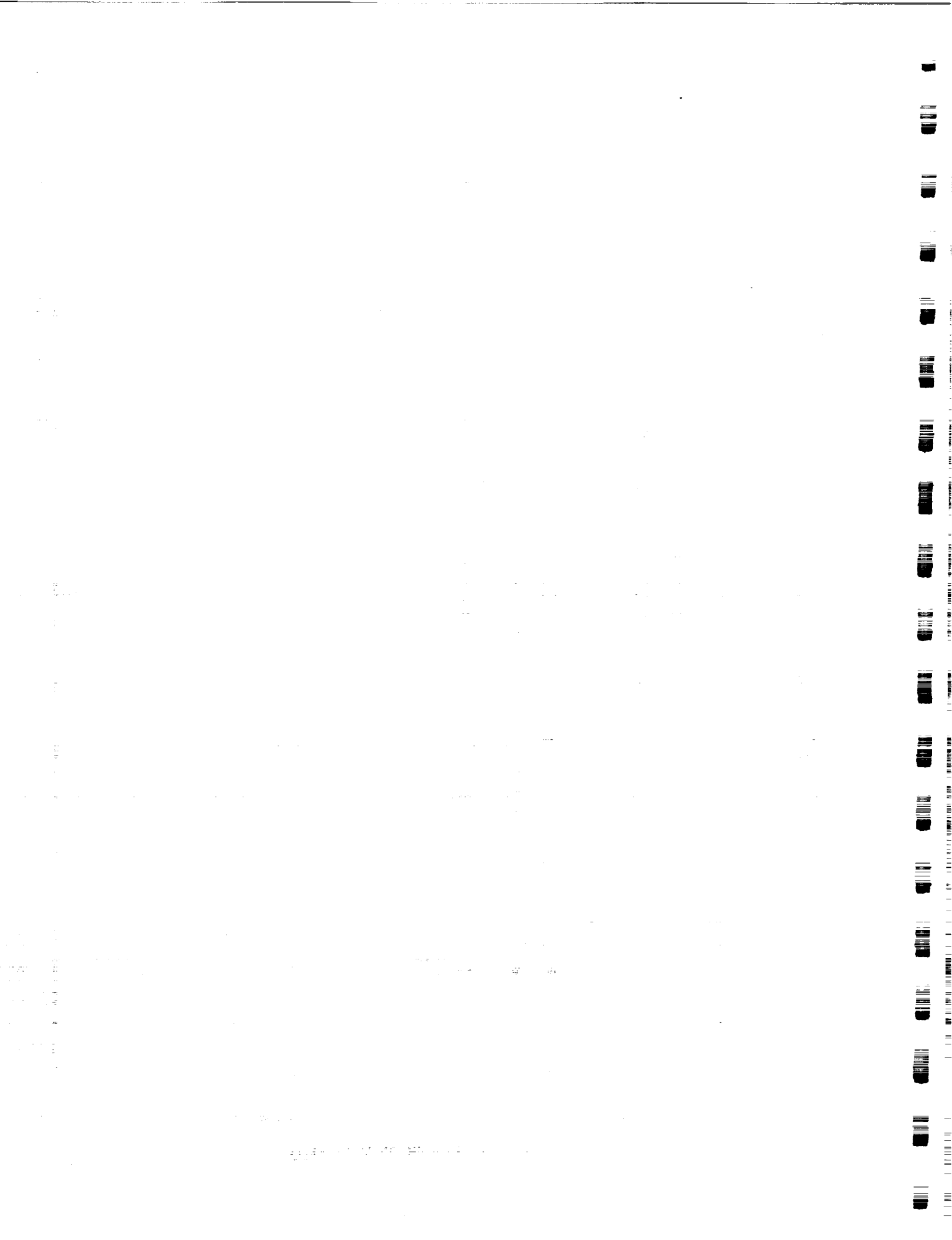
where

$$0 = A_i Q_i + Q_i A_i^T + B_i B_i^T$$



Design Algorithms

- Open loop
 - Compute expected value of gramians over entire uncertainty set
 - Reduce number of s/a options by straight ranking
- Closed loop
 - Use existing techniques for optimization
 - Cost is expected value over uncertainty set
 - Trade off degree of open loop reduction vs. size of set for closed loop optimization



Approach

- Structural dynamic analysis
 - Nominal plant model using standard Rayleigh-Ritz or f. e. techniques
 - Represent uncertainty by small number of fundamental parameters in stiffness and mass distribution - based on laboratory experience
 - Recompute model for range of values of uncertain parameters
- MATLAB analysis
 - State space system representation (for each value of uncertainties)
 - Calculate exact expected controllability/observability, weight by uncertainty distribution function, and average
 - Reduce possible s/a choices by straight ranking
 - Reduce model and design controller with iteration on state and control weighting for each design
 - Calculate exact expected closed loop cost, weight by uncertainty distribution function, and average
 - Check controllers on evaluation model

The primary test case for the study is the interferometer multipoint alignment testbed. However, a much simpler beam problem is being considered first. In this case, the number of possible transducer combinations is easily within brute force direct search techniques. More sophisticated search algorithms, restrictions, and approximations will have to be applied to the placement problem.

The question of how to any sort of structural control experiment involving robustness is an interesting one. Since the finite element model and the laboratory testbed represent only two distinct points in the space of uncertain parameters, experimental results are not necessarily sufficient to demonstrate results conclusively. An option under consideration is the deliberate introduction of uncertainties through moderate manipulation of mass distribution in the system.

Current Efforts

- Analytical sample problem: cantilevered beam
 - 6 sensors, 6 actuators
 - LQG control (SISO and TITO)
- Interferometer testbed
 - Analysis based on finite element model
 - Uncertainty description provided from system ID data
 - Main focus is active strut placement problem
 - Experimental demonstration of improved closed loop performance based on sensor/actuator location and type

The analysis is based on

N. Hagood, A. von Flotow, and W. Chung, "Piezoelectric Actuator Dynamics for Structural Control," *J. Intell. Mater. Syst. and Structures*, 1, 3, July 1990, pp. 327-354.

The self-sensing concept was demonstrated by

Dosch, J.J., Inman, D.J., and Garcia, E., "A Self-Sensing Actuator for Collocated Control," *ADPA Int'l. Symp. on Active Materials and Adaptive Structures, Alexandria, VA, Nov. 1991*. (submitted to *J. Intell. Mater. Syst. and Structures*)

and by the authors

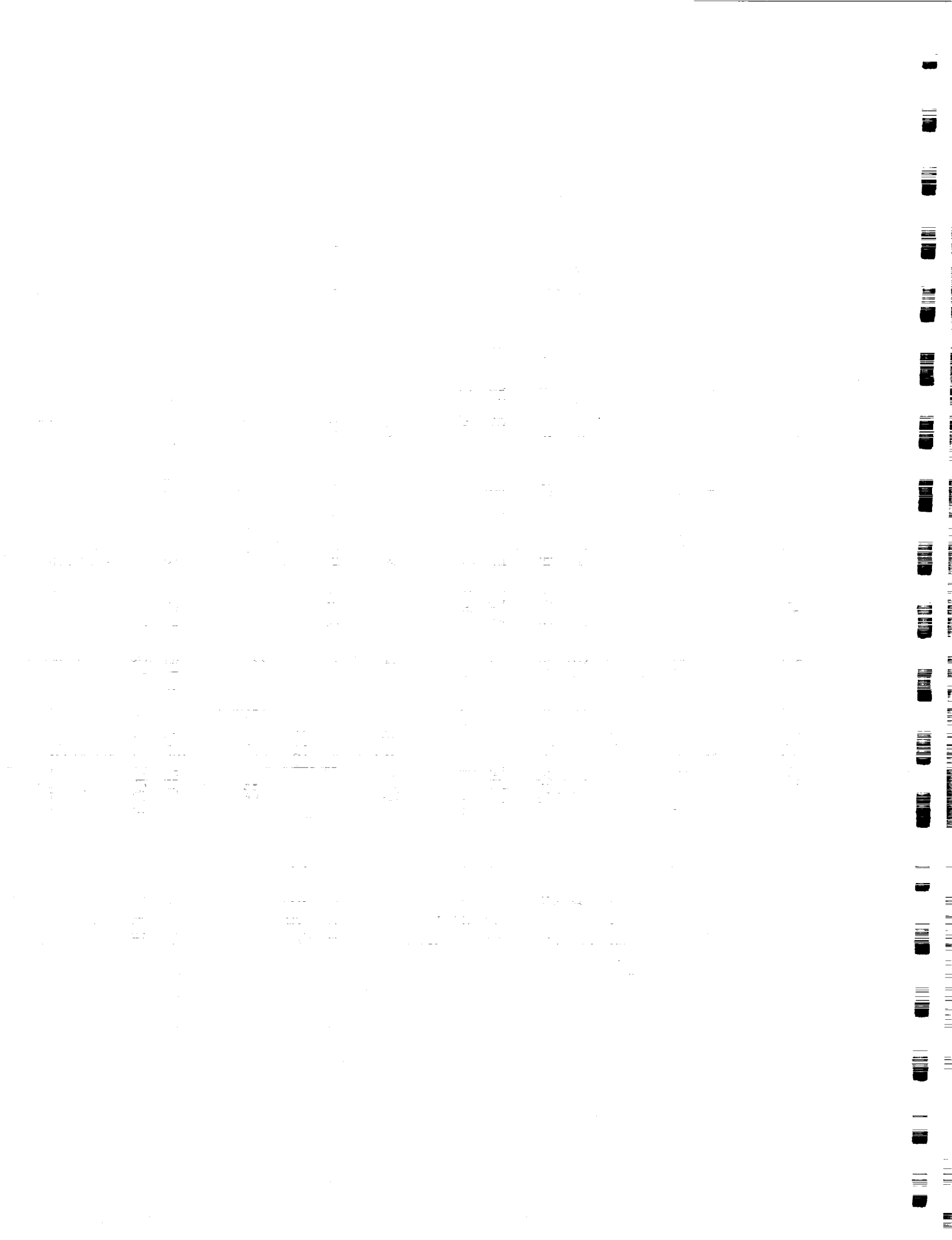
Hagood, N.W., and Anderson, E.H., "Simultaneous Sensing and Actuation Using Piezoelectric Materials," *SPIE Conf. on Active and Adaptive Optical Components*, July 1991, SPIE 1543-40.

A more complete presentation, including sensitivity to errors in implementation is described in

E. Anderson, N. Hagood, and J. Goodliffe, "Self-Sensing Piezoelectric Actuation: Analysis and Application to Controlled Structures," *33rd AIAA Structures, Structural Dynamics, and Materials Conf.*, Dallas, Apr. 1992, AIAA Paper 92-2645.

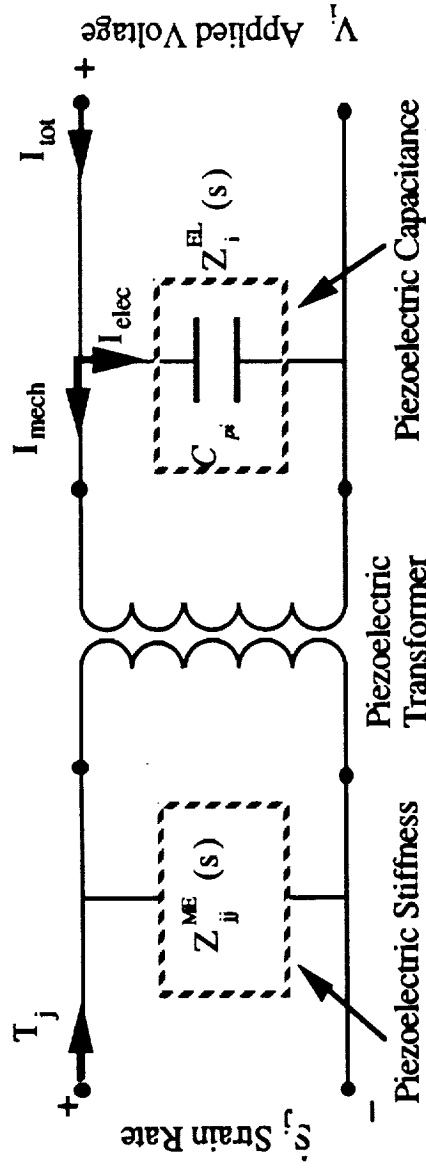
Simultaneous Sensing and Actuation

- **Concept:** Use the same piece of piezoelectric simultaneously as both a structural sensor and an actuator.
- **Motivation:**
 - Eliminates need for separate sensor. Reduced signal conditioning.
 - Perfectly collocated dual sensor useful for structural control.
- **Modelling:** If the applied current and piezoelectric electrode voltage is known, one can reconstruct the mechanical strain or strain rate.
$$\Theta^T \mathbf{r} = \mathbf{q} - C_p \mathbf{v} \quad \Theta^T \dot{\mathbf{r}} = \mathbf{i} - C_p \dot{\mathbf{v}}$$
- The $\Theta^T \mathbf{r}$ term is proportional to averaged strain state as for the charge based sensor.
$$\Theta^T \mathbf{r} = \int_{V_p} [e_{31} S_1 + e_{31} S_2 + e_{33} S_3] dv$$
- More insight can be gained on the physical significance of the terms by a piezoelectric circuit analogy.



Physical Interpretation

- The piezoelectric transformer analogy is useful for determining the physical significance of the terms. The piezoelectric element is represented as a transformer converting mechanical energy to electrical and vice versa.



- The sensor equation can be interpreted physically as measuring the difference in between applied current and the capacitance current.

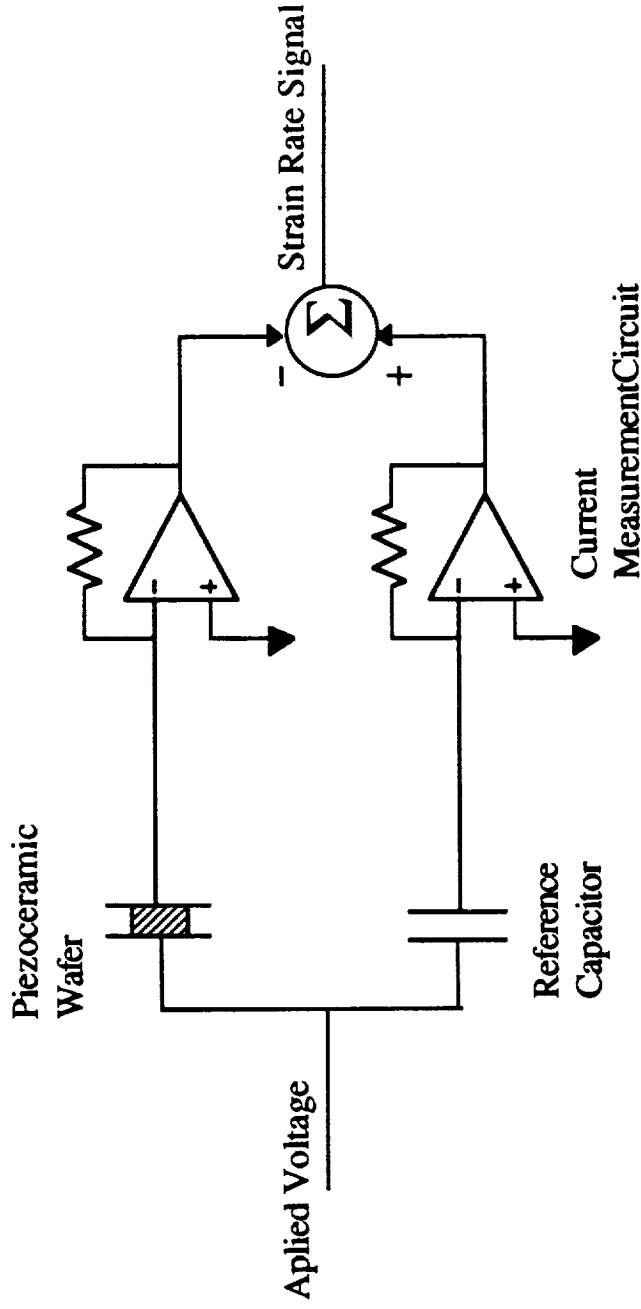
$$\Theta^T \dot{\mathbf{r}} = \underbrace{\mathbf{i}_{\text{mech}}}_{\mathbf{i}_{\text{tot}}} - \underbrace{C_p \dot{\mathbf{v}}}_{\mathbf{i}_{\text{elec}}}$$

It is also possible to use a capacitive bridge to extract measurement of the charge. See Dosch 1991 and Anderson, et al., 1992.

MIT Space Engine Research Center

Simple Circuit Implementation

- Strain Rate Circuit



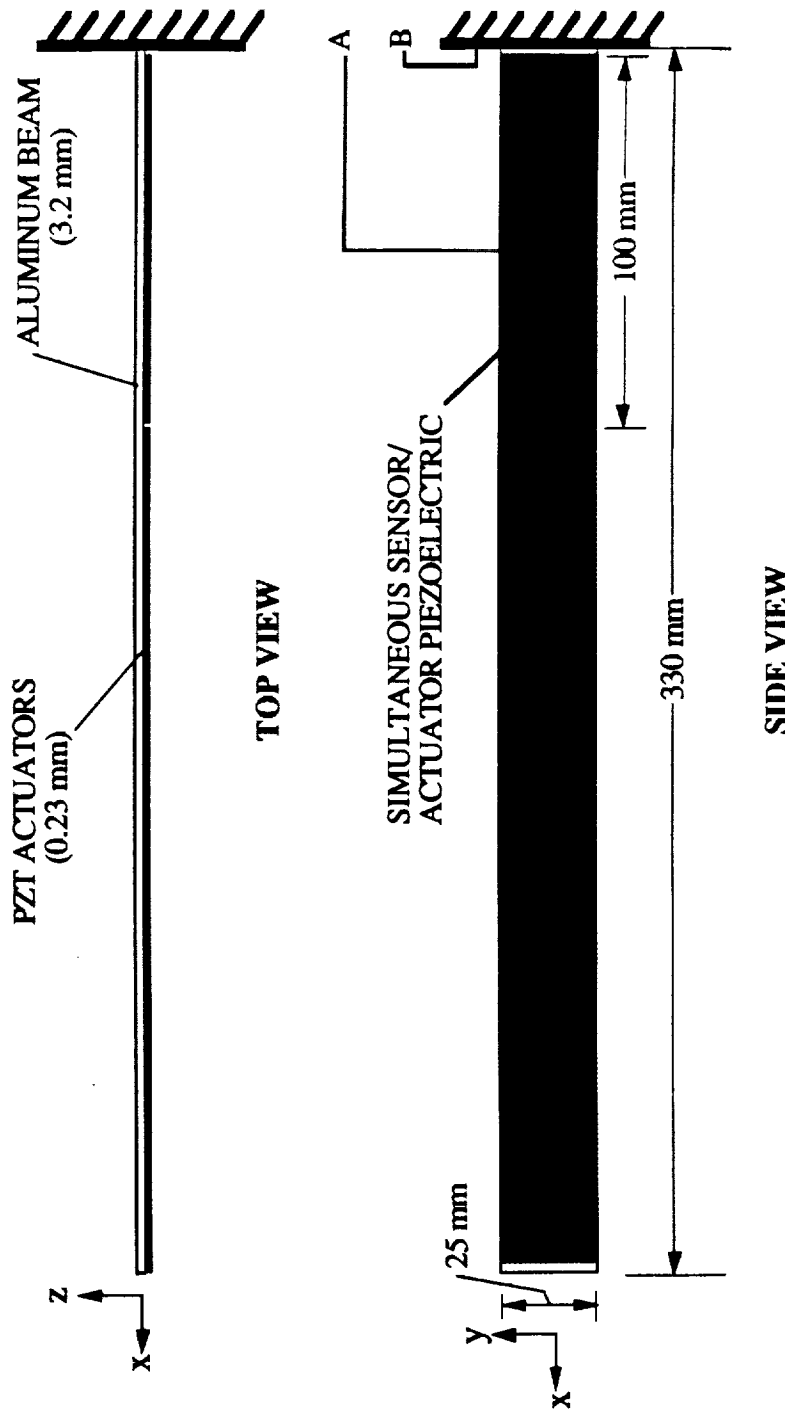
B) Strain-Rate Sensing Configuration

- Also possible to implement simple strain sensing circuit by measuring a charge rather than current.

A cantilevered beam was used in the experiments. A force transducer disturbance was introduced near the tip. Performance was measured with a laser displacement sensor, also near the tip.

System for Experimental Demonstration

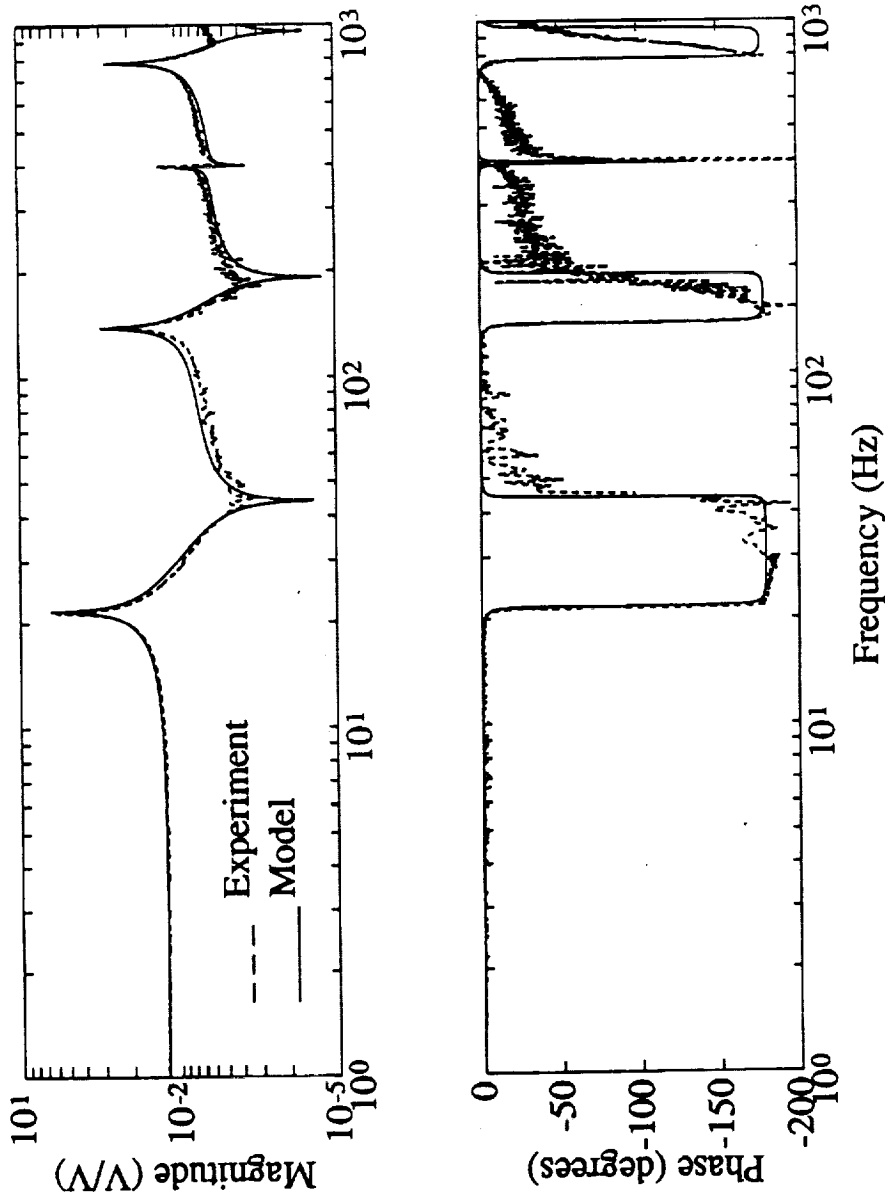
- Cantilevered beam with PZT wafers on the surface.



This is the colocated sensor output/actuator input transfer function.

The linear modeling of the “sensation” is well understood. The main difficulty is obtaining the sharpness of the analytically predicted zeros. Because of piezoelectric hysteresis, there are small (< 1 degree) phase errors between the two signals being differenced. Thus, they cannot yield a true 0 value. The effect is to damp the collocated transfer function zeros.

Open Loop Results



This is the laser performance output/disturbance force input for the LQG controller. The gain was kept low because of low frequency unmodeled dynamics of the optical bench.

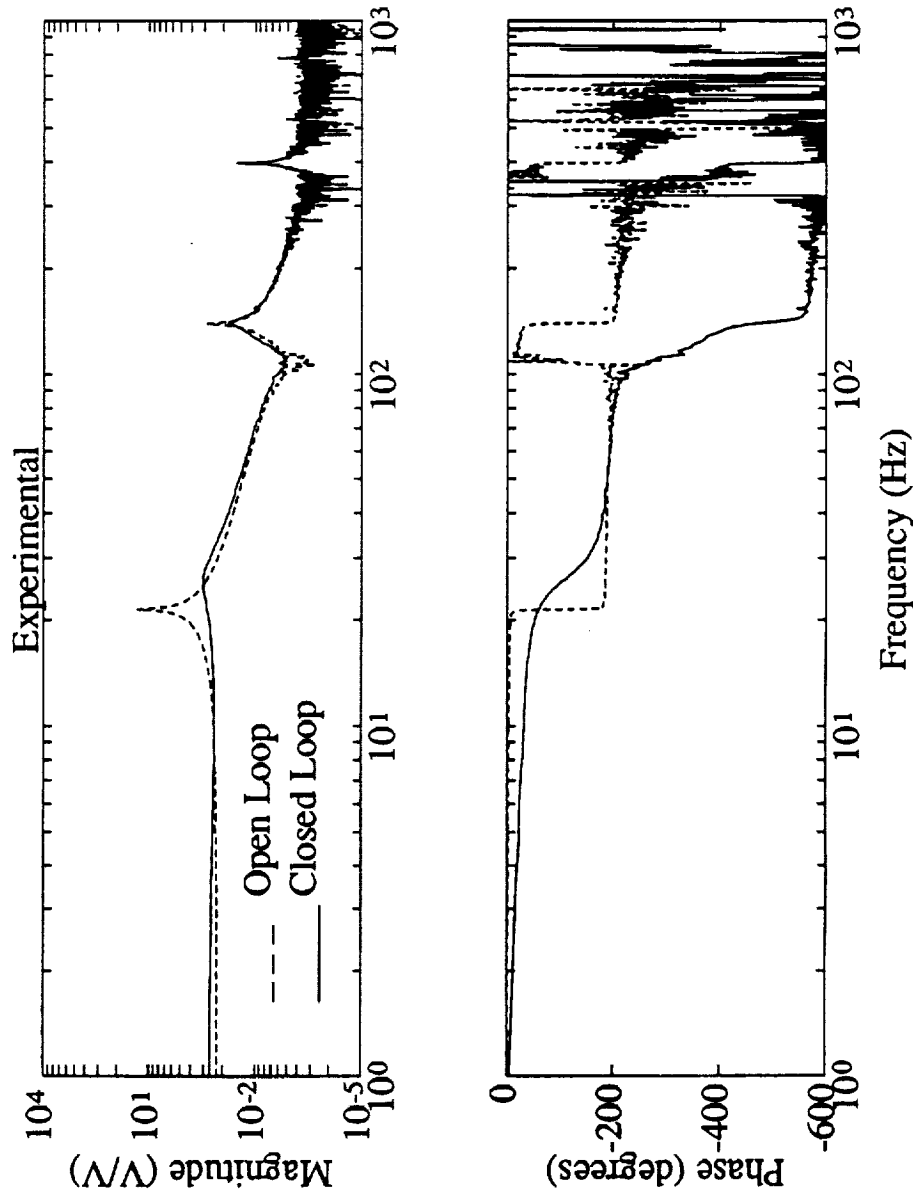
Strain rate feedback (SRF), positive position feedback (PPF) and LQG compensators were all designed based on the system model and implemented on the beam system. Results agree well with predictions.

The simultaneous strain sensor is a direct substitute for a sensor such as a strain gage.

In the AIAA paper, results of the effect of small errors in the circuit implementation are presented. Both the open loop zeros and the closed loop performance are significantly influenced.

Closed Loop Results

- Tip displacement/force input with “sensuator” loop closed

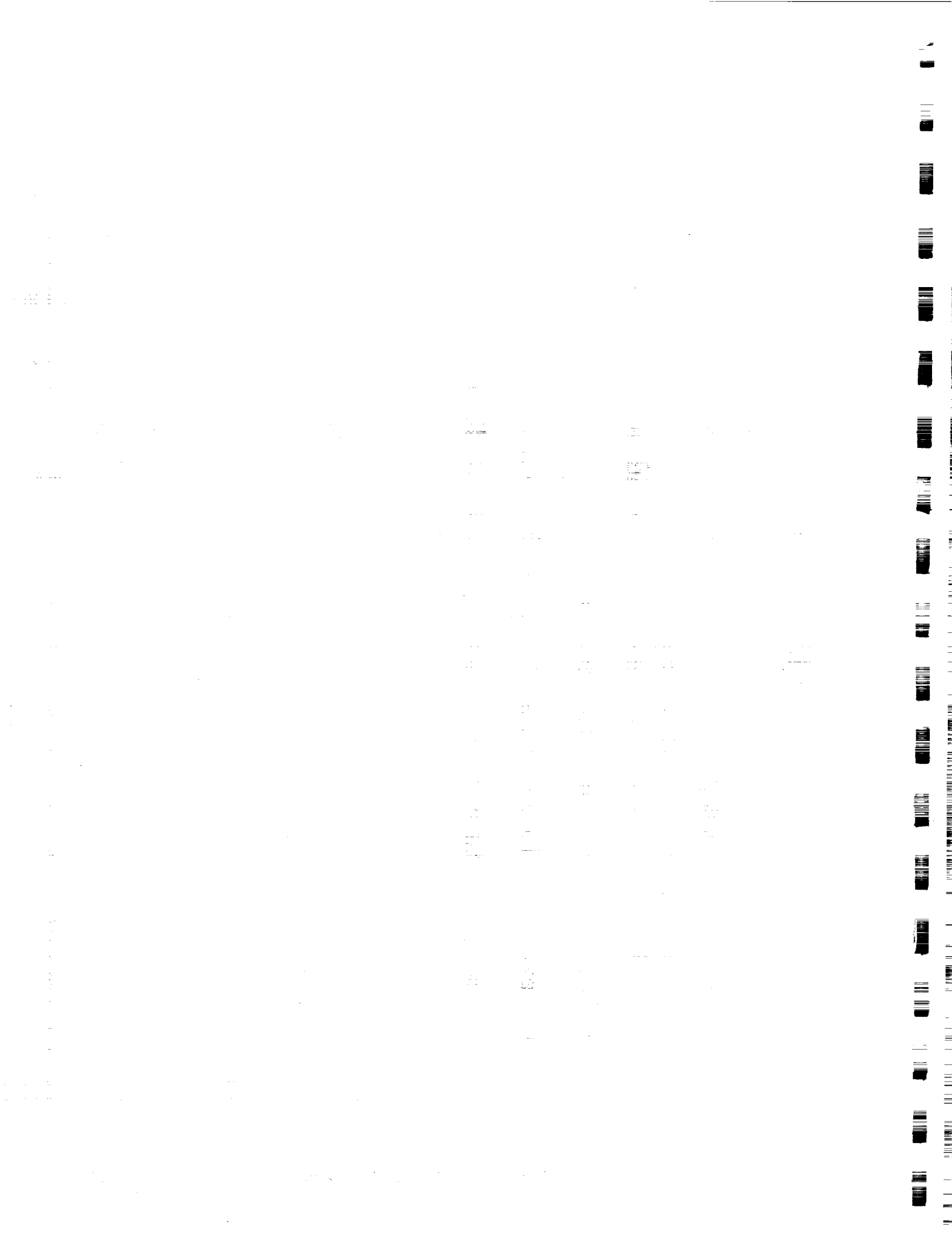


The simultaneous sensing was shown to be identical to a colocated strain gage measurement when the system was implemented on an active piezoelectric strut on the SERC interferometer multipoint testbed.

The possibility of a deliberately mistuned sensor that provides an impedance matched measurement was suggested in the strut implementation.

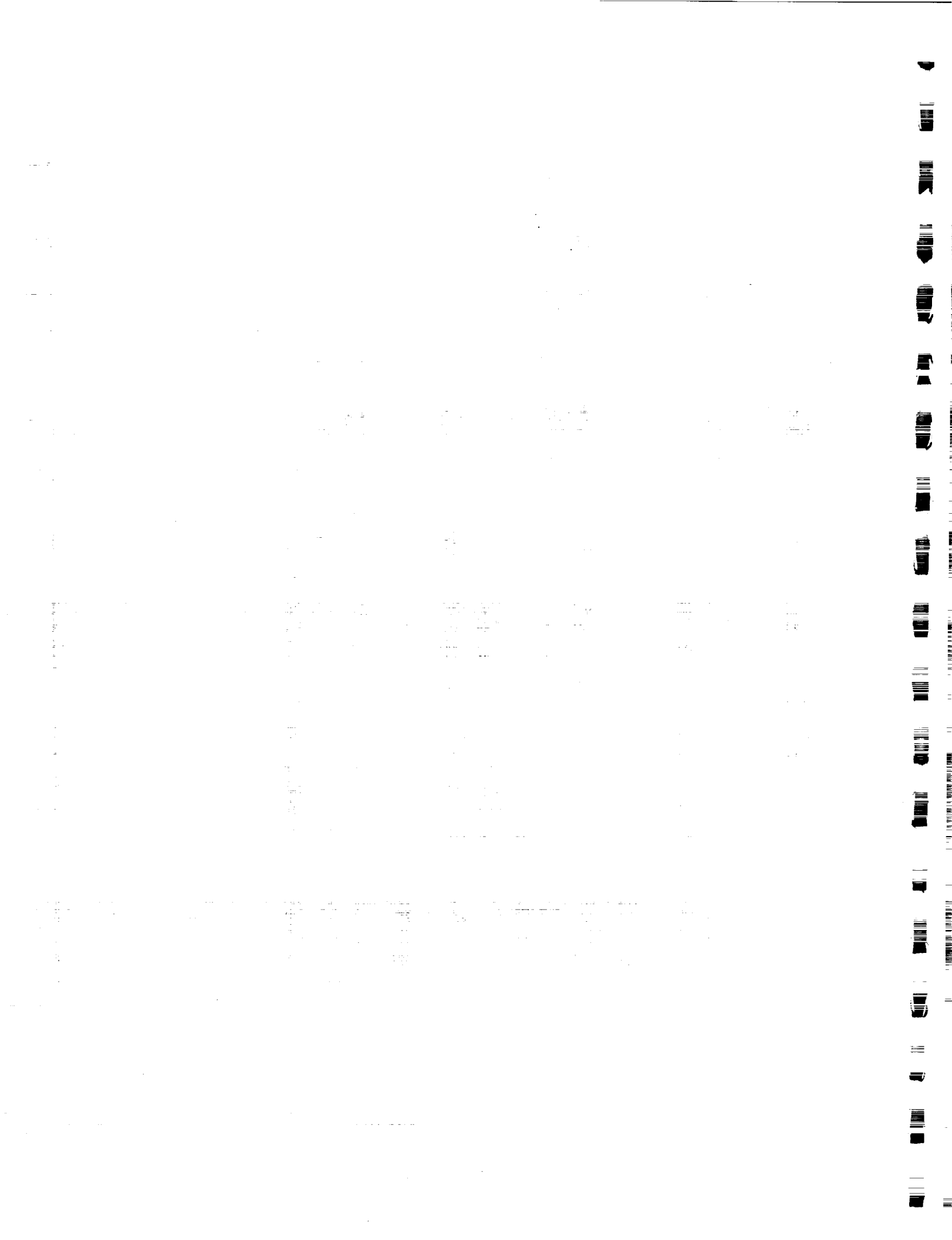
Applications

- Retrofit of sensing capability on existing actuator systems
 - Information on local deformation
 - Information for collocated control (addition of damping)
- Linearization of actuator response
- Health monitoring and system identification
- Active structural control (high gain collocated loops)



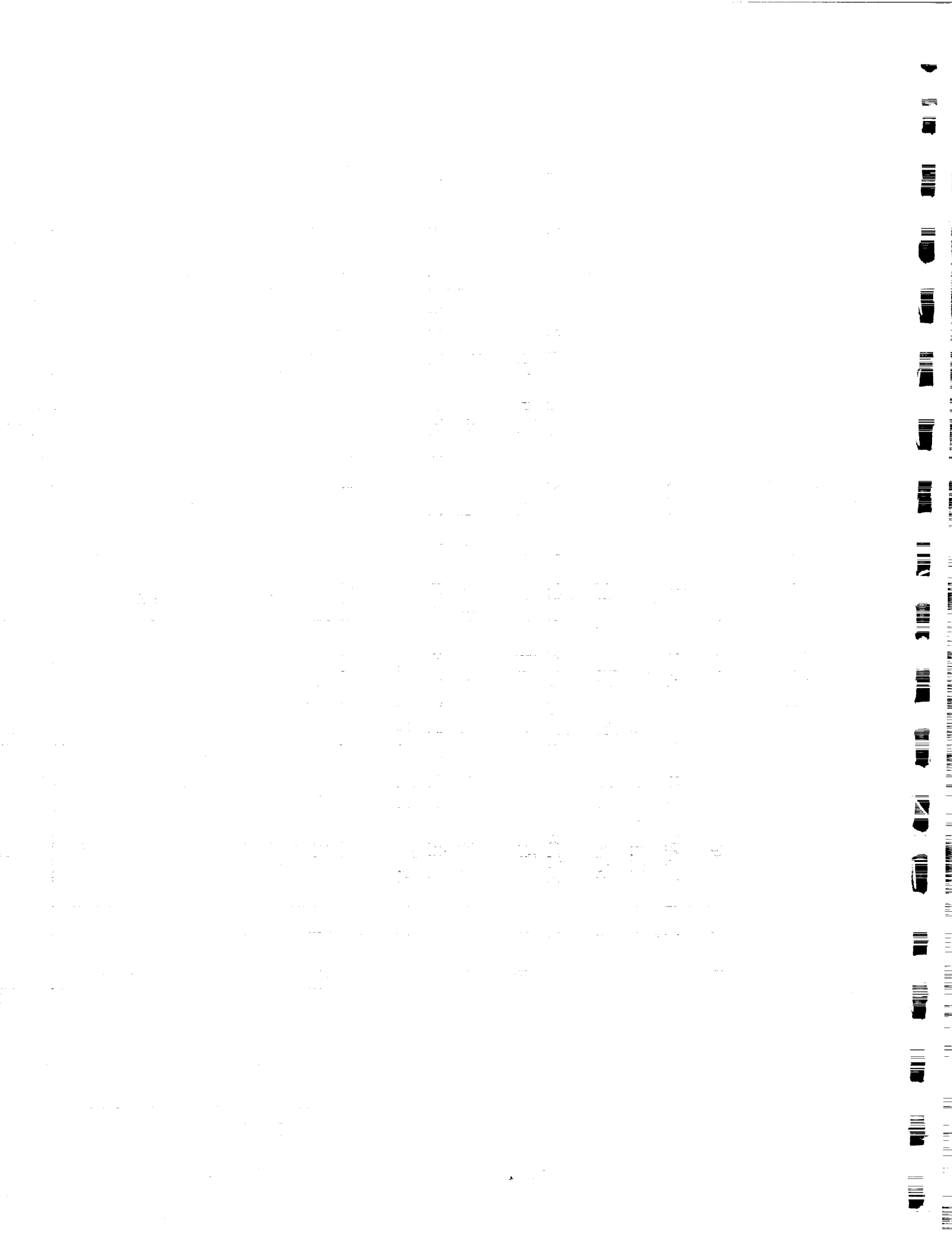
Nonlinear Actuation Models

- **Concept:** Develop models of actuated structures capable of handling actuation material nonlinearities
- **Motivation:**
 - Piezoelectric material properties are nonlinear at high strains.
 - Higher actuation performance available from inherently nonlinear materials.
- **Electrostrictive materials**
New high-strain, shape-memory ceramics.
- **Approach:**
 - Microscopic material models for capturing relevant physics.
 - Macroscopic phenomenological models for nonlinear structural response using energy methods.



Conclusions

- Ongoing work in three areas:
 - Robust Actuator and Sensor Placement
 - Self-Sensing Actuation
 - Nonlinear Actuation Modeling
- Robust actuator and sensor placement addresses a clear need but faces the difficulty of good error model development.
- Self-sensing actuation has been demonstrated and modeled, works well in active control systems for simple structures, and is being applied to built up structures.
- New research on nonlinear actuation models holds promise for high fidelity modeling of high strain actuation materials.





IMPLEMENTATION OF INPUT COMMAND SHAPING TO REDUCE VIBRATIONS IN FLEXIBLE SPACE STRUCTURES

Kenneth W. Chang
Professor Warren P. Seering
B. Whitney Rappole

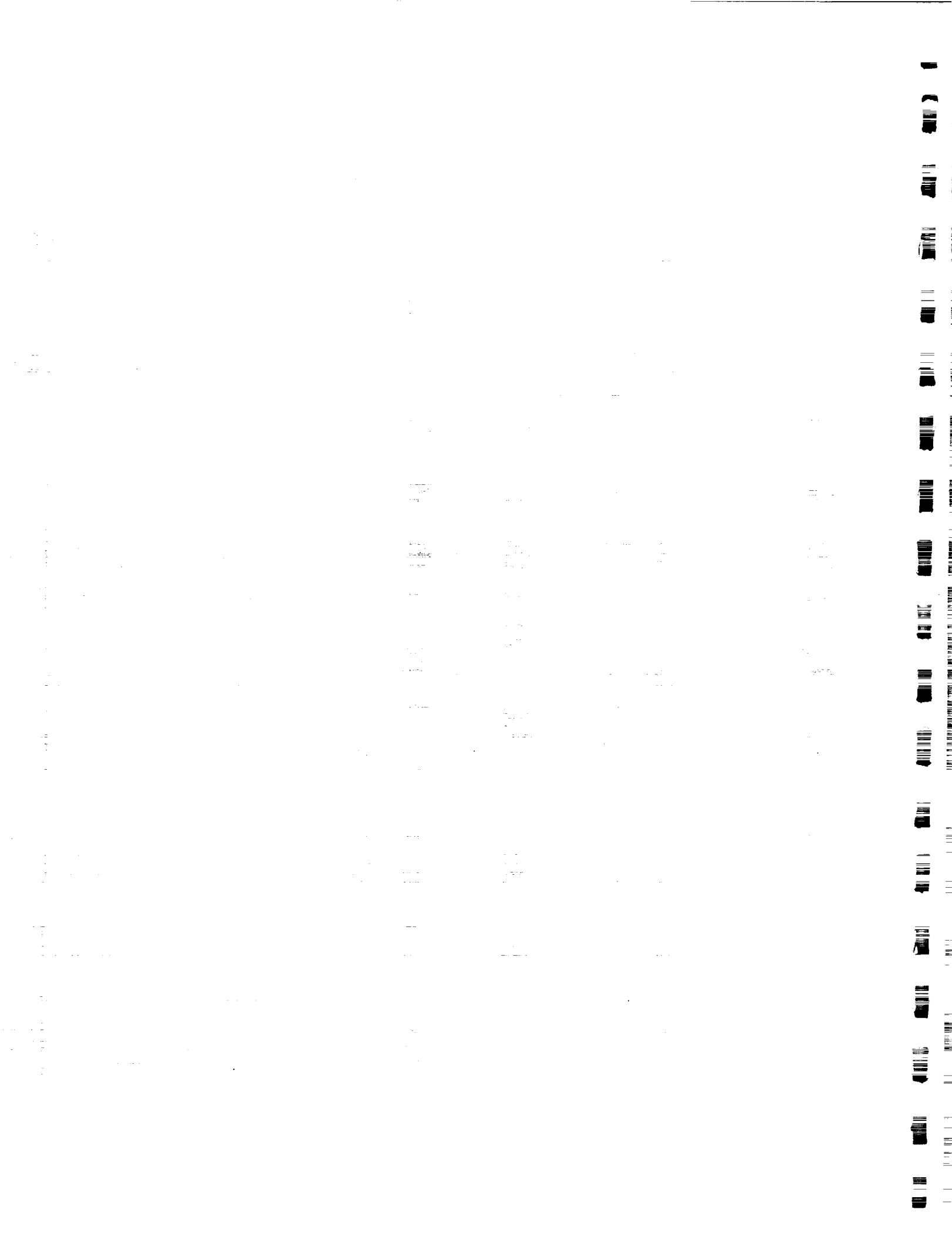
SERC Steering Committee Meeting
January 23, 1992

PRECEDING PAGE BLANK NOT FILMED

THE GOALS OF OUR RESEARCH CAN BE BROKEN DOWN INTO THE THEORETICAL AND EXPERIMENTAL. WE WANT TO EXPLORE THE THEORY OF INPUT SHAPING FURTHER TO FIND IMPULSE SEQUENCES WHICH ARE MORE EFFECTIVE. WE ALSO WANT TO IMPLEMENT THESE THEORETICAL RESULTS ON THE MACE TEST ARTICLE.

GOALS OF RESEARCH

- Explore theory of input command shaping to find an efficient algorithm for flexible space structures.
- Characterize MACE test article.
- Implement input shaper on the MACE structure; interpret results.



OUTLINE

- Background on Input Shaping.
- Simulation Results.
- Experimental Results.
- Future Work.

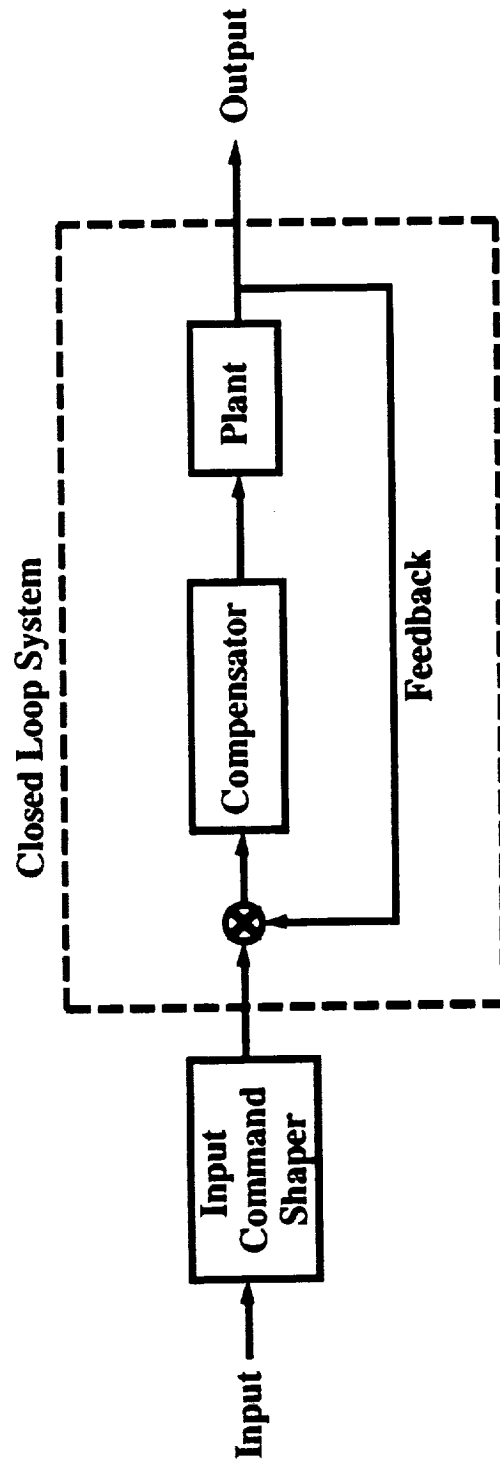
C-4

PRECEDING PAGE BLANK NOT FILMED

INPUT COMMAND SHAPING IS AN OPEN LOOP APPROACH TO REDUCING VIBRATION. AS CAN BE SEEN IN THE DIAGRAM, THE SHAPER RESIDES OUTSIDE OF OUR CONTROLLED SYSTEM. THE DYNAMIC SYSTEM, WHETHER OPEN LOOP OR CLOSED LOOP, IS SEEN AS AS BLACK BOX WITH CERTAIN DYNAMIC CHARACTERISTICS.

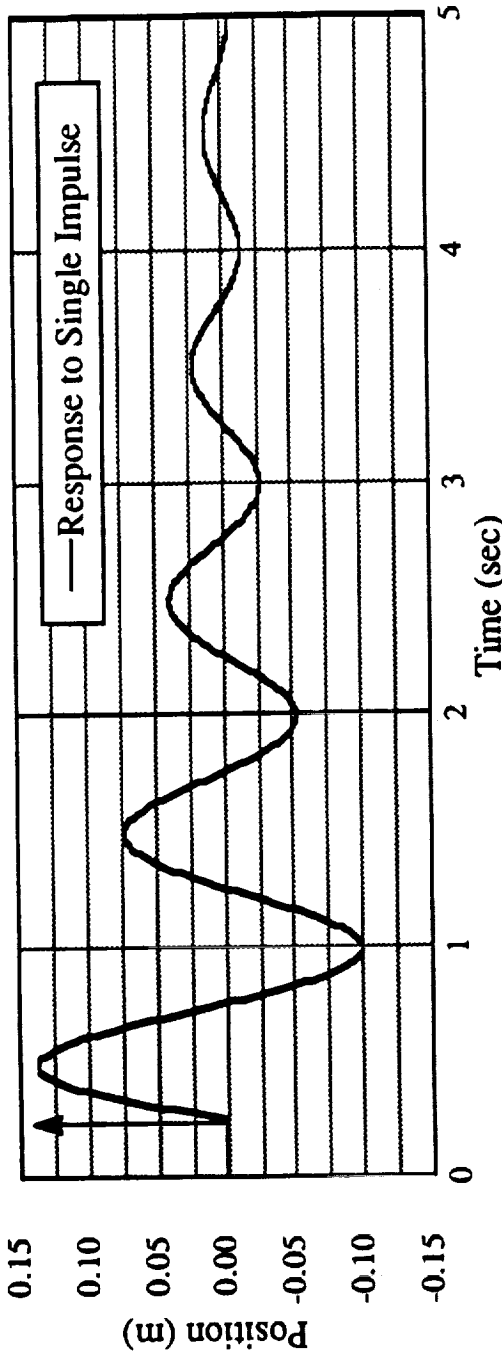
WHAT IS INPUT COMMAND SHAPING?

An OPEN-LOOP method of reducing residual vibration by manipulating the input to a dynamic system.



IMPULSE COMMAND SHAPING MODELS YOUR SYSTEM AS A SUM OF SECOND ORDER LINEAR SYSTEMS. THE IMPULSE RESPONSE OF A SECOND ORDER SYSTEM IS THE BASIS FOR THE IMPULSE SHAPING THEORY.

IMPULSE COMMAND SHAPING ASSUMES SECOND ORDER LINEAR RESPONSE.

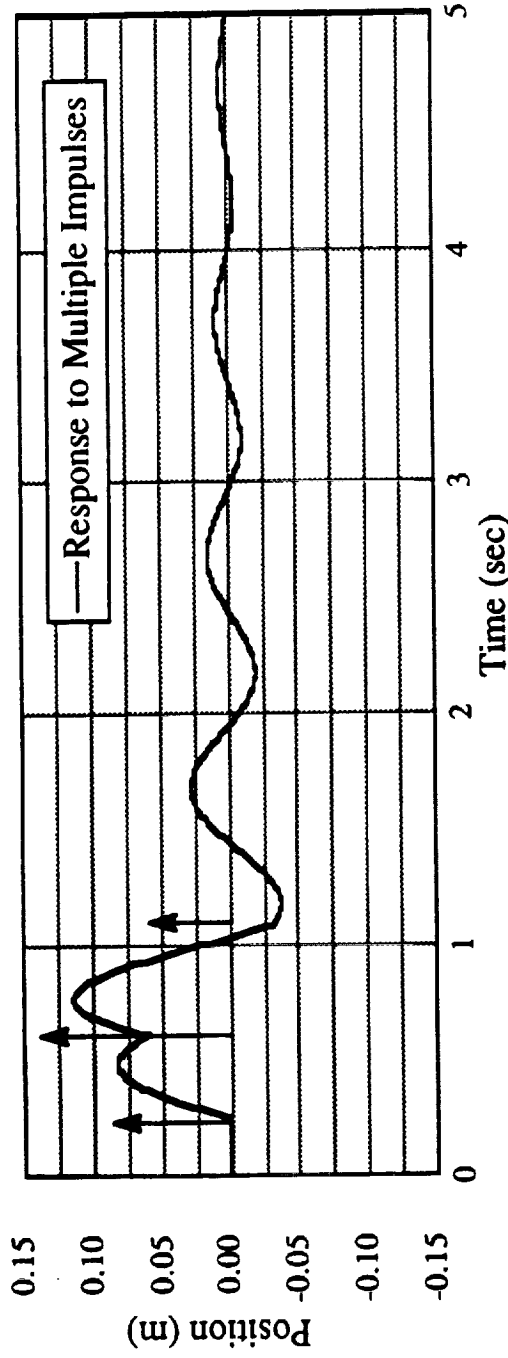


$$y_i(t) = A_i e^{-\zeta \omega (t - t_i)} \sin((t - t_i) \omega \sqrt{1 - \zeta^2})$$

y_i Response to Impulse i
 A_i Magnitude of Impulse i
 t_i Time of Impulse i
 ω System Natural Frequency
 ζ System Damping Ratio

BY LINEAR THEORY, WE CAN USE SUPERPOSITION TO FIND THE RESPONSE TO AN ARBITRARY NUMBER OF IMPULSES.

BY SUPERPOSITION, WE CAN CALCULATE THE RESPONSE TO MULTIPLE IMPULSES.



$$y_i(t) = \sum_{i=1}^N A_i e^{-\zeta \omega (t - t_i)} \sin((t - t_i) \omega \sqrt{1 - \zeta^2})$$

i Impulse Counter
 N Number of Impulses

WE CAN DERIVE AN EXPRESSION FOR THE AMPLITUDE OF THE VIBRATION ENVELOPE AT THE TIME OF THE LAST IMPULSE.

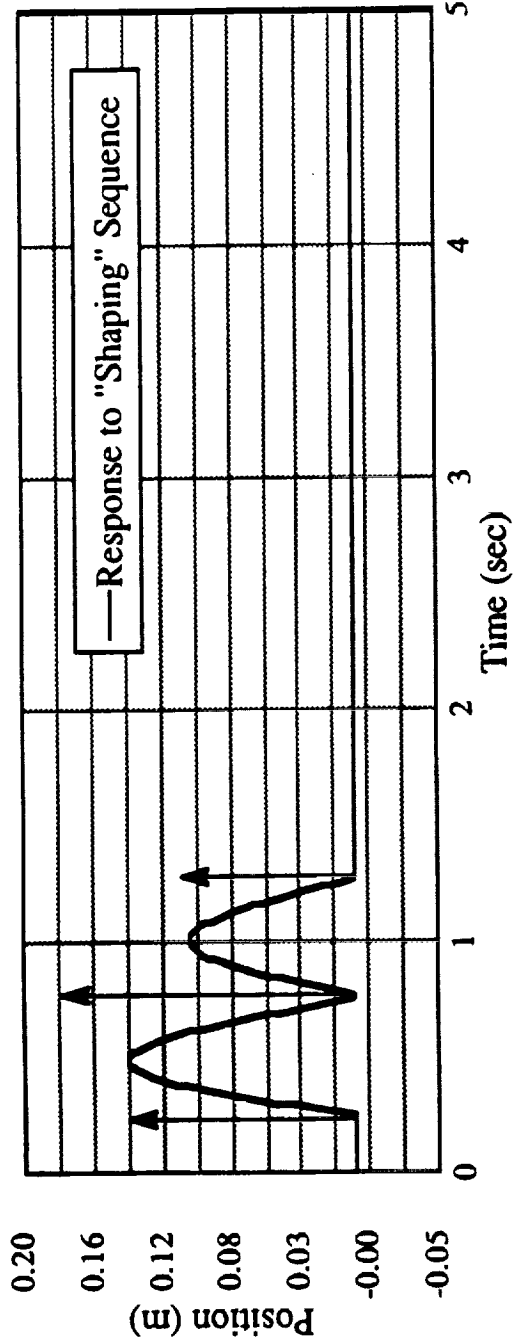
AN EXPRESSION FOR THE AMPLITUDE
OF RESIDUAL VIBRATION.

$$\text{Amp} = \left[\left(\sum_{i=1}^N A_i e^{-\zeta \omega (t_N - t_i)} \sin(t_i \omega \sqrt{1 - \zeta^2}) \right)^2 + \left(\sum_{i=1}^N A_i e^{-\zeta \omega (t_N - t_i)} \cos(t_i \omega \sqrt{1 - \zeta^2}) \right)^2 \right]^{1/2}$$

Expression for envelope amplitude at t_N ,
the time of the final impulse.

IN ORDER FOR THE RESIDUAL VIBRATION TO BE ZERO, THE EXPRESSION FOR THE AMPLITUDE OF VIBRATION HAS TO BE ZERO. FROM THE PREVIOUS PAGE, WE CAN SEE THAT IN ORDER FOR THE AMPLITUDE EXPRESSION TO BE ZERO, THE TWO SQUARED SINE AND COSINE TERMS NEED TO BE ZERO. ALSO, WE ADD A CONSTRAINT THAT THE DERIVATIVES OF THESE TERMS WITH RESPECT TO TIME BE ZERO. THIS ADDS A ROBUSTNESS CONSTRAINT TO THE IMPULSE SEQUENCE, MAKING THE SEQUENCE MORE INSENSITIVE TO ERROR. IN EFFECT, WHAT WE ARE DOING IS ADDING A THIRD IMPULSE TO THE SEQUENCE TO CANCEL ANY OF THE VIBRATION THAT THE SECOND IMPULSE DIDN'T GET.

TO ELIMINATE RESIDUAL VIBRATION, THESE CONSTRAINTS MUST BE MET.



$$\sum_{i=1}^N A_i t_i e^{-\zeta \omega t} \sin(t_i \omega \sqrt{1-\zeta^2}) = 0$$

$$\sum_{i=1}^N A_i t_i e^{-\zeta \omega t} \cos(t_i \omega \sqrt{1-\zeta^2}) = 0$$

WE CAN EXTEND THIS METHOD TO MULTIPLE MODES BY SIMPLY REPEATING THE CONSTRAINT EQUATIONS FOR AN ARBITRARY NUMBER OF MODES "J." WE CAN SOLVE THESE EQUATIONS FOR THE AMPLITUDE AND TIMES OF THE IMPULSES BY USING A LINEAR OPTIMIZATION ROUTINE AND USING THOSE RESULTS AS GUESSES FOR A NON-LINEAR EQUATION SOLVER.

WE CAN EXTEND THIS METHOD TO MULTIPLE MODES.

$$\sum_{i=1}^N A_i e^{-\zeta_j \omega_j t} \sin(t_i \omega_j \sqrt{1 - \zeta_j^2}) = 0$$

$$\sum_{i=1}^N A_i e^{-\zeta_j \omega_j t} \cos(t_i \omega_j \sqrt{1 - \zeta_j^2}) = 0$$

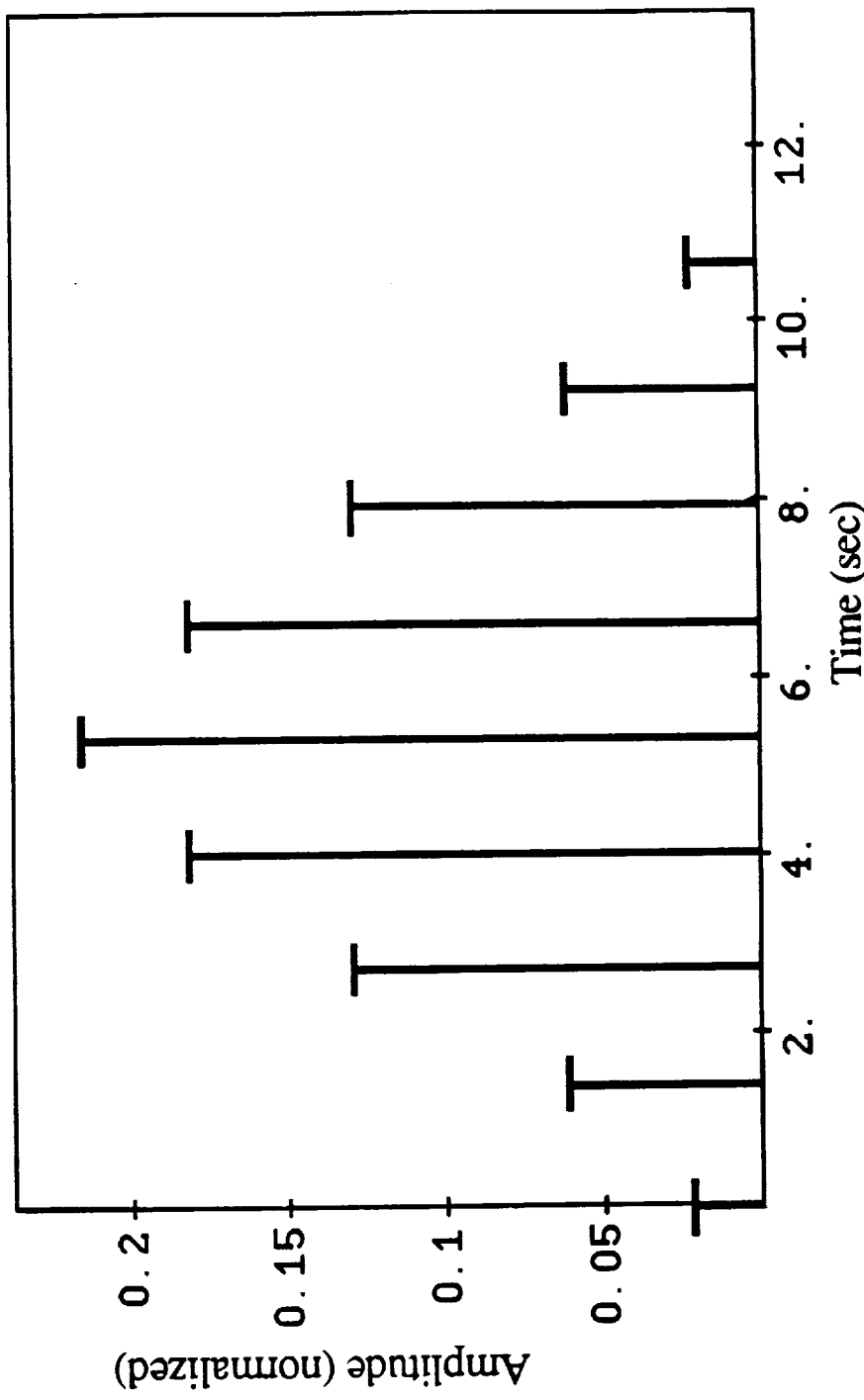
$$\sum_{i=1}^N A_i t_i e^{-\zeta_j \omega_j t} \sin(t_i \omega_j \sqrt{1 - \zeta_j^2}) = 0$$

$$\sum_{i=1}^N A_i t_i e^{-\zeta_j \omega_j t} \cos(t_i \omega_j \sqrt{1 - \zeta_j^2}) = 0$$

These four equations are repeated for each mode "j"

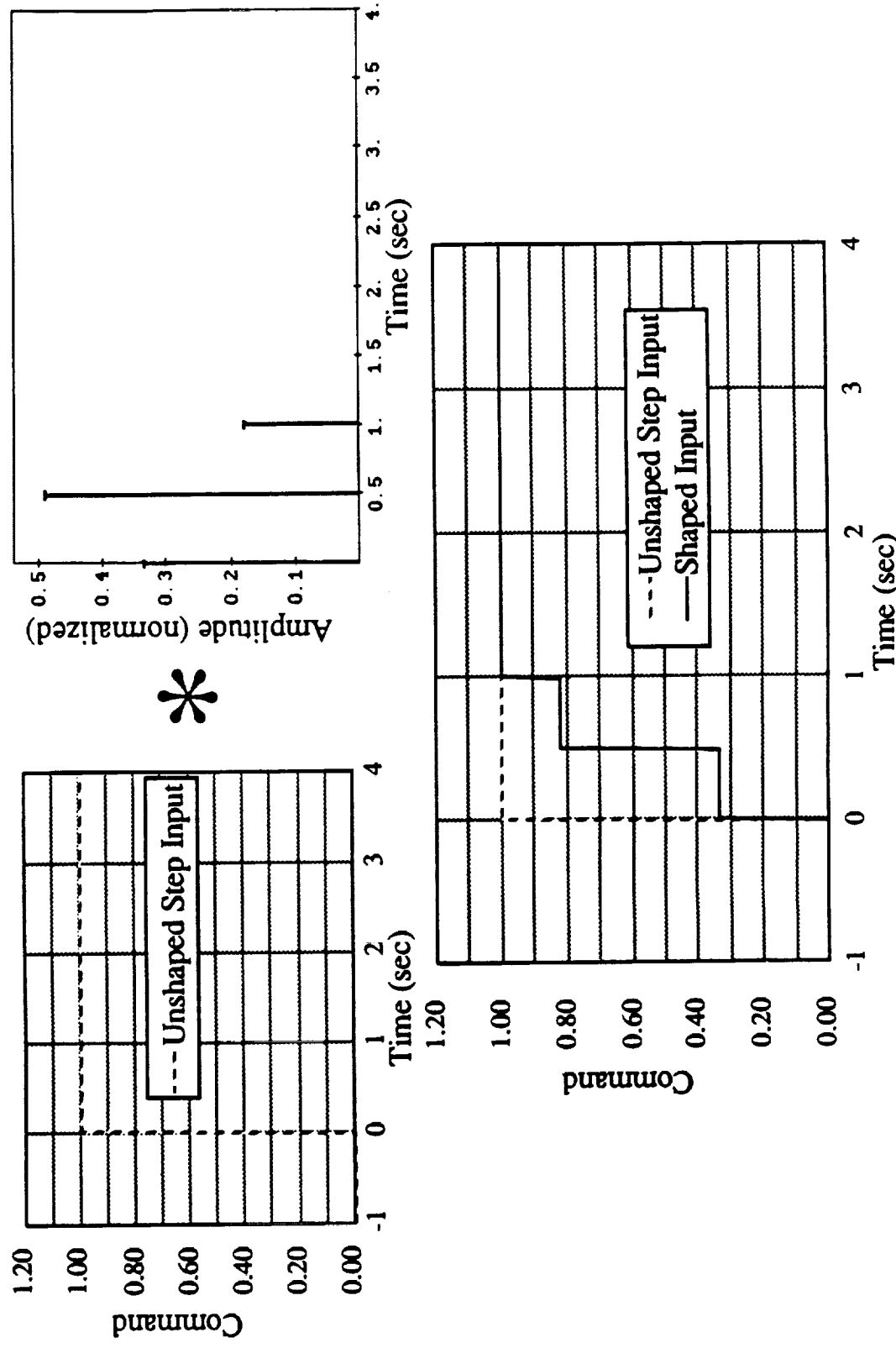
SHOWN IS AN EXAMPLE OF AN IMPULSE SEQUENCE GENERATED FOR A 4 MODE PROBLEM. THE MULTIPLE MODE METHOD ALWAYS GENERATES $2M+1$ IMPULSES, "M" BEING THE NUMBER OF MODES.

AN EXAMPLE SOLUTION OF IMPULSES FOR A 4 MODE PROBLEM.



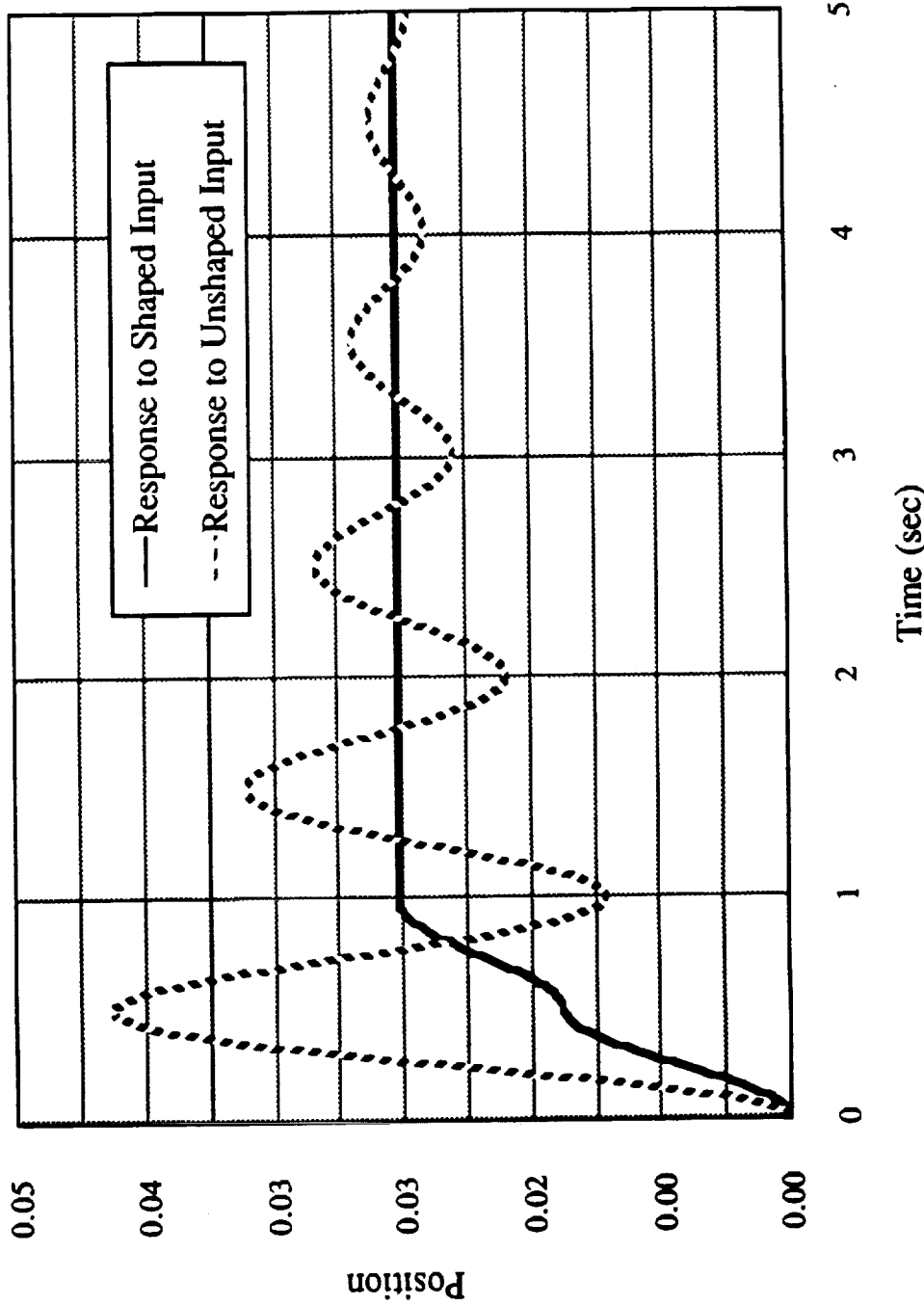
WE DON'T ACTUALLY INPUT IMPULSES INTO THE SYSTEM. WE CONVOLVE THE DESIRED INPUT WITH THE IMPULSE SEQUENCE. FOR EXAMPLE, IF THE DESIRED COMMAND WAS A STEP COMMAND, THE SHAPED INPUT WOULD LOOK LIKE THREE STEPS, AS SHOWN IN THE FIGURE. THE INPUT SHAPER CAN, THEREFORE, BE USED IN REAL-TIME, AS A FILTER TO DESIRED INPUTS.

THE SHAPER IS IMPLEMENTED BY CONVOLVING THE INPUT WITH THE IMPULSES.



FOR A SIMPLE ONE MODE, SECOND ORDER SYSTEM, THE RESPONSE TO A SHAPED INPUT WOULD LOOK LIKE THIS. THIS ASSUMES THAT IT IS A LINEAR SECOND ORDER SYSTEM, AND THAT WE HAVE ACCURATELY IDENTIFIED THE NATURAL FREQUENCY OF THE SYSTEM. IN THE NON-LINEARITY OF THE REAL WORLD, HOWEVER, IT'S NOT ALWAYS SO EASY.

RESPONSE TO INPUTS FOR A SIMPLE MODE SYSTEM.

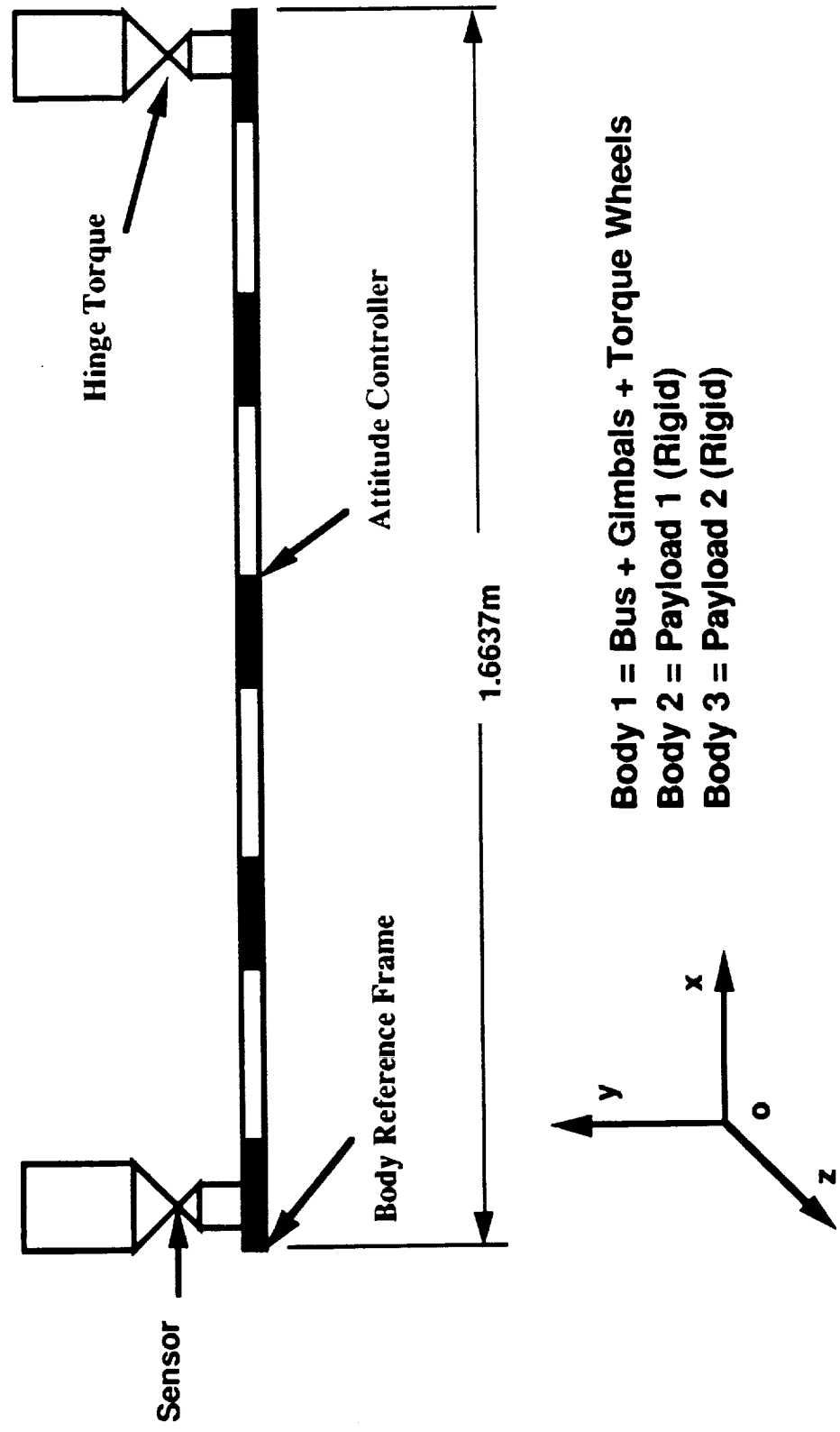


**DISCOS (DYNAMIC INTERACTIONS SIMULATIONS OF CONTROLS AND
STRUCTURES) IS A NON-LINEAR SIMULATION CODE DEVELOPED BY GODDARD AND
MARTIN MARIETTA FOR THE SIMULATION OF LARGE MULTI-BODY SPACE
STRUCTURES.**

DISCOS SIMULATION RESULTS.

**DISCOS SEES YOUR MODEL AS A COLLECTION OF BODIES. WE HAVE
MODELLED MACE AS A COLLECTION OF BODIES; THE FIRST BEING THE FLEXIBLE
BUS WITH THE GIMBALS AND TORQUE WHEELS ATTACHED, AND BODIES 2 AND 3
BEING THE TWO RIGID PAYLOADS WHICH ARE HINGED TO THE BUS AT THE
GIMBALS.**

DISCOS MODEL OF MACE.



WE IDENTIFIED THE CLOSED LOOP FREQUENCIES FOR THE PAYLOAD POINTING AT 60° INBOARD AND 60° OUTBOARD. YOU CAN SEE THE KINEMATIC CHANGES IN FREQUENCY THAT THE NON-LINEAR SIMULATION IS EXHIBITING.

IDENTIFIED CLOSED LOOP FREQUENCIES (NON-LINEAR DISCOS MODEL)

**60° Outboard (Hz)
(Beginning of 120° Slew)**

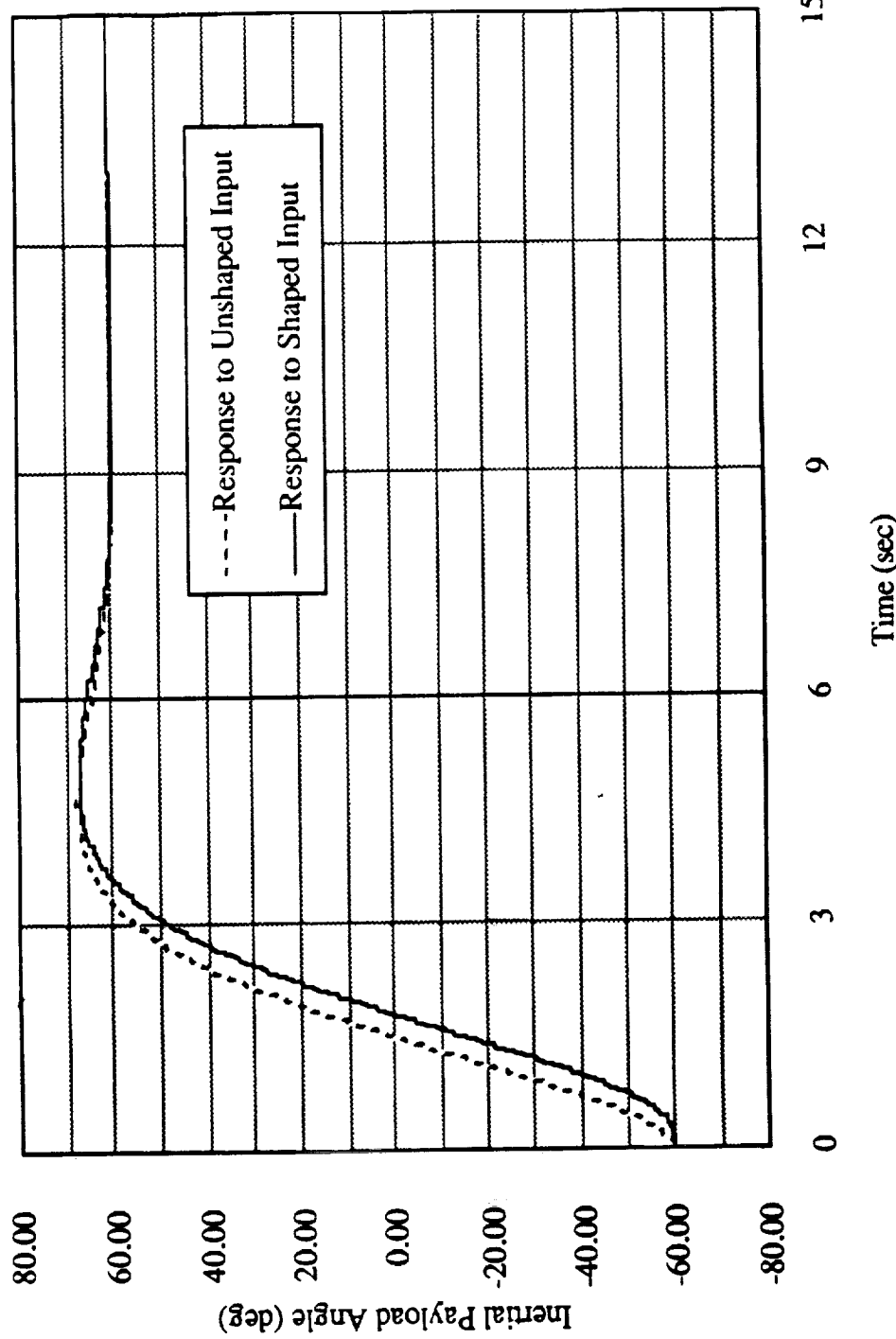
2.18
14.25
15.25
15.90

**60° Inboard (Hz)
(End of 120° Slew)**

1.88
13.40
14.20
15.90

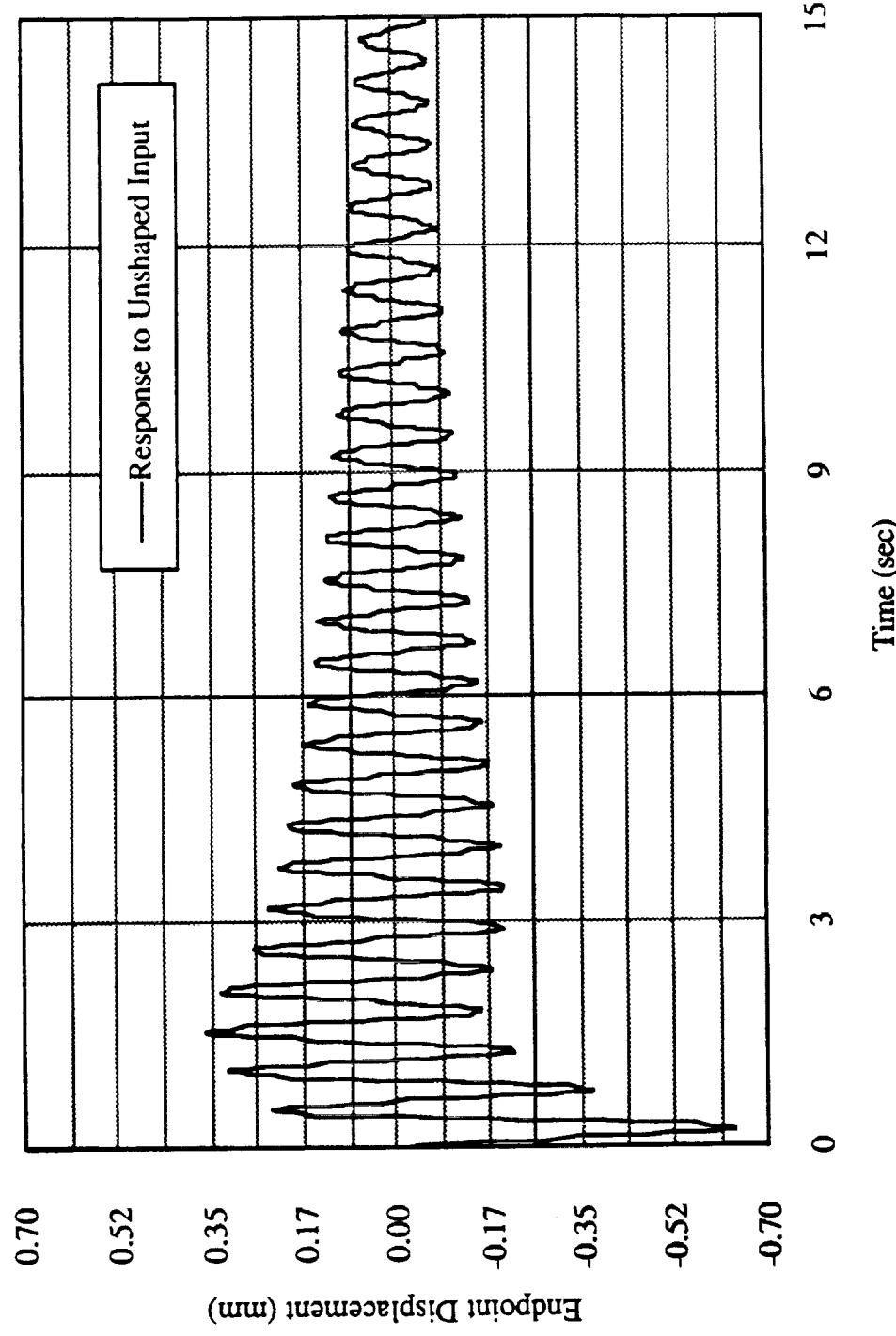
THIS IS THE SIMULATION RESPONSE TO A 120° PAYLOAD SLEW, FOR THE SHAPED AND UNSHAPED RUNS. WE ARE LOOKING AT THE INERTIAL ANGLE OF THE GIMBAL PAYLOAD. WHAT WE CAN NOTICE HERE IS THE DELAY IN THE RESPONSE TIME CAUSED THE IMPULSE SHAPER. SINCE THE SLOWEST MODE WE'RE SHAPING FOR HAS A PERIOD OF ABOUT .5 SECONDS, WE CAN SEE THE DELAY IN RESPONSE IS ALSO ABOUT THAT MUCH.

TIME TRACE OF 120° PAYLOAD SLEW



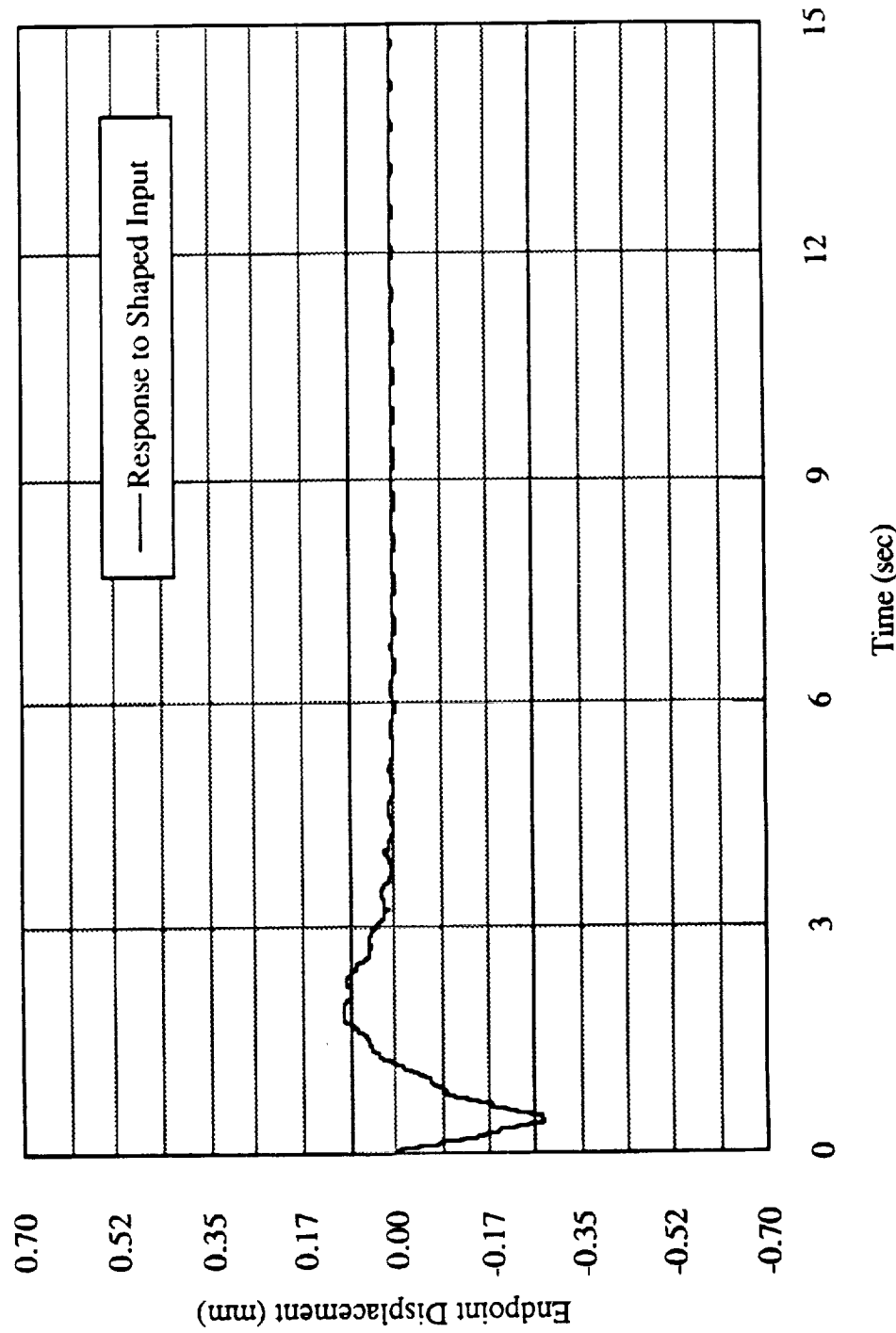
SHOWN IS A PLOT OF THE ENDPOINT DEFLECTION RESPONSE TO THE UNSHAPED 120° SLEW. THIS DEFLECTION IS RELATIVE TO THE STRUCTURE ITSELF, AND HENCE IT OSCILLATES AROUND 0. YOU CAN NOTICE THE MULTI-MODE VIBRATION IN THE RESIDUAL RESPONSE.

ENDPOINT RESPONSE TO UNSHAPED SLEW



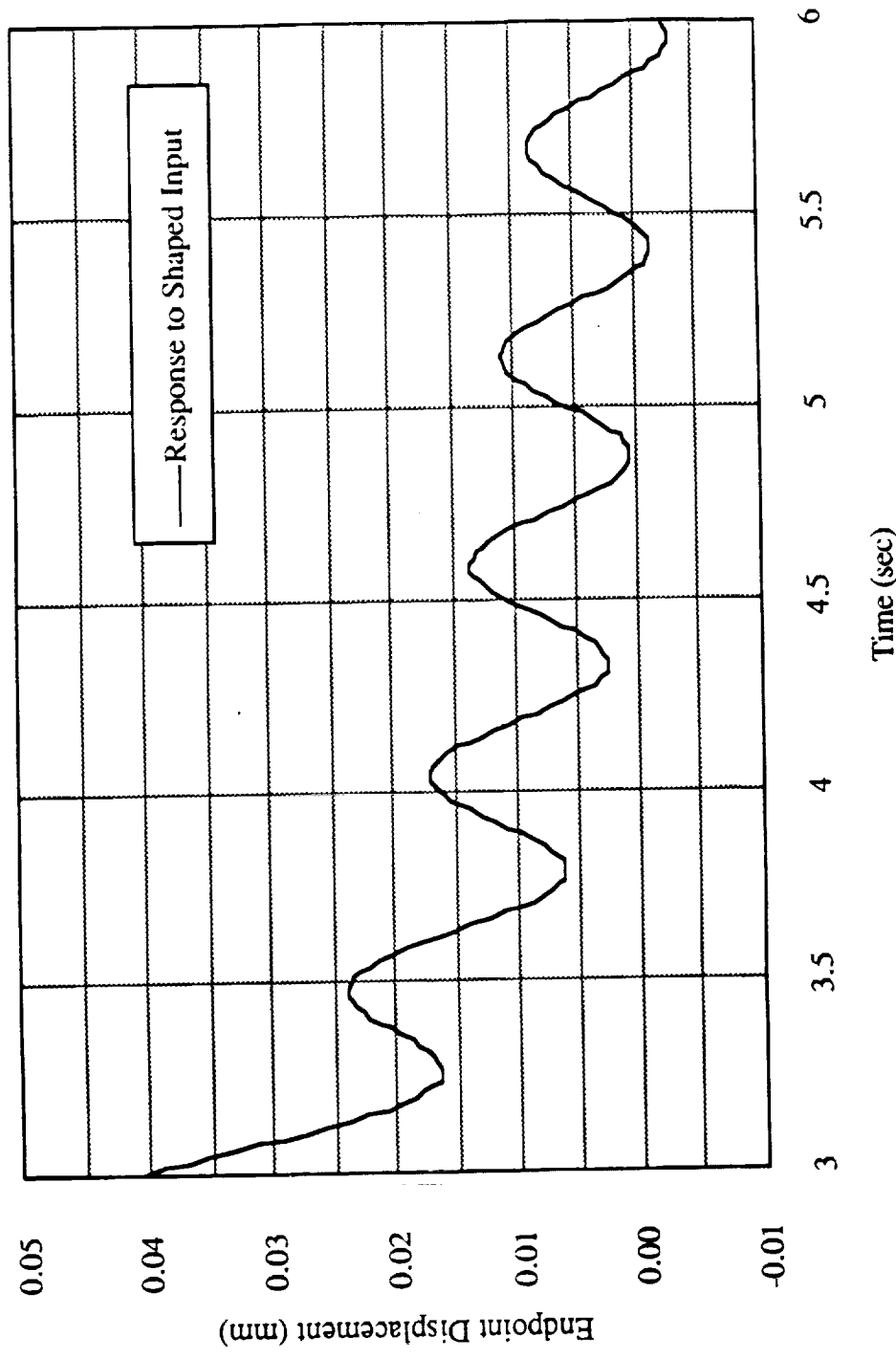
THE SHAPED SLEW SHOWS A SIGNIFICANT IMPROVEMENT IN THE ENDPOINT RESPONSE. THE VIBRATION IS CANCELLED VERY EFFECTIVELY.

ENDPOINT RESPONSE TO SHAPED SLEW



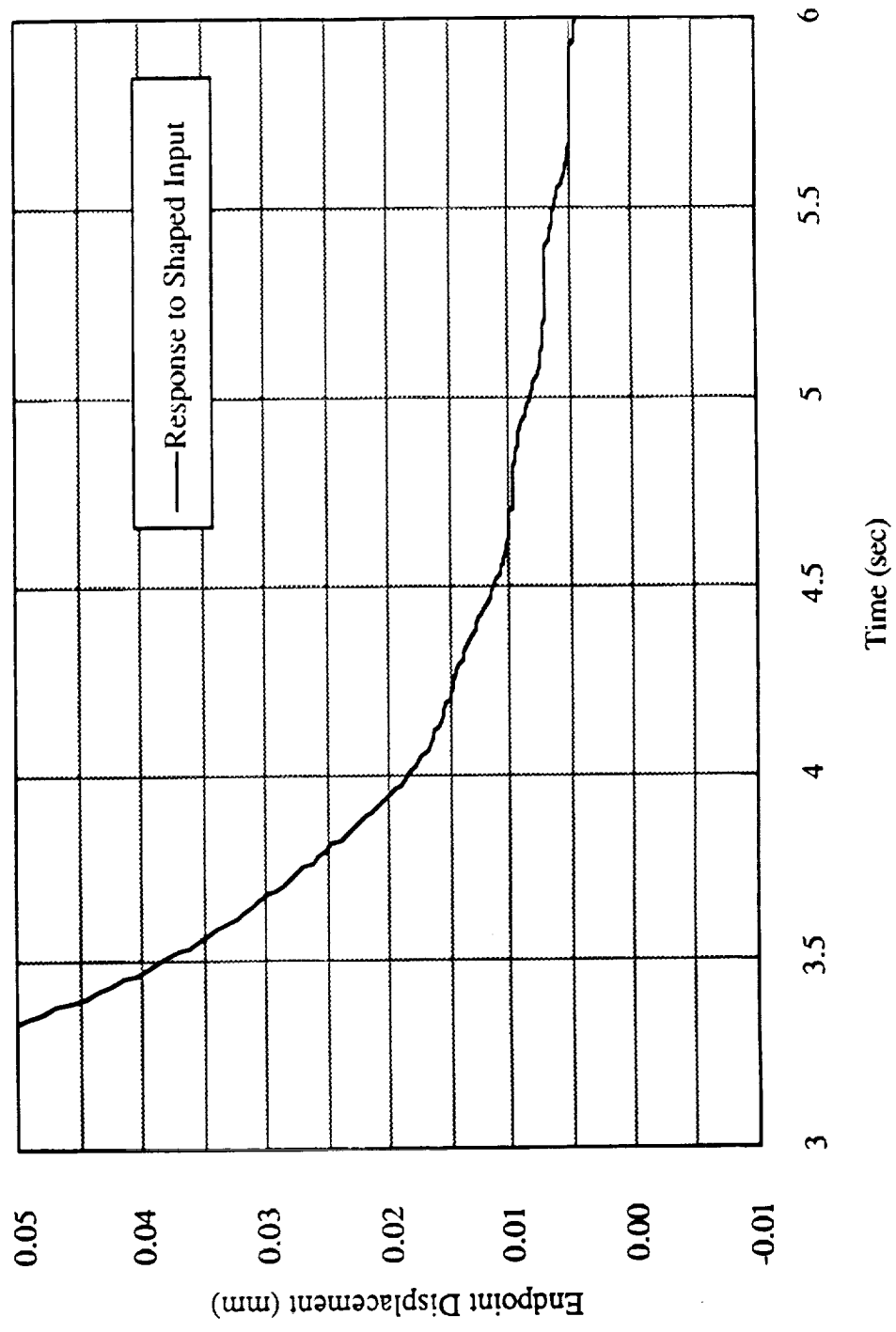
A DETAIL PLOT OF THE RESPONSE SHOWS THAT THERE IS STILL SOME,
ALTHOUGH VERY SMALL, RESIDUAL VIBRATION IN THE SHAPED RESPONSE. THIS
CAN BE ATTRIBUTED TO THE FACT THAT THIS IS NOW A NON-LINEAR SYSTEM AND
WE HAVE NOT ACCURATELY IDENTIFIED THE CHANGING FREQUENCIES ENOUGH
TO CANCEL THEM TO GO TO ZERO.

SHAPED RESPONSE DETAIL



WE FOUND THAT WE CAN COMPENSATE FOR THIS NON-LINEARITY BY SHAPING THE INPUT FOR THE BEGINNING, MIDDLE, AND ENDING FREQUENCIES FOR THE ENTIRE 120° SLEW. THE PLOT SHOWS AN IMPROVEMENT OVER THE PREVIOUS PLOT. THIS, HOWEVER, COMES AT THE COST OF ADDING ABOUT A SECOND OF DELAY TO THE IMPULSE SHAPER. AT THIS POINT, IT IS NOT CLEAR WHETHER THIS IS A WIN IN TERMS OF VIBRATION CANCELLATION.

RESPONSE DETAIL FOR SHAPER WITH ADDITIONAL MODES.

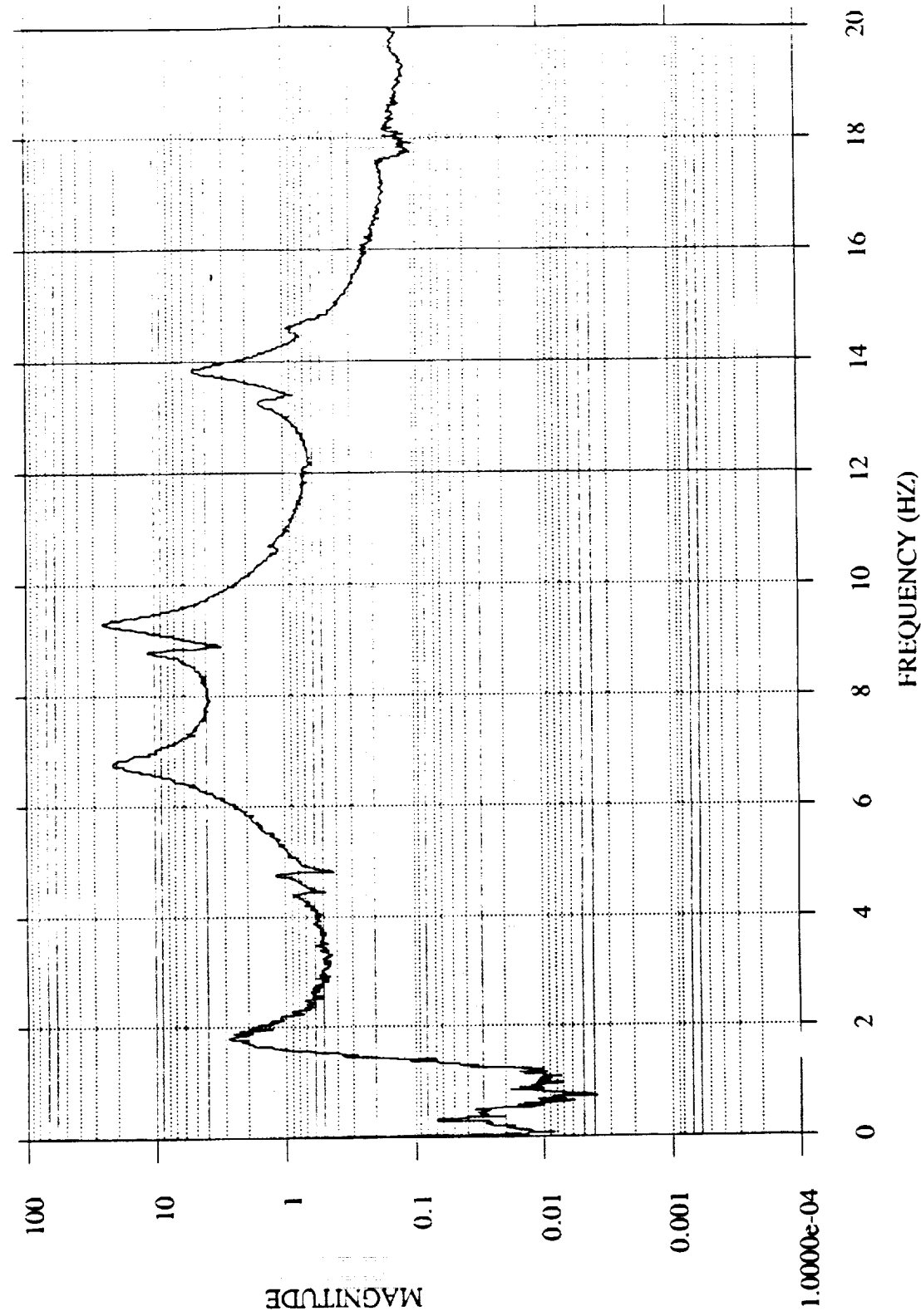


THE EXPERIMENTAL RESULTS WERE TAKEN FROM THE DEVELOPMENT MODEL
OF MACE THAT SITS IN THE BASEMENT OF MIT BUILDING 37.

EXPERIMENTAL RESULTS

THE MACE DEVELOPMENT MODEL HAS A FREQUENCY RESPONSE IN THE
20HZ BANDWIDTH RANGE THAT LOOKS LIKE THIS. NOTICE THE SEMILOG
PLOTTING THAT WE ARE USING THE ACCENT THE HIGHER MODES.

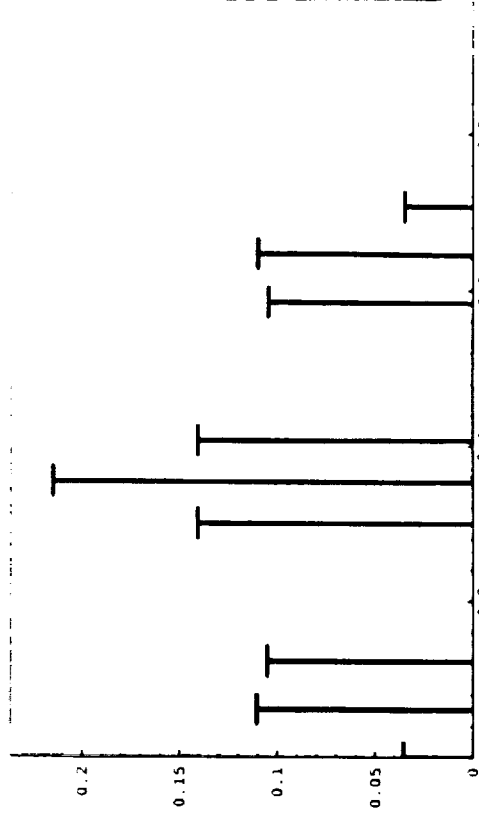
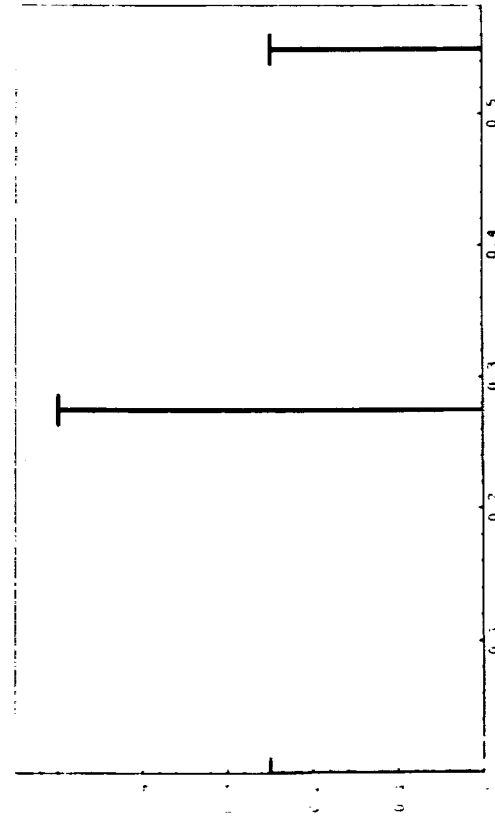
MACE PLANT FREQUENCY RESPONSE



WE RAN TWO TESTS. THE FIRST WAS TO TRY TO CANCEL THE FIRST MODE ONLY. THE SEQUENCE FOR CANCELLING THE FIRST MODE IS A SIMPLE 3 IMPULSE SEQUENCE. WE THEN RAN A TEST TO CANCEL THE FIRST FOUR MODES. THE IMPULSE SHAPERS FOR BOTH OF THESE CASES ARE SHOWN.

IMPULSE SHAPERS CALCULATED FOR FIRST FOUR MODES.

1.82 hz
6.82 hz
8.79 hz
9.29 hz

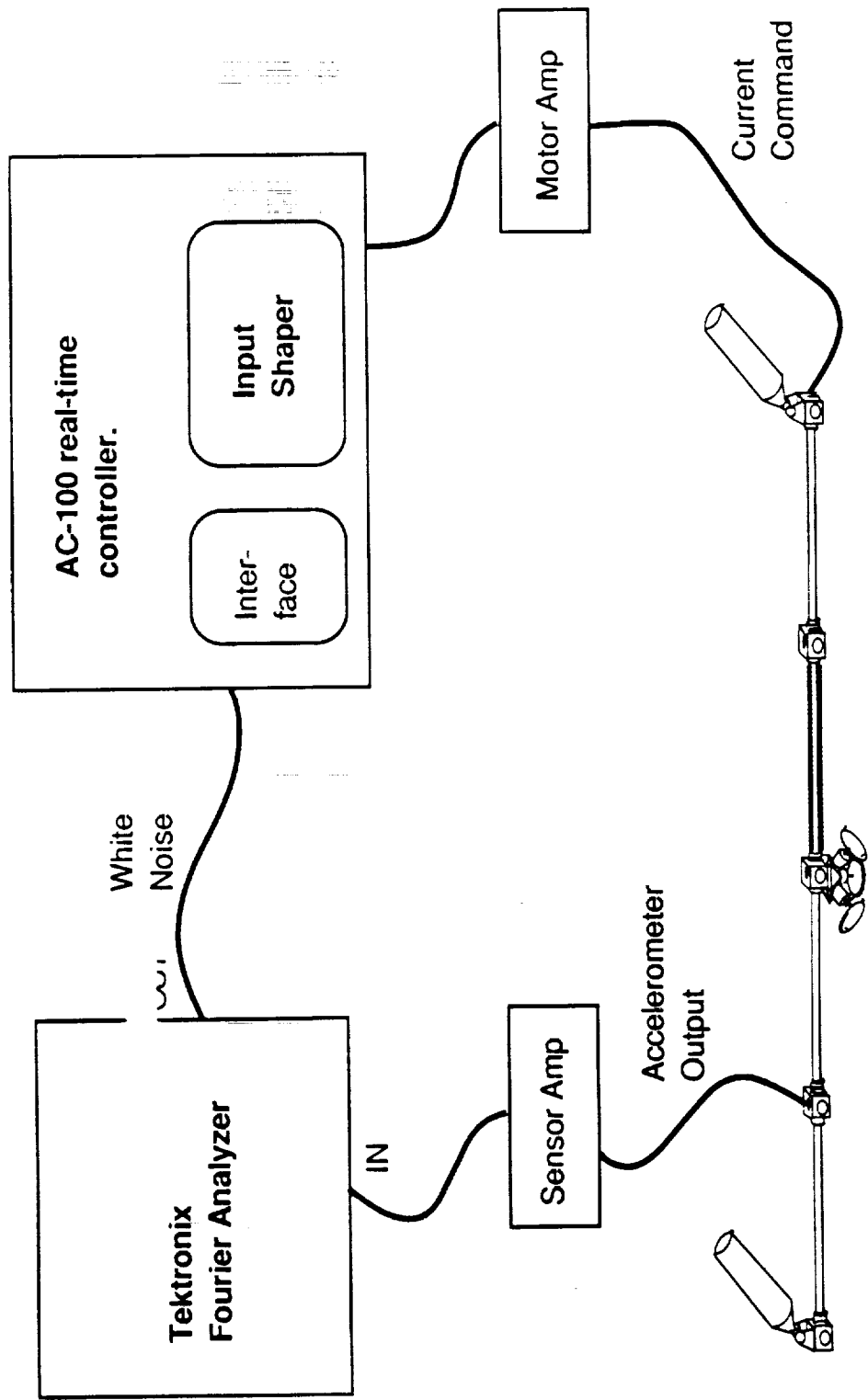


FIRST MODE ONLY

FOUR MODES

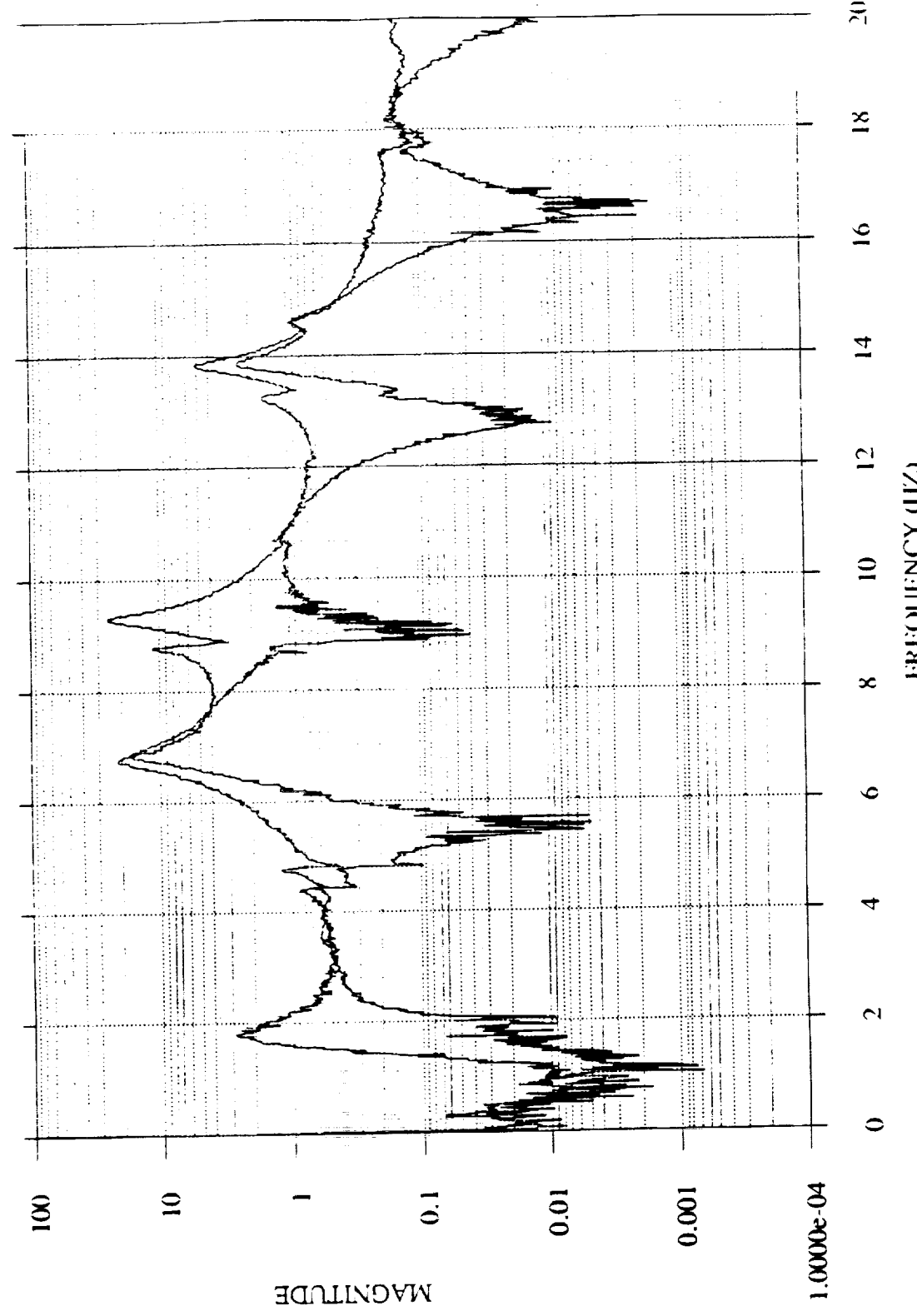
THE DATA WAS COLLECTED BY USING A TEKTRONIX FOURIER ANALYZER TO TAKE THE TRANSFER FUNCTION OF THE OUTPUT OF THE ACCELEROMETER TO THE INPUT INTO THE GIMBAL MOTOR AMPLIFIER. ALL THE CODING FOR THE INPUT SHAPERS WERE DONE ON THE AC-100 REAL-TIME COMPUTER.

EXPERIMENTAL SETUP



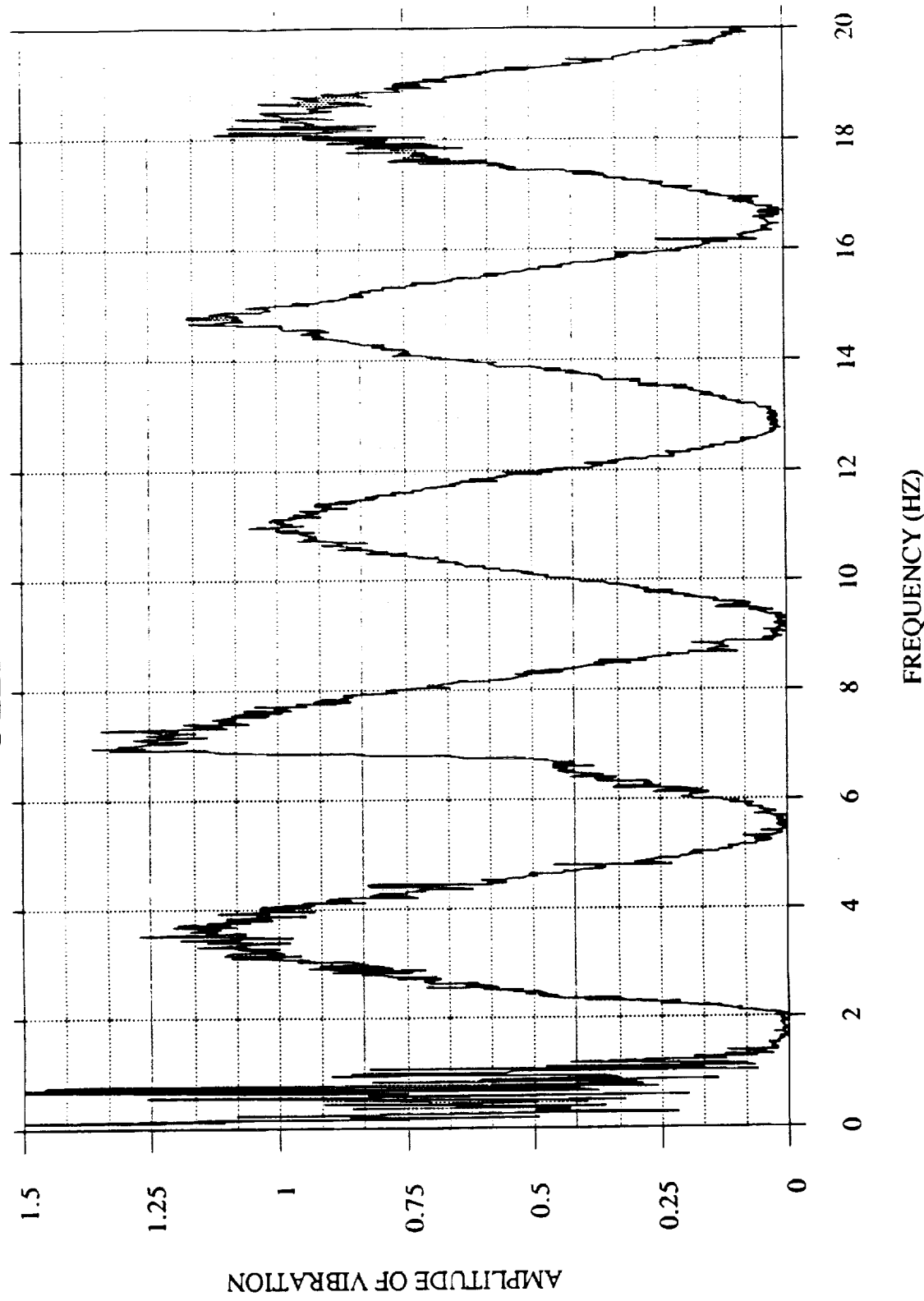
SHOWN IS THE TRANSFER FUNCTION TAKEN BEFORE AND AFTER THE INPUT SHAPER FOR THE FIRST MODE WAS UTILIZED. NOTICE THE DECREASE IN AMPLITUDE OF THE FIRST MODE BY ALMOST TWO ORDER OF MAGNITUDE. ALSO INTERESTING TO SEE IN THIS PLOT IS THE REPEATING NATURE OF THE IMPULSE SHAPER. BECAUSE THE IMPULSES HIT AT HALF PERIODS OF THE FREQUENCY IT IS TRYING TO CANCEL, THEY ALSO HAPPEN TO CANCEL THOSE MODES WHICH ARE AN ODD MULTIPLE OF THE THAT MODE.

MACE PLANT WITH SHAPER FOR 1ST MODE



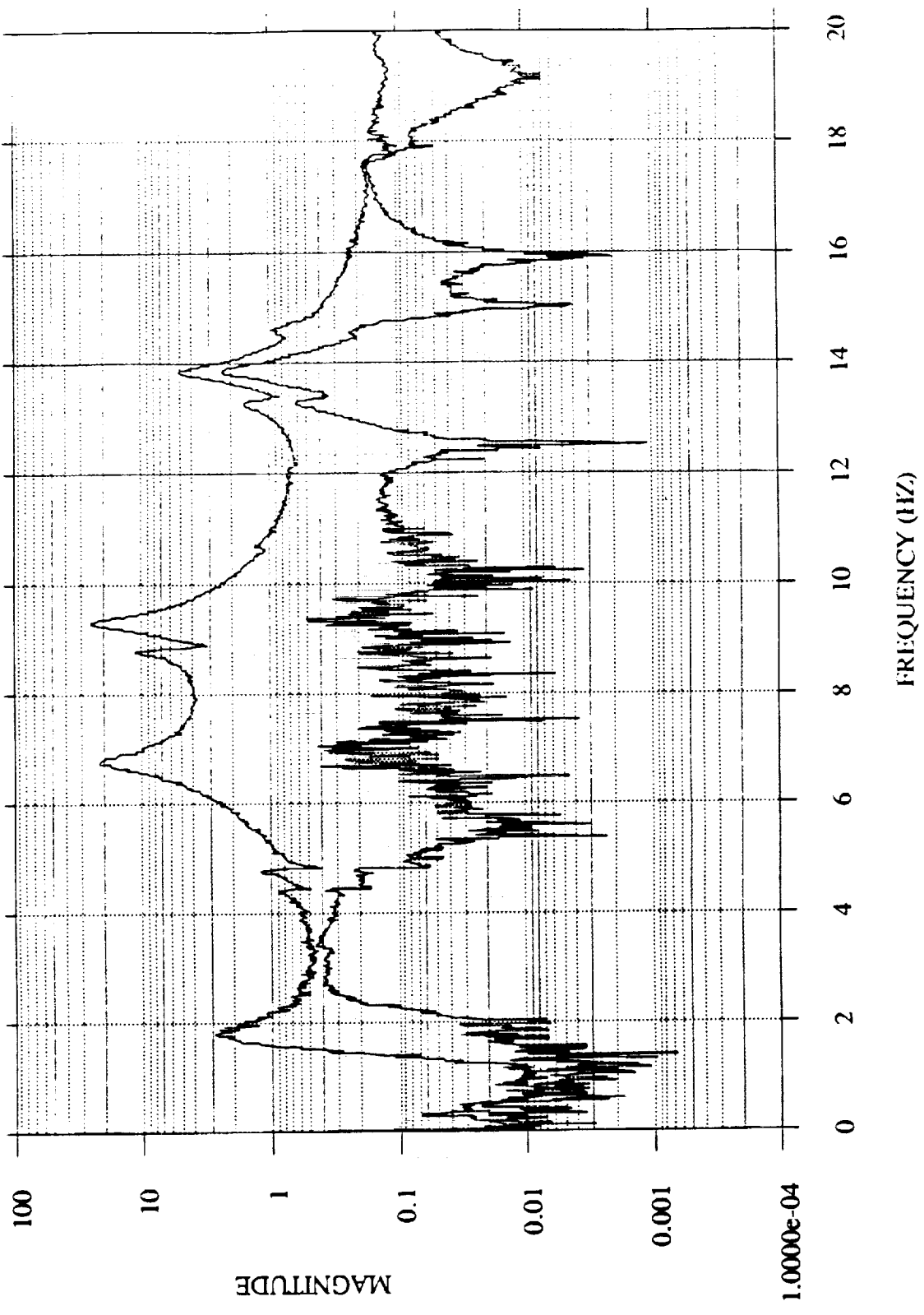
WE CAN VIEW THE EFFECTIVENESS OF THE SHAPING SEQUENCE BY LOOKING AT WHAT WE CALL AN "INSENSITIVITY CURVE." WHAT WE HAVE DONE IS TO DIVIDE THE AMPLITUDE AT EACH DISCRETE FREQUENCY OF THE TRANSFER FUNCTION WITH THE IMPULSE SHAPER BY THE TRANSFER FUNCTION WITHOUT THE IMPULSE SHAPER AND PLOT IT ON A LINEAR SCALE. WHAT WE SEE IS THE ROBUSTNESS OF THIS SHAPER IN THE 1.8HZ RANGE.

INSENSITIVITY CURVE FOR ONE MODE SHAPER



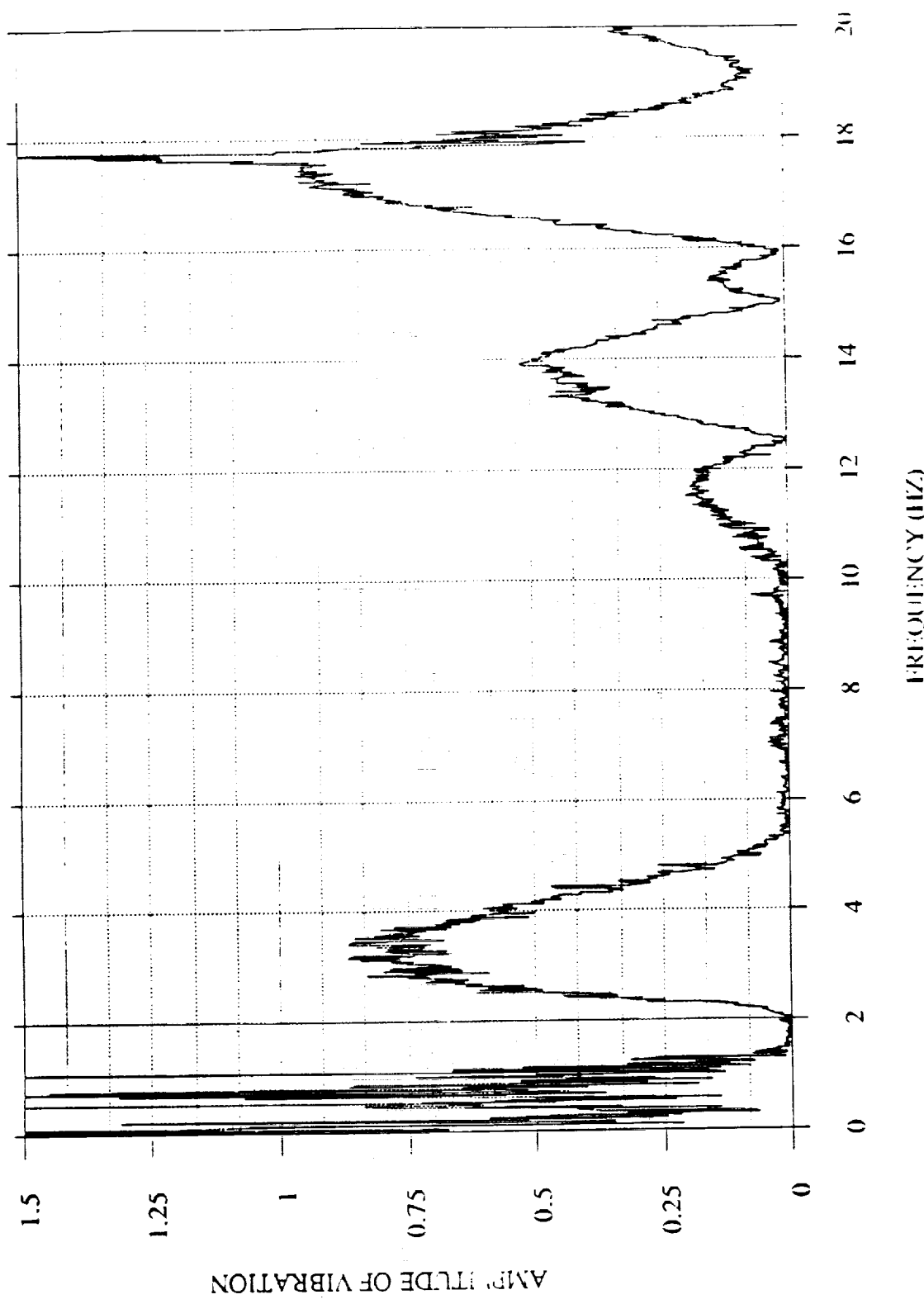
WE THEN REPEATED THE EXPERIMENT FOR THE 4 MODE SHAPER.

FREQUENCY RESPONSE WITH SHAPER FOR FIRST FOUR MODES



LOOKING AT THE INSENSITIVITY CURVE FOR THE 4 MODE SEQUENCE, WE CAN SEE THE EXTREMELY GOOD ROBUSTNESS IN THE 5 TO 10HZ RANGE. THIS IS THE CONSEQUENCE OF THE 3 MODES IN THAT AREA BEING SO CLOSE TO EACH OTHER.

INSENSITIVITY CURVE FOR 4 MODE SHAPER



WE HAVE SEEN THAT INPUT SHAPING CAN REDUCE VIBRATION IN COMPLICATED MULTIPLE-MODE SYSTEMS SUCH AS MACE. WE HAVE SHOWN THIS BY DOING THE NON-LINEAR SIMULATIONS IN DISCOS AND BY PERFORMING SOME INITIAL EXPERIMENTS ON THE MACE DEVELOPMENT MODEL. HOWEVER, REAL SYSTEM NON-LINEARITIES WILL DECREASE THE EFFECTIVENESS OF SHAPING ONCE WE START DOING LARGE ANGLE SLEWS. THESE NON-LINEARITIES ARE THE CENTER OF THE FUTURE WORK WE HAVE PLANNED FOR MACE.

CONCLUSIONS

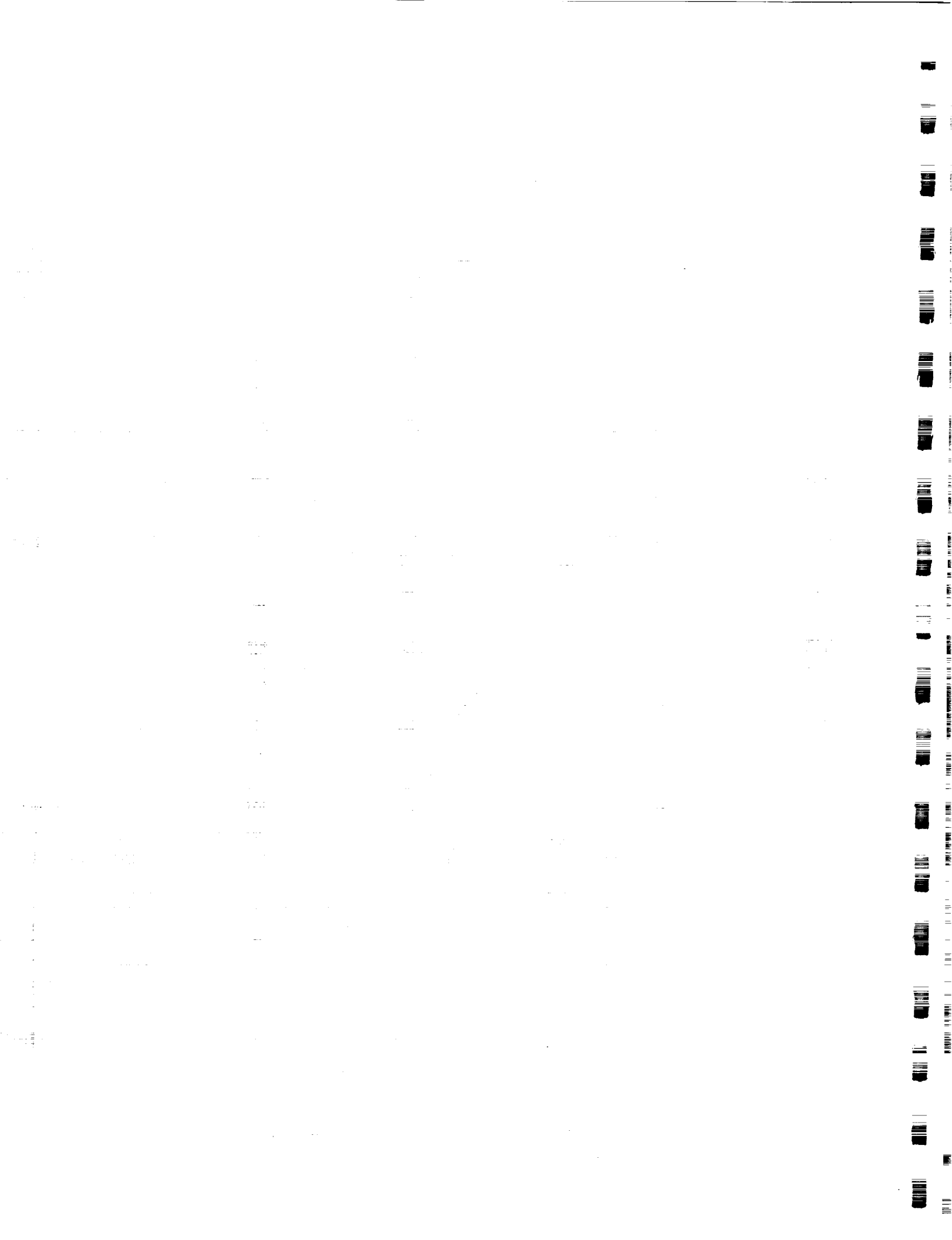
- Input shaping can reduce vibration in multiple-mode systems (MACE).
- Real system non-linearities decrease effectiveness of impulse shaping.

Space Engineering Research Center



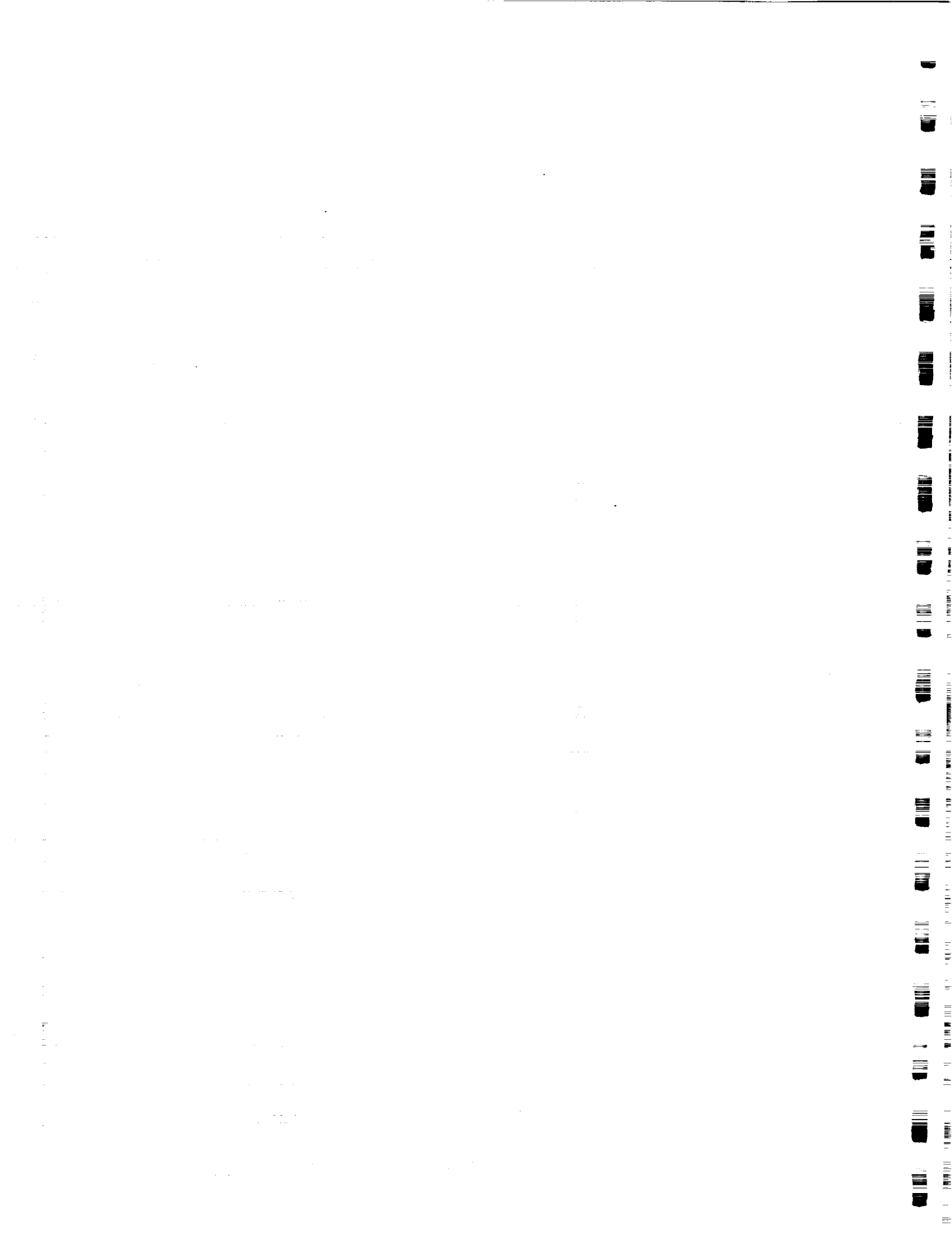
FUTURE WORK

- Identify relevant non-linearities in MACE test article. (friction, kinematic changes in frequency, gravity effects ...)
- Implement an input shaper which most efficiently reduces residual vibration in the presence of non-linearities.
- Generalize observations for all systems.



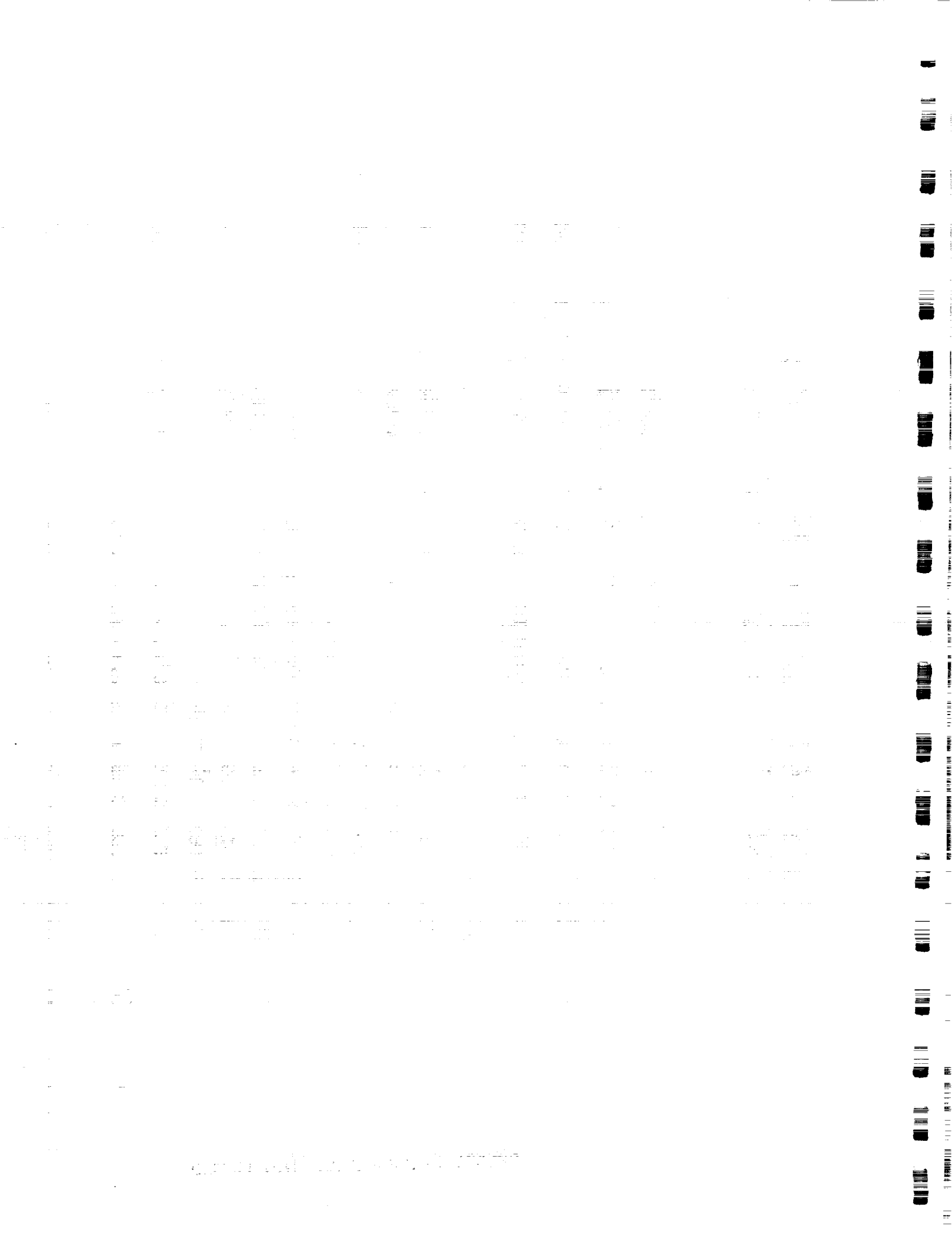
OTHER ONGOING RESEARCH

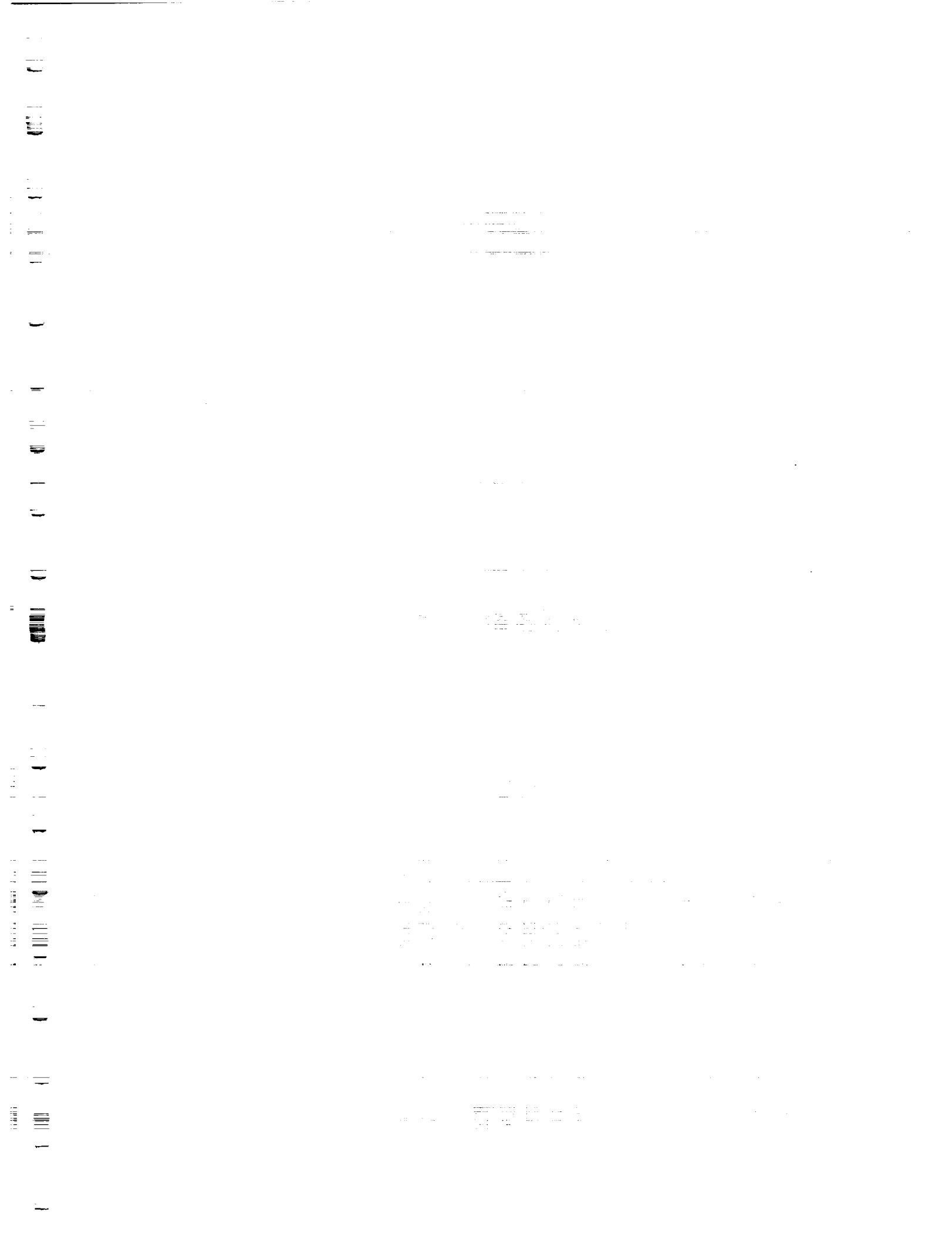
PRECEDING PAGE BLANK NOT FILMED



PRESSURE ACTUATOR WITH VISCOSUS FLUID DAMPING

- OBJECTIVE: The design, manufacture, and testing of a pressure-controlled actuator with viscous fluid damping
- PRINCIPLE: Controlled pressurization will alter the dimensions of the structure while eliminating high frequency excitations
- APPROACH:
 - Application of theory to a first generation design including actuator size, shape and critical subcomponents
 - Design and manufacture of an actuator based on an isotropic (Aluminum) pressure cavity
 - Testing and analysis of first generation design
 - Second generation design and manufacture based on an anisotropic (composite) cavity to maximize axial stroke and hoop stress tolerance
 - Incorporation of actuator into a controlled truss structure
- STATUS: Initial component design completed





PREVIOUS WORK, DUE TO HAGOOD[1], HAS SHOWN THAT SHUNTING A PIEZOELECTRIC MATERIAL WITH SIMPLE PASSIVE CIRCUITS INVOLVING RESISTORS AND POSSIBLY INDUCTORS WILL CREATE A TUNABLE DAMPING ELEMENT FOR STRUCTURAL APPLICATIONS. IN THE PRESENT EFFORT WE SEEK TO DEVELOP A CONTROL-THEORETIC APPROACH TO THE DESIGN OF MORE GENERAL SHUNTING CIRCUITS.

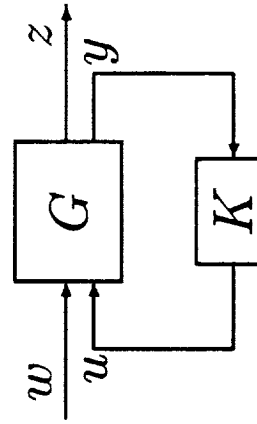
OUR APPROACH IS FIRST TO DEVELOP A STRUCTURAL MODEL SUITABLE FOR CONTROL DESIGN, IN WHICH THE CONTROL INPUT/OUTPUT ARE CURRENT AND VOLTAGE AT THE ELECTRODES OF AN INTEGRAL PIEZOELECTRIC ELEMENT. THE TRANSFER FUNCTION FROM U TO Y (SEE FIGURE) IS THEN A DRIVING-POINT IMPEDANCE. W IS A VECTOR OF DISTURBANCE FORCES AND Z IS THE PERFORMANCE VARIABLE TO BE REGULATED, SUCH AS LINE-OF-SIGHT ERROR. THUS THE OTHER THREE TRANSFER FUNCTIONS DEFINED BY THE FIGURE RELATE EITHER MECHANICAL TO MECHANICAL VARIABLES, ELECTRICAL TO MECHANICAL, OR VERSA. THIS MODEL IS OBTAINED FROM A MODEL OF THE BASIC STRUCTURE (WITHOUT INTEGRAL PIEZOELECTRICS) AND AN ELECTRO-MECHANICAL MODEL OF THE PIEZOELECTRIC ELEMENT.

[1] HAGOOD, N., AND VON FLOTOW, A., "DAMPING OF STRUCTURAL VIBRATIONS WITH PIEZOELECTRIC MATERIALS AND PASSIVE ELECTRICAL NETWORKS," JOURNAL OF SOUND AND VIBRATION, VOL. 146, NO. 2, PP. 243-268, 1991.

Passive Control/Damping: Spangler, Hall

- Objective: Design and implementation of optimal structural control using integral piezoelectrics shunted with strictly passive electrical networks.

- Approach
 - Modeling for Control Design:



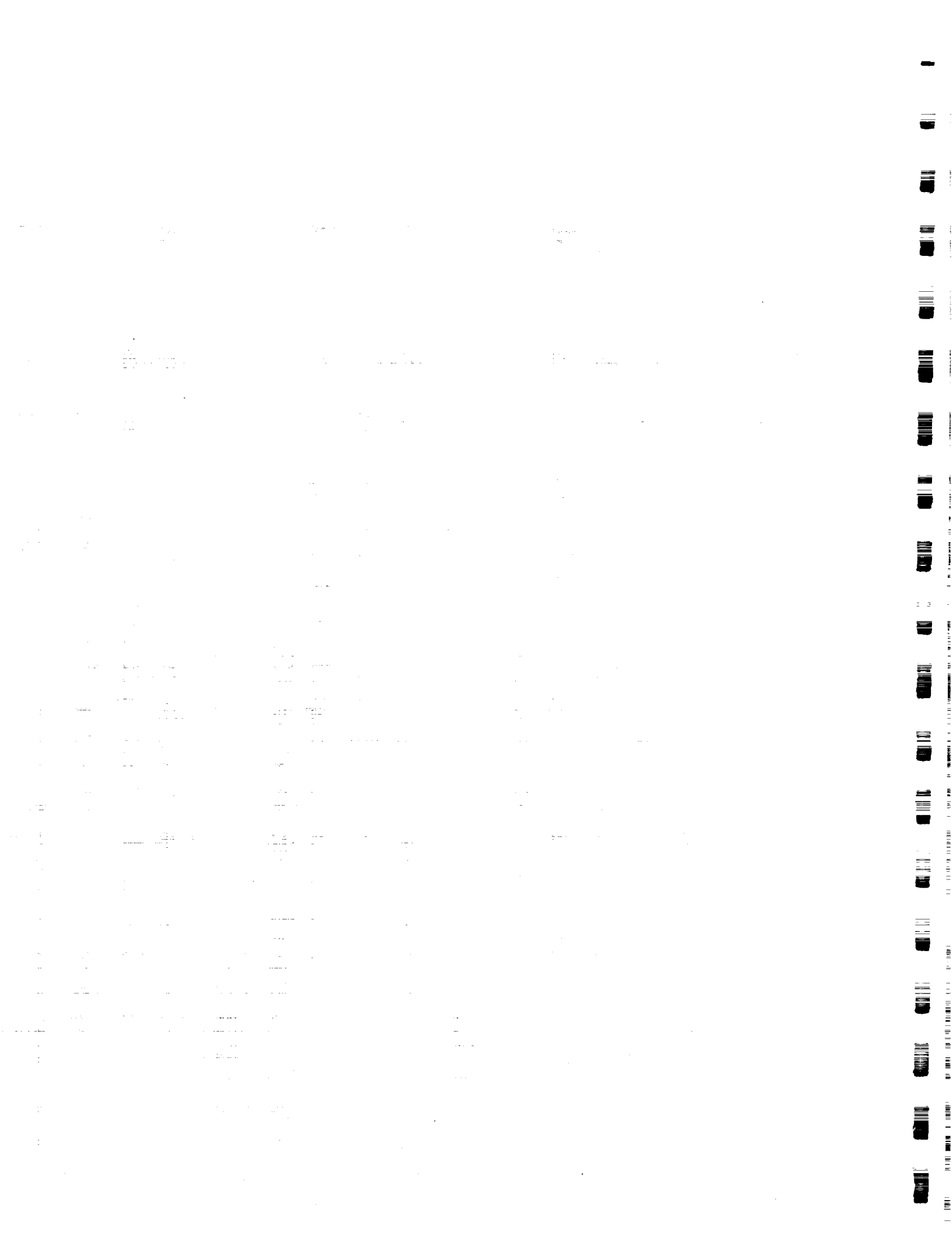
- * Controller input/output are voltage/current at piezo electrodes.
- * Piezo is both sensor and actuator, *truly collocated*.
- * G_{22} is an electrical impedance which exhibits the combined effects of the piezo capacitance and the structure's dynamics.

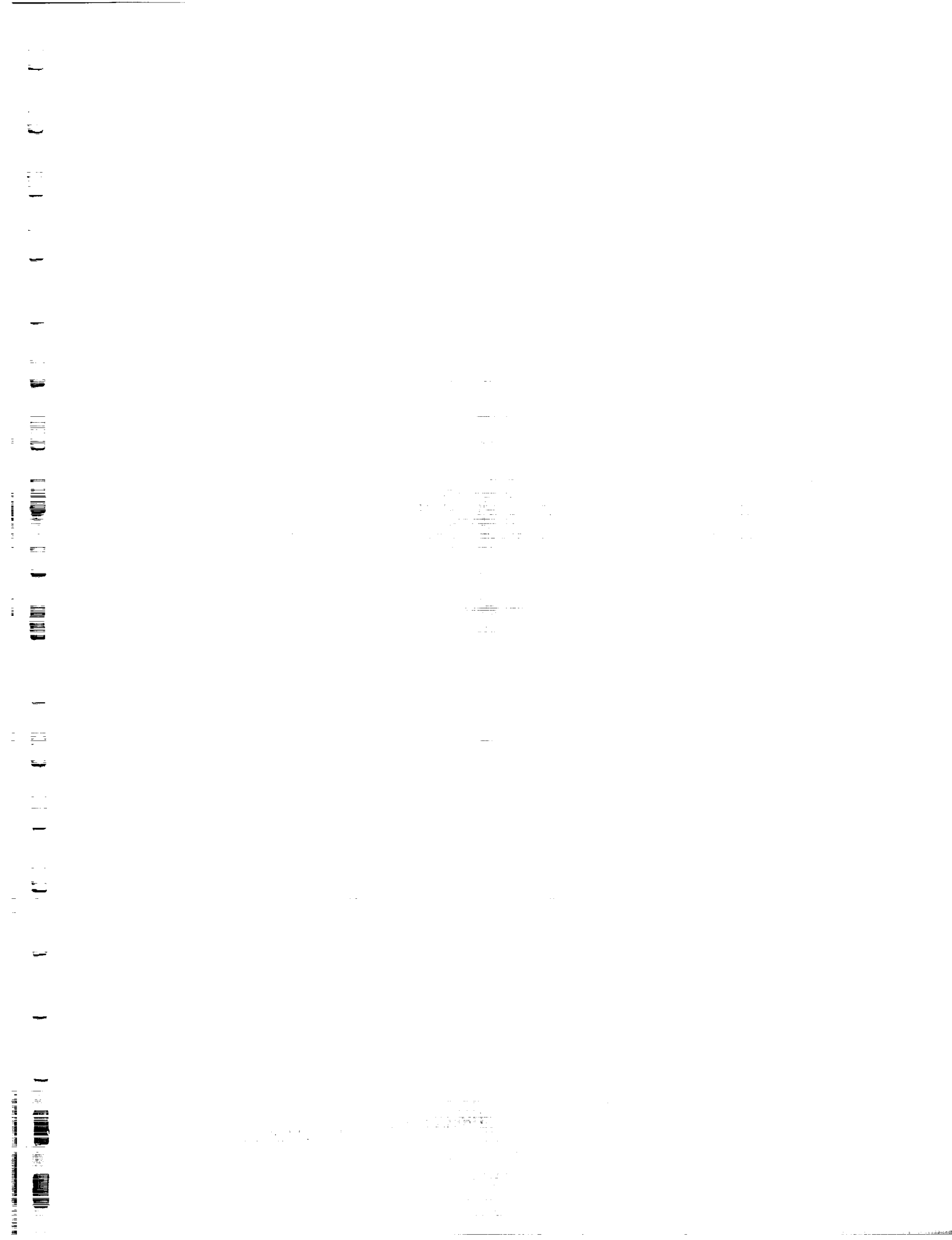
THE APPROACH TO CONTROL DESIGN INVOLVES DEFINING A COST FUNCTIONAL OF Z, SUCH AS ITS H₂ OR H_∞ NORM, AND OPTIMIZING IT OVER THE SET OF ALL PASSIVE CONTROLLERS. THIS PASSIVITY CONSTRAINT CAN BE FORMULATED AS A CONSTRAINT ON THE STATE-SPACE REALIZATION OF THE CONTROLLER NETWORK. IT CAN ALSO BE DESIRABLE TO RESTRICT THE CONTROLLERS TO CIRCUITS INVOLVING ONLY RESISTORS AND CAPACITORS, THUS AVOIDING MASSIVE INDUCTORS. A DIFFERENT SET OF CONSTRAINTS CAN BE DEVELOPED FOR THIS CASE.

TO DATE NO ANALYTICAL SOLUTION HAS BEEN FOUND FOR THESE OPTIMIZATION PROBLEMS, BUT A NUMERICAL SOLUTION PROCEDURE HAS BEEN FORMULATED FOR THE H₂ COST WITH FIXED-ORDER RC CONTROLLERS. SOLUTIONS HAVE BEEN OBTAINED FOR CERTAIN LOW-ORDER EXAMPLES WHICH SUGGEST THAT THE OPTIMAL CONTROLLER ORDER IS FINITE, THOUGH NOT NECESSARILY EQUAL TO THE ORDER OF THE PLANT AS IN THE CONVENTIONAL LQG PROBLEM.

Passive Control: Spangler, Hall (cont.)

- Control Design:
 - * Passivity constraint is formulated in terms of constraints on the state-space realization of the controller network.
 - * Cost (some functional of z) is optimized numerically over the constrained controller.
- Status:
 - Frequency domain modeling technique developed - extension of [Hagood '91] - and examples worked.
 - \mathcal{H}_2 controllers developed for benchmark examples, with networks restricted to RC.
- Future:
 - Develop a more fundamental, elegant solution technique for the \mathcal{H}_2 /RC design problem (riccati equations).
 - Experiment on the Interferometer Testbed.





Status:

- Simulation of planar, two-link flexible manipulator has been created.
- Investigation of nonlinear system dynamics, degree of nonlinearity of desired trajectories, and choice of mode shapes for control design are under way.
- Theory of output regulation for nonlinear systems used as a framework to elucidate tradeoffs between Feedforward and Feedback control.
- Performance limitations inherent in nonlinear nonminimum phase (NMP) systems made transparent in this way and are reducible locally to limits of performance on linear NMP systems.
- Concepts from Lyapunov-based Sliding Control and Adaptive control for rigid robots and robots with flexible joints are combined with differential geometric concepts to extend results to flexible link robots.
- Hamiltonian approach to Lyapunov function selection promises stabilizing control results without neglecting higher order dynamics through modal truncation.
- Extensions to tracking control and to controllers with robustness to parameter uncertainty seem possible.

PRECEDING PAGE BLANK NOT FILMED

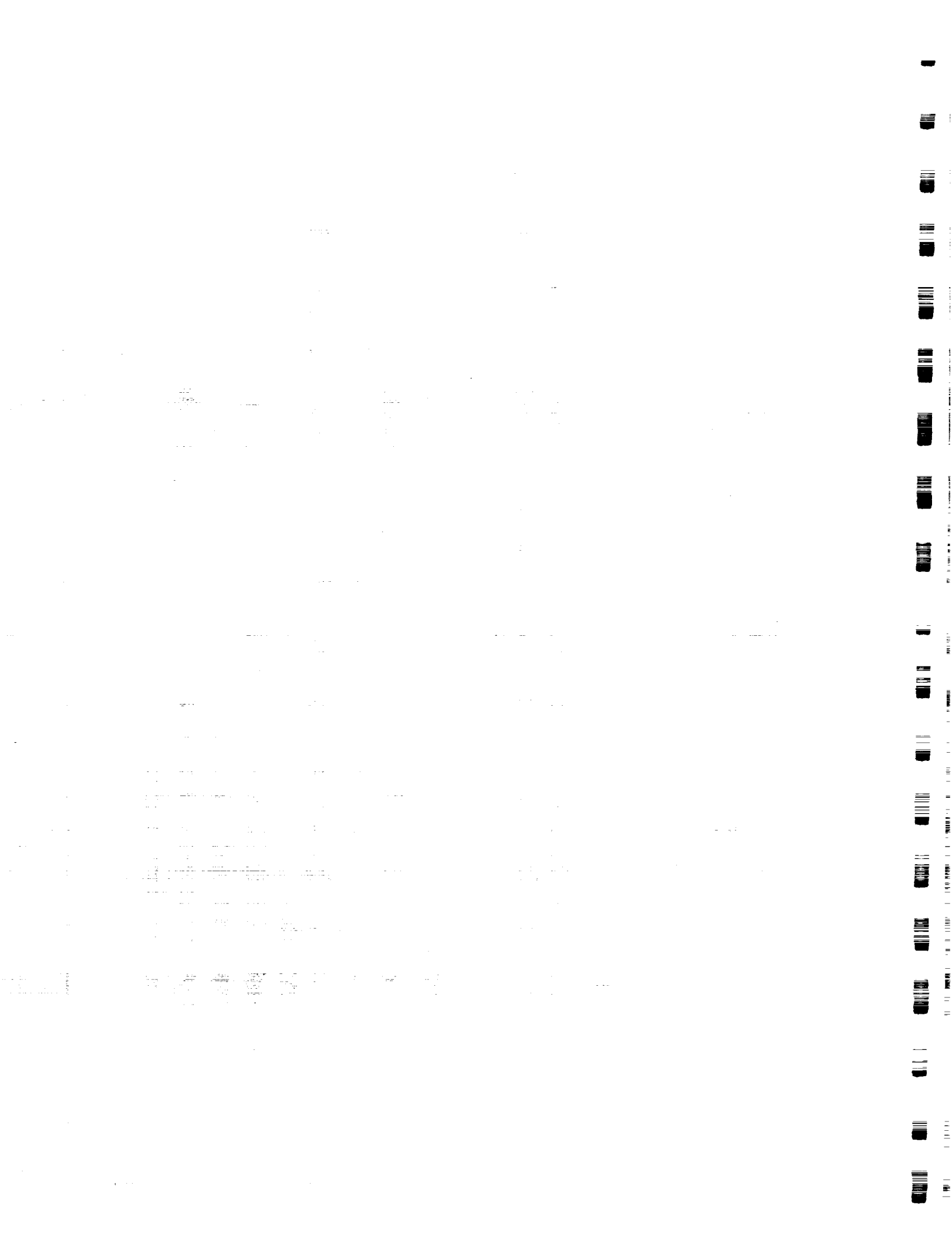
END-POINT CONTROL OF FLEXIBLE MANIPULATOR ARMS

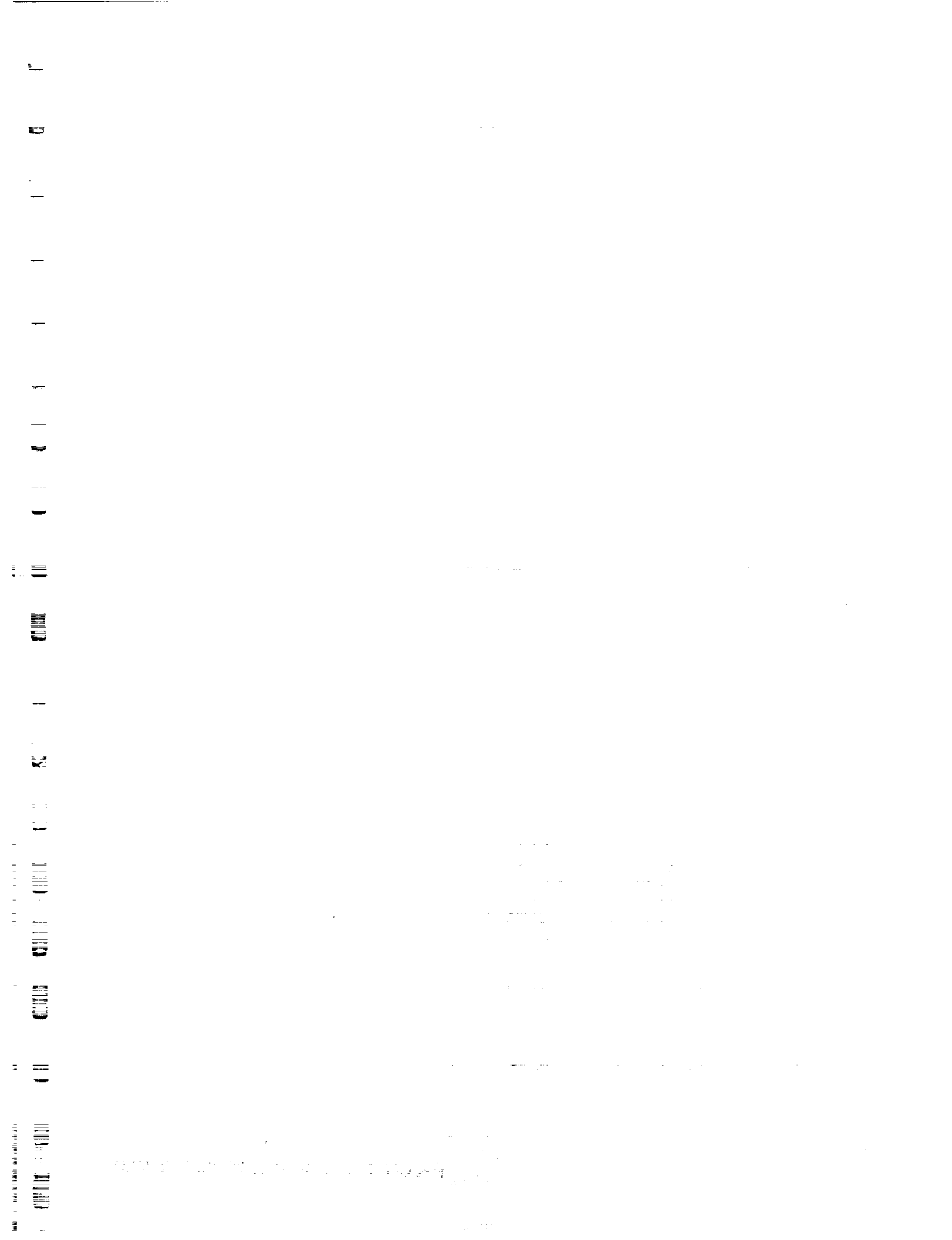
Objective:

- To achieve high-bandwidth, robust, end-point position control of a two-link, planar manipulator with distributed flexibility in the links.

Approach:

- Model distributed flexibility using assumed modes.
- Investigate maximum performance achievable.
- Obtain analytical stability and performance results for desired controllers.
- Design controllers for robustness to model uncertainties, both structured and unstructured.
- Exploit the use of simplified models when possible.
- Conduct simulations.





AMONG THE PUBLISHED REFERENCES FOR THIS WORK ARE:

HALL, S., CRAWLEY, E., HOW, J., AND WARD, B., "HIERARCHIC CONTROL ARCHITECTURE FOR INTELLIGENT STRUCTURES," *AIAA JOURNAL OF GUIDANCE, CONTROL, AND DYNAMICS*, MAY-JUNE 1990, PP.503-512.

WARKENTIN, D. AND CRAWLEY, E., "PROSPECTS FOR ELECTRONIC COMPONENT DISTRIBUTION IN INTELLIGENT STRUCTURES," PRESENTED AT THE ADPA CONFERENCE ON ACTIVE MATERIALS AND ADAPTIVE STRUCTURES, ALEXANDRIA, VIRGINIA, NOVEMBER 1991.

WARKENTIN, D., CRAWLEY, E., AND SENTURIA, S., "THE FEASIBILITY OF EMBEDDED ELECTRONICS FOR INTELLIGENT STRUCTURES," TO APPEAR IN THE JULY 1992 ISSUE OF *JOURNAL OF INTELLIGENT MATERIAL SYSTEMS AND STRUCTURES*.

PRECEDING PAGE BLANK NOT FILMED

Embedded Electronics for Intelligent Structures

Recent work in the center has established potential advantages of distributing and embedding large numbers of sensors, actuators, and processors for precision control of flexible structures

A technique to embed electronic devices in addition to sensors and actuators in structural members has been demonstrated

Current research is focusing on the distribution of power and signals to embedded electronic components

- Thermal, structural, and electrical design models of a prototypical intelligent structure are being developed to explore functional requirements for embedded components
- These requirements will drive the custom design of an efficient, single-chip amplifier suitable for driving piezoelectric actuators

The work is expected to culminate in a graphite/epoxy beam test article in which both an actuator and an amplifier are embedded, possibly with additional control circuitry

